Réactivité et devenir des micropolluants dans le canyon sous-marin de Capbreton.

Alyssa Azaroff

ECOLE DOCTORALE DE SCIENCES EXACTES ET LEURS APPLICATIONS ED 211

THESE

EN VUE DE L'OBTENTION DU GRADE DE

DOCTEUR DE L'UNIVERSITE DE PAU ET DES PAYS DE L'ADOUR

DISCIPLINE

CHIMIE ET MICROBIOLOGIE DE L'ENVIRONNEMENT

SOUTENUE PAR

ALYSSA AZAROFF

LE 17 DECEMBRE 2019

REACTIVITE ET DEVENIR DES MICROPOLLUANTS DANS LE CANYON SOUS-MARIN DE CAPBRETON

JURY

ANDREA BRAVO	CSIC– BARCELONE - ESPAGNE	RAPPORTEUR
JOEL KNOERY	IFREMER – NANTES - FRANCE	RAPPORTEUR
DANIEL COSSA	ISTERRE – GRENOBLE - FRANCE	EXAMINATEUR
HERVE GILLET	EPOC– BORDEAUX - FRANCE	EXAMINATEUR
MATHILDE MONPERRUS	IPREM – ANGLET - FRANCE	DIRECTRICE DE THESE
REMY GUYONEAUD	IPREM – PAU - FRANCE	DIRECTEUR DE THESE
EMMANUEL TESSIER	IPREM – PAU - FRANCE	MEMBRE INVITE

Structure d'accueil :

Institut des sciences analytiques et de physico-chimie pour l'environnement et les materiaux

Cette thèse a été co-financée par la région Nouvelle Aquitaine (Fonds Européen de Développement Régional) et par l'Agence de l'eau Adour Garonne dans le cadre du programme de recherche MICROPOLIT « état et évolution de la qualité du milieu littoral Sud Aquitain ».

Remerciements

Je remercie Mathilde Monperrus pour m'avoir fait confiance pour relever ce challenge, et pour m'avoir poussée dans mes retranchements et m'obliger à aller toujours plus loin. Merci à Rémy Guyoneaud, qui m'a ouvert la porte du monde passionnant qu'est la microbiologie. Il m'a transmis son intérêt pour ce monde invisible mais qui pourtant recèle de tant de secrets à mettre au grand jour.

Je remercie naturellement toutes les personnes qui ont participé à ce projet et sans qui tout cela n'aurait vu le jour :

Emmanuel Tessier, qui m'a instruit sa technique et sa rigueur pour les analyses de mercure,

Carole Miossec, qui a été d'un appui technique incontestable pour l'analyse des micropolluants organiques,

Jonathan Deborde, qui m'a initié à la géochimie et qui a permis la caractérisation de mes échantillons,

Claire Gassie pour son appui technique en biologie moléculaire,

Marisol Goni, qui m'a initié à l'étude des bactéries méthylantes.

Toutes ces personnes ont été capitales pour aller jusqu'au bout de mes raisonnements. J'ai vraiment apprécié travailler au sein de cette équipe. Cette aventure m'a beaucoup apporté aussi bien sur le plan professionnel qu'humain.

Je suis vraiment reconnaissante d'avoir eu la chance d'évoluer dans ce cadre. Pour cette raison, je tiens aussi à remercie la région Nouvelle-Aquitaine, Le FEDER et l'Université de Pau et des Pays de l'Adour.

Je remercie aussi UPPA-E2S et l'Ecole Doctorale pour m'avoir soutenue dans mon projet de mobilité internationale à l'Université de Californie, Santa Cruz. Je remercie Carl Lamborg pour son invitation et le Moss Landing Marine Lab pour avoir rendu possible une étude comparative entre le canyon de Capbreton et celui de Monterey. Cette expérience a été révélatrice et m'a permis d'élargir mes horizons.

Finalement, je remercie toutes les personnes qui m'ont soutenue, entourée et m'ont aidée à supporter les moments de doutes, mais qui aussi ont été près de moi pour partager tous les moments de joie que m'a apporté cette thèse.

Inconnu

SOMMAIRE

INTRODUCTION GENERALE

1 Les micropolluants : un enjeu environnemental

A la suite de la seconde guerre mondiale, les trente glorieuses fût une période qui s'est caracatérisée par un dévelopemment sans précédent dans les secteurs de la technologie et de l'ingénierie. Bien qu'une prise de conscience s'élève face à l'impact de cette industrialisation de masse depuis les années 60 [1], le nombre de substances chimiques, lui ne cesse de s'accroître. On définit alors un polluant comme une substance introduite par l'homme impactant l'environnement et que l'on catégorise selon qu'elle soit physique (radiation ionisant, pollution sonore ou thermique), organique (matières organiques mortes, microorganismes pathogènes, ...) ou chimique (hydrocarbures, matières plastiques, pesticides, nitrates, phosphates, métaux lourds, fluorures, ...) [2]. La notion de micropolluant, ici, ne tient compte que du groupe des polluants chimiques, dont les concentrations dans l'environnement sont inférieures ou de l'ordre du microgramme par litre (ou par kilogramme).

La production et la création constante de nouvelles substances conduisent aujourd'hui à plus de 150 millions de substances organiques et inorganiques reportées dans la littérature scientifique et répertoriées dans le registre « Chemistry Abstract Service », où chaque substance est identifiée par un numéro CAS (http://www.cas.org). Néanmoins, il n'existe pas de liste exhaustive comprenant l'ensemble des micropolluants car celle-ci évolue en même temps que l'on découvre leur présence dans l'environnement et que l'on étudie leurs effets. Ce progrès s'est aussi accompagné d'un récent développement des outils analytiques, rendant possible l'étude de nouveaux micropolluants, appelés émergents. Au sens de la définition donnée par le réseau européen NORMAN (http://www.norman-network.net/), une substance émergente est une substance qui a été détectée dans l'environnement mais qui n'est pas incluse dans des programmes de surveillance de routine et dont le comportement, le devenir et les effets sont mal connus

Il est difficile d'estimer le nombre de substances pouvant être classées comme micropolluants puisqu'on ne connait que celles que l'on étudie. Toutefois, 45 substances (métalliques et organiques) considérées comme étant des micropolluants prioritaires selon la Directive Cadre sur l'Eau (DCE) [3] sont suivies, régulièrement ou épisodiquement, dans les eaux européenes, dont l'objectif est d'atteindre un bon état écologique et chimique des masses d'eau (eaux de surface, souterraines, intérieures et de transition).

1.1 Définition

De manière générale, le terme « micropolluant » désigne un ensemble de substances essentiellement anthropogéniques, présentant des effets nocifs avérés ou suspectées sur l'environnement, à des concentrations de l'ordre du µg L^{-1} (voire du ng L^{-1}). Ils entrent dans la

composition de nombreuses formulations et interviennent dans de nombreux procédés (industriels, agricoles). Ils sont aussi retrouvés dans les activités quotidiennes des usagers (combustion des produits pétroliers, rejet de substances dans les réseaux de collecte des eaux usées, …). Ils peuvent aussi être d'origine naturelle dans l'environnement tels que les métaux par exemple. Même à de très faibles concentrations, ils peuvent engendrer des effets négatifs sur les organismes vivants en raison de leur toxicité, de leur persistance et de leur bioaccumulation [4].

1.2 Groupes et familles de micropolluants

La classification des micropolluants peut se faire selon différents critères, par exemple par familles chimiques, usages, effets ou statut réglementaire. La grande diversité de substances induit un large spectre de micropolluants aux propriétés et aux usages extrêmement variables (Fig. 1). Ils sont introduits dans l'environnement via les effluents industriels, les rejets urbains, l'agriculture et les produits agricoles. Alors que les hydrocarbures aromatiques polycycliques (HAPs), polychlorobiphényles (PCBs) et pesticides organochlorés sont relativement bien étudiés depuis les années 1970, la récente découverte des micropolluants émergents est préoccupante, car ils sont très peu étudiés. En effet, leurs impacts sur l'environnement restent à ce jour au cœur des problématiques liées aux micropolluants. D'autant plus que le spectre de ces micropolluants émergents, issus d'émissions domestiques, est large: médicaments, cosmétiques, lessives, détergents, tensioactifs, plastifiants, retardateurs de flammes, etc ….

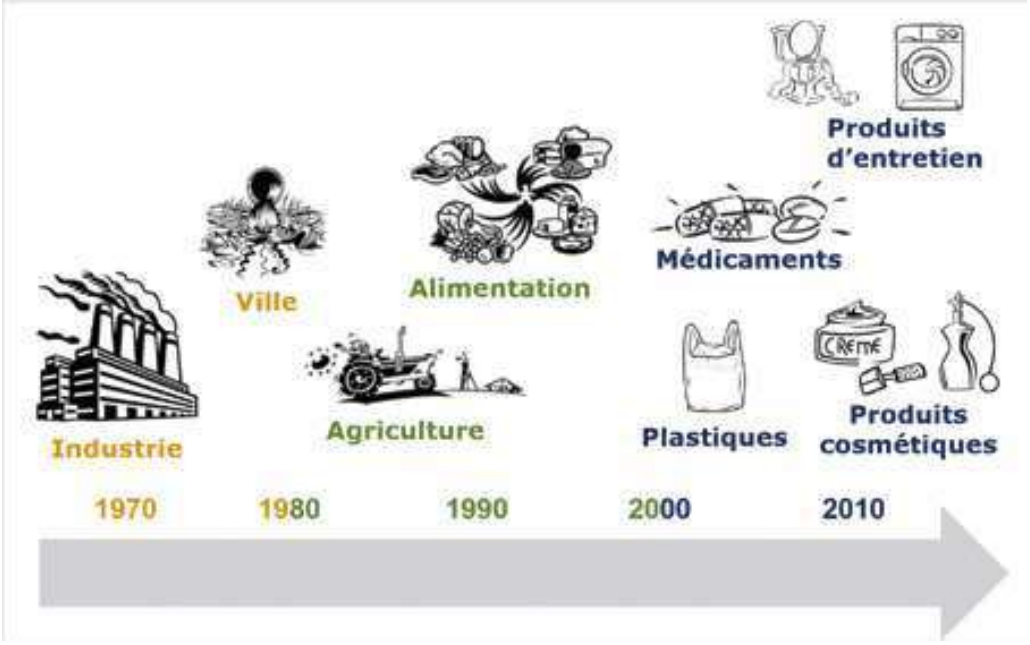

Figure 1 - Evolution de la prise de conscience des sources de micropolluants [5].

Les regroupements se font classiquement en fonction de :

leur structure chimique : composés aromatiques (comme les hydrocarbures aromatiques polycycliques; HAPs), organophosphorés , les polychlorobiphényles (PCBs), alkylphénols,…

leurs propriétés physico-chimiques : éléments traces métalliques vs. micropolluants organiques, molécules hydrophiles vs. hydrophobes,

leurs usages/familles : les composés impliqués dans la formulation des pesticides, cosmétiques, pharmaceutiques, …

leur devenir dans le milieu comme les composés organiques volatils (COV), polluants organiques persistants (POP), les substances très persistantes et très bioaccumulables (vPvB),

du types d'effets sur la santé humaine et les écosystèmes : perturbateurs endocriniens, cancérigènes, mutagènes, reprotoxiques, …

leur statut réglementaire : « substances prioritaires », « substances dangereuses prioritaires », « polluants spécifiques de l'état écologiques », « substances pertinentes à surveiller », « émergents »...

2 Suivi réglementaire dans les milieux marins

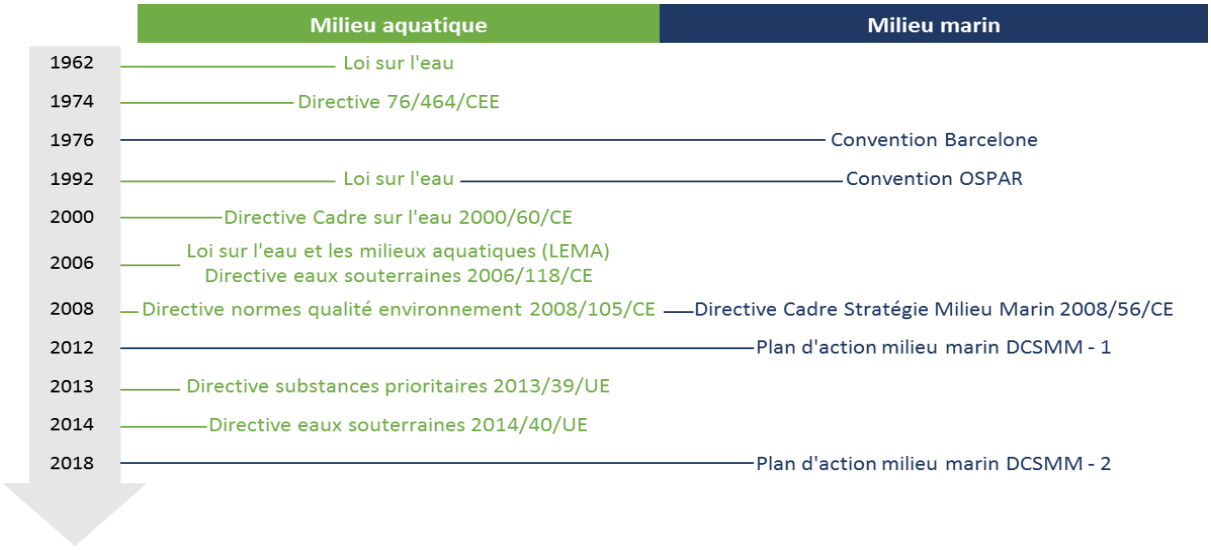

Figure 2 Chronologie des principaux textes réglementaires visant les micropolluants dans les milieux aquatiques en France.

En France, les lois sur l'eau de 1964 et 1992 ont permis de fixer un cadre pour une gestion intégrée des eaux, par grand bassin hydrographique. La directive n°76/464/CEE du 4

mai 1976 déterminait une réglementation générale pour la pollution causée par certaines substances. En 2000, la réglementation s'est établie à l'échelle européenne par la Directive Cadre sur l'Eau (DCE/2000/60) et les directives filles qui en ont découlées (DCE 2008/105/CE, 2013/39/CE) visant l'harmonisation des lois et des outils pour chaque états membres (Fig. 2). En parallèle des textes réglementaires voient le jour dans en 1976 (Convention de Barcelone) et s'harmonisent à l'échelle européenne avec la Directive Cadre Stratégie pour le Milieu Marin (DCSMM) (Fig. 2).

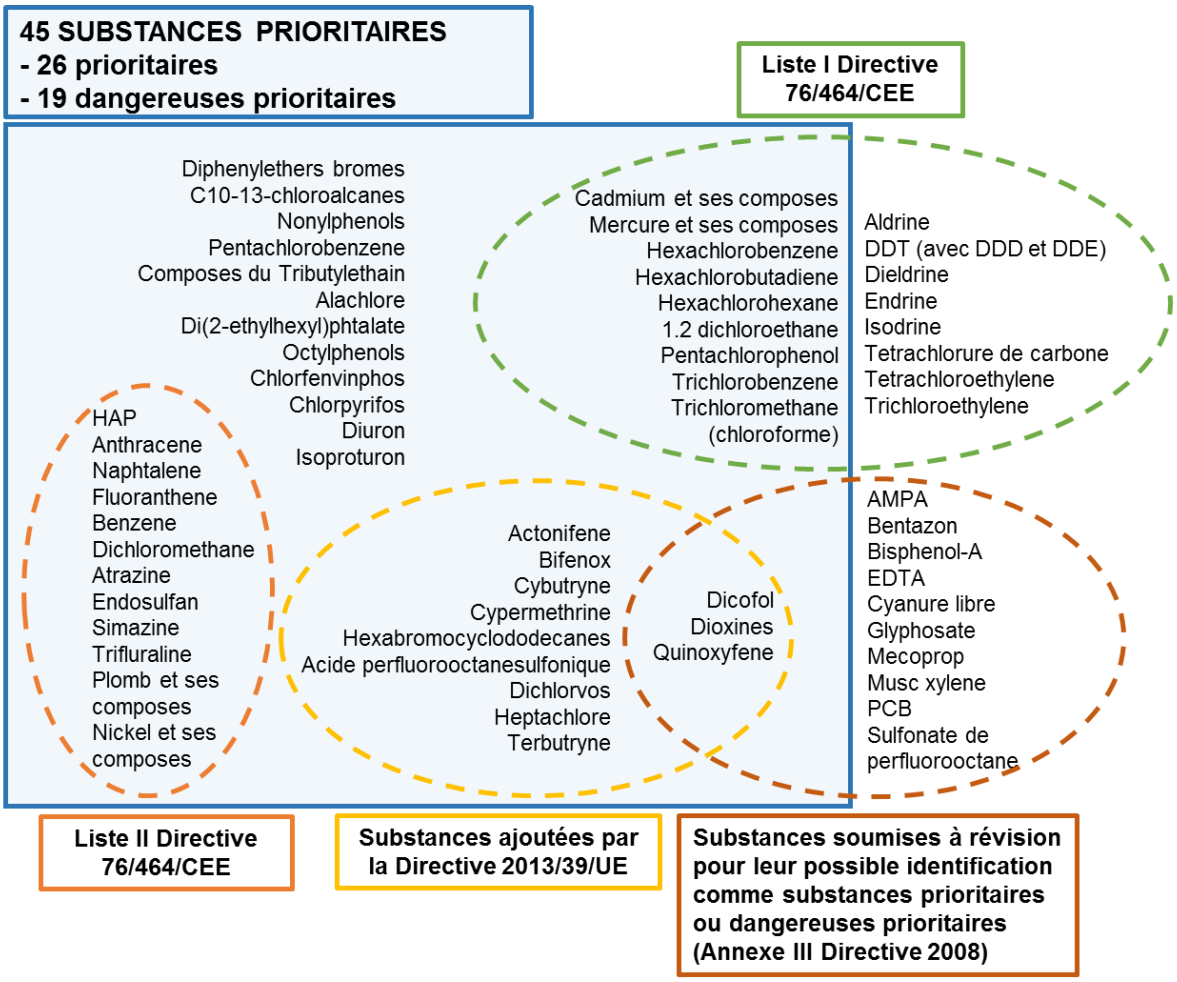

Figure 3 Schéma récapitulant la liste des substances prioritaires selon la DCE et des substances soumises à révision (d'après DCE 2000/60, DCE 2008/105/CE, DCE2013/39/CE.)

Ainsi, 45 substances prioritaires (Fig. 3) sont suivies en routine car «la pollution chimique des eaux de surface constitue une menace tant pour le milieu aquatique, avec des effets tels qu'une toxicité aiguë et chronique pour les organismes aquatiques, l'accumulation des polluants dans les écosystèmes, la disparition d'habitats et la perte de biodiversité, que pour la santé humaine. Il convient en priorité de déterminer les causes de pollution et de lutter contre les émissions de polluants à la source, de la façon la plus efficace possible du point de vue économique et environnemental » (DCE 2013/39/CE).

Alors qu'il est largement admis que l'océan est le récepteur final des pollutions aquatiques, les lacunes de connaissances sur l'état chimique, physique et écologique persistent pour le milieu marin. En 2008, la DCSMM (DCSMM 2008/56/CE) a été mise en place pour y palier. Dans le même esprit que la DCE, la DCSMM a pour objectif d'atteindre un bon état écologique (BEE) d'ici 2020. Cette directive indique qu'il faut « prévenir et réduire les apports dans le milieu marin afin d'éliminer progressivement la pollution telle que définie à l'article 3, point 8, pour assurer qu'il n'y ait pas d'impact ou de risque significatif pour la biodiversité marine, les écosystèmes marins, la santé humaine ou les usages légitimes de la mer. ». Ainsi, en France, la DCSMM s'applique aux zones sous juridiction française, divisées en 4 sous-régions marines : la Manche-Mer du Nord, les mers celtiques, le golfe de Gascogne et la Méditerranée occidentale.

Pour chaque sous-région marine, un plan d'action pour le milieu marin est établi pour une durée de 6 ans (Fig. 4) selon 11 descripteurs dont le descripteur 8 « contaminants » qui évalue la concentration des contaminants dans les matrices appropriées (8.1), les effets biologiques (8.2.1) et l'occurrence, l'origine des contaminants et leurs effets physiques sur le biote (8.2.2). Alors que le premier cycle de 2012 fût plutôt qualitatif, celui de 2018 fût plus quantitatif. Cela met en avant la complexité de la tâche à relever pour atteindre un BEE d'ici à 2020.

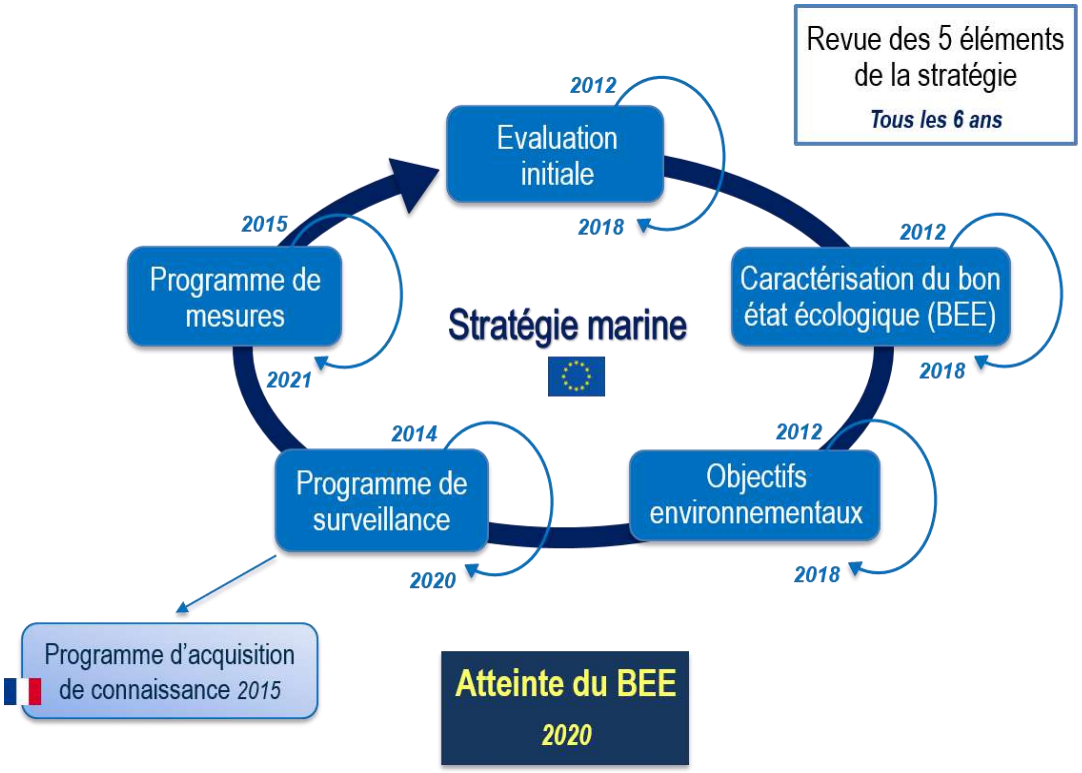

Figure 4 – Plan d'action pour le milieu marin (source :http://www.dcsmm-d4.fr/la-directive-cadre-strategir-pour-le-milieu-marin-dcsmm))

80 % de la pollution en milieu côtier est anthropique, c'est-à-dire qui provient des activités humaines sur le continent. Ainsi, les micropolluants marins ont des origines multiples : rejets urbains (eaux usées et pluviales), rejets industriels et rejets agricoles. Le cadre réglementaire européen prend en compte à la fois l'état des eaux de surface continentales (DCE 2000/60/CE), des eaux souterraines (Directive 2006/118/CE), eaux de transition (estuaires et lagunes) et eaux marines côtières (s'étendant à 1 mille du trait de côte) (DCSMM 2008/56/CE), régule les eaux résiduaires urbaines (directive 91/721/CE) et modère les émissions (règlement REACH n°1907/2006, directives pesticides 2009/128/CE). Cela permet une prise en compte globale pour une meilleure gestion de l'eau. Néanmoins, d'autres sources potentielles proviennent directement des activités qui se déroulent en mer telles que l'exploitation des hydrocarbures liquides et gazeux / activité offshore, incinération, eaux de ballast, antisalissure, marées noires, ect.

Partant de l'ensemble des contaminants présents dans le milieu marin, la DCSMM-D8 a sélectionné ceux qui correspondent aux substances pertinentes de la Directive 2000/60/CE (DCE), celles des conventions sur les mers régionales (OSPAR, Barcelone pour les sous-régions marines françaises), et celles des substances ou groupes de substances affectant l'environnement marin. Un récent travail a permis de compiler les susbtances potentielles à suivre dans le milieu marin. Il fait état d'une liste 2700 substances (ou groupes de substances) [6] parmi lesquelles figurent :

-substances persistantes, bioaccumulables et toxiques, dites « PBT »,

-des substances prioritaires de la DCE

-des substances anti-salissures introduites directement dans le milieu marin,

-des substances dites émergentes : composés perfluorés, pharmaceutiques, et nanomatériaux par exemple.

En l'état actuel des connaissances, la DCSMM inclut plusieurs seuils environnementaux pour l'évaluation du BEE, tels que les indicateurs de seuil de la Convention OSPAR que sont les Environnmental Assessment Criteria (EAC), les Background Assessment Concentrations (BAC), et celui de la DCE qui est la Norme de Qualité Environnementale (NQE) [7]. A ce jour, ces seuils ne sont pas définis pour l'ensemble des substances suivies. Concernant les substances émergentes, la réglementation et les seuils environnementaux sont toujours en cours d'élaboration ou n'existent pas encore.

3 Micropolluants dans le milieu marin

3.1 Sources

Selon leurs propriétés physio-chimiques et leurs sources, les micropolluants sont libérés dans l'océan par les cours d'eaux, les effluents côtiers et les estuaires, par retombées atmopshériques, par les eaux souterraines et encore par des apports sous-marins (Fig. 5). On distingue des pollutions dites chroniques, c'est-à-dire un apport constant dans l'environnement, des pollutions dites aigues, c'est-à-dire ponctuelles.

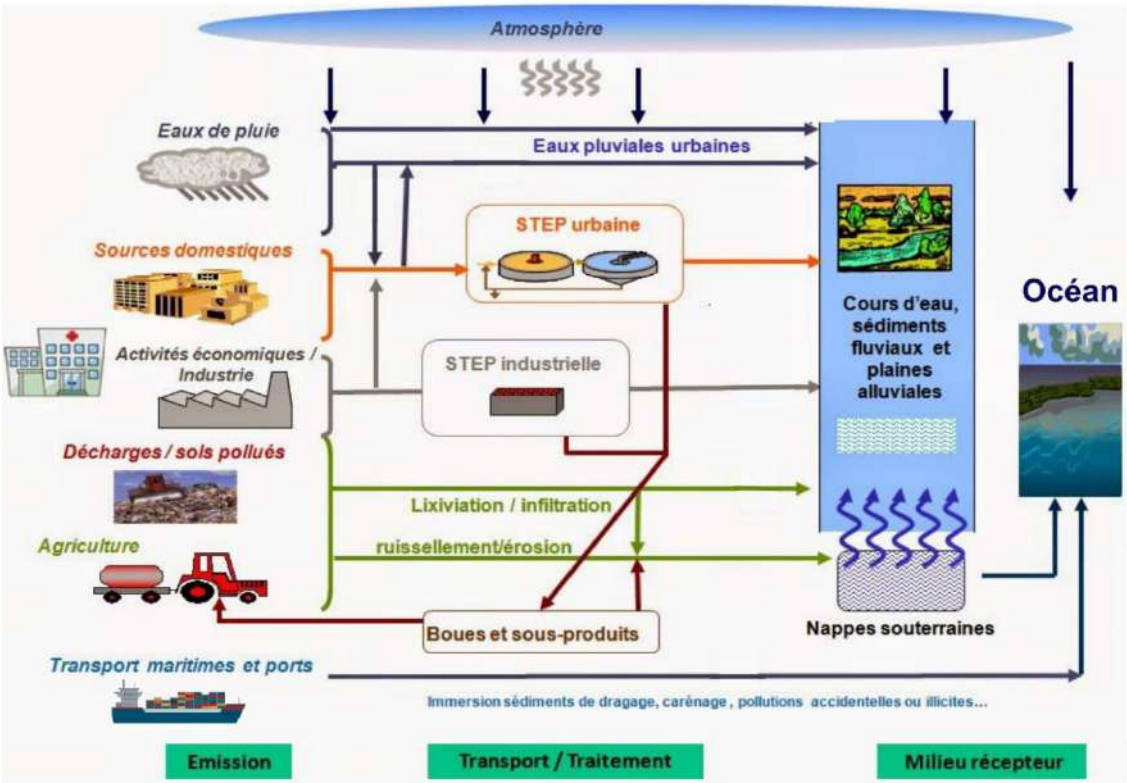

Figure 5 - Sources des micropolluants dans l'océan

3.1.1 Pollutions chroniques

80 % de la pollution marine est d'origine continentale, liée aux activités anthropogénétiques. Ces pollutions proviennent essentiellement des eaux de rejets industriels, agricoles et urbains mais aussi des eaux de lessivage des sols (routes, zones agricoles et forêts). Ces pollutions sont diffuses, chroniques et les quantités déversées dans l'environnement sont croissantes. Les systèmes de traitement des eaux usées (STEUs) restent à ce jour inefficaces pour éliminer la totalité des micropolluants. Les grandes agglomérations côtières et fluviales déversent par conséquent plusieurs millions de tonnes de substances [8] dans l'environnement qui finissent dans l'océan, réceptacle de toutes pollutions. Certaines d'entre elles s'accumulent dans les profondeurs des océans et/ou sont

transportées au large jusqu'en pleine mer [9]. Ces substances subissent des transformations en fonction d'un ensemble de facteurs environnementaux et biologiques (e.i. biostranformation microbienne par exemple), rendant possible leur introduction dans la chaîne alimentaire. Ces polluants chimiques sont communément des pesticides, herbicides, fertilisants, détergents, pétrole et produits industriels.

3.1.2 Pollutions aigües

Les autres sources potentielles proviennent directement des activités qui se déroulent en mer : exploitation des hydrocarbures liquides et gazeux / activité offshore, incinération, eaux de ballast, antisalissure, transport maritimes et ports. Contrairement aux pollutions d'origines continentales, elles sont caractérisées par des épisodes de pollution aigües, telles que les marées noires (Amoco Cadiz et de l'Erika par exemple). Par ailleurs, leur impact est plus faible à long terme. Il convient toutefois de noter que des facteurs océanographiques et géologiques naturels, y compris l'activité géothermique, peuvent parfois être responsables de concentrations élevées de certains contaminants (tels que les métaux lourds) (Europa MWFD).

3.1.3 Quelques exemples de pollutions marines

Parmis les pollutions marines on peut lister les déchets industriels, déchets urbains et routiers, eaux d'égouts, gaz d'échappement via l'atmosphère, engrais et pesticides, eaux de refroidissement, précipitations atmosphériques (métaux lourds et hydrocarbures), marées noires, armement et munitions diverses, déchets en provenance de bateaux, déchets industriels et nucléaires, épaves ou encore les stations de forage pétrolier offshore.

3.2 Activités et niveaux de concentration dans les sédiments marins

La matrice sédimentaire constitue une matrice intégratrice de la pollution. En effet, les métaux et les substances organiques hydrophobes ont une forte affinité pour les particules. Dans ce travail, une centaine de substances prioritaires et émergentes ont été suivies. Ici, les niveaux de concentration retrouvés dans les sédiments estuariens, côtiers et marins sont recensés afin de faire un état des lieux des niveaux de concentrations dans le milieu marin. A partir des listes de substances pertinentes à suivre définies par la DCE ou encore la DCSMM, les micropolluants prioritaires que nous avons ciblés sont les hydrocarbures aromatiques polycycliques (HAPs), les pesticides organochlorés (OCPs), les polychlorobiphényles (PCBs) et les métaux/métalloïdes. Les micropolluants émergents ont été sélectionnés en fonction de leur présence dans l'environnement, tels que les parfums de synthèse, écrans anti UV et les composés pharmaceutiques.

3.2.1 Les substances prioritaires

3.2.1.1 Hydrocarbures Aromatiques Polycycliques (HAPs)

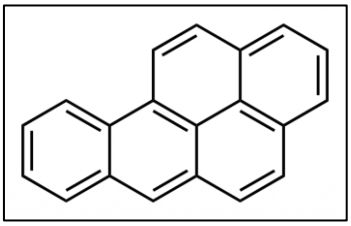

Figure 6 - benzo[a]pyrène, polluant ubiquiste, cancérigène, toxique, représentatif des HAPs dans les milieux marins

Les HAPs sont un proupe d'hydrocarbures dont la molécule est constituée par la fusion d'un nombre variable de cycles benzéniques [10], les rendant hydrophobes, persistants et bioaccumulables. Les HAPs présents dans l'environnement résultent de différents processus tels que la biosynthèse par des organismes vivants, les pertes à partir du transport ou de l'utilisation des carburants fossiles, charbons, pétroles et la pyrolyse des matières organiques à haute température (feu de forêt, combustions des charbons et pétroles). Les feux de forêt sont une source importante d'introduction d'HAPs dans l'atmosphère (Fig. 7), parmi lesquels figure le benzo(a)pyrène (Fig. 6). Par des processus de remobilisation et sédimentation, les HAPs sont stockés dans le compartiment sédimentaire. Les activités telles que les usines de production d'aluminium, les raffineries de pétrole ou les rejets urbains contribuent également de manière importante aux apports atmosphériques et aquatiques (Fig. 7).

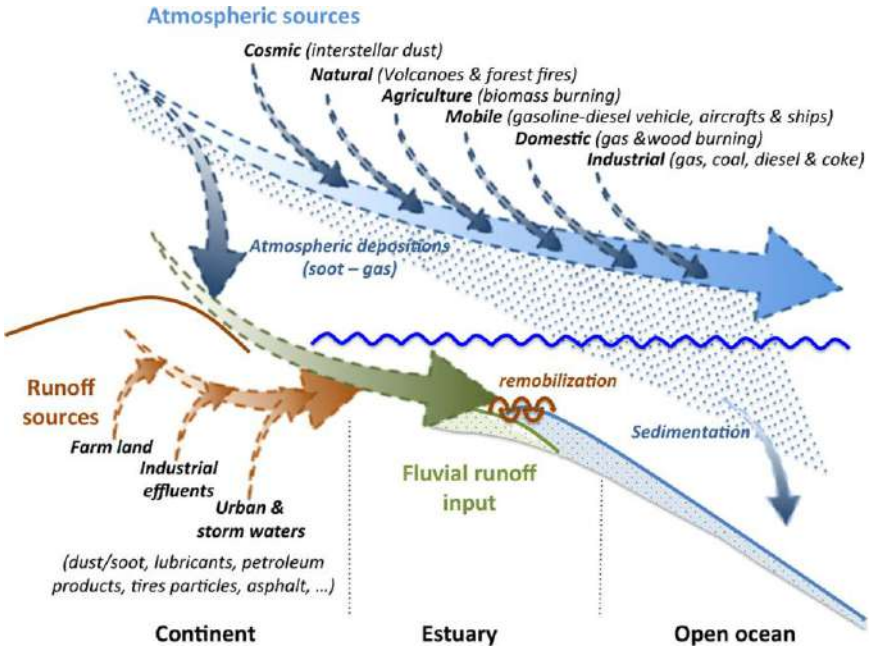

Figure 7 – Principales sources de HAPs dans le milieu marin [11]

16 d'entre eux sont communément suivis (EPA USA (1984), CE, OMS) dans les suivis environnementaux car ils sont connus pour être cancérigènes (HAP ayant des chaines carbonées polycycliques allant généralement de 18 à 22 carbones ($C_{18}H_{12}$ à $C_{22}H_{14}$)). Ils ont été retrouvés à des concentrations maximales allant jusqu'à près de 1 million de ng g^{-1} (sédiment sec) dans des sédiments côtiers en Inde (Table 1).

Table 1 Concentrations de HAPs dans les sédiments marins à travers le monde (ng g^{-1} sédiment sec).

Pays	Sites	∑HAPs	Références
Croatie	Baie de Rijeka	32 - 13 681	[12]
Espagne	Côte Atlantique	20 - 602	[13]
Espagne	Port de Barcelone	1 740 - 8 420	[14]
Espagne	Baie de Santander	20 - 344 600	[15]
France	Estuaire de Gironde	19 - 4 888	[16]
France	Côte Méditerranéenne	86 - 48 000	[17]
Grèce	Côte Méditerranéenne	100 - 26 000	[18]
Italie	Mer Adriatique	39 - 572	[19]
Italie	Port de Naples	9 - 31 774	[20]
Alaska	Mer de Beaufort	159 - 1 092	[21]
Brésil	Baie de Guanabara	77 - 7 751	[22]
Chine	Baie de Zhanjiang	42 - 934	[23]
Chine	Estuaire de Pearl	53 - 1 369	[24]
Inde	Côtes Bhavnagar	5 020 - 981 180	[25]
Egypte	Côte Méditerranéenne	3.5 - 14 100	[26]
Qatar	Golf Arabique	3 146 - 14 350	[27]
Etats Unis d'A.	Baie de San Francisco	2 653 - 27 680	[28]

3.2.1.2 Pesticides organochlorés

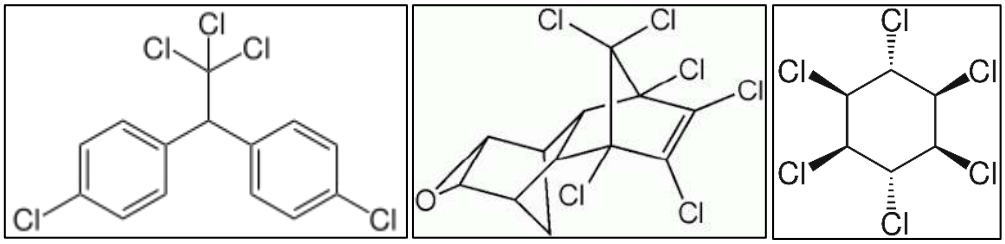

Figure 8 - Formules chimiques du DDT, Dieldrin et Lindane

Le terme "pesticides" regroupe les substances ou produits qui éliminent les organismes considérés comme nuisibles, qu'ils soient utilisés dans le secteur agricole ou dans d'autres applications. Ce sont des poisons destinés à éliminer les herbes (herbicides), les insectes (insecticides), à lutter contre les maladies (fongicides), ou à se débarrasser de divers animaux jugés nuisibles. Les pesticides se retrouvent partout : dans nos aliments, dans l'eau des rivières, dans les eaux souterraines, dans l'air, dans les sols, dans les sédiments, dans la biomasse vivante et morte, dans le sang et le lait maternel [29,30]. En 1961, dans son ouvrage « Printemps silencieux » [1], Rachel Carson mettait en garde contre l'utilisation du Dichloro-Diphényl-Trichloréthane (DDT) (Fig. 8), un pesticide largement utilisé, notamment pour lutter contre le paludisme. Il fut progressivement interdit (en 1973 en France) et remplacé par une nouvelle génération de pesticides organochlorées ou des carbamates. Malgré de nombreuses mises en garde sur l'utilisation de ces pesticies, l'Europe représente à elle seule 25% de leur utilisation à l'échelle globale [31]. En France son utilisation semble plus intensive au abord des grands fleuves qui se jettent dans la zone côtière (Fig. 9).

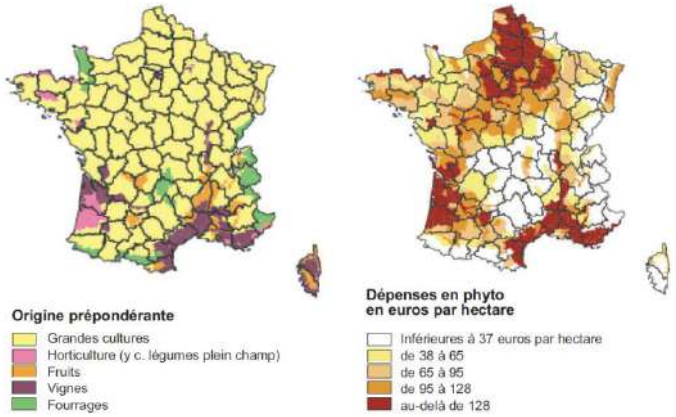

Figure 9 - Répartition des petites régions agricoles selon l'origine et le niveau de la pression phytosanitaire (pesticides par hectare)[32]

De nombreux pesticides sont caractérisés comme cancérigènes, mutagènes et reprotoxiques (CMR). Par conséquent, les pesticides et leurs résidus posent un sérieux

enjeu sanitaire, impliquant notamment une dégradation de la qualité des milieux aquatiques. En 2008, la France lançait son plan « Ecophyto » pour réduire de 50% l'utilisation des pesticides d'ici 2018. Malheureusement il fut sans effet, repoussant cet objectif de réduction pour 2025. Nombreux d'entre eux sont compris dans la liste des polluants organiques persistants à éliminer ou à restreindre établit par la convention de Stockholm dont le DDT, dieldrine, endosulphan, heptachlore ou encore le lindane (Fig. 8).

Table 2 Concentrations de pesticides organochlorés dans les sédiments marins à travers le monde (ng g^{-1} sédiment sec). ∑DDT correspond à la somme DDT et ses résidus, DDE et DDD ; ∑HCH correspond à la somme des lindanes ∑HCH = αHCH +βHCH + ϒHCH + δHCH. <LD signifie que les concentrations étaient inférieures à la limite de détection.

Pays	Sites	∑DDT	Dieldrine	∑HCH	Références
Atl. ocean	-	0.08 -32	<0.005 - 1.86	-	[33]
Espagne	Côte Cantabrie	0.5 - 0.9	0.4 -0.7	-	[33]
France	Cortiou	0.7 - 114.3	0 - 41.3	0.1 - 31.4	[34]
France	Etang de Berre	0.37 - 1.52	-	-	[35]
Italie	Mer Adriatique	0.1 - 4.3	-	-	[19]
Egypte	Port d'Alexandrie	<0.25- 885	< LD	< LD	[26]
USA	New Jersey	100–300	-	-	[36]
USA	Long Island Sound	1.31 - 33.2	0.05 - 5.27	-	[37]
Chine	Singapour	2.2 - 11.9	-	3.3 – 46.2	[38]
Chine	Hong Kong	0.3–14.8	-	0.1–16.7	[39]
Chine	Haihe	0.32–80.18	-	1.88–18.76	[40]
Inde	Mer d'Arabie côte	1.47–25.17	0.70–3.33	0.85–7.87	[41]
Inde	Mer d'Arabie offshore	1.14–17.59	0.20–1.41	0.10–6.20	[41]
Taiwan	estuaire Wu-Shi	0.53–11.4	-	0.99–14.5	[42]

Les teneurs en pesticides les plus élevées dans les milieux marins sont habituellement retrouvées dans les zones où la population est dense et dans les régions industrialisées, proches de grands estuaires [43]. Par exemple, en dépit de leur interdiction ou de leur restriction depuis un cinquantaine d'année, le DDT et ses résidus (DDD et DDE) sont toujours détectés dans les sédiments côtiers. Ainsi des concentrations atteignant 885 ng g^{-1} ont été retrouvées dans les sédiments du port d'Alexandrie (Table 2). D'autres pesticides tels que le dieldrine et le lindane (HCH) et ses résidus, ont été retrouvés à des concentrations atteignant 41.3 ng^{-1} g et à 46.2 ng g^{-1}, respectivement (Table 2). Cela illustre une fois encore que l'océan est un récepteur final de pollution continentale mais également la persistance de ces pesticides.

3.2.1.3 Polychlorobiphényles (PCBs)

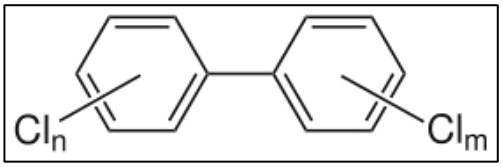

Figure 10 – Structure chimique des PCBs, C12H(10-x)Clx avec x = n+m > 2

Les PCBs forment une famille de 209 composés aromatiques organochlorés (Fig. 10) dérivés du biphényle et sont des CMRs. Les PCBs et les dioxines qui en dérivent proviennent de processus industriels ou de phénomènes naturels comme les éruptions volcaniques ou des incendies de forêt. Les PCBs ont été remplacés les chloralcanes (halogénoalcanes utilisés comme retardateurs de flammes). De par leurs propriétés, ils sont largement utilisés comme: fluides dans les échangeurs thermiques, fluides diélectriques dans les condensateurs, diluants organiques dans les plastiques et les encres, dans la préparation de certains insecticides ou comme agents électriques dans les transformateurs électriques.

Table 3 Concentrations de PCBs dans les sédiments marins à travers le monde (ng g^{-1} sédiment sec). ∑PCBs correspond à la somme des 7 isomères usuellement étudiés comprenant les PCB 28, 52, 101, 118, 138, 153 et 180.

Pays	Sites	∑PCBs	Références
Espagne	Côte Atlantique	1,1 -12,1	[44]
France	Cortiou	11,5 - 751,5	[34]
France	Etang de Berre	0.03 - 13.13	[35]
France	Rivière Huveaune	2.8 to 435	[45]
France	Etang de Thau	0 -28.3	[46]
Italie	Mer Adriatique	<LD - 4,3	[19]
Italie	Lagune Venise	2 - 2049	[47]
Egypte	Port d'Alexandrie	0.9 to 1210	[26]
Chine	Singapour	1.4 to 329.6	[38]
Inde	Bengale	0.18–2.33	[48]

7 d'entre eux sont communément suivis depuis 1987 (Bruxelles, CE) : PCB 28, 52, 101, 118, 138, 153 et 180. Au même titre que les HAPs ou les pesticides organocholorés, ils sont souvent retrouvés à de plus fortes concentrations dans les zones côtières industrialisées proches des estuaires. La somme des concentrations de ces 7 PCBs, noté ∑PCBs, dans les sédiments marins atteint ainsi 1210 ng g^{-1} dans le port d'Alexandrie.

3.2.1.4 Composés métalliques – Cas du mercure

Seul métal volatil à température ambiante, le mercure, naturel ou anthropique, peut être transporté en grandes quantités par l'atmosphère. Les sources naturelles sont le dégazage de l'écorce terrestre, les feux de forêt, le volcanisme et le lessivage des sols. Sa très forte toxicité fait qu'il est soumis à de nombreuses réglementations d'utilisation et de rejet. Les sources anthropiques proviennent des processus de combustion (charbon, pétrole, ordures ménagères, etc.), de la fabrication de la soude et de chlore ainsi que de l'orpaillage [49]. Dangereux neurotoxique, la forme organique du mercure, le méthylmercure (MeHg), est bioaccumulable et pose de nombreux problèmes environnementaux et sanitaires. Le plus connu est celui qui avait affectés les habitants de la baie de Minamata en 1955 (maladie de Minamata) [50]. Les niveaux de concentrations du mercure total (HgT) dans les sédiments marins sont généralement autours de 100 ng g^{-1} [51] alors que sa forme organique (MeHg) représente en moyenne une proportion autours de 1% du HgT [51] (Table 4).

Table 4 Concentrations de mercure total (HgT) et de mercure organique (MeHg) dans les sédiments marins à travers le monde (ng g^{-1} sédiment sec)

Pays	Sites	HgT	MeHg	Références
France	Canyon du Var (Mer Med.)	18-61		[52]
France	Estuaire de l'Adour (Atl. Ocean)	20-461	0,1-1,6	[56]
Espagne	Basque country background	130		[57][58]
Portugal	Canyons Cascais (Atl. Ocean)	43-59		[53]
Portugal	Canyon de Nazaré (Atl. Ocean)	2-363		[54]
Portugal	Canyon de Cascais (Atl. Ocean)	110-431		[55]
Portugal	Nazaré canyon (Atl. Ocean)	2-363		[54][55]
Espagne	Basque country background	130		[58]

3.2.2 Les substances émergentes

Au-delà des substances surveillées classiquement (métaux, organochlorés, pesticides, hydrocarbures), une forte préoccupation émerge sur les éventuels effets des substances émergentes (parfums de synthèse, les écrans anti UV ou encore les résidus pharmaceutiques). Ce sont des substances entrant notamment dans la formulation des cosmétiques et des produits d'hygiène corporelle. Certaines d'entres elles sont suspectées d'être des perturbateurs endocriniens (PE) [58]. Ces substances sont retrouvées dans l'environnement et jusque dans les océans. Et cela, même après les différentes étapes de traitement dans les STEUs [59,60].

3.2.2.1 Parfums de synthèse

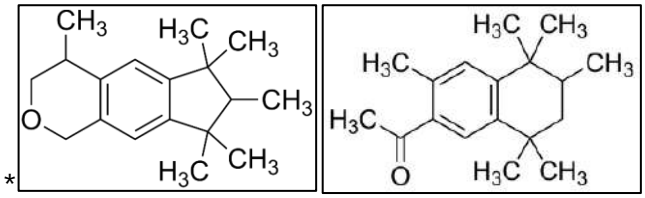

Figure 11 - Formule chimique du galaxolide (HHCB) et du tonalide (AHTN)

Deux types de substances sont synthétisées industriellement : les nitromuscs (muscs xylène MX, cétone MK) et les muscs polycycliques (galaxolide HHCB, tonalide AHTN) (Fig. 11). Selon Daughton et Ternes [61], la production mondiale des muscs synthétiques pour l'industrie des parfums et cosmétiques était de 7 000 tonnes en 1988. Les nitromuscs (MX et MK) ont été restreints en Europe depuis les années 1990. Ils ont été remplacés par des muscs polycycliques, où l'utilisation industrielle des muscs polycycliques (HHCB et AHTN) et des muscs nitrés (MX et MK) était respectivement de 3285 et 298 tonnes (HERA, 2004). En Europe, la consommation de HHCB et AHTN, représentait 1473 et 385 tonnes en 1998 [62,63]. Aujourd'hui on les retrouve dans les différents compartiments environnementaux et également dans la chaîne trophique aquatique, les tissus adipeux humains et le lait maternel [64]. Néanmoins, l'étude récente de ces molécules se traduit par un manque de données dans le compartiment sédimentaire marin. A ce jour, ces études montrent que HHCB et AHTN peuvent atteindre des concentrations de 156.2 et 27.9 ng g^{-1}, respectivement (Table 5), dans les sédiments marins.

Table 5 Concentrations de galaxolide (HHCB) et tonalide (AHTN) dans les sédiments marins à travers le monde (ng g^{-1} sédiment sec); minimum et maximum.

Pays	Sites	HHCB	AHTN	Références
Espagne	Côte Atlantique	2,9 -156,2	0,6 -26,2	[44]
Italie	Mer Adriatique	0,6 - 24,3	<LD - 16	[19]
Brésil	Côte Bahia	2,39 - 52,5	2,81 - 27,9	[65]
Chine	Estuaire Pearl river	<LD - 56	<LD - 24	[24]
Chine	Estuaire Pearl river	4.55–27.1	1.89–13.6	[66]

3.2.2.2 Ecrans anti UV

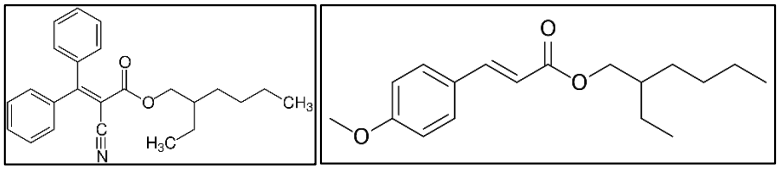

Figure 12 – Formule chimique de octocrylène (OC) et 2-ethyl-hexyl-4-trimethoxycinnamate (EHMC)

Les écrans anti UV sont des molécules chimiques absorbant les rayonnements dans l'UVA (400-315 nm) et l'UVB (315-280 nm). Ils peuvent représenter jusqu'à 10% des formulations de produits cosmétiques et sont également utlisés dans les plastiques [67]. Les principales molécules retrouvées sur le marché sont la benzophénone-3 (Bp-3), l'homosalate (HMS), l'octyl-méthoxycinnamate (OMC), et l'octyl-dimethyl-PABA (OD-PABA). La Bp-3, l'HMS, le 4-MBC et le OD-PABA circuleraient à plus de 10 tonnes par an en Europe et l'OMC [68,69]. Ils sont libérés dans l'environnement indirectivement par les eaux usées des STEUs ou directement lors des baignades et activités récréationnelles dans l'océan [70].

Les études environnementales ont montré que l'OC et EHMC (Fig. 12) sont souvent retrouvés dans les sédiments marins (Table 6). A contrario l'OD-PABA est retrouvé plus sporadiquement. Néanmoins il atteint une concentration autours de 20 ng g^{-1} dans les sédiments côtiers de Hong Kong [71].

Table 6 Concentrations d'écrans UV, octocryléne (OC) et 2-ethyl-hexyl-4-trimethoxycinnamate (EHMC) dans les sédiments marins à travers le monde (ng g^{-1} sédiment sec).

Pays	Sites	OC	EHMC	Références
Espagne	Côte Atlantique	1,7 - 43,6	0,4 - 23,8	[44]
Italie	Mer Adriatique	0,8 - 40,7	-	[19]
China	Hong Kong	0,04 - 15,6	0,3 – 447	[71]
Chine	Estuaire des Perles	<LD - 105,2	<LD - 30,1	[24]
Chine	Estuaire des Perles	6.26–27.8	-	[66]
Colombie	Zone côtière	-	nd–17.8	[72]

3.2.2.3 Produits pharmaceutiques

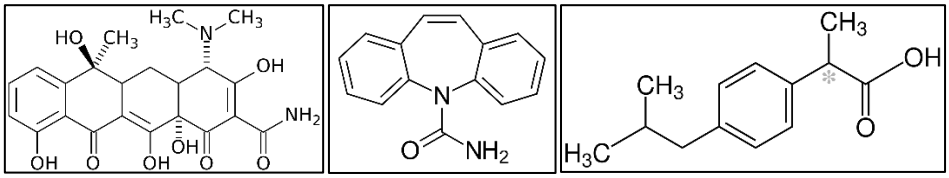

Figure 13 - Formule chimique de tétracycline, carbamazépine et ibuprofen

Parmi les produits pharmaceutiques, les plus employés sont les antibiotiques. A usage humain ou vétérinaire, ils transitent dans le milieu aquatique via les effluents des hôpitaux, les effluents des eaux usées et des eaux provenant d'exploitation agricoles. Bien que ces effluents chargés de résidus soient en partie traités, ils finissent par rejoindre le milieu aquatique. Au cours de la dernière décennie, on estime leur consommation à 12 500 tonnes par an [73]. En 2000, la consommation d'antibiotiques vétérinaires s'élevait à 1391 tonnes en France, traduisant une augmentation de 5% entre 1999 et 2000 (tétracyclines, sulfamides et bêta-lactamines représentant 76% des ventes) [73]

D'autres produits pharmaceutiques, tels que les anti-inflammatoires non stéroïdiens (ibuprofène et dicloflénac) ou les antiépileptiques (carbamazépine, également utilisée comme stabilisateur d'humeur pour les personnes atteintes de troubles bipolaires) (Fig. 13), sont couramment retrouvés dans les eaux en sorties de STEUs. Ils sont aussi détectés dans les sols et sédiments [74] indiquant qu'ils sont transportés et persistants.

Table 7 Concentrations de composés pharmaceutiques : antibiotique (Tetracycline, TC), anti épileptique (Carbamazépine, CBZ) et antalgique (Ibuprofen, IBU) dans les sédiments marins à travers le monde (ng g -1 sédiment sec). <LD signifie que la concentration était inférieure à la limite de détection. N.Z pour Nouvelle-Zélande

Pays	Sites	TC	CBZ	IBU	Références
Brésil	Bahia coast	-	<0,1 - 4,81	0,77 - 18,8	[65]
Espagne	Baie de Cadiz	-	90 - 15	98 - 100	[44]
Espagne	Baie de Cadiz	-	< 0.1 – 88.8	-	[75]
USA	Baie de San Francisco	-	0.04 - 0.12	-	[76]
USA	Estuaire Puget	-	-	21.7	[77]
N-Z	Estuaire Auckland	-	0.2 - 1.1	-	[78]
Chine	Rivière Huangpu	<LD - 21,4	-	-	[79]
Chine	Sédiments marins	1.74–7.13	-	-	[60]

Continuellement déversés dans l'environnement, difficilement dégradables, ces produits pharmaceutiques sont au cœur des préoccupations des pollutions émergentes. A ce jour très peu de données existent au niveau des sédiments marins et côtiers. Par exemple, Gaw et al. [80] reportaient qu'il n'y avait eu jusqu'alors que 22 études sur le sujet en 2014. En effet, pour trois d'entre eux, tétracycline, ibuprofen et carbamazépine, les concentrations dans les sédiments côtiers (ou proches des estuaires), étaient comprises entre 0.6 - 21.4 (min – max), 0.2 – 88.8, 0.77 – 100 ng g^{-1}, respectivement (Table 7), soulignant le caractère persistant de ces substances.

4 Les processus impliqués dans le devenir des micropolluants

Les micropolluants ont des sources multiples et des natures différentes qui leur confèrent des propriétés physico-chimiques (dégradabilité, volatilité, solubilité...) qui détermineront leur devenir dans le milieu dans lequel ils sont rejetés. Ils circulent selon un double processus d'advection horizontale et verticale. Les courants et les vents peuvent les transporter sur des milliers de kilomètres alors que d'autres peuvent se fixer sur le matériel particulaire et sédimenter avant d'être remis en suspension. La forte persistance des micropolluants pose la question de la résilience naturelle du milieu impacté. En effet, leur dégradation est sous le contrôle de processus abiotiques et biotiques. Cela définit le temps au bout duquel les micropolluants seront éliminés par le milieu. Le temps de demi vie d'une molécule renseignera sur son degré de persistance. Par exemple, malgré l'arrêt progressif de l'usage de certaines substances dans les années 1980, les PCBs persistent et se retrouvent encore dans l'environnement. Néanmoins, pour des molécules à fort poids moléculaire, ces processus peuvent être à l'origine de la formation de produits de dégradation. Ces résidus peuvent être, dans certain cas, plus toxiques que la substance mère. Cette partie présentera succinctement les processus physico-chimiques et les processus biologiques (à l'échelle microbiologique) qui conditionnent la transformation, la dégradation ou la séquestration des micropolluants dans le milieu marin, plus particulièrement dans le compartiment sédimentaire.

4.1 Processus physico-chimiques

4.1.1 Répartition dissous/particulaire

Selon ses paramètres physico-chimiques et les conditions environnementales, un micropolluant peut se retrouver sous différentes formes physiques (ou « espèces » que l'on appelle la spéciation). Il peut se retrouver alors dans la phase dissoute ou la phase particulaire. Dans la phase dissoute, les micropolluants sont libres ou bien complexés à la

matière organique dissoute (MOD). Dans la phase particulaire, ils sont adsorbés sur la phase solide (organique ou minérale) qui peut être en suspension ou immobile (matière en suspension, sédiments, sols). Cette répartition contrôle l'exposition de ces micropolluants aux organismes vivants et la manière dont ils sont biodisponibles (fraction dissoute). Ce qui par conséquent, peut déterminer la résilience naturelle du milieu.

Les substances dont la constante de partition octanol-eau (log K_{ow}) est supérieure à 5 vont préférentiellement s'adsorber sur la phase particulaire [5] (Fig. 14). Or les polluants organiques persistants sont généralement définis comme des substances dont le log K_{ow} est supérieure à 5. L'étude des micropolluants dans le compartiment sédimentaire est alors pertinente vis-à-vis de sa forte capacité de stockage. L'adsorption est un processus qui peut notamment empêcher la dégradation (biodégradation, photodégradation) et réduire sa biodisponibilité, contrôlant en partie le devenir des substances dans l'environnement.

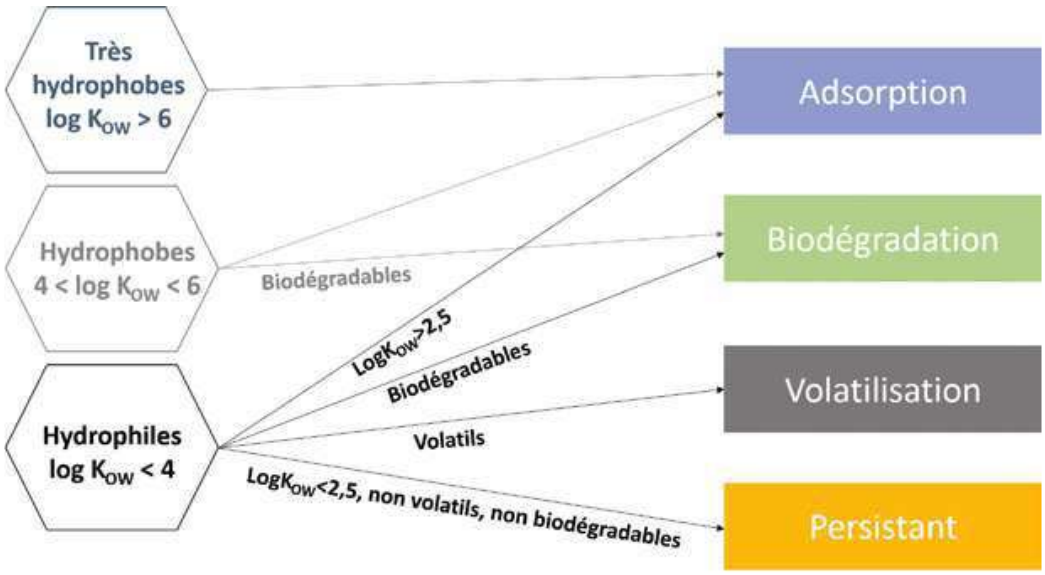

Figure 14 - Exemple de différents devenirs de micropolluants en fonction des propriétés des molécules [5] et d'après Mailer 2015

4.1.2 Processus de transfert/rétention

Dans le compartiment particulaire, le processus principal impliqué dans la rétention de micropolluants est l'adsorption. Selon l'hydrodynamisme et la taille des particules, les micropolluants sont transportées par advection ou piégées par sédimentation ou adsorption sur le substrat. Certains micropolluants sont métabolisables et d'autres sont bioaccumulés chez les organismes incapables de les métaboliser ou de les évacuer. Par exemple, le mercure est adsorbé par le phytoplancton, puis par bioamplification, les poissons atteignent des concentrations entre 10^5 et 10^7 fois plus élevés. Cela à pour conséquence un danger pour la santé humaine par la consommation de ces poissons contaminés.

4.1.3 Processus de transformation

Bien que ces micropolluants peuvent présenter un caractère persistant, plusieurs processus conduisent à la diminution de la concentration d'un micropolluant dans un compartiment donné. Ces processus peuvent être abiotiques ou biotiques. Il s'agit de :

- La photolyse qui détruit des liaisons chimiques par les radiations UV
- L'hydrolyse par l'action directe ou indirecte de l'eau, avec l'apparition de nouvelles molécules
- Les réaction d'oxydoréduction consistant par le transfert d'électron(s)
- La volatilisation au contact de l'air qui transfère les micropolluants de l'eau vers l'atmosphère,
- La biodégradation sous l'action des microorganismes présents dans l'eau et dans les sédiments (uniquement pour les micropolluants organiques et les organo-métalliques ; organo-SN, MeHg).

La dégradation peut être complète ou partielle et peut également conduire des produits de dégradation ou des métabolites ayant des propriétés physico-chimiques différentes du composé parent (Fig. 15). Par exemple, le galaxolide (un parfum de synthèse) se dégrade en galaxolide lactone, dont les propriétés sont différentes [81] pouvant être plus toxique que le galaxolide lui même.

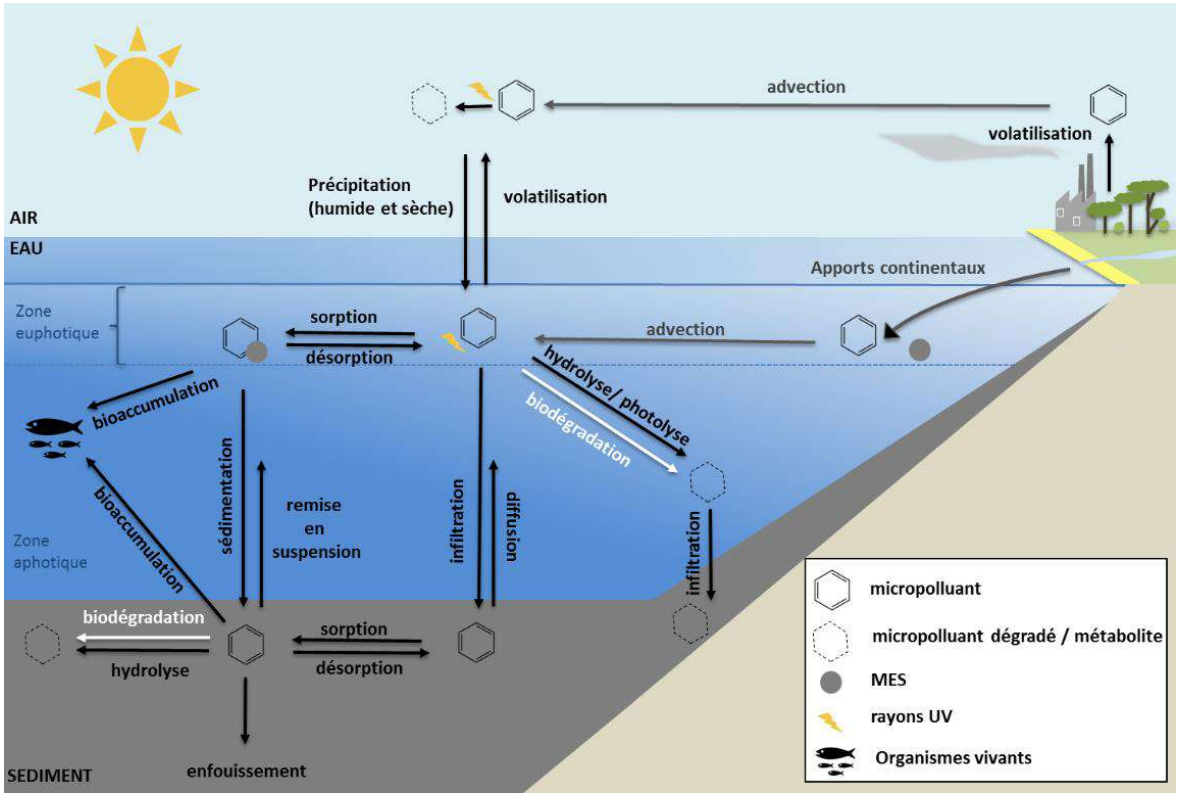

Figure 15 - Processus physico-chimiques (en noir) et biologiques (en blanc) ayant lieu dans le compartiment eau et sédiment, aux interfaces atmosphère/eau, eau/sédiment en milieu marin. D'après Briand 2018.

4.2 Transformation microbienne

Chaque élément parcourt un cycle géochimique spécifique, mais le cycles de ces éléments sont étroitement couplés et interdépendants. La croissance des êtres vivants n'est possible qui si l'ensemble des éléments biogènes, dont fait partie les micropolluants organiques, sont disponibles et à des concentrations bien définies. La minéralisation de la matière organique (MO) et des micropolluants organiques, restitue au milieu naturel des éléments minéraux, dont certains sont des accepteurs ou donneurs d'électrons au cours de réaction d'oxydo-réduction. Ces derniers sont à la base des cycles biogéochimiques permettant le recyclage de la MO et la dégradation de micropolluants organiques.

Les processus microbiens sont en grande partie responsable de cette minéralisation. Ils sont particulièrement importants lors du traitement des eaux usées (boues actives), dont la composition de la communauté microbienne, les conditions environnementales (température, pH, salinité, oxygène, and nutriments) et les caractéristiques de la substance définiront le devenir de cette dernière.

Dans le cadre de ce travail, deux processus seront étudiés : les processus de biotransformation impliqués dans la méthylation du mercure inorganique (4.2.1) et des processus de biodégradation les micropolluants organiques (4.2.2).

4.2.1 Cas du mercure

L'intoxication au Hg des habitants de la baie de Minamata a été le premier incident qui permis de prendre conscience de l'ampleur des répercussions du mercure à l'échelle globale. En effet, par un processus de transformation, appelé méthylation, le mercure inorganique est transformé en mercure organique par l'addition d'un groupement méthyl (-CH_3). Cela se produit par l'intermédiaire de microorganismes que l'on trouve dans la colonne d'eau et les sédiments principalement en condition anoxique (Fig. 16). Bio-amplifiable le long de la chaîne alimentaire, le MeHg est un problème sanitaire et environnemental d'envergure, notamment parce qu'on le retrouve à de très fortes concentrations dans les espèces piscicoles marines d'intérêt commercial.

Bien que des processus de déméthylation et méthylation abiotiques soient impliqués dans le cycle biogéochimique du mercure, nous nous focaliserons ici uniquement sur la méthylation du mercure par voie biotique. Il est à ce jour admis que ces processus abiotiques sont régis par des transformations photochimiques (réduction, dégradation du

MeHg en Hg^0) et transformations chimiques (transfert de $–CH_3$ ou $–CH_3^-$, oxydation, hydrolyse) [82–84].

La **bio-méthylation** du mercure s'exerce sous l'action d'une activité microbienne intense. En milieu aquatique, notamment en condition d'anoxie (dépourvue d'oxygène), cette méthylation est principalement due aux bactéries sulfacto-réductrices (BSR)[85], utilisant le sulfate (SO_4^{2-}) comme accepteur d'électrons. Néanmoins, les conditions environnementales définissent les accepteurs d'électrons disponibles pour les microorganismes, typiquement utilisés dans l'ordre des O_2, NO_3^-, $Mn_{(VI)}$, $Fe_{(III)}$, et SO_4^{2-} suivi par la méthanogénèse et/ou la fermentation [86]. Alors que les BSR sont identifiées comme étant les principaux acteurs de la méthylation du mercure, la méthylation est aussi associée à l'activité des bactéries ferri reducteurs (FeRB), archeae méthanogènes and d'autres anaérobes [87].

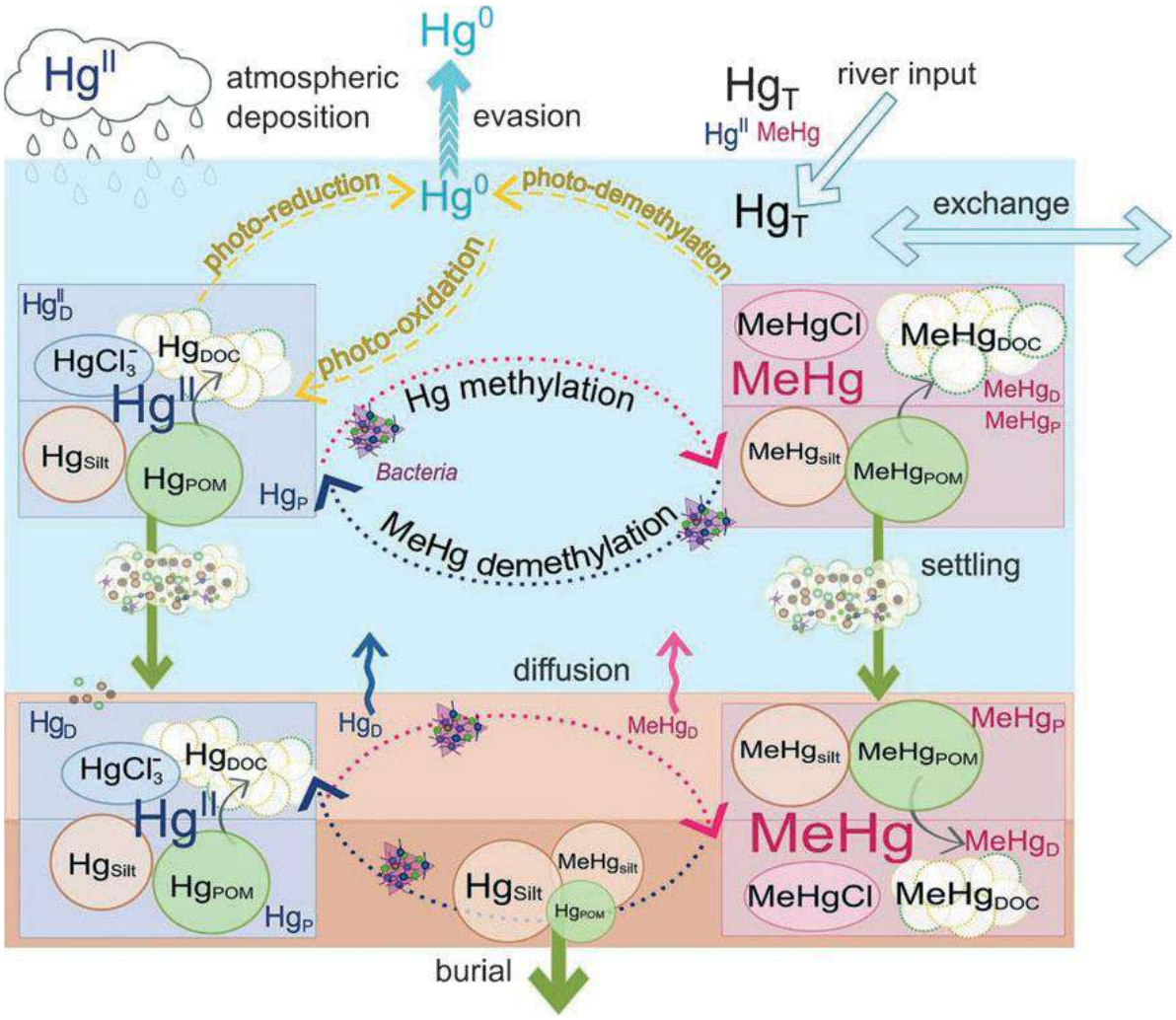

Figure 16 Cycle biogéochimique du mercure dans le milieu [88]

Le développement des outils de biologie moléculaire a récemment permis la découverte de gènes spécifiquement impliqués dans ces processus de méthylation et de déméthylation du mercure, *hgcA* et *hgcB*, respectivement [89]. Cela permet ainsi de

nombreuses opportunités pour l'identification de nouvelles souches microbiennes impliquées dans ces processus. *hgcA* est présent dans le génome de BSR, FeRB des *Deltaprotéobacteria*, *Clostridium* (*Firmicutes*), méthanogènes parmi les *methanomicrobia* et aussi des fermenteur et organismes acétogènes [87,90,91]. D'autres phylums microbiens, suspectés de porter également ce gène, se trouveraient parmi les *Chloroflexi*, *Chrysiogenetes*, *Nitrospina*, PVC superphylum ou *Spirochaetes* [92]. Néanmoins, leur potentiel de méthylation demeure inconnu et nécessite des études futures afin de déterminer leur implication dans la production de MeHg. De plus, bien que de récentes études aient permis l'étude de ce gène *hgcA* dans de nombreuses zones potentiellement productrice de MeHg (zones humides, rizières, lacs, réservoirs de barrage hydroélectrique et effluents de STEUs), les microorganismes méthylants dans les sédiments marins n'ont jamais été identifiés par l'utilisation du gène *hgcA*.

4.2.2 Cas des micropolluants émergents

La création de nouvelles molécules et leur rejet constant de substances émergentes dans les milieux aquatiques sont au cœurs de nombreuses préoccupations qui visent à quantifier, comprendre et réduire leurs impacts sur l'environnement notamment dans le milieu marin [93].

De nombreuses technologies voient le jour et sont en constant développement afin d'augmenter les taux d'abattement au niveau des STEUs. L'optimisation de plusieurs technologies dont les boues activées sont en cours pour augmenter les taux abattements des STEUs vis-à-vis des micropolluants [94]. Cette technologie, en milieu contrôlé, s'inspire du milieu naturel et met en jeu des processus que l'on retrouve dans le compartiment sédimentaire. Les deux processus majeurs impliqués dans la l'élimination de polluants sont la bio-absorption (ex. bio-sorbants tels que les plantes, les algues, les bactéries, les champignons et les levures) et la bio-remédiation, qui sont eux même dépendant des conditions physico-chimiques du milieu (ex. pH, granulométrie) qui détermineront la biodisponibilité de ces substances [95].

La bio-remédiation comprend des processus biologiques qui permettent d'éliminer, de réduire, de précipiter, d'accumuler, de dégrader ou d'immobiliser les composés toxiques tels que les substances émergentes. On distingue la phyto-remédiation et le remédiation microbiennes (e.i. champignons et bactéries). La biodégradation représente un service écosystémique non négligeable puisqu'elle contribue à la résilience naturelle du milieu. Il n'y pas de règle générale pour la biodégradation des micropolluants émergents [59]. De plus, si

les gènes sont déjà présents pour dégrader ces xénobiotiques, ces gènes peuvent aussi être hérités par transfert horizontal de gènes [96].

5 Canyon de Capbreton – zone de transfert particulaire du continent aux plaines abyssales

5.1 Généralités et caractéristiques des canyons sous-marins

D'après Sherpard [97], un canyon est « vallée caractérisées par des pentes abruptes, sinueuses, avec un fort dénivelé amont-aval et des sections transversales en forme de V. Les profondeurs peuvent atteindre de 1000 à 3000 mètres. Ils assurent le transfert de sédiments provenant des continents vers les grands fonds »

Le développement des techniques pour l'étude des fonds océaninques a permis de dénombrer à ce jour près de 5 849 canyons sous-marins [98].

Les canyons possèdent des caractéristiques physiques et écologiques particulières [99] :

- une migration verticale nycthémérale de zooplancton
- des courants de turbidité pouvant être causés par la topographie et le forçage climatique
- de fortes concentrations de matière en suspension (MES)
- transport de la matière organique (MO) des zones côtières vers la plaine abyssale
- la présence d'upwelling favorisant la productivité primaire et des populations pélagiques.

5.2 Caractéristique générales du canyon de Capbreton

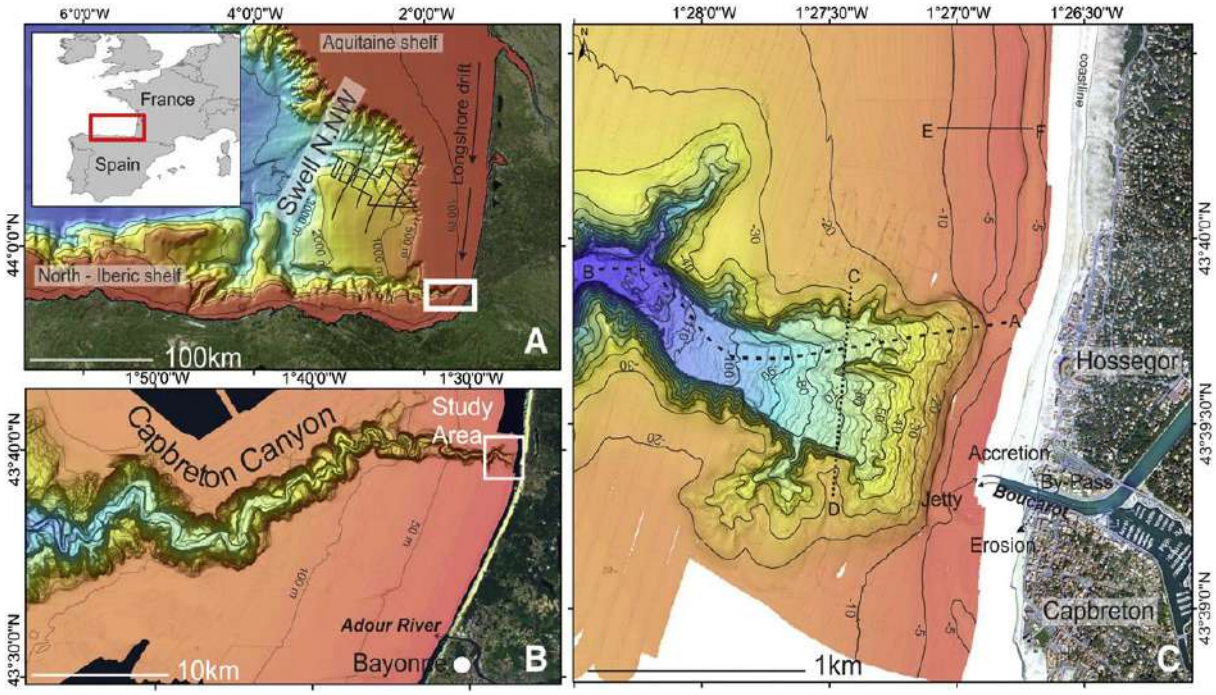

Figure 17 - Cartographie du canyon sous-marin de Capbreton, (A,B) Zone d'étude dans le golfe de Gascogne montrant la proximité avec la zone cotière et (C) la bathymétrie détaillée de la tête du Canyon montrant la continuité continent/ocean [100].

Le canyon de Capbreton (Sud-Est du golfe de Gascogne, océan Atlantique Nord Est) est un des plus long du monde (270 km). Il débute à 250 mètre de la côte, à 15 km de l'embouchure de l'estuaire de l'Adour (Fig 17). Cet estuaire draine un bassin versant qui couvre environ 17 000 km^2 et connecte le piedmont Pyrénéen occidental jusqu'à l'océan Atlantique. La partie amont de l'estuaire traverse des zones agricoles, tandis que la partie avale se situe dans la ville de Bayonne et est soumise à des intrants industriels [56]. Le débit annuel moyen du fleuve est d'environ 300 $m^3 s^{-1}$ et atteint 2 000 $m^3 s^{-}1$ pendant les périodes de crues [56]. Il s'agit donc d'une zone de transfert sédimentaire naturelle entre le continent et la plaine abyssale.

D'un point de vue morphologique, le canyon de Cabreton comporte une tête creusée en forme d'amphithéâtre à proximité immédiate du littoral [100] et une entaille profonde qui longe la côte espagnole et oblique en angle droit au nord au niveau de la ville de Santander avant de se jeter dans la plaine abyssale [101]. Le anyon de Capbreton est une entaille sous-marine dans le plateau continental dont la morphologie est complexe. Ce qui constitue un espace marin remarquable donc l'accès et l'échantillonnage reste difficile.

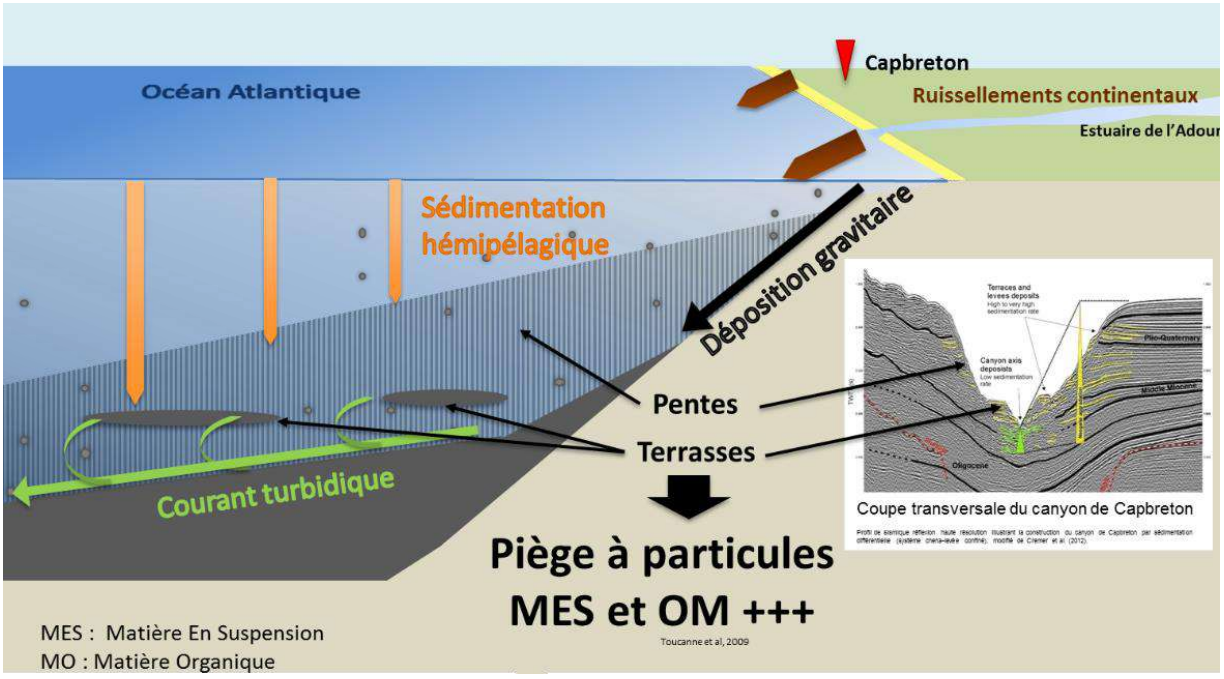

Figure 18 – Schéma représentant les principaux processus de la dynamique sédimentaire du canyon de Capbreton. A droite, une coupe transversale du canyon de Capbreton représentation le profil sismique haute résolution illustrant la construction de canyon de Capbreton par sédimentation différentielle [102]

Le canyon de Capbreton est dit « actif » en ce qui concerne sa dynamique sédimentaire. Cela signifie que les courants et les apports de matériel sédimentaire contribuent à l'accumulation de sédiments le long du canyon jusqu'à la plaine abyssale.

Les apports de matériel particulaire proviennent essensiellement des rivières, de la dérive littorale et de la sédimentation hémipélagique (provenant de la colonne d'eau par la sédimentation du plancton) [103,104]. Les courants turbidiques contribuent notamment au transfert de ce matériel vers l'aval du canyon [105]. Ce qui se traduit par le stockage de sédiments dans des zones d'accumulation telles que les terrasses [102]. Des taux de sédimentation ont été enregistrés jusqu'à 30 mètres par 1000 ans sur ces terrasses [106] (Fig. 18). Par conséquent, le canyon de Capbreton est considéré comme piège à matériel particulaire.

5.3 Des écosystèmes essentiels pour la biodiversité

L'apport de ce matériel particulaire (organique et inorganique) stimule la productivité primaire locale. L'ensemble des micro-habitats qu'offre le canyon de Capbreton sont des zones de refuges, de reproduction et de nurseries pour de nombreuses espèces. Il est déjà communément admis que les marges continentales sont d'importants réservoirs de biodiversité marine et de productivité. Dans le contexte particulier des canyons sous marins, il a été déjà démontré leur importance en terme de richesse et d'abondance spécifiques [107–109]. Les pressions anthropiques (ex. pression de pêche, rejets de boues de dragage des ports, des rejets industriels)[110] rendent les canyons sous-marins vulnérables à préserver. En effet, d'après l'Organisation des Nations Unies pour l'Alimentation et l'Agriculture (F.A.O), ces canyons sont reconnus pour être des écosystèmes marins vulnérables (VME) [99].

OBJECTIFS

Problématiques - Pourquoi s'intéresser aux micropolluants dans le milieu océanique ?

L'océan joue un rôle primordial dans notre subsistance. Il constitue une source importante de nourriture, est un élément essentiel de la biosphère et produit la majorité du dioxygène de notre atmosphère. Pourtant, depuis des décennies, les activités humaines grandissant et s'amplifiant, des micropolluants y sont déversés continuellement ou épisodiquement, menant à une dégradation de l'environnement océanique.

Les océans et les mers recouvrent 70 % de la surface de la Terre, représentant 97% de l'eau sur Terre et génèrant jusqu'à 32 % de la production primaire nette à l'échelle globale [111]. De plus, 90 % du volume de la biosphère est marine et abrite 50 % de la production primaire et des cycles de nutriments [112]. L'usage et le rejet constant de micropolluants dans les milieux aquatiques dont l'océan est le récepteur final, constitue donc un enjeu environnemental prioritaire. A ce jour, le milieu marin reste encore sous étudié face à cette problématique des micropolluants. Les contraintes techniques pour l'échantillonnage dans les sédiments marins profonds, telles que les canyons sous-marins conduit à un manque de données en ce qui concerne l'étude des micropolluants dans de tels écosystèmes. Bien que de récents développements d'outils analytiques permettent l'analyse d'un large spectre de substances chimiques, notamment celles réglementées par l'Union Européenne [113] pour les eaux continentales et marines [114], dites prioritaires, de nombreuses substances émergentes sont sous étudiées (https://www.norman-network.net/). Des lacunes sont à noter sur leur identification, leur quantification et sur leur devenir dans le milieu marin. L'objectif de ce travail de thèse est donc d'étudier pour la première fois le devenir et la réactivité de ces micropolluants dans les sédiments du canyon de Capbreton.

Ce travail de recherche s'insère dans un programme pluridisciplinaire qui a pour objectif d'étudier l'état et l'évolution de la qualité du milieu littoral sud aquitain. Pour ce faire ce programme prend en compte comme zones d'études l'estuaire de l'Adour, la zone côtière ainsi que le canyon de Capbreton. Les objectifs sont de surveiller, évaluer et réduire la contamination chimique du milieu littoral par i/ l'identification des substances chimiques et leurs sources, ii/ l'évaluation du transfert et du devenir des micropolluants dans le milieu littoral, iii/ l'amélioration des connaissances sur leurs impacts sur l'environnement, iv/ le développement de nouveaux procédés de traitement pour réduire les rejets et leur transfert dans le milieu et v/ le développement d'éléments d'aide à la décision aux différents gestionnaires et acteurs de l'eau. C'est un projet qui implique un large consortium d'équipes de recherche travaillant sur la thématique commune des micropolluants. Les travaux de ce programme de recherche se sont donc focalisés sur 3 sites ateliers (l'estuaire de l'Adour, la

côte rocheuse et le canyon de Cabpreton) dont le canyon de Capbreton représente une station référence marine profonde.

La forte affinité des micropolluants pour la phase particulaire suggère que les micropolluants se dispersent et s'accumulent dans le compartiment sédimentaire. Or le Canyon de Capbreton est une zone de transfert du matériel particulaire du continent vers le milieu marin profond. Il constitue donc une zone atelier de fort intérêt pour étudier les sources, la réactivité et les impacts des micropolluants dans le compartiment sédimentaire.

Une première partie sera dédiée à l'étude des micropolluants, de leurs réactivités et de leurs sources alors qu'une seconde partie sera dédié à l'étude des processus de transformation de ces micropolluants, notamment ceux liés aux activités microbiennes.

Objectifs de la thèse

Dans ce contexte, les objectifs de mon travail de thèse étaient nombreux et peuvent être regroupés en différents items qui sont les suivants:

- **Identifier et quantifier les différents micropolluants, prioritaires et émergents**

Dans ce travail, les familles de micropolluants ciblées appartiennent aux substances dites prioritaires, habituellement étudiées en routine (i.e. les éléments traces tel que le mercure, les hydrocarbures aromatiques polycycliques ou les polychlorobiphényles) et aux substances dites émergentes provenant essentiellement de sources domestiques (i.e. muscs de synthèse, écrans anti UV, composés pharmaceutiques). Dans le cadre de la Directive Cadre Stratégie pour le Milieu Marin, dont l'objectif est d'atteindre un bon état écologique et chimique, ce travail pourra également proposer le suivi plus détaillé de certaines substances émergentes pertinentes. Ce travail sera présenté dans le **Chapitre 1A** qui présente à la fois les familles identifiées, leurs concentrations ainsi que leur risque écotoxicologique selon les normes existantes.

- **Evaluer la réactivité des micropolluants dans le compartiment sédimentaire**

Une fois émis dans l'environnement, les micropolluants peuvent se transformer par des mécanismes naturels (biotiques et/ou abiotiques). Etudier les cinétiques de dégradation et/ou de transformation permettent donc d'obtenir des renseignements sur la persistance des substances et sur leur résilience naturelle dans le milieu. Deux points sont développés pour répondre à cet objectif. Un premier concerne les potentiels de dégradation de certains micropolluants émergents (muscs de synthèse, écrans anti UV et pharmaceutiques) au travers d'incubation de sédiments prélevés dans le canyon de Capbreton en condition

contrôlées au laboratoire (**Chapitre 2.A**). Un second concerne les processus de transformation du mercure inorganique en mercure organique (i.e. méthylation et déméthylation) avec l'utilisation de traceurs isotopiques du mercure au travers d'incubations de sédiments prélevés dans le canyon de Capbreton en condition contrôlées au laboratoire (**Chapitre 1B**).

- **Evaluer les sources et le transport de ces micropolluants**

L'hydrodynamisme au sein du canyon de Capbreton facilite le transfert et la remobilisation de particules des zones côtières vers la plaine abyssale. Cela amène à se demander si les micropolluants sont aussi transportés des points de sources continentales vers des zones éloignées de la côte. L'affinité des micropolluants organiques et des éléments traces avec ces particules conduit à se demander si les sources de micropolluants sont systématiquement d'origine continentale. Plusieurs approches seront mises en œuvre pour répondre à cet objectif. Les isotopes stables du carbone et du mercure permettent de suivre les sources et les transformations du C et du Hg, respectivement. Or le devenir du mercure est intimement lié à l'origine et l'état de la matière organique. Par conséquent, il est intéressant de les étudier ensemble en tant qu'outils de compréhension des sources et de transport du mercure dans les sédiments du Canyon de Capbreton. Ce point sera développé en partie dans les parties **1B et 1C du Chapitre 1**. Ensuite, l'étude de l'occurrence des micropolluants émergents (utilisés comme traceurs des activités humaines domestiques) dans les sédiments du canyon de Capbreton pourra aussi renseigner sur la capacité du canyon à transférer ces micropolluants vers le milieu marin profond **(Chapitre 1A**).

- **Mettre en relation la biodiversité bactérienne et son rôle vis-à-vis de ces micropolluants**

La biotransformation microbienne des micropolluants est un processus déterminant dans leur devenir dans l'environnement. Avec les processus abiotiques (i.e. photolyse, hydrolyse, réactions d'oxydo-réduction), elle contribue à la dégradation des micropolluants organiques (i.e. minéralisation) ou à leur transformation. Dans ce contexte, des souches bactériennes ont été isolées à partir d'échantillons de sédiments provenant du canyon de Capbreton en présence de micropolluants émergents. Leur potentiel de dégradation a été aussi étudié pour la première fois. Cela constituera une première étape pour permettre la compréhension des transformations microbiennes et leur implication dans la résilience du milieu naturel. Ce point sera développé dans le **Chapitre 2A**. Contrairement à la minéralisation de la matière organique, des processus de transformation microbienne sont aussi à l'origine de la méthylation et de la déméthylation du mercure. Ces processus sont simultanés et peuvent conduire à la formation nette de méthylmercure, un neurotoxique

bioaccumulable dans la chaîne alimentaire. Un gène impliqué dans la méthylation (*hgcA*) a été étudié pour la première fois dans des sédiments marins, ceci dans le but d'identifier les procaryotes portant *hgcA*, et donc impliqués dans la méthylation du mercure. Ce point sera développé dans le **Chapitre 2B**.

Des approches pluridisciplinaires et des outils innovants pour l'étude des micropolluants

Dans ce travail, plusieurs approches seront mises en œuvre afin de répondre aux objectifs décrits précédemment. Une combinaison d'outils innovants de chimie analytique, de microbiologie et de biologie moléculaire seront utilisés pour mener à bien ce travail. Ces outils sont regroupés dans la table 19 en fonction des objectifs posés et du type d'outils. Ils seront décrits dans les différentes parties de ce manuscrit où les méthodes y seront également développées (Table 19).

Objectifs	Identifier et quantifier les différents micropolluants prioritaires et émergents	Evaluer la réactivité des micropolluants dans le compartiment sédimentaire	Evaluer les sources et le transport de ces micropolluants	Mettre en relation la biodiversité bactérienne et la présence de ces micropolluants
Outils de chimie analytique	ICP-MS *(métaux traces)* GC-MS *(HAPs,PCBs, OCPs, écrans UV, muscs)* LC-MS/MS *(composés pharmaceutiques)* ID-ICP-MS *(espèces mercurielles)* Analyseur de Hg total *(HgT)*	GC-MS *(écran UV, muscs, carbamazépine)* double spikes ID-ICP-MS *(espèces mercurielles)* Granulométrie Spectrometrie infraroure *(TS, TC, OC)* TOC-LCSH/CSN/SSM-5000A *(POC)* Analyseur élémentaire couplé IRMS *(C et N isotopes)*	Analyseur élémentaire couplé IRMS *(isotopes N et C)* cold-vapor-MC-ICP-MS *(Isotopes du Hg)* GC-MS	GC-MS *(écran UV, muscs, carbamazépine)*
Outils de biologie moléculaire	-	-	-	16 rRNA gene (séquençage MiSeq et Sanger) *hgcA* gene (clonage et séquençage Sanger)
Outils de microbiologie	-	Incubation de sédiments en présence : -de micropolluants émergents *(potentiel de dégradation)* -de traceurs isotopiques du Hg *(potentiel de méthylation et déméthylation)*	-	Isolement de souches dégradant les micropolluants émergents Evaluation des potentiels de dégradation de ces souches
Correspondance avec les parties du manuscrit	Chapitre 1A	Chapitre 1B Chapitre 2A	Chapitre 1A Chapitre 1B Chapitre 1C	Chapitre 2A Chapitre 2B

Figure 19 – Outils utilisés pour répondre aux différents objectifs de ce travail. Les paramètres analysés sont écrits en italique.

CHAPITRE 1

ETAT DES LIEUX DES NIVEAUX DE MICROPOLLUANTS

SOURCES

REACTIVITE

CHAPITRE 1 – ETAT DES LIEUX DES NIVEAUX DE MICROPOLLUANTS – SOURCES - REACTIVITE –- DANS LES SEDIMENTS DU CANYON DE CAPBRETON

Le Canyon de Capbreton est une entaille dans le plateau continental qui débute à 250 mètres de la côte avant de finir dans la plaine abyssale à 3500 mètres. Sa proximité avec la côte et son fort hydrodynamisme contribuent au transfert de matériel particulaire de continent vers le large. Il est également admis que les micropolluants ont une forte affinité pour le cette phase particulaire. Des études ont déjà démontré que les canyons peuvent faciliter l'apport et l'export de substances inorganiques et organiques vers les fonds marins. Or depuis l'ère pré-industriel, il est reconnu que l'utilisation de ces substances sont en constante augmentation et ne cessent d'être rejetées dans les milieux aquatiques, dont le récepteur final est l'océan.

Les données relatives à l'identification et la quantification de micropolluants dans les sédiments du Canyon de Capbreton sont sporadiques, incomplètes et ne concernent que certaines substances prioritaires (éléments traces, PCBs, HAPs).

L'objectif de ce chapitre est de répondre aux problématiques suivantes :

- Identifier les différents micropolluants prioritaires et émergents
- Déterminer les niveaux de concentration de ces différents micropolluants
- Evaluer le risque écotoxicologique sur les organismes benthiques
- Evaluer la réactivité de ces micropolluants dans le compartiment sédimentaire
- Identifier les sources des micropolluants.

Une première partie 1.A « Priority and emerging micropollutants distribution from coastal to seaward sediments: a case study of Capbreton Submarine Canyon (North Atlantic Ocean) » a pour objectif de dresser, pour la première fois, un état des lieux de substances prioritaires et émergentes retrouvées dans les sédiments du Canyon de Capbreton et d'en déterminer leurs concentrations. De plus, afin d'estimer leur impact sur le milieu, une évaluation de risque écotoxicologique est effectuée sur la base de seuils de qualité environnementale disponibles. Un large spectre d'une centaine de substances prioritaire (HAPs, PCBs, OCPs, éléments traces) et émergentes (parfums de synthèse, écrans UV et composés pharmaceutiques) sont analysés par l'utilisation d'un panel d'outils analytiques et de méthodes innovantes (e.i. GC-ICP-MS, ICP-MS, GC-MS, LC-MS/MS).

Une deuxième et une troisième partie sont dédiées à l'étude du mercure, un micropolluant prioritaire, qui est un dangereux neurotoxique (e.i. sa forme organique, methylmercure) se bioaccumulant dans les poissons. Pour la première fois, la réactivité du

mercure (partie 1.B) et l'indentification de ses sources et des processus géochimiques (partie 1.C) sont étudiés dans les sédiments du Canyon de Capbreton.

La partie 1.B « Mercury and methylmercury concentrations, sources and distribution in submarine canyon sediments (Capbreton, SW France): Implications for the net methylmercury production » cible l'étude de la réactivité du mercure par l'intermédiaire de traceurs isotopiques du mercure en milieu contrôlé au laboratoire, à partir d'échantillons de sédiment frais. La dilution isotopique, une technique permettant l'étude simultanée de processus de méthylation et de déméthylation, a permis d'estimer leurs potentiels de transformation et indirectement d'estimer la production nette de méthylmercure de cet écosystème marin particulier.

La partie 1.C « Stable isotopes of Carbon and Mercury as tracers of particulate inputs in submarine canyon sediments of Capbreton (North Atlantic Ocean) » est complémentaire à la précédente. Le mercure en milieu marin est connu pour être prinicipalement d'origine atmosphérique. Or, depuis l'ère pré-inidistruelle, il a été observé une forte augmentation du mecure dans l'environnement, essentiellement d'origine anthropique. L'objectif est donc d'identifier les sources et de caractériser les processus géochimiques du mercure dans les sédiments du Canyon de Capbreton par l'étude de la composition isotopique du mercure total tout en croisant ces résultats avec la composition isotopique du carbone (e.i. également utilisé comme un traceur de sources).

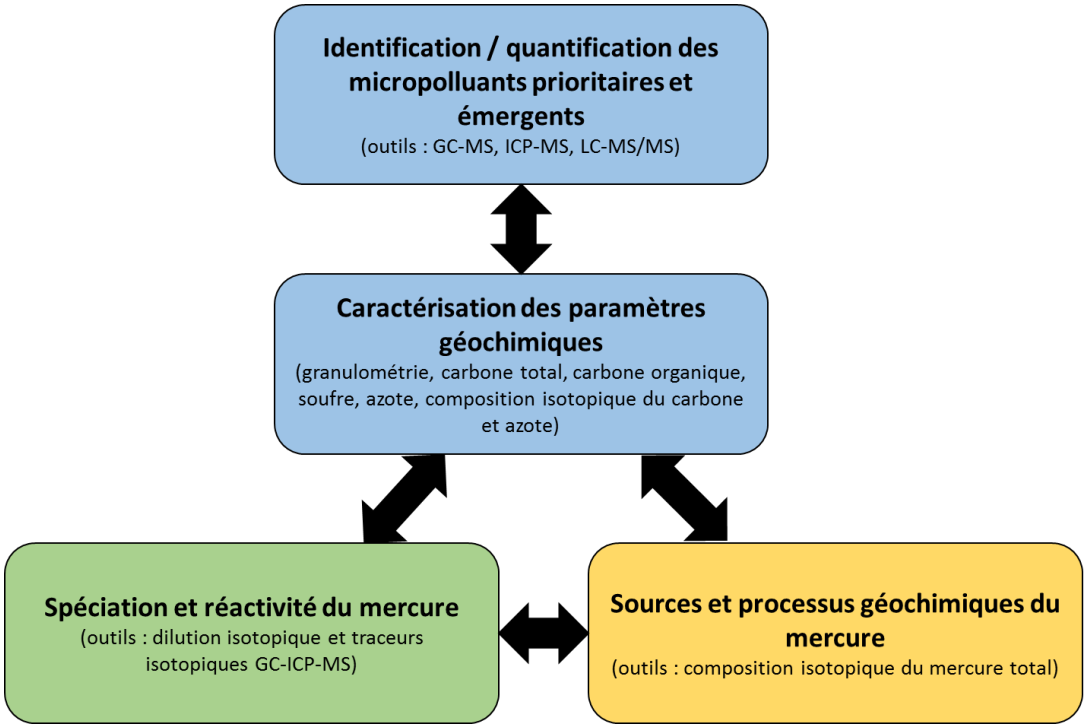

Valorisation de ce chapitre :

Publications :

- "Priority and emerging micropollutants distribution from coastal to continental slope sediments: A case study of Capbreton Submarine Canyon (North Atlantic Ocean), Alyssa Azaroff, Carole Miossec, Laurent Lanceleur, Rémy Guyoneaud, Mathilde Monperrus"– 2020 - https://doi.org/10.1016/j.scitotenv.2019.135057
- "Mercury and methylmercury concentrations, sources and distribution in submarine canyon sediments (Capbreton, SW France): Implications for the net methylmercury production", Alyssa Azaroff, Emmanuel Tessier, Jonathan Deborde, Rémy Guyoneaud, Mathilde Monperrus, 2019, https://doi.org/10.1016/j.scitotenv.2019.04.111
- "Mercury and carbon isotopes evidences for biogeochemical cycle of Hg in Capbreton submarine canyon sediments (Atlantic ocean)", Alyssa Azaroff, Emmanuel Tessier, Rémy Guyoneaud, Mathilde Monperrus (***in preparation***)

Présentations :

- "Priority and emerging micropollutants in Capbreton canyon sediments (SW France), Alyssa Azaroff, Carole Miossec, Laurent Lanceleur, Rémy Guyoneaud, Mathilde Monperrus" The 16th International Symposium on Oceanography of the Bay of Biscay (ISOBAY), June 2018, France, Anglet. (***Poster***)
- "Mercury species reactivity in deep sea sediments of the Capbreton Canyon (Biscay Bay, SW France)"; Alysss Azaroff, Emmanuel Tessier, Jonathan Deborde, Claire Gassie, Rémy Guyoneaud, Mathilde Monperrus, The 16th International Symposium on Oceanography of the Bay of Biscay (ISOBAY), June 2018, France, Anglet. (***Oral***)
- "Mercury and carbon isotopes evidence for biogeochemical cycle of Hg in Capbreton submarine canyon sediments (Atlantic Ocean, SW France)"; Alyssa Azaroff., Emmanuel Tessier, Rémy Guyoneaud, Jonathan Deborde, Mathilde Monperrus ; Krakow, Poland, The 14th International Conference on Mercury as a Global Pollutant (ICMGP), September 2019. (***Poster***)

1.A - PRIORITY AND EMERGING MICROPOLLUTANTS DISTRIBUTION FROM COASTAL TO CONTINENTAL SLOPE SEDIMENTS: A CASE STUDY OF CAPBRETON SUBMARINE CANYON (NORTH ATLANTIC OCEAN)

Alyssa Azaroff, Carole Miossec, Laurent Lanceleur, Rémy Guyoneaud, Mathilde Monperrus

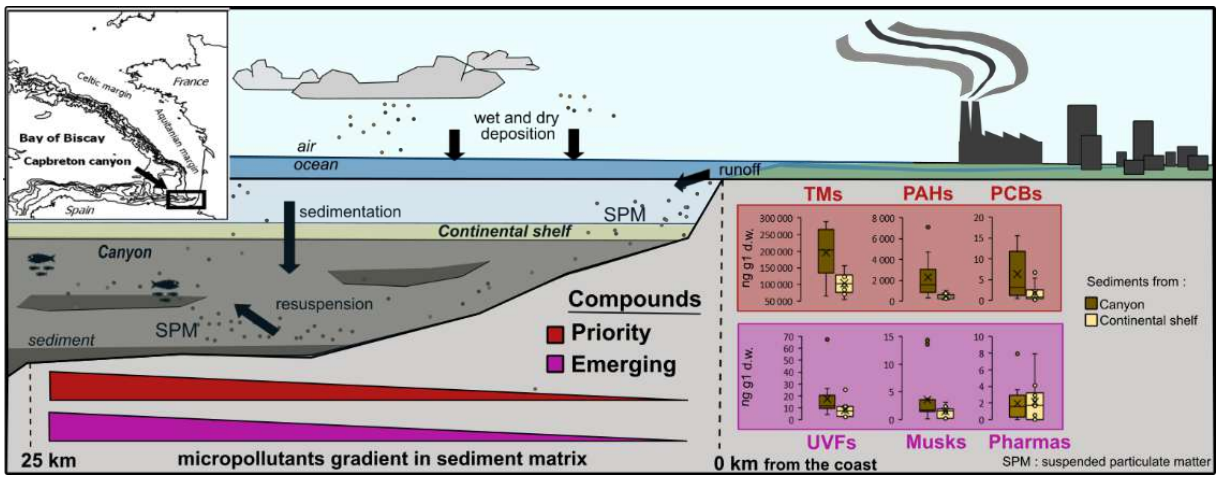

Published, Science of the Total Environment, 2020, https://doi.org/10.1016/j.scitotenv.2019.135057

Résumé

L'incision des marges continentales par des canyons sous-marins sont des questions essentielles pour comprendre les échanges de micropolluants entre les plates-formes et les fonds marins, impactant les écosystèmes marins et les cycles géochimiques mondiaux. La présence et la distribution de 100 micropolluants prioritaires et émergents ont été étudiées dans le compartiment sédimentaire des 25 premiers kilomètres du Canyon de Capbreton. Les substances prédominantes étaient les hydrocarbures aromatiques polycycliques (HAPs), les métaux traces et les métalloïdes (TMs) (e.g. mercure, plomb et arsenic), les muscs de synthèse (e.g. musc kétone, galaxolide), les écrans UV (e.g. EHMC et octocrylène), ainsi que certains composés pharmaceutiques (e.g. azithromycine, acétaminophène). De fortes concentrations ont été mesurées dans les sédiments du canyon situés au large, éloignés de la côte, et sont corrélés aux teneurs en carbone organique et en fraction fine, où les concentrations en HAP, EHMC et musc kétone atteignaient 7116, 32 et 7 ng g^{-1}, respectivement. Ces résultats démontrent probablement que les apports atmosphériques de HAPs d'origine pyrogénique, à la fois par le piégeage et le transport de particules polluées le long du continuum littoral / milieu profond via le Canyon de Capbreton, ce qui pourrait conduire à une accumulation de micropolluants anthropiques. L'évaluation des risques pour l'environnement indique également que les micropolluants prioritaires posent un risque potentiellement élevé pour les organismes benthiques (e.g. les HAPs, les MTs). Cela suggère une préoccupation particulière quant à la manière dont l'Homme peut influer sur cet écosystème marin.

Mots clefs: Polluants organiques persistants, polluants inorganiques, Directive Cadre Stratégie pour le Milieu Marin, sédiments de canyon sous-marin, évaluation du risque de toxicité

Abstract

Incising continental margins, submarine canyons are key issue for understanding shelf/ deep sea exchange of particulate pollutant, impact on marine ecosystem and global geochemical cycling. The occurrence and distribution of 100 priority and emerging micropollutants were investigated in sediments within the first 25 km of the Capbreton submarine area. The most predominant compounds were polycyclic aromatic hydrocarbons (PAHs), trace metals and metalloid (TMs) (e.g. mercury, lead and arsenic), synthetical musks (e.g. musk ketone, galaxolide), UV filters (e.g. EHMC and octocrylene) as well as some pharmaceuticals (e.g. azithromycin, acetaminophen). Highest concentrations were measured in submarine canyon sediments, distant from the coast and were correlated with both organic carbon and fine fraction contents, where PAHs, EHMC and musk ketone concentrations up to 7116, 32 and 7 ng g^{-1} dry weight, respectively. Those results likely demonstrate, that atmospheric inputs of pyrogenic PAHs, and both trapping and transporting of polluted particles along the continuum shore/deep sea by the Capbreton Canyon, might lead to an accumulation of anthropogenic micropollutants. The ecological risk assessment indicates that priority pollutants raise a potentially high risk for benthic organisms (e.g. PAHs, TMs).This might raised a specific concern about how the human can impact this ecosystem.

Keywords: Persistent organic pollutants, inorganic pollutants, marine strategy framework directive, seaward sediments, toxicity risk assessment

1 Introduction

The industrial revolution in the 1950s' led to a huge development of technology and engineering. Nowadays, more than 150 million organic and inorganic substances have been reported in the scientific literature and registered in CAS registry. Environmental monitoring appeared in Europe, U.S, Canada or more recently in China, to assess the potential effects of chemicals on health and environment. The European water policy focus on priority substances set by the Water Framework Directive (WFD, Directive 2013/39/EC 2013) and was implemented in the Marine Strategy Framework Directive, MSFD (Directive 2008/56/EC 2008) to achieve Good Environmental Status of EU's marine waters by 2020. Priority substances include for instance, traces metals (TMs), polycyclic aromatic hydrocarbons (PAHs), polychlorinated biphenyls (PCBs), and organochlorine pesticides (OCPs). Coastal and marine systems are the final receptors for pollutant emissions and the MSFD describes 8 monitored hazardous substances classes which are relevant for the marine environment such as pesticides, pharmaceuticals, resulting from diffuse sources, pollution by ships, atmospheric deposition, riverine input. In addition to the priority compounds, the European Chemical Agency has compiled a list of 2,700 new potential chemical contaminants for the human health and the environment (EC, Brussels, 13 February 2001). Their distribution and reactivity are still poorly studied, defining among those new contaminants, the "emerging contaminants" group [58] with a recent high concern to develop methods in order to assess them. Indeed, they are substances that have often long been present in the environment but whose presence and significance are only now being elucidated. (NORMAN project; http://www.norman-network.net). For instance, pharmaceuticals and personal care products (PPCPs) are emerging substances widely consumed and continuously introduced in the environment, mainly through treated and untreated wastewater discharges, could be considered as anthropogenic markers [115].

Marine sediments are an integrative matrix reflecting the pollution state in given area [116,117] where affinity of micropollutants with the suspended particulate matter (SPM) lead them to be readily scavenged from the water column and accumulated into sediments. The physicochemical properties of the sediment, such as organic carbon or grain size, control most of its interactions with the contaminants [118]. However, this matrix not only acts as a reservoir for contaminants, but also serves as a source of toxicants to marine fauna due to resuspension resulting from either natural (bioturbation and bio-irrigation, resuspension by storms, waves and tidal currents, diffusive fluxes, etc.) or anthropogenic (dredging, trawling) causes [119,120]. The knowledge on the distribution and fate of contaminants, both priority and emerging compounds, in marine sediments is still limited due to the huge number of

compounds release and the multi-inputs into the ocean. However, previous studies demonstrated that estuaries and coastal areas are the most impacted by regulated compounds [19,44,65]. However, both priority and emerging contaminants distribution from sediments of submarine canyons are poorly studied.

Marine pollution is usually studied in sediment compartment for monitoring environmental quality. Sediment-dwelling benthic organisms, as one of the primary source to support the existence of all higher trophic life forms, can be sensitive to toxicants. Environmental quality standards (EQS) are defined by different approaches, as a maximum concentration allowed. For example, ERL (Effect Range Low) and ERM (Effect Range Median) were defined for the biota and sediment (Environmental Protection Agency, US) as the concentration which has a biological effect on 10 or 50 percentile of organism, respectively [121]. From those thresholds, WFD and the MSFD defined predicted no effect concentration (PNEC) as the EQS used in the ecological risk assessment (ERA) where ambient concentration higher than PNEC might indicate that the compound is hazardous for the benthic organisms.

Capbreton Canyon is located nearby the coast, with strong urban and agricultural activities. Consequently, wastewater discharges from adjacent populations can be a source of priority and emerging substances in this area. Indeed, submarine canyon act as transfer zone of SPM between the continent and the open ocean, depending of gravity deposition, nepheloid flow, and hemipelagic inputs [106,122], accentuated with storms [123] may lead to an accumulation of pollutants [53,124] into this vulnerable ecosystem [107,125]. As expected, a previous study demonstrated that the sediments of this canyon accumulated both rich organic fine particles and mercury compounds along the canyon transect [126], constituting a potential ecological risk.

The aim of this study was to identify and quantify priority (TMs, PAHs, PCBs, OCPs) and emerging micropollutants (synthetic musks, UV filters and pharmaceutical compounds) in surface sediments along the Capbreton canyon and this adjacent continental shelf. The purpose was to provide for the first time, data about the distribution and occurrence of these 100 pollutants in Capbreton Canyon sediments, and provide for the first time a large screening of emerging micropollutants in submarine canyons sediments. Additionally, a risk assessment has been performed to estimate their potential hazard on the benthic sediment organisms, one of the primary sources into the food web

2 Material and methods

2.1 Study area and sampling strategy

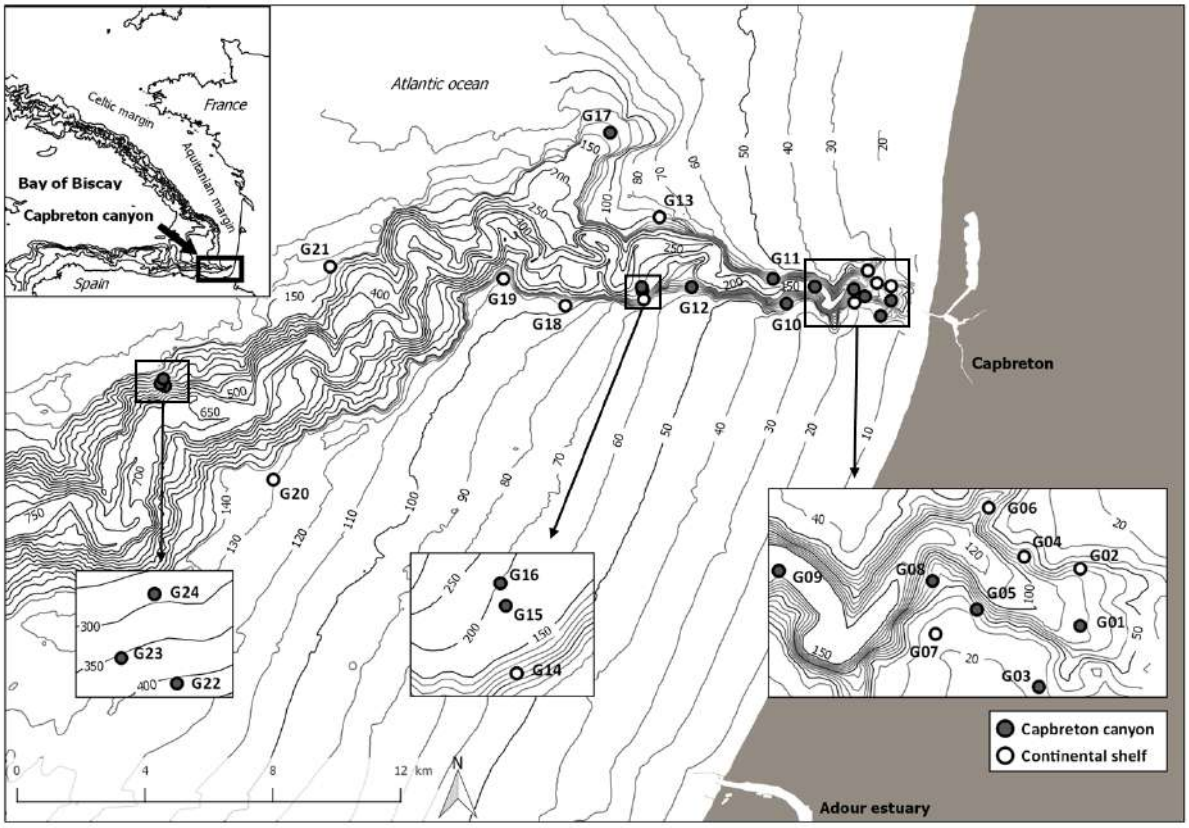

Figure 1 - Sediment sampling sites in the Capbreton Canyon (grey circles) and on the adjacent continental shelf (white circles) Isobath data from SEDIMAQ3 (Gillet 2012).

The Capbreton Canyon (South-Eastern Bay of Biscay, NE Atlantic) is one of the deepest in the world. It begins at 250 m from the coastline and located nearby the Adour Estuary. The Adour watershed, covering about 17,000 km^2, connects the occidental Pyrenean piedmont to the Atlantic Ocean. The upstream part of the estuary flows through agricultural areas, while the downstream part is within the urban district of Bayonne and is subject to industrial inputs [56]. The mean annual river discharge is about 300m^3 s^{-1} and reaches 2000m^3 s^{-1} during brief flood events [56]. Thus, it is a natural sedimentary transfer area between the continent and the abyssal plain. Micropollutants (i.e. priority and emerging) have strong affinity for the particulate matter (i.e. mineral and organic). Previous studies have shown high accumulation of sediments on the slopes and terraces of the Capbreton Canyon [103,106] and thus, likely constitute an accumulative area for micropollutants. Twenty-four surface sediments were sampled in the first 25 km of the Capbreton Canyon with a Hybrid Remotely Operated Vehicle (HROV Ariane, Ifremer) in order to sample surface sediments (0–10 cm) using cores and a Shipeck grab sampler (HAPOGE and ATLANTROV oceanographic cruises, in June and July 2017, respectively). Canyon sediments (n=14) were

sampled in terraces and in adjacent slopes, between 40 and 399 meters' depth and extending from 1.2 Km to 23.5 Km from the coast (Fig. 1). To compare, adjacent continental shelf sediments (n=10) were sampled between 40 and 136 meters' depth, at 1.4 Km of the coastline and extending to 19.1 Km from shore (Fig. 1). The station number increases with the distance from the coast (G1 o G24). Continental shelf sediments are considered as shallow sediments comparatively to the deep sediments sampled in the Capbreton Canyon, 200 meters below the surface water. After collection, sediment samples were homogenized, and placed into sterile polyethylene bags or cryotubes, sealed and stored in the dark at −20 °C until further analysis. Micropollutants and geochemical parameters were analysed in each sample.

2.2 Sample processing and geochemical parameters

All frozen samples were freeze-dried (Zirbus, Bad Grund, Germany) before further processing, except sediments for grain-size analysis, which were thawed at room temperature. Granulometry was analysed using a Malvern® Mastersizer 2000 laser diffractometer able to analyse between 0.02 and 2000 µm particle sizes. The percentages of the following three groups of grain sizes were determined: < 2 µm (clay), 2–63 µm (silt), and > 63 µm (sand) where fine fraction is inferior to 63 µm. Others subsamples were homogenized and ground with an agate pestle and mortar before each analytical and extraction procedures. Particulate organic carbon (POC) was measured after removal of carbonates with 1.2N HCl from 200 mg of powdered sample with Shimadzu® TOC-LCSH/CSN/SSM-5000A analyser. Analytical associated uncertainties were ≤ 0.05% for POC.

2.2.1 Extraction and analysis

Reagents, materials, internal standards (IS), analytical performances and abbreviations of compounds are summarized are summarized Table S1, Supporting information.

2.2.2 Trace metals

Briefly, 50 mg of freeze-dried sediment was pre-digested overnight with a mixture of nitric acid:hydrochloric acid (3:1) and then digested (4 hours at 85°C) using a DigiPREP Jr block digestion system (SCP science, Canada), before the addition of hydrogen peroxide solution. After centrifugation, the supernatant was then accordingly diluted with nitric acid 2% and spiked with the IS (bismuth) prior to the analysis, using inductively coupled plasma-mass spectrometry (ICP-MS, Agilent 7500, Agilent Technologies, Waldbronn, Germany). Instrument control, data acquisition and data treatment were performed using Agilent

Chemstation software. Recoveries achieved for all target elements in standard reference materials (SRM®1944), ranged from 86 to 113% (Table S1, Supporting information).

Total mercury (THg) concentrations were determined from the concentrations of mercury (Hg) species, inorganic (IHg) and methylmercury (MeHg), analysed in a previous work (Azaroff et al, 2019). We consider here, that the sum of species concentrations is equal to THg.

2.2.3 PAHs, PCBs, OCPs, musks and sunscreens

PAHs, PCBs, OCPs, musks and UV filters (UVFs) were extracted from sediments following a procedure based on a QuEChERS extraction and purification method, described by Miossec et al. [127]. Briefly, 2 g of freeze-dried sediment were spiked at 100 ng g^{-1} with an IS mixture (naphthalene-d8, acenaphthene-d10, perylene-d12, atrazine-d5 and MX-d15) before the extraction with 4 mL of ultrapure water and 10 mL of ethyl acetate:toluene (75:25; v:v) with homogenization by vortex for 1 min. Afterwards, the citrate buffer salt mixture was added to the tube, shaken by vortex for 1 min and centrifuged (5 min at 4,000 rpm). The supernatant was transferred in dispersive SPE tube, vortexed (1 min) before centrifugation (5 min at 4,000 rpm). Extracts were then dried to 1 mL under a gentle air stream, vortexed, transferred into vials and kept at −20°C until analysis.

Extracts were analysed by 7890A Gas Chromatograph coupled with 5975C Mass Spectrometer (GC/MS) with an Electron Ionization (EI) source using a Large Volume Injection (LVI) (Agilent Technologies). The GC/MS system was equipped with a single taper ultra-inert liner with glass wool and a HP-5MS UI capillary column (30 m length × 0.25 mm diameter and 0.25 µm film thickness). Carrier gas was helium (He) with a purity greater than 99.999% (Linde). Separation was performed at a constant He flow of 1.5 mL/min, and the GC oven temperature was programmed to hold at 50 °C for 3 min, then increase at 25 °C/min until 195 °C (hold 1.5 min), then 8 °C/min until 265 °C (hold 1 min) and 20 °C/min until 310 °C (hold 5 min). Injection volume was 20 µL in splitless mode. Instrument control, data acquisition and data treatment were performed using Agilent Chemstation software. Quantification was carried out in Selected Ion Monitoring (SIM) mode, selecting two characteristics fragments ions for each compounds. Recoveries achieved for all target compounds in a sediment spiked at 50 ng g^{-1}, ranged from 48 to 143% (Table S1, supporting information).

2.2.5 Pharmaceuticals

Pharmaceuticals were extracted from sediments following a procedure adapted from Siedlewicz et al. (2016). Briefly, 0.2 g of freeze-dried sediment was spiked with IS (atenolol-d7, carbamazepine-d10, ibuprofen-d3, nordiazepam-d5 and ofloxacin-d3) at concentrations of 400, 400, 10,000, 400, and 2,000 ng g^{-1}, respectively. After addition of 1 mL of MeOH, 1 mL of supersaturated NH_4Cl water solution and 0.2 mL of Na_2EDTA 0.1M, the tube was shaken by vortex for 1 min and sonicated for 20 min. After centrifugation (5 min at 4,500 rpm), the supernatant was diluted with water. The solid phase extraction was carried out with a SPE vacuum manifold. Oasis HLB (60 mg, 3 mL) cartridges were conditioned with both 3 mL of MeOH and ultrapure water. 50 mL of diluted sample were applied to the SPE cartridges. Prior rinse of SPE colum with 3 mL of water, elution performed with 5mL of MeOH, The eluate was collected, evaporated to dryness and re-dissolved in 1 mL water:MeOH (95:5; v:v). Finally, extracts were vortexed, transferred into vials and kept at -20°C until analysis.

Liquid Chromatographic analyses were carried out using an Acquity UPLC system connected to a Xevo TQ MS (Triple quadrupole) with an electrospray (ESI) interface (Waters). Chromatographic separation was performed using an Acquity UPLC HSS T3 column (1.8µm particle size, 50mm x 2.1mm i.d.) preceded by a guard column (1.8µm particle size, 5mm x 2.1mm i.d.), at a flow rate of 0.4 mL/min. Column was kept at 40°C and sample manager was maintained at 15°C. The analysis in positive ionization mode was performed using ultrapure water with 0.1% formic acid as eluent (A) and ACN as eluent (B). For the analysis in negative ionization mode, eluent (A) was ultrapure water with 0.01% formic acid. Sample injection volume was 5 µL.

Instrument control, data acquisition and data treatment were performed using MassLynx software (Waters). Quantification was carried out in Multiple Reaction Monitoring (MRM) mode, selecting two characteristics transitions for each compound (Miossec et al., 2019; submitted in Food Chemistry). Recoveries achieved in a sediment spiked at 200 ng g^{-1} were between 80 to 120% for 35 compounds out of 43 (Table S1, Supporting information).

2.3 Data analysis and risk assessment

Principal component analysis (PCA) was applied to assess compositional differences among sediment properties usually known to play a key role in micropollutants adsorption (POC and grain size inferior to 63 µm) as well as the distance to the coast gradient and the sum of target compounds concentrations (TMs, PAHs, PCBs, synthetic musks and UVFs) in

surface sediments samples. The Factoextra package [129] was used from FactoMineR package [130] import in R statistical language was used for the PCA.

An ERA was also performed for those target compounds which were detected in sediments and for which ecotoxicological data on benthic species were available. Briefly, according to EC, to estimate the toxicity of a substance, a risk quotient (RQ) is defined as the ratio of the exposure concentration to the effect concentration for a specific medium (e.g. sediment). A RQ for a substance should be calculated as :

$$RQ_i = C_i/PNEC_i$$

C_i : measured environmental concentration for the substance i and $PNEC_i$: predicted no effect concentration for the substance i. If PNEC values were not available in literature, they were calculated by applying an Assessment Factor (AF) (calculation in table S5, Supporting information) where this factor was 1000 for an acute toxicity data (e.g., EC50 or ERM) and 100 for a chronic toxicity data (e.g., no observed effect concentration, NOEC) according to EC [131].

To estimate the toxicity of a mixture, the RQ for all substances in the group of substances are summed:

$$\sum RQ_{mixture} = \sum RQ_i$$

RQ_i and $\sum RQ_{mixture}$ values were then used for risk assessment following the criterion recommended by Dudhara et al.[25]: $RQ_i = 0$: no significant risk; $RQ_i \geq 1$: moderate risk and $\sum RQ_{mixture} = 0$: free risk; $1 \leq \sum RQ_{mixture} < 800$ and $\sum RQ_{mixture} > 800$: moderate to high risk.

3 Results and discussion

3.1 Concentrations and spatial distribution of micropollutants

The OCPs and 39 pharmaceutical compounds that not have been quantified in this study are listed in Table S2 in Supporting information.

3.1.1 Priority contaminants

3.1.1.1 TMs

The average of ∑TMs concentrations, including one metalloid (arsenic), were 2 times higher in Canyon sediments than in continental shelf sediments where TMs were up to 287 960 and 155 819 ng g^{-1}, respectively (Table 1). Furthermore, TMs concentrations increased onto the canyon sediments from the coast to the offshore, where priority metals such as

Cadmium, lead and mercury, were 4, 8 or 30 times higher in the offshore station (G24) than in the closest coastal location G01 (Fig. 2, A), respectively. This enrichment of TMs is in accordance with the deposition of TMs observed in the Foix submarine Canyon in the Mediterranean sea and Portuguese submarine Canyons in the Atlantic Ocean [53,132]. MTs concentrations in canyon sediments are mainly higher than MTs levels observed in West Gironde Mud Patch located at the north of the Capbreton Canyon [133] and the metal background level determined in the coast of the Basque country, nearby the Capbreton canyon [57]. To compare with ŦthisŦ regional mean background levels (estimated in the <63 µm fraction, which were at 12,000; 240; 33,000; 26,000; 130; 29,000 and 31,000 ng g^{-1} d.w. for arsenic, cadmium, copper, chromium, mercury, nickel and lead, respectively) [57], only sediments with more than 90% of fine fraction were selected (G11, G15, G16, G17, G22, G23 and G24, see Table S3, Supporting information). Although levels of Cd, Cu and Ni are similar to their background concentrations, As, Cr, Hg and Pb are 2.5, 1.9, 4.4 and 2.8 times more elevated than the regional background. In the offshore sediment (G24), enrichment factors were up to 4 and 7 for Pb and Hg, respectively. This likely indicate an abnormal accumulation of TMs, such as Hg and Pb, in the Capbreton canyon sediments due to the transport of particles along the canyon axis, as reported in Portuguese submarine canyons [53]. Furthermore, Hg is an ubiquitous pollutant (i.e. atmosphere, water and particulate compartments) and could also arise from the pelagic sedimentation and favour this accumulation in these sediments.

Table 1 Minimum, maximum and mean concentrations (ng g-1, dry weight) with standard deviation (SD), and detection frequency (% Det) of every class of compounds, in surface sediments from the two sampling areas: Canyon and Continental shelf (n=14 and 10, respectively). <LOQ means the concentration of the compound was inferior to the limit of quantification (Table S1, Supporting information). Mean concentrations were calculated with <LOQ = 0.

	Canyon (n= 14)					**Continental shelf (n=10)**				
Compounds	**Min**	**Max**	**Mean**	**SD**	**% Det.**	**Min**	**Max**	**Mean**	**SD**	**% Det.**
Arsenic	12172	36852	25009	7040	100	9335	30889	18089	7137	100
Cadmium	71	302	217	67	100	47	133	87	32	100
Cobalt	5136	15491	10966	2565	100	4620	11340	8011	2132	100
Chromium	14794	57393	39410	12270	100	12465	32636	22126	6148	100
Copper	7158	42388	27567	11408	100	5219	15468	10178	3590	100
Mercury	31	975	345	318	100	18	264	102	71	100
Nickel	11286	43691	29260	8624	100	9344	23311	15404	5122	100
Lead	14045	122474	62551	32052	100	11022	55104	29392	13481	100
∑Trace Metals	**64693**	**287960**	**195326**	**71532**		**54703**	**155819**	**103390**	**31567**	
Naphtalene	1.1	77.8	22.7	26.9	100	<LOQ	9.9	4.1	2.9	90
Acenaphtylene	1.0	59.7	17.9	18.8	100	<LOQ	6.5	1.7	2.1	80
Acenaphthene	<LOQ	49.4	10.6	14.7	71	<LOQ	3.5	0.4	1.1	20
Fluorene	1.9	68.2	19.4	19.0	100	0.5	8.0	3.4	2.5	100
Phenanthrene	13.9	299.8	110.3	76.4	100	4.3	56.8	22.0	15.2	100
Anthracene	4.7	132.3	50.7	39.9	100	3.5	21.7	8.7	5.9	100
Fluoranthene	25.2	503.9	196.9	128.3	100	16	122	40.2	30.8	100
Pyrene	23.5	390.5	168.5	100.0	100	14.3	95.7	35.1	23.5	100
Chrysene	13.1	269.1	104.3	70.2	100	8.0	52.7	22.5	13.3	100
Benzo[*a*]anthracene	16.1	281.8	116.0	76.8	100	8.4	54.7	25.0	13.9	100

Benzo[*b*]fluoranthene	37.3	1192.3	319.6	330.3	100	24.9	115.5	63.2	31.8	100
Benzo[*k*]fluoranthene	33.5	945.1	268.4	254.2	100	27.6	106.7	55.9	29.9	100
Benzo[*a*]pyrene	31.8	1046.4	297.3	280.2	100	21.9	119.6	54.9	33.3	100
Indeno[*1.2.3.cd*]pyrene	36.1	871.4	265.8	246.6	100	25.7	106	53.6	27.1	100
Dibenzo[*a.h*]anthracene	11.1	219.8	65.8	60.2	100	8.1	26.2	14.9	6.0	100
Benzo[*g.h.i*]perylene	30.4	708.5	227.5	194.7	100	18.3	93	43.2	24.2	100
∑PAHs	**280.5**	**7116.1**	**2261.6**	**1889.8**		**198.8**	**993.9**	**448.8**	**252.6**	
PCB 18	<LOQ	<LOQ	<LOQ	-	0	<LOQ	<LOQ	<LOQ	-	0
PCB 28+31	<LOQ	<LOQ	<LOQ	-	0	<LOQ	<LOQ	<LOQ	-	0
PCB 52	<LOQ	2.9	0.2	0.8	7	<LOQ	<LOQ	<LOQ	-	0
PCB 44	<LOQ	1.6	0.2	0.6	14	<LOQ	<LOQ	<LOQ	-	0
PCB 101	<LOQ	2.0	0.6	0.8	37	<LOQ	<LOQ	<LOQ	-	0
PCB 118	0.1	0.8	0.4	0.3	100	<LOQ	0.2	0.1	0.1	90
PCB 138	0.1	2.9	1.1	0.9	100	<LOQ	0.8	0.3	0.3	90
PCB 149	0.1	2.1	0.8	0.6	100	<LOQ	0.8	0.2	0.2	100
PCB 153	0.1	2.8	1.1	0.9	100	<LOQ	1.0	0.3	0.3	90
PCB 180	0.1	1.8	0.6	0.6	100	<LOQ	1.0	0.2	0.3	100
PCB 194	<LOQ	3.3	1.4	1.6	43	<LOQ	3.1	0.6	1.3	20
∑PCBs	**0.5**	**15.5**	**6.4**	**5.7**		0.1	6.7	1.8	2.3	
ADBI	<LOQ	<LOQ	<LOQ	-	0	<LOQ	<LOQ	<LOQ	-	0
AHMI	<LOQ	<LOQ	<LOQ	-	0	<LOQ	<LOQ	<LOQ	-	0
MA	<LOQ	<LOQ	<LOQ	-	0	<LOQ	<LOQ	<LOQ	-	0
ATII	<LOQ	<LOQ	<LOQ	-	0	<LOQ	<LOQ	<LOQ	-	0
HHCB	<LOQ	3.6	0.6	1.3	29	<LOQ	<LOQ	<LOQ	-	0
AHTN	<LOQ	1.7	0.4	0.6	86	<LOQ	0.2	0.1	0.1	100
MX	<LOQ	2.2	0.3	0.6	57	<LOQ	0.8	<LOQ	-	10
MM	<LOQ	0.2	0.1	0.1	79	<LOQ	0.1	<LOQ	-	80
MK	<LOQ	7.0	2.2	2.1	86	<LOQ	2.9	1.2	0.9	70
∑Musks	**0.1**	**14.3**	**3.5**	**4.5**		**0.1**	**3.1**	**1.4**	**0.9**	
3-BC	0.7	6.2	3.0	1.7	100	0.5	4.0	2.0	1.2	100
Benzophenone 3	0.4	1.9	1.3	0.4	100	0.3	1.6	0.8	0.4	100
4-MBC	<LOQ	7.7	4.2	2.8	86	0.2	5.3	2.0	1.9	100
OD-PABA	<LOQ	0.8	-	-	7	<LOQ	<LOQ	<LOQ	-	0
EHMC	<LOQ	31.8	4.8	8.7	71	<LOQ	6.5	1.1	2.0	50
OC	<LOQ	29.2	3.6	7.5	93	<LOQ	12.7	1.6	4.0	30
∑UV filters	**4.3**	**67.4**	**17.1**	**15.6**		**1.9**	**25.1**	**7.6**	**7.2**	
Azithromycin	<LOQ	7.9	1.3	2.2	50	<LOQ	2.9	0.9	1.2	50
Clarithromycine	<LOQ	<LOQ	<LOQ	-	0	<LOQ	2.4	-	-	10
Antibiotics	**-**	**-**	**-**	**-**		**-**	**-**	**-**	**-**	
Acetaminophen	<LOQ	3.0	0.6	0.9	57	<LOQ	7.9	1.0	2.5	30
Analgesics and NSAIDs	**-**	**-**	**-**	**-**		**-**	**-**	**-**	**-**	
Amiodarone	<LOQ	0.6	-	-	7	<LOQ	<LOQ	<LOQ	-	0
Various pharmaceuticals	**-**	**-**	**-**	**-**		**-**	**-**	**-**	**-**	

3.1.1.2 PAHs

Like TMs, the average and the highest concentrations of ∑16PAHs (selected by the US EPA) were 4 and 7 times higher in canyon sediments than in continental shelf sediments, where maximum concentrations up to 7116 and 994 ng g^{-1}, respectively (Table 1). These relatively high concentrations of ∑16PAHs increased onto the canyon sediments from the coast to the offshore, with an enrichment factor at 25 between the offshore station (G24) and the closest coastal location G01 (Fig. 2, B). No trend was observed in continental shelf sediments, highlighting an accumulation along the canyon transect. PAHs are characterized by low vapour pressure and low aqueous solubility. More number of rings increase, more

these characteristics decrease and increase the persistence of PAHs. The 2-3 rings PAHs (Naphtalene to Anthracene in the Table 1) were detected in lower concentrations than 4-6 rings PAHs (Fluoranthene to benzo(g,h,i)perylene in the Table 1). High concentrations ~~of~~ observed within high molecular weight PAHs are similar to the results observed in polluted sediments [15]. Indeed, these PAHs are known to indicate a pyrogenic source, suggesting the PAHs found in those studied sediments are from humans activities such as heavy transportation, incineration, and scrapping activities [25]. Moreover, similar accumulation factors between the G01 and G24 are observed for the low and high weight PAHs (30 and 25, respectively) where concentrations are significantly strongly correlated (Pearson correlation, R^2 = 0.98, p-value <0.0001, n=24) might suggest a common origin of PAHs in this canyon sediments. To determinate the sources of PAHs in environmental samples, the ratios of PAHs isomers having same molecular mass and physico-chemical properties such as Ant/Phe, Flt/Pyr, Ant/Ant + Phe, have been used as distinct chemical tracers. The ratio of Ant/Phe, Flt/Pyr, Ant/Ant + Phe are superior to 0.1, 1 and 0.1, respectively, confirming the PAHs are pyrogenic source, i.e. combustion processes, in all surface sediments sampled in this study [134,135]. Consequently, the PAHs contamination in the Capbreton canyon sediments might come from atmospheric fallout deposition (terrestrial and/or aquatic), then can be absorbed in SPM, themselves accumulating in the bottom sediment by deposition and remobilization processes along the canyon axis. Moreover, the significatively strong correlation with Hg concentrations (Pearson correlation, R^2= 0.85, p-value <0.0001, n=24) and a similar enrichment factor observed in 2.1.1.1., might suggest the same geochemical processes were applied for both Hg and PAHs.

The PAHs concentrations in the Capbreton Canyon sediments were higher than those of other Northern Atlantic Ocean locations, up to 20 and 35 times higher than Cadiz Bay (242.7 ng g^{-1}) and Huelva Estuary (197.2 ng g^{-1}) levels, respectively [13]. Nevertheless, PAHs concentrations are very low compared to Santander Bay located in the North Spain where PAHs reached 344 600 ng g^{-1} [15] and individual PAHs measured in the continental shelf are similar to thus previously measured in the same area [136]. The same author measured high PAHs concentrations in the Hossegor Lake, which is a laguna in front of the mouth of the Capbreton Canyon. Consequently, we may hypothesis that each low tide brings fine sediment loaded in PAHs from this lake into the canyon, and may contribute to increase the PAHs concentrations in the canyon sediments. Moreover, settling sediments from the column water can also increase the PAHs levels in surface sediments. Indeed, Salvadó et al. (2017) have demonstrated high levels of PAHs in settling sediments (until 2700 ng g^{-1}) collected in the Cap de Creus and Lacaze-Duthiers submarine Canyons (Mediterranean sea, France).

3.1.1.3 PCBs

Like TMs and PAHs, PCBs concentrations in canyon sediments are higher than the concentrations observed in the continental shelf, where means were 6.4 and 1.8 ng g^{-1}, respectively (Table 1). PCBs with smaller molecular weight (e.g. PCB 18, 28, 31) were not detected in both areas (Table 1) in accordance with Gouriou et al. (2018) in canyon location (Doigt mordu), likely due to of their degradation by a microbial reductive dechlorination process [138]. Like TMs and PAHs, Fig.2 C shows an increase of PCB 118, 138, 149, 153, 180, 194 congener concentrations along canyon axis gradient, with an enrichment factor between 10 and 25, indicating persistence of high molecular weight PCBs. Concentrations observed in the adjacent continental shelf are in accordance with the concentrations measured in coastal sediments in the North Atlantic Ocean [44,139,140]. Although these PCBs are banned since 30 years ago [141], higher concentrations were observed in the offshore locations and reinforce that there is an enrichment of priority substances in this submarine canyon sediments.

3.1.2 Emerging micropollutants

3.1.2.1 Musks

HHCB, AHTN, MX, MM and MK were detected in these sediment samples where ∑musks mean concentration in Canyon sediments is relatively higher than the mean in continental shelf sediment, where means are at 3.5 and 1.4 ng g^{-1}, respectively (Table 1). In general term, Fig.2 D shows that transport and distribution patterns are not similar than these previously discussed for priority compounds, where the highest concentrations are still observed for G22 and G23 reaching up 14.3 ng. g^{-1} but do not increase along this canyon axis (Fig.2 D).

Musks detected in this canyon are mainly polycyclic musks (i.e. HHCB, ATHN and MM). Indeed nitro musks (MX and MK) were restricted in Europe since the 1990s' and replaced by polycyclic musks, where industrial usage of polycyclic musks (HHCB and AHTN) and nitro musks (MX and MK) were at 3285 and 298 tons, respectively [142]. Nevertheless, MK is detected around 1.5 ng. g^{-1} in all the sediments analysed and quantified 7 times more in G22 and G23 sediments, could explain those locations are a specific accumulative area of anthropogenic inputs.

Effluent from waste water treatment plants (WWTPs) is the predominant pathway through which PPCPs enter surface water [115] with high concentrations of synthetic musks (mg L^{-1} range). Cavalheiro et al. (2017) have shown HHCB, AHTN and MK were detected in Adour estuary water. This estuary is close to Capbreton canyon where the plume of SPM are

often transferred to the north [144], and may transport these MK, AHTN and HHCB in the canyon sediments.

Lack of data of musks concentrations in submarine canyon sediments does not allow comparison with these present data. Although the mean concentration levels are lower than Cadiz Bay [44], estuaries across the world [13,145] and Adriatic Sea [19], the detection of these anthropogenic compounds highlights that the Capbreton canyon is also an accumulative area for the emerging micropollutants.

3.1.2.2 UV filters

All UVFs analysed were detected at least once in sediments (Table 1), except OD-PABA. Indeed, OD-PABA in water can be fastly degraded by UV radiation [146] thus allowed a decontamination of SPM which are accumulated in the bottom sediments. UVFs mean concentration was 2 times higher in canyon sediments than in continental shelf sediments where sums of UVFs concentrations reach 67.4 and 25.1 ng g^{-1} in canyon and continental shelf sediments, respectively (Table 1). The four more represented UVFs were 3-BC, 4-MBC, EHMC and OC. Maximum concentrations were observed in the G22 station at 31.8 ng g^{-1} and 29.2 ng g^{-1} for EHMC and OC, respectively (Fig.2 E). The presence of these UVFs might be due to their strong sorption affinity and relatively high stability [146,147].

3-BC concentrations in Canyon sediments are in accordance with coastal and freshwater sediments located in Spain or Chile [44,148] and clearly lower than sediments located in China and Japan [71]. As 3-BC, EHMC concentrations are in accordance with coastal and freshwater sediments located in Spain and were lower than concentrations found in Columbia, China and Japan. Previous studies of OC occurrence in sediments have shown that their concentrations are often higher than the other UVFs concentrations, mainly around 100 ng g^{-1} and reaching 600 ng g^{-1} in freshwater and marine sediments [13,149]. In general term, UVFs in this submarine canyon are lower or in accordance with coastal and freshwater sediments analysed across the world, might indicating a dilution and degradation from the source, but still accumulated in sediments.

3.1.2.3 Pharmaceuticals

Regarding analysis of pharmaceuticals, 4 of the 43 compounds analysed were quantified. Azithromycin (antibiotic) and acetaminophen (analgesic) were detected in both canyon and continental shelf locations (Table 1).

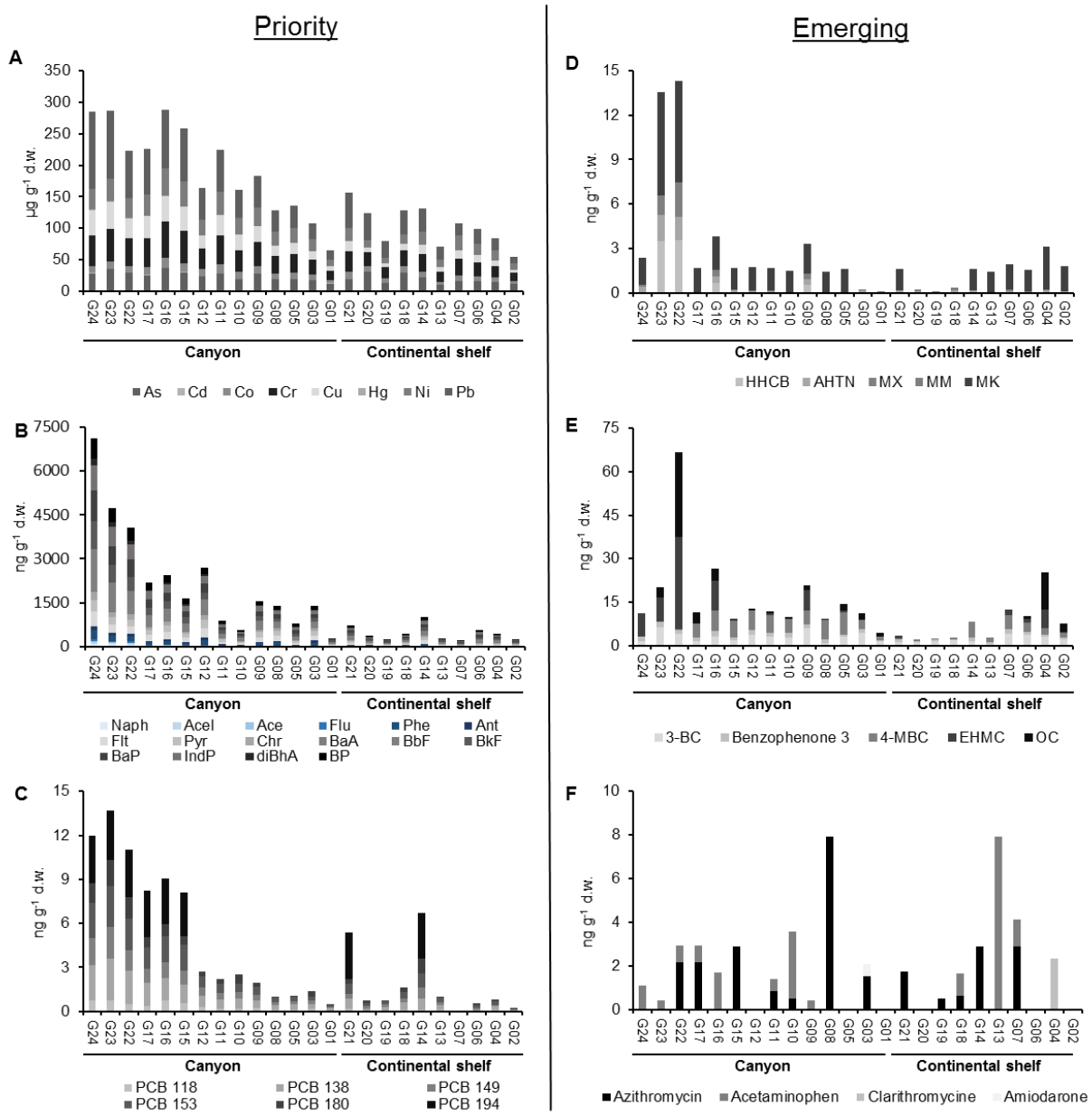

Figure 2 - Concentrations of priority pollutants (A, Trace Metals (TMs) ; B, Polycyclic Aromatic Hydrocarbons (PAHs) ; C, PolyChorinated Biphenyl (PCBs)) and emerging compounds (D, Musks; E, UV Filters; F, Pharmaceuticals) from Capbreton canyon and continental shelf sediments expressed per dry weight as a function of the distance from the coast. Abbreviation for PAHs are Naphtalene (Naph), Acenaphtylene (Acel), Acenaphthene (Ace), Fluorene (Flu), Phenanthrene (Phe), Anthracene (Ant), Fluoranthene (Flt), Pyrene(Pyr), Chrysene (Chr), Benzo[a]anthracene (BaA), Benzo[b]fluoranthene (BbF), Benzo[k]fluoranthene (BkF), Benzo[a]pyrene (BaP), Indeno[1,2,3,c,d]pyrene (IndP), Dibenzoa[h]anthracene (diBhA) and Benzo[g,h,i]perylene (BP)

Clarithromycin and amiodarone were quantified once in continental shelf and canyon sediments, respectively.

Pharmaceuticals are hydrophilic compounds and hence, they are less absorbed on the particulate matter. Moreover, pharmaceuticals are anthropogenic compounds, from

domestic or medical uses, that are released into aquatic environment by domestic wastewater, hospital discharges, improper manufacturer disposal, sewage treatment plants (STPs), and water treatment plants (WTPs) [115,150]. Acetaminophen is a common analgesic, used across the world. It has been detected in water at high concentration after STPs [115]. The Capbreton Canyon is located at 200 meters from the coast, and the presence of such pharmaceuticals might infer that STPs and WTPs wastewater loaded of PPCPs, impact the canyon sediments.

Contrary to the priority and previous emerging compounds (i.e. musks and UVFs), there is no trend of the concentrations of the two detected pharmaceutical compounds in those sediments (Fig. 2 F). Nevertheless, detection of these pharmaceuticals, as well musks and UVFs, demonstrated an anthropogenic source of this global contamination.

3.2 Geochemical parameters favour micropollutants enrichment in Submarine canyon

To a better visualization of the PCA, the first and the third dimensions of the PCA (Dim1 and Dim3, representing 77.6 % of the total inertia) where selected. Dim1 showed strong correlations with all micropollutants groups (Table S4, Supporting Information) illustrating both contaminants and particles gradients. Regarding the Dim3, correlations for each variable, were lower than the Dim1 but higher contribution of emerging micropollutants, explained this axis indicated an emerging micropollutants gradient. POC and fine fraction are usually directly related to higher concentration of contaminants, as they provide a greater surface for sorption of pollutants, with a positive correlation for the TMs [57] and organic compounds such as PAHs [137,151,152], PCBs [153], pesticides [124] and emerging organic substances [66]. In this study, occurrence of priority and emerging pollutants is significantly positively correlated with their POC content and fine fraction (Fig.S1, Supporting information), confirming they are strongly associated to fine-grained sediments and thus, may explain the increasing of micropollutants concentrations (Fig.3, Table S3, Supplementary information). Furthermore, the greater contribution of G22, G23 and G24 samples on the Dim1 might indicate that priority and emerging pollutants are more accumulated into the submarine Canyon sediments, particularly in the offshore locations. Inputs of fine particles in this accumulative area could come from turbiditic currents, which transport fine sediments from the coast to the abyssal plain and come from the hemipelagic sedimentation of particles settling from the column water [103,105]. Moreover, organic pollutants and TMs have strong affinity with settling particles and may enhance the micropollutants accumulation in sediments [137,152]. Finally, nearshore sand is trapped in the head of the Capbreton Canyon [100]. This could explain the higher sand fraction in

coastal sediments as compared to ~~seaward~~ submarine canyon sediments (G15 to G24), and the enrichment of micropollutants observed along the canyon axis (Fig.2). Moreover, abiotic (i.e. photolysis and hydrolysis) and biotic [154] processes could explain a higher degradation within first kilometres of the canyon. For instance, high UVFs and musks concentrations in offshore locations seem to confirm, that anthropogenic organic compounds were well bind to particulate matter and transported during sediments transfer from the continent to the first 25 km of the canyon in sediments accumulative areas, like terraces and canyon slopes. Indeed, most of the UVFs are lipophilic substances with high log octanol/water partition coefficient (k_{ow}) in the range 4-8 as well as poor biodegradable, they also tend to accumulate in biota [155] like persistent organic pollutants in deep sea biota [156].

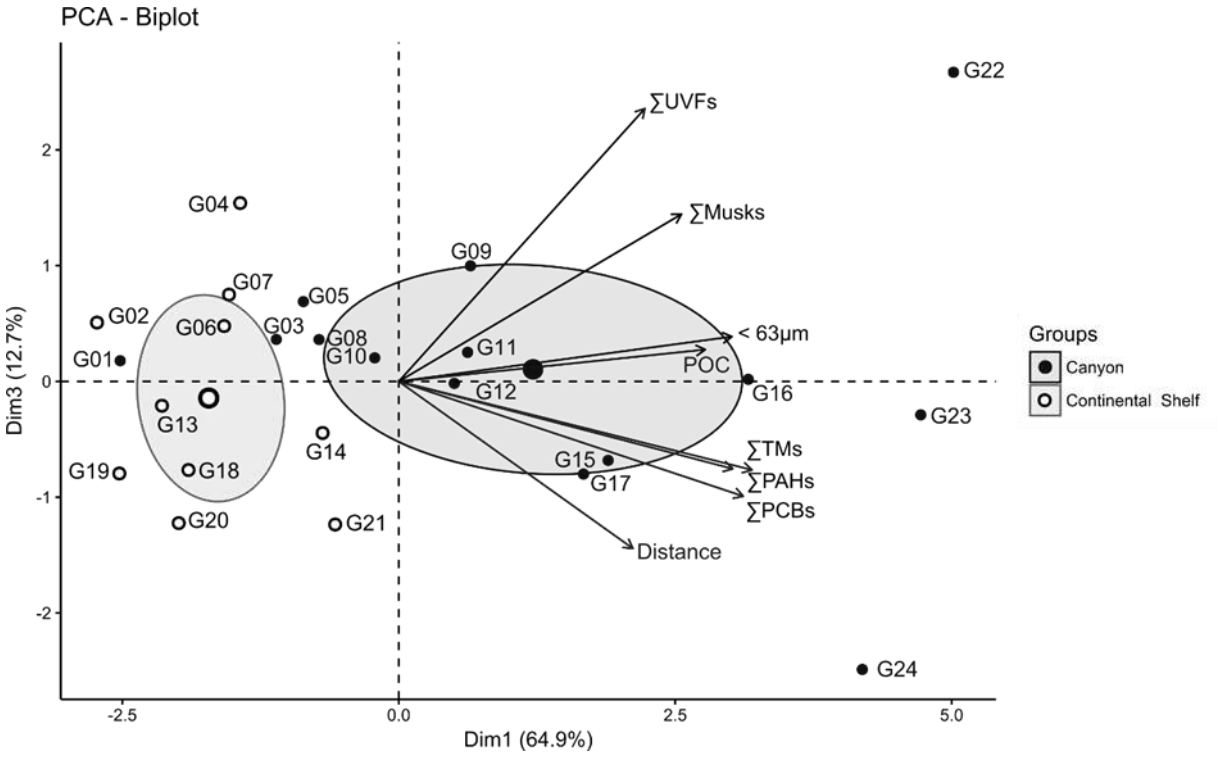

Figure 3 - PCA of contaminant concentrations summed per type groups (TMs, PAHs, PCBs, Musks and UVFs), properties of the sediment (particulate organic carbon, POC, fine grain size, <63µm fraction) and distance from the coast of the first and third dimensions (Dim1 and Dim 3 representing 64.9 and 12.7 % of the total variance). Data points in this figure indicate the location of sediments sampled both on Continental Shelf and on Canyon. Arrows indicate the loadings onto the two dimensions of the percentage of POC, <63µm fraction, distance to the coast gradient and the sums of each contaminant groups. Confidence ellipses around the individual sediments are in function of their location in this area: from the Canyon and from the Continental Shelf

3.3 Ecological risk assessment

The ERA for the TMs is not evaluate with the same method than used for the organic substances, as TMs are neither created nor destroyed by biological or chemical processes.

Naturally present in the environment, organisms have evolved mechanisms to regulate their accumulation and storage. Nevertheless, excess amounts of certain metals are potentially toxic [131]. As described in section 2.1.1.1, TMs amounts in the Capbreton area are higher than the nearby estimated background levels [57]. Previous work on the mercury compounds distribution in the same samples [126] have shown a potential risk for the organisms where both IHg and MeHg overpassed the ERL, as well as observed here for As, Cu, Ni and Pb [121], mainly in the offshore deep canyon sediments. The highest concentrations of As, Hg and Pb in the canyon sediments are clearly higher than both the background level and ERL where high factor are observed between the ambient concentration and those ERL, for Hg (6.5), As (5.5) and Pb (2.6), may indicate an anthropogenic input with adverse effects on local benthic organisms.

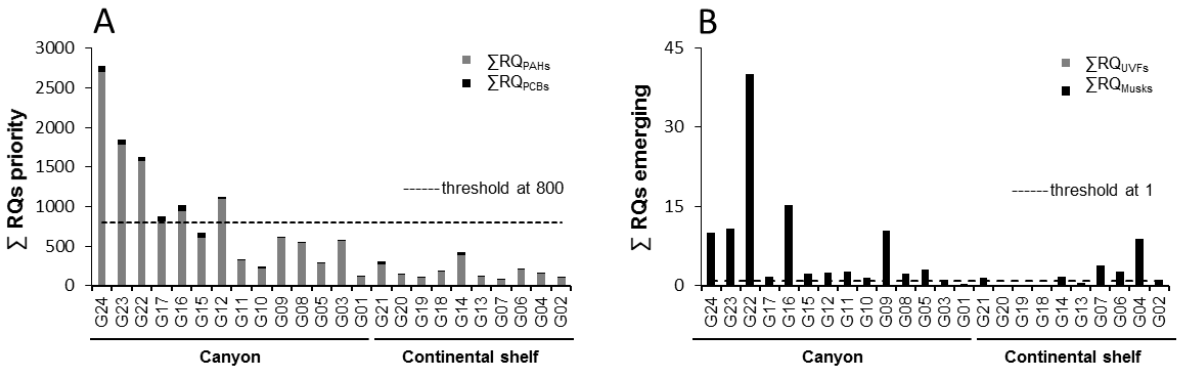

Figure 4 - Evaluation of the toxicity (∑RQs) of priority (A) and emerging (B) contaminants in surface sediments of Capbreton Submarine Canyon and adjacent Continental Shelf. Free, moderate and high risk toxicity correspond to ∑RQmixture = 0, 1 ≤ ∑RQmixture < 800 and ∑RQmixture > 800, respectively. Thresholds at 800 and 1 are added on (A) and (B), respectively

RQ_i were calculated for organic priority and emerging micropollutants for sediment samples (Table S6, Supporting Information). Maximum RQ_i values were observed for the priority compounds, among PAHs, at 845.4, 654.0 and 199.9 for dibenzo(a,h)anthracen, benzo(a)pyrene and phenanthrene. These RQ_i demonstrate a potential adverse effect on the dwelling sediment benthic organisms. RQ_i of emerging compounds were mainly inferior to 1, except for EHMC and 4-MBC. This means there is no significant risk for both of them except for EHMC with significant potential adverse effects, particularly in G22. However, most of sediments from deep and distance to the coast locations in the canyon showed high concentrations of priority compounds which were above ERL [121], the low effect range for which the concentration has a biological effect on 10 percentile of organism. This is observed for 4-6 rings PAHs where benzo(g,h,i)perylene concentrations were above the ERL (85 ng g^{-1}) in 11 sediments of 14 from canyon location, although priority compounds analysed in continental shelf sediments were always under those environmental thresholds.

In order to assess the global impact of organic priority and emerging compounds, the sum of the RQ_i were calculated for priority, $\sum RQ_{priority}$, and emerging compounds, $\sum RQ_{emerging}$ (Fig.4). The $\sum RQ_{priority}$ increased along the canyon axis, from 73 in continental shelf sediment to 2782 in offshore sediments (G24), indicating significant potential adverse effects and adverse effects for benthic organisms, and huge adverse effects are observed in the canyon sediments. In general term, these concentrations of priority and emerging substance observed in Capbreton Canyon sediments can be toxic for benthic organisms, and consequently can be bioaccumulated in higher trophic levels, such commercial crustaceans and fish. That is consistent with the concentrations of persistent organic pollutants in deep sea organisms measured higher in the Blanes Canyon (Mediterranean sea) than the adjacent open slope[157]. This study assume that submarine canyons are a route of persistent anthropogenic pollutants to the deep sea, improving their accumulation in surface sediments and thus far, might be toxic for this kind of productive ecosystem, known to be an hotspot of biodiversty.

4 Conclusion

While WFD and MSFD have set recommendations for achieving the objective the concentrations of contaminants are at levels not giving rise to pollution effects in 2020, very high concentrations of priority compounds and the presence of emerging compounds were observed in Capbreton Canyon sediments. This likely demonstrates that both trapping and transport of micropollutants along the Capbreton Canyon might lead to an accumulation of those anthropogenic pollutants in the sediment compartment. Moreover, the pyrogenic source of the PAHs may indicate an additional atmospheric source involved into this global contamination, where the strong affinity of micropollutants for the SPM and phytoplankton, lead to the micropollutants are readily scavenged from the column water and deposited to the bottom sediment.

In parallel, the risk assessment demonstrated the strong implication of the PAHs level in those sediment with a huge risk for benthic organisms. PAHs can cause serious damages in some organisms, including mutagenic and carcinogenic properties. In addition, the potential risk of Hg, Pb, As and also some emerging micropollutants, may play a synergic effect and consequently increase the impact on the local benthic organisms. These relatively high concentrations of priority and emerging organic compounds in those sediments, can be bioaccumulative, toxic and/or persistent, are as primary source to support the existence of all higher trophic life forms. This can be an ecological risk for the local biodiversity, and indirectly for the human health with the consumption of fish of commercial interest in this area.

More than 2000 submarine canyons incise the continental shelf across the world [158] that represented an area of $4{,}4.10^6$ km^2 which can act as transfer zone of SPM between the continent and the open ocean. This study demonstrates that anthropogenic micropollutants are released from the continent and can dramatically impact the continental slope sediments through submarine canyons. The distribution of those micropollutants in others submarine canyons should be explored in further studies in order to estimate their implication at a global scale. Nevertheless, their decontamination and their degradation (biotic and abiotic processes) along the coastal/deep sea continuum should be experimented in order to estimate the natural resilience of this dynamic ecosystem.

Reagents and materials for priority and emerging micropollutants analysis

Nitric acid (69-70%), hydrochloric acid (33-36%) and hydrogen peroxide solution (30-32%) were of trace metals grade and supplied by Fisher (Hampton, USA). All organic solvents (2-propanol, acetonitrile, toluene, ethyl acetate and methanol) were of analytical grade and supplied by Sigma Aldrich (Saint-Louis, USA). Formic acid (98-100%), ethylenediaminetetraacetic acid disodium (Na_2EDTA) and ammonium chloride (NH_4Cl) were purchased from Sigma Aldrich.

Acetone (laboratory reagent. 99.5%), nitric acid (65%) and hydrochloric acid (37%) were used for cleaning the glassware and were supplied by Fisher. Ultrapure water was obtained with a PURELAB Classic water purification system from Veolia (Paris, France).

Reference standards of arsenic (As), cadmium (Cd), cobalt (Co), chromium (Cr), copper (Cu), nickel (Ni) and lead (Pb), as well as bismuth (Bi) used as internal standard as individual solutions were supplied at 1000 mg L^{-1} each component in nitric acid 10%. All standard working solutions were prepared in nitric acid 2% and stored at 4°C.

Reference standards of 16 PAHs (10 µg mL^{-1} each component in acetonitrile) (naphthalene, acenaphthylene, acenaphthene, fluorene, phenanthrene, anthracene, fluoranthene, pyrene, benzo[a]anthracene, chrysene, benzo[b]fluoranthene, benzo[k]fluoranthene, benzo[a]pyrene, indeno[1,2,3-cd]pyrene, dibenzo[a,h]anthracene, benzo[ghi]perylene). 12 PCBs congeners (10 µg/mL each component in heptane) (PCB 18, 28, 31, 44, 52, 101, 138, 118, 153, 149, 180 and 194) and 7 OCPs (2000 µg mL^{-1} each component in hexane:toluene (1:1)) (4,4′-DDE, 4,4′-DDD, dieldrin, α-endosulfan, β-endosulfan, endrin, heptachlor epoxide) were purchased from Sigma Aldrich, as well as deuterated PAHs internal standards (4000 µg mL^{-1} each component in methylene chloride containing naphthalene-d8, acenaphthene-d10 and perylene-d12) and atrazine-d5. All standard working solutions were prepared in acetonitrile and stored at -20°C.

Reference standards of musk moskene (MM), galaxolide (HHCB), oxybenzone (benzophenone 3), 3-(4-methylbenzylidene)camphor (4-MBC), 2-ethylhexyl 4-methoxycinnamate (EHMC), octocrylene (OC), padimate O (OD-PABA), 3-benzylidenecamphor (3-BC) were purchased from Sigma–Aldrich. Musk ambrette (MA), phantolide (AHMI), tonalide (AHTN), celestolide (ADBI), traseolide (ATII), musk ketone (MK), musk xylene (MX) were purchased from LGC Standards (Molsheim, France). Internal standard musk xylene-d15 (MX-d15) (100 ng/µL in acetone) was also purchased from LGC Standards. All standard stock and working solutions were prepared in 2-propanol and stored at −20°C.

Reference standards of acetaminophen, acetazolamide, acetylsalicylic acid, amiodarone, ampicillin, atenolol, azithromycin, caffeine, carbamazepine, ciprofloxacin, clarithromycin, cyclophosphamide, diclofenac, doxycycline, erythromycin A, flumequine, gemfibrozil, hydrochlorothiazide, ibuprofen, josamycin, ketoprofen, lorazepam, losartan, metoprolol, metronidazole, niflumic acid, nordiazepam, 19-norethindrone, norfloxacin, ofloxacin, oxazepam, oxolinic acid, phenazone, piperacillin, rifampicin, roxithromycin, spiramycin, sulfadiazine, sulfamethazine, sulfamethoxazole, tetracycline, trimethoprim and tylosine were supplied by Sigma Aldrich and classified as analytical grade (>98%). Isotopically labelled compounds used as internal standards were atenolol-d7, carbamazepine-d10, ibuprofen-d3, nordiazepam-d5 and ofloxacin-d3 also purchased from Sigma Aldrich. All standard stock and working solutions were prepared in methanol and stored at −20°C.

Quick, Easy, Cheap, Effective, Rugged and Safe (QuEChERS) extraction tubes containing the citrate buffer salt mixture 4 g of magnesium sulfate, 1 g of sodium chloride, 0,5 g of disodium citrate sesquihydrate and 1 g of sodium citrate (EN method), and dispersive SPE tubes containing 1200 mg of magnesium sulfate, 400 mg of PSA and 400 mg of C18EC (AOAC method) were supplied by Agilent Technologies (Les Ulis. France). Cartridges used for solid phase extraction were Oasis HLB (60mg, 3cc) from Waters (Milford, USA).

Table S1 *– Analytical methods performances, including internal standard (IS), coefficient of determination (R2), limit of quantification (LOQ), recovery mean and relative standard deviation (RSD) for each compound. Linearity (R2) was calculated in the range 0-20 ng g-1 and 0-500 ng g-1 for TMs and organic compounds, respectively. LOQ of TMs were estimated from the RSD of procedural blanks in triplicate multiplicate by 10. LOQ of organic compounds were estimated as the lowest injected compound concentration in matrix that yielded a signal-to-noise (S/N) ratio of 10. LOQ units for Trace Metals and for organic compounds are µg g-1 and ng g-1, respectively. Recoveries were performed in triplicate with Standard Reference Material (SRM 1944, sediment) for trace Metals and with natural sediments (from Adour Estuary and Capbreton canyon) spiked with organic analytes. Precision was calculated as the RSD of three replicates.*

Compounds	**Method**	**IS**	**R^2**	**LOQ**	**Recovery performance method**	**Recovery (%)**	**RSD (%)**
As	ICP-MS	Bi	0.9998	<0.1	SRM	100	8
Cd	ICP-MS	Bi	0.9999	<0.1	SRM	113	5
Co	ICP-MS	Bi	0.9996	<0.1	SRM	87	6
Cr	ICP-MS	Bi	0.9998	0.3	SRM	86	2
Cu	ICP-MS	Bi	0.9997	1.8	SRM	104	5
Hg	ID-GC-ICP-MS	199iHg/201MeHg	-	<0.1	SRM	95	3
Ni	ICP-MS	Bi	0.9997	0.1	SRM	110	6
Pb	ICP-MS	Bi	0.9998	0.1	SRM	107	7
Trace Metals							
Naphtalene	GC-MS	Naphtalene-d8	0.9997	0.3	spiked matrix	93	6
Acenaphtylene	GC-MS	Naphtalene-d8	0.9988	0.1	spiked matrix	108	5
Acenaphthene	GC-MS	Acenaphthene-d10	0.9999	1.5	spiked matrix	96	10
Fluorene	GC-MS	Acenaphthene-d10	0.9997	0.2	spiked matrix	97	4
Phenanthrene	GC-MS	Acenaphthene-d10	0.9998	0.2	spiked matrix	93	3
Anthracene	GC-MS	Acenaphthene-d10	0.9998	0.2	spiked matrix	94	6
Fluoranthene	GC-MS	Acenaphthene-d10	1.0000	0.1	spiked matrix	100	7
Pyrene	GC-MS	Acenaphthene-d10	0.9998	0.1	spiked matrix	89	2
Chrysene	GC-MS	Acenaphthene-d10	0.9992	0.1	spiked matrix	94	13
Benzo[*a*]anthracene	GC-MS	Acenaphthene-d10	0.9934	0.1	spiked matrix	100	8
Benzo[*b*]fluoranthene	GC-MS	Perylene-d12	0.9996	0.1	spiked matrix	89	4
Benzo[*k*]fluoranthene	GC-MS	Perylene-d12	0.9998	0.1	spiked matrix	74	2
Benzo[*a*]pyrene	GC-MS	Perylene-d12	0.9996	0.1	spiked matrix	68	6
Indeno[*1.2.3.cd*]pyrene	GC-MS	Perylene-d12	0.9988	0.1	spiked matrix	48	5
Dibenzo[*a.h*]anthracene	GC-MS	Perylene-d12	0.9994	0.1	spiked matrix	61	7

Benzo[*g.h.i*]perylene	GC-MS	Perylene-d12	0.9998	0.1	spiked matrix	51	12
PAHs							
Dieldrine	GC-MS	Atrazine-d5	1.0000	2.7	spiked matrix	69	5
α-Endosulfan	GC-MS	Atrazine-d5	0.9999	7.3	spiked matrix	56	2
β-Endosulfan	GC-MS	Atrazine-d5	0.9998	9.6	spiked matrix	76	4
Endrin	GC-MS	Atrazine-d5	0.9995	2.3	spiked matrix	49	5
Heptachlor Epoxide	GC-MS	Atrazine-d5	0.9999	0.4	spiked matrix	76	2
4.4'-DDD	GC-MS	Atrazine-d5	1.0000	0.03	spiked matrix	58	4
4.4'-DDE	GC-MS	Atrazine-d5	0.9999	0.1	spiked matrix	74	7
OCPs							
PCB 18	GC-MS	Atrazine-d5	1.0000	0.04	spiked matrix	71	4
PCB 28+31	GC-MS	Atrazine-d5	0.9999	0.2	spiked matrix	72	4
PCB 52	GC-MS	Atrazine-d5	0.9999	0.1	spiked matrix	79	4
PCB 44	GC-MS	Atrazine-d5	0.9999	0.1	spiked matrix	78	3
PCB 101	GC-MS	Atrazine-d5	1.0000	0.1	spiked matrix	63	2
PCB 118	GC-MS	Atrazine-d5	0.9998	0.1	spiked matrix	63	4
PCB 138	GC-MS	Atrazine-d5	0.9994	0.2	spiked matrix	57	3
PCB 149	GC-MS	Atrazine-d5	1.0000	0.1	spiked matrix	66	4
PCB 153	GC-MS	Atrazine-d5	0.9999	0.2	spiked matrix	65	2
PCB 180	GC-MS	Atrazine-d5	0.9996	0.3	spiked matrix	79	3
PCB 194	GC-MS	Atrazine-d5	0.9997	0.5	spiked matrix	84	3
PCBs							
ADBI	GC-MS	MX-d15	0.9985	0.03	spiked matrix	65	2
AHMI	GC-MS	MX-d15	0.9998	0.04	spiked matrix	109	6
MA	GC-MS	MX-d15	0.9995	0.9	spiked matrix	117	4
ATII	GC-MS	MX-d15	0.9994	0.1	spiked matrix	129	2
HHCB	GC-MS	MX-d15	0.9987	0.1	spiked matrix	101	2
AHTN	GC-MS	MX-d15	0.9999	0.1	spiked matrix	100	2
MX	GC-MS	MX-d15	0.9986	0.1	spiked matrix	106	1
MM	GC-MS	MX-d15	0.9998	0.1	spiked matrix	134	2
MK	GC-MS	MX-d15	0.9996	0.2	spiked matrix	129	3
Musks							
3-BC	GC-MS	MX-d15	0.9993	1.4	spiked matrix	129	6
Benzophenone 3	GC-MS	MX-d15	0.9998	0.6	spiked matrix	143	8

4-MBC	GC-MS	MX-d15	0.9999	0.7	spiked matrix	132	1
OD-PABA	GC-MS	MX-d15	0.9996	0.1	spiked matrix	115	3
EHMC	GC-MS	MX-d15	0.9998	0.2	spiked matrix	135	4
OC	GC-MS	MX-d15	0.9998	1.9	spiked matrix	132	8
UV filters							
Ampicillin	LC-MS/MS	Carbamazepine-d10	0.9205	19.7	spiked matrix	52	7
Azithromycin	LC-MS/MS	Ofloxacin-d3	0.9922	0.4	spiked matrix	85	7
Ciprofloxacin	LC-MS/MS	Ofloxacin-d3	0.9984	4.3	spiked matrix	124	15
Clarithromycine	LC-MS/MS	Carbamazepine-d10	0.9977	2.1	spiked matrix	93	7
Doxycycline	LC-MS/MS	Ofloxacin-d3	0.9913	3.0	spiked matrix	134	1
Erythromycin A	LC-MS/MS	Carbamazepine-d10	0.9980	1.2	spiked matrix	83	6
Flumequine	LC-MS/MS	Carbamazepine-d10	0.9996	0.7	spiked matrix	84	4
Josamycin	LC-MS/MS	Ofloxacin-d3	0.9805	1.5	spiked matrix	80	5
Metronidazole	LC-MS/MS	Carbamazepine-d10	0.9957	0.1	spiked matrix	91	5
Norfloxacin	LC-MS/MS	Ofloxacin-d3	0.9883	4.7	spiked matrix	101	6
Ofloxacin	LC-MS/MS	Ofloxacin-d3	0.9957	0.9	spiked matrix	91	5
Oxolinic acid	LC-MS/MS	Carbamazepine-d10	0.9990	1.1	spiked matrix	81	7
Piperacillin	LC-MS/MS	Carbamazepine-d10	0.8482	27.5	spiked matrix	22	17
Rifampicin	LC-MS/MS	Ofloxacin-d3	0.9976	35.7	spiked matrix	121	1
Roxithromycine	LC-MS/MS	Ofloxacin-d3	0.9912	4.1	spiked matrix	101	8
Spiramycin	LC-MS/MS	Carbamazepine-d10	0.9977	8.1	spiked matrix	119	6
Sulfadiazine	LC-MS/MS	Carbamazepine-d10	0.9999	1.0	spiked matrix	92	6
Sulfamethazine	LC-MS/MS	Carbamazepine-d10	0.9981	0.1	spiked matrix	96	5
Sulfamethoxazole	LC-MS/MS	Ofloxacin-d3	0.9947	1.6	spiked matrix	94	4
Tetracycline	LC-MS/MS	Carbamazepine-d10	0.9982	2.4	spiked matrix	122	1
Trimethoprim	LC-MS/MS	Ofloxacin-d3	0.9904	0.1	spiked matrix	94	5
Tylosine	LC-MS/MS	Ofloxacin-d3	0.990	3.6	spiked matrix	88	5
Antibiotics							
Acetylsalicylic acid	LC-MS/MS	Ibuprofen-d3	0.9374	57.5	spiked matrix	94	8
Acetaminophen	LC-MS/MS	Carbamazepine-d10	0.9978	0.3	spiked matrix	94	3
Diclofenac	LC-MS/MS	Ibuprofen-d3	0.9998	3.2	spiked matrix	95	8
Ibuprofen	LC-MS/MS	Ibuprofen-d3	0.9997	34.6	spiked matrix	100	1
Ketoprofen	LC-MS/MS	Carbamazepine-d10	0.9973	1.8	spiked matrix	91	10
Niflumic acid	LC-MS/MS	Ibuprofen-d3	0.9995	0.8	spiked matrix	92	2

Phenazone	LC-MS/MS	Carbamazepine-d10	0.9993	3.9	spiked matrix	89	2
Analgesics and NSAIDs							
Atenolol	LC-MS/MS	Atenolol-d7	0.9990	0.9	spiked matrix	89	3
Losartan	LC-MS/MS	Carbamazepine-d10	0.9997	0.1	spiked matrix	103	2
Metoprolol	LC-MS/MS	Carbamazepine-d10	0.9980	0.1	spiked matrix	91	2
β-blockers							
Cyclophosphamide	LC-MS/MS	Carbamazepine-d10	0.9995	0.6	spiked matrix	93	1
Anti-cancer					spiked matrix		
Carbamazepine	LC-MS/MS	Carbamazepine-d10	0.9999	0.7	spiked matrix	103	3
Anti-epileptic							
Caffeine	LC-MS/MS	Carbamazepine-d10	0.9958	0.3	spiked matrix	51	2
Human indicator							
Lorazepam	LC-MS/MS	Nordiazepam-d5	0.9987	1.1	spiked matrix	98	3
Nordiazepam	LC-MS/MS	Nordiazepam-d5	0.9990	0.1	spiked matrix	94	2
Oxazepam	LC-MS/MS	Nordiazepam-d5	0.9990	1.3	spiked matrix	97	4
Anxiolytics							
Acetazolamide	LC-MS/MS	Carbamazepine-d10	0.9889	1.4	spiked matrix	85	5
Amiodarone	LC-MS/MS	Carbamazepine-d10	0.9671	0.3	spiked matrix	54	1
Gemfibrozil	LC-MS/MS	Ibuprofen-d3	0.9985	0.9	spiked matrix	88	15
Hydrochlorothiazide	LC-MS/MS	Ibuprofen-d3	0.9972	0.4	spiked matrix	88	7
19-Norethindrone	LC-MS/MS	Carbamazepine-d10	0.9982	3.1	spiked matrix	91	11
Various pharmaceuticals							

Table S2 *- List of compounds analysed in Capbreton canyon sediments and adjacent continental shelf sediments with concentrations inferior to the limit of quantification (LOQ).*

Groups	Subgroups	Substances
OCPs		Dieldrine, α-Endosulfan, β-Endosulfan, Endrin, Heptachlor Epoxide, 4.4'-DDD, 4.4'-DDE
Pharmaceuticals	Antibiotics	Ampicillin, Ciprofloxacin, Doxycycline, Erythromycin A, Flumequine, Josamycin, Metronidazole, Norfloxacin, Ofloxacin, Oxolinic acid, Piperacillin, Rifampicin, Roxithromycine, Spiramycin, Sulfadiazine, Sulfamethazine, Sulfamethoxazole, Tetracycline, Trimethoprim, Tylosine
	Analgesics and NSAIDs	Acetylsalicylic acid, Diclofenac, Ibuprofen, Ketoprofen, Niflumic acid, Phenazone
	Various pharmaceuticals	Acetazolamide, Gemfibrozil, Hydrochlorothiazide, 19-Norethindrone
	β-blockers	Atenolol, Losartan, Metoprolol
	Anxiolytics	Lorazepam, Nordiazepam, Oxazepam
	Anti-cancer	Cyclophosphamide
	Anti-epileptic	Carbamazepine
	Human indicator	Caffeine

Table S3 *– Particulate organic carbon (POC) and grain size contents (sant, silt, clay and fine fraction <63 µm corresponding to fraction > 63 µm, 2–63 µm, < 2 µm and 2–63 µm + < 2 µm, respectively) from sediments of Capbreton Canyon and continental shelf.*

	POC (%)	Sand (%)	Silt (%)	Clay (%)	<63 µm (%)
Capbreton Canyon					
G01	0,6	63,0	35,6	1,4	37.0
G03	1,5	46,1	52,2	1,8	53.9
G05	1,3	39,1	58,1	2,8	60.9
G08	1,5	35,9	61,4	2,7	64.1
G09	1,8	15,1	81,0	3,9	85.4
G10	1,6	23,7	72,7	3,6	76.3
G11	2,1	8,9	86,3	4,8	91.1
G12	2,2	36,6	60,2	3,2	63.4
G15	2,5	8,5	86,7	4,8	91.5
G16	2,6	9,7	85,9	4,4	90.3
G17	1,8	9,8	85,8	4,4	90.2
G22	1,9	5,5	89,0	5,5	94.5
G23	2,0	3,5	90,5	5,9	96.2
G24	2,0	2,8	91,0	6,0	97.2
Continental Shelf					
G02	0,4	76,7	22,3	1,0	23.3
G04	0,8	58,9	39,6	1,5	41.1
G06	0,8	45,7	52,2	2,1	54.3
G07	0,8	44,7	52,0	3,4	55.3
G13	0,5	65,9	32,0	2,0	34.1
G14	0,9	54,3	43,2	2,5	45.7
G18	0,5	77,2	21,2	1,6	22.8
G19	0,3	87,5	11,3	1,2	12.5
G20	0,3	83,0	15,7	1,3	17.0
G21	0,7	54,1	42,8	3,1	45.9

Table S4 *– Correlation and contribution of variables for DIM1 and DIM3 from PCA of the global distribution of the sum of each group of compounds with geochemical parameters for all locations (n=24).*

	Inertia		Contribution	
Variables	**Dim.1**	**Dim.3**	**Dim.1**	**Dim.3**
∑TMs	0.93	-0.22	16.53	4.84
∑PAHs	0.88	-0.22	14.77	4.72
∑PCBs	0.90	-0.29	15.71	8.13
∑Musks	0.74	0.42	10.58	17.27
∑UVFs	0.65	0.68	8.02	45.95
POC	0.80	0.08	12.44	0.63
<63µm	0.87	0.11	14.7	1.24
Distance	0.61	-0.42	7.26	17.23

Table S5 *– Ecotoxicological data used for RQ calculation. Concentration and PNEC units are ng g^{-1}. AF is assessment factor used to convert endpoint in predicted no effect concentration. PNEC.*

Groups	Compounds	Organism	Endpoint	Concent.	AF	PNEC	References
TMs	**Ag**	several species	ERM	3.7	1000	**0.0037**	[121]
	As	several species	ERM	70000	1000	**70**	
	Cd	several species	ERM	9600	1000	**9.6**	
	Cr	several species	ERM	370000	1000	**370**	
	Cu	several species	ERM	270000	1000	**270**	
	Hg	several species	ERM	710	1000	**0.71**	
	Ni	several species	ERM	51600	1000	**51.6**	
	Pb	several species	ERM	218000	1000	**218**	
	Zn	several species	ERM	410000	1000	**410**	
PAHs	**Naphtalene**	several species	ERM	2100	1000	**2.1**	[121]
	Acenaphtylene	several species	ERM	640	1000	**0.64**	
	Acenaphthene	several species	ERM	500	1000	**0.5**	
	Fluorene	several species	ERM	540	1000	**0.54**	
	Phenanthrene	several species	ERM	1500	1000	**1.5**	
	Anthracene	several species	ERM	1100	1000	**1.1**	
	Fluoranthene	several species	ERM	5100	1000	**5.1**	
	Pyrene	several species	ERM	2600	1000	**2.6**	
	Chrysene	several species	ERM	2800	1000	**2.8**	
	Benzo[a]anthracene	several species	ERM	1600	1000	**1.6**	
	Benzo[a]pyrene	several species	ERM	1600	1000	**1.6**	
	Dibenzo[a.h]anthracene	several species	ERM	260	1000	**0.26**	
PCBs	**Total PCBs**	several species	ERM	180	1000	**0.18**	[121]
Musks	**HHCB**		PNEC	1970		**1970**	EU risk assessment
	AHTN		PNEC	1720		**1720**	EU risk assessment
	MX		PNEC	300		**300**	EU risk assessment
UVFs	**Benzophenone 3**	QSAR	PNEC	370		**370**	QSAR
	4-MBC	QSAR	PNEC	3		**3**	QSAR
	EHMC	*Potam. antipodarum*	NOEC	80	100	**0.8**	[159]
	OC	QSAR	PNEC	180		**180**	QSAR

Table S6 *– Risk Quotients (RQ_i) calculated from Capbreton Canyon and continental shelf sediments for priority compounds (A) and emerging compounds (B) in all locations.*

(A) PRIORITY	Naph	Acel	Ace	Flu	Phe	Ant	Flt	Pyr	Chr	BaA	BaP	diBhA	PCBs
Canyon													
G01	0.5	1.5	0,0	3.5	9.3	4.2	4.9	9.1	4.7	10.1	19.8	42.6	2.7
G03	3.2	17.1	2.8	18.9	65.6	67.8	32.2	60.2	33.5	63.7	81.4	112.7	7.5
G05	1.8	4,0	0,0	8.3	23.9	9,0	12.5	21.2	11.9	24.4	76,0	87,0	6.1
G08	2.5	11,0	10.4	17.5	79.7	23.7	38.7	66.2	29.5	54.5	89.1	120.3	5.7
G09	4.3	15.3	19.5	21.6	62.5	27.5	30.9	66.8	30.3	63,0	115.2	153.1	10.8
G10	2.5	6.1	0,0	8.9	17,0	9.3	11.9	19.9	11,0	21.4	43.1	68.2	20.4
G11	4.2	7.2	0,0	13.7	29.2	12.9	17.3	28.5	14,0	29.2	69.4	93.4	12.1
G12	4.1	23.5	15.8	35,0	113.6	86.2	62.9	105.6	60,0	129.4	192.1	273,0	15.2
G15	8.9	13.6	5.5	25.7	53.9	28.2	28.2	48.6	27.8	46.1	136.1	186.3	54.3
G16	9.8	31.6	24.6	32.7	76.8	48.7	51.9	89.8	45.1	86.3	176.3	269.4	77.1
G17	8.3	24,0	8.3	31.1	65.5	42,0	37.8	66,0	38.8	77.9	184.6	230.2	62.3
G22	29.1	74.3	51.2	72.6	117.4	82.3	51.9	84.5	58.9	111.6	361.6	473.4	61.2
G23	35.1	69.7	60.8	86.5	115.7	83.5	60.4	90.3	59.9	120.9	402.9	590.7	75.9
G24	37.1	93.3	98.8	126.2	199.9	120.3	98.8	150.2	96.1	176.1	654,0	845.4	86.1
Continental Shelf													
G02	0,0	0,0	0,0	0.9	7.1	3.2	5,0	9.5	5.3	10.8	18.1	37.2	1.1
G04	1.3	0,0	0,0	5.2	13.4	4.7	6.7	13.7	6.9	13.7	34.2	56.4	4.6
G06	1.5	0.9	0,0	4,0	11.4	6.8	6.9	12.4	9.9	20.3	52.6	71.4	3.2
G07	0.4	0.7	0,0	2.2	2.9	3.3	3.1	5.5	2.9	5.2	14.8	31.3	0.3
G13	1.4	1.3	0.2	3.1	9,0	5.4	4.7	8.5	4.9	10.2	20,0	42.6	5.6
G14	2.5	10.2	7.1	14.8	37.9	19.7	23.9	36.8	18.8	34.2	74.7	100.7	37.2
G18	3.1	2.9	0,0	7.8	19.2	9.7	7.2	12.6	8.2	15.4	33.5	61.2	9,0
G19	1.8	0,0	0,0	3.4	7.7	4.7	4.4	7.5	4.9	10.2	13.7	36,0	4.1
G20	2.8	3.9	0,0	8.2	14.6	7.2	5.7	9.5	5.8	11.2	23.8	51,0	4.1
G21	4.7	6.1	0,0	13.1	23.5	14.5	11.1	19.1	12.8	25.3	57.4	86.5	29.7

Table S6 *– Risk Quotients (RQ_i) calculated from Capbreton Canyon and continental shelf sediments for priority compounds (A) and emerging compounds (B) in all locations.*

(B) EMERGING	HHCB	AHTN	MX	BP-3	4-MBC	EHMC	OC
Canyon							
G01	0.00	<0.01	<0.01	<0.01	0.4	0.00	<0.01
G03	0.00	<0.01	0.00	0.00	1.0	0.00	0.01
G05	0.00	0.00	0.00	0.00	2.5	0.42	0.01
G08	0.00	0.00	0.00	<0.01	2.2	0.00	<0.01
G09	<0.01	<0.01	<0.01	<0.01	1.5	8.91	<0.01
G10	0.00	0.00	0.00	<0.01	1.6	0.00	<0.01
G11	0.00	0.00	<0.01	<0.01	1.9	0.82	<0.01
G12	0.00	0.00	0.00	<0.01	2.2	0.19	<0.01
G15	0.00	0.00	<0.01	<0.01	1.8	0.37	<0.01
G16	<0.01	<0.01	<0.01	<0.01	2.3	12.85	0.02
G17	0.00	<0.01	0.00	<0.01	1.5	0.20	0.02
G22	<0.01	<0.01	<0.01	<0.01	0.1	39.72	0.16
G23	<0.01	<0.01	<0.01	<0.01	0.0	10.70	0.02
G24	0.00	<0.01	<0.01	<0.01	0.0	9.98	0.00
Continental Shelf							
G02	0.00	<0.01	0.00	<0.01	0.4	0.70	0.01
G04	0.00	<0.01	0.00	<0.01	0.7	8.08	0.07
G06	0.00	<0.01	0.00	<0.01	1.1	1.51	<0.01
G07	0.00	<0.01	0.00	<0.01	1.6	2.21	0.00
G13	0.00	<0.01	0.00	<0.01	0.5	0.00	0.00
G14	0.00	<0.01	0.00	<0.01	1.7	0.00	0.00
G18	0.00	<0.01	0.00	<0.01	0.1	0.00	0.00
G19	0.00	<0.01	0.00	<0.01	0.1	0.00	0.00
G20	0.00	<0.01	0.00	<0.01	0.1	0.00	0.00
G21	0.00	<0.01	0.00	<0.01	0.0	1.45	0.00

Fig. S1 *– Matrix of coefficients of determination from relationship between pollutants groups and geochemical parameters. Size of the circle and dark color indicate strong correlation between variables. Significance of codes: 0.0001 '***' ; 0.001 '**' ; 0.01 '*' ; 0.05 '.' , 0.1 ' ' 1 for p-value.*

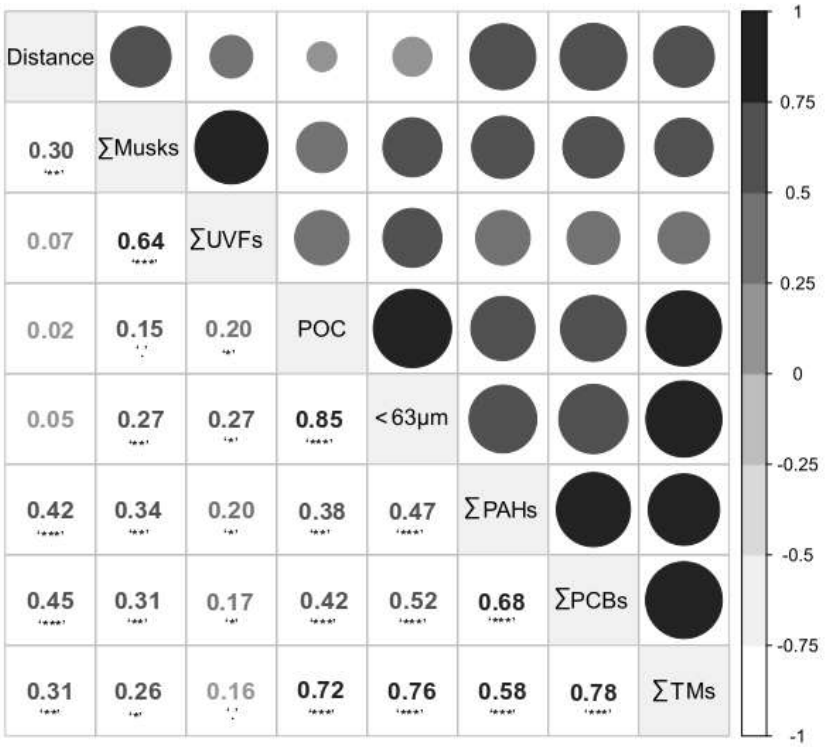

References

European Union Risk Assessment Report on AHTN a. http://echa.europa.eu/documents/10162/26e223a9-eda9-4e79-8c4d-650d2a3c1124

European Union Risk Assessment Report on HHCB b. http://echa.europa.eu/documents/10162/947def3b-bbbf-473b-bc19-3bda7a8da910

European Union Risk Assessment Report on Musk xylene c. http://echa.europa.eu/documents/10162/dc1a179e-699e-44c2-b4ad-371b9b89efab

1.B - MERCURY AND METHYLMERCURY CONCENTRATIONS, SOURCES AND DISTRIBUTION IN SUBMARINE CANYON SEDIMENTS (CAPBRETON, SW FRANCE): IMPLICATIONS FOR THE NET METHYLMERCURY PRODUCTION

Alyssa Azaroff, Emmanuel Tessier, Jonathan Deborde, Rémy Guyoneaud, Mathilde Monperrus

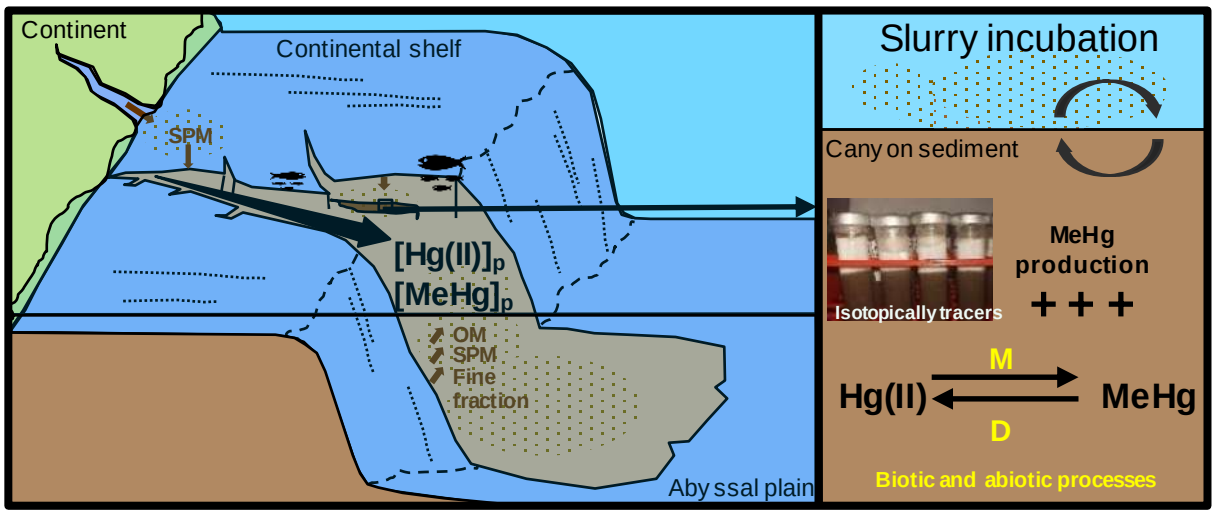

Published, Science of Total Environment, 2019, https://doi.org/10.1016/j.scitotenv.2019.04.111

Résumé

Les canyons sous-marins sont d'importants stocks de poisson à intérêt commercial, dont la consommation est l'un des principaux risques d'exposition des humains au monométhymercure (MeHg). Actuellement, la biogéochimie du mercure dans ces systèmes biologiquement productifs est inconnue. Dans ce travail, la distribution du mercure inorganique (Hg (II)) et du mercure organique (MeHg) a été étudiée dans des zones d'accumulation sédimentaire (pentes et terrasses) par rapport aux sédiments du plateau continental adjacent. Les concentrations des espèces mercurielles dans ces sédiments montrent une large gamme de concentrations (allant de 18 à 973 ng g^{-1} pour Hg(II) et 0,07 à 2,03 ng g^{-1} pour MeHg) présentant des facteurs d'enrichissement de 50 et 20, respectivement. Des valeurs plus élevées ont été observées dans les sédiments du canyon, suggérant une forte accumulation de mercure associée aux valeurs plus élevées de la fraction d'argileuse et de la teneur en matière organique. La réactivité du mercure a été étudiée au laboratoire à partir de sédiment collectés sur trois sites le long de l'axe du canyon sous-marin de Capbreton à l'aide de traceurs isotopiques. Les constantes spécifiques du taux de méthylation et de déméthylation (k_M et k_D) ont été calculées. Les résultats ont clairement montré que les concentrations de MeHg dans ces sédiments sont contrôlées par des réactions de méthylation et de déméthylation concurrentes et simultanées, principalement médiées par un processus biotique. La réactivité du mercure semble être plus élevée dans les stations côtières que dans la station offshore, en raison de la présence de matières organiques plus labiles, susceptibles de stimuler les activités microbiennes. Cependant, la production nette de MeHg pour la station au large a été estimé plus élevée que les stations côtières en raison de la concentration plus élevée en Hg(II), suggérant une source potentielle de MeHg pour de tels environnements marins.

Mots clefs : Composés mercuriels, milieu marin profond, méthylation, déméthylation, processus biologiques

Abstract

Submarine canyons are important stocks of commercial interest fish, whose consumption is one of the main monomethymercury (MeHg) exposure to humans. Currently, biogeochemistry of mercury in those biologically productive system is unknown. In this work, inorganic mercury (Hg(II)) and organic mercury (MeHg) distributions were measured in sedimentary accumulative zones (slopes and terraces) against adjacent continental shelf sediments. Hg compound concentrations in these sediments show a huge range of concentrations (Hg(II) ranging from 18 to 973 ng g^{-1} and MeHg ranging from 0.07 to 2.03 ng g^{-1}) exhibiting factors 50 and 20 fold, respectively. Higher values of mercury compounds were observed in canyon locations suggesting a high accumulation of mercury associated with higher values of clay fraction and organic matter content. The reactivity of mercury was investigated in sediment of three locations along Capbreton submarine canyon axis using slurry incubations experiments and isotopic tracers. Specific methylation and demethylation rate constants (k_M and k_D) were calculated. Results clearly showed that MeHg concentrations in these sediments are controlled by competing and simultaneous methylation and demethylation reactions mainly mediated by biotic process. Mercury reactivity was found higher in coastal stations compared to the offshore station due to more labile organic matter which may stimulate microbial activities. However, higher net MeHg production was estimated for the offshore station due to high Hg(II) concentrations suggesting a potential MeHg source for such marine environments.

Key words: Mercury compounds, deep marine environment, methylation, demethylation, biotic processes

1 Introduction

Mercury (Hg) is a global pollutant due to its long-range transport from source regions to remote parts of the world [160]. Most Hg, from anthropogenic or natural sources, is exported to marine ecosystems [161]. Due to its affinity for particulate matter, Hg is readily scavenged from the water column and deposited to sediment, particularly in estuaries and coastal areas [162]. During the biogeochemical cycling of Hg, methylmercury (MeHg), a potent neurotoxin, can be produced and subsequently bioaccumulated along the food chain in aquatic ecosystems. Methylation of inorganic mercury (Hg(II)) to MeHg and demethylation of MeHg are the two most important processes in the cycling of MeHg, determining the concentration of MeHg in aquatic ecosystems

MeHg formation is influenced by a number of abiotic environmental factors including temperature, pH, redox potential, and inorganic and organic complexing agents (Merritt and Amirbahman, 2009; Zhu et al., 2018). It is also influenced by biotic factors including activity and structure of bacterial communities [163]. In sediment, anaerobic prokaryotes, including sulfate-reducing bacteria (SRB), iron-reducing bacteria (FeRB), methanogens, and fermentors that possess the genes (*hgcAB*) have been identified as Hg methylators [85,164,165,87,89]. MeHg production is limited by geochemical parameters controlling the solubility and availability of Hg(II) for bacterial uptake such as Hg(II) speciation in the solid/adsorbed [84,166] and dissolved [167,168] phase. Dark reduction of Hg(II) to elemental mercury (Hg^0) [169,170] is also potentially important factor controlling the availability of Hg(II). Similar to methylation of Hg(II), demethylation of MeHg can proceed through both biotic, reductive [171,172], and oxidative [173,174] processes, and abiotic processes. .Nevertheless, biotic process was suggested to be the dominant pathway of Hg demethylation in sediment [163]. Both SRB and methanogens could be the primary microorganisms for this process [175,176].

The determination of Hg methylation and demethylation rates is important for quantitatively estimating the net production of MeHg which in turn is necessary for identifying the major sources and sinks of MeHg in aquatic ecosystems. These rates can be found using the technique of adding isotopically labelled Hg compounds to samples and has been applied in this field since the mid-1990s (Hintelmann and Evans, 1997) due to its high accuracy and precision, short incubation time, and ability of simultaneously determining the methylation and demethylation rates.[177–179].

Submarine canyons act as channels for the transfer of sediments from the continent to the deep sea [97,180]. They accumulate organic-rich-sediments, transported along the inner shelf zone [181,123] that affect the sedimentology, and thus the ecology of the oceans.

Local productivity at the head of submarine canyon [107] can lead to an enrichment in abundance and diversity of biological communities [108,125], including commercially important stocks of fish and shellfish [182].Submarine canyons are also considered as vulnerable marine ecosystems [183,184] and act as a trap for pollutants [185,186]. The sediments which are transported through submarine canyons between the shelf and the deep sea can be contaminated [132,54,55] and lead to the accumulation of Hg that can be converted into MeHg. Terrigenous inputs, in addition with sedimentary dynamics can play an important role in Hg accumulation and its geochemical cycle. However, Hg distribution and its reactivity, especially the net methylation production potential, in sediment of submarine canyons are poorly studied.

In the present study, Hg(II) and MeHg were determined in sediments along the Capbreton Canyon axis, adjacent terraces and continental shelf up to 23.5 km from the coast (maximum depth of 399 m). Ambient concentrations were correlated to geological parameters (grain size, organic carbon content, sulphur). Incubations of sediment slurries with isotopically labelled Hg compounds were performed to determine methylation/demethylation potentials and rates in three stations along the Capbreton Canyon in order to estimate the net MeHg production in such sediment.

2 Material and methods

2.1 Study area and sampling strategy

The Capbreton Canyon is located in the south-eastern Bay of Biscay (NE Atlantic) and deeply incises the Aquitaine continental shelf over 300 km in length [187]. It begins 250 m away from the coastline and reaches up to 3000 m water depth [188]. Sediment were sampled in July 2017 during the HAPOGE oceanographic cruise. Twenty-four stations were sampled within the first 23.5 km of the Capbreton Canyon area with a Hybrid Remotely Operated Vehicle (HROV Ariane, Ifremer) in order to sample overlying water with Go-Flo bottle and surface sediments (0–10 cm) using cores and a Shipeck grab sampler. Ten stations were located on the continental shelf between 40 and 136 m depth, beginning at the head of the canyon (G01 and G02) at 1.4 km of the coastline and extending to 19.1 km from shore (Fig. 1). Fourteen stations were located in the canyon and in adjacent slopes or terraces, between 40 and 399 m depth, extending from 1.2 km to 23.5 km from the coast (Fig. 24, Annexe 9). After collection, sediment samples were homogenized, and placed into sterile polyethylene bags or cryotubes, sealed and stored in the dark at −20 °C until further analysis. For each sample, Hg speciation analysis and geochemical parameters were

analysed. Methylation/demethylation potentials and rates were determined for G10 and G24 canyon samples and for G14 continental shelf sample (described below).

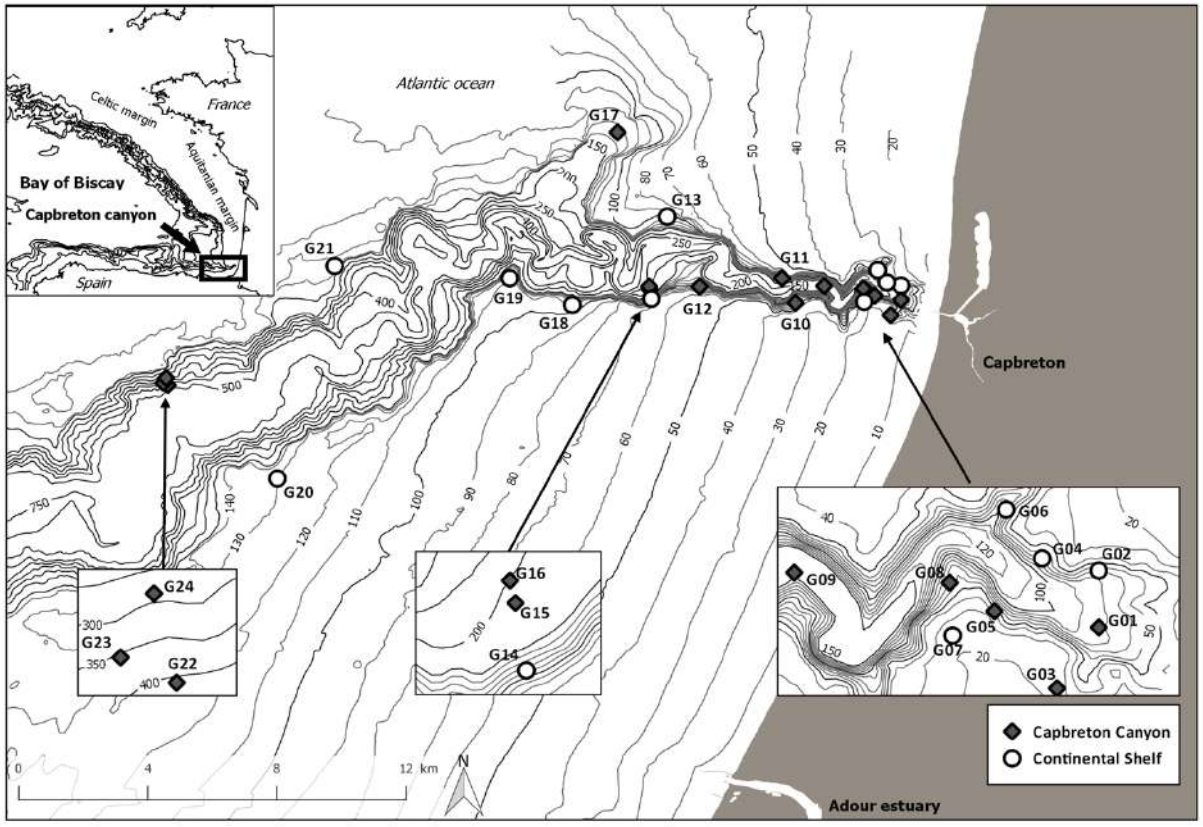

Figure 1 Sediment sampling sites in the Capbreton Canyon (grey diamonds) and on the adjacent continental shelf (white circles) Isobath data from SEDIMAQ3 (Gillet 2012).

2.2 Sample processing and geochemical parameters

All frozen samples were freeze-dried before further processing, except sediments for grain-size analysis that were thawed at room temperature. The subsample for granulometry was analysed using a Malvern® Mastersizer 2000 laser diffractometer capable of analysing particle sizes between 0.02 and 2000 µm. The percentages of the following three groups of grain sizes were determined: < 2 µm (clay), 2–63 µm (silt), and > 63 µm (sand). Others subsamples were homogenized and ground in an agate pestle and mortar before analytical procedures.

Total and organic carbon (TC and OC) were analyzed by infrared spectroscopy via high temperature combustion on a Shimadzu® TOC-LCSH/CSN/SSM-5000A analyzer. Particulate organic carbon (POC) was measured after removal of carbonates with 1.2N HCl from 200 mg of powdered sample. Total sulphur (TS) was measured by infrared spectroscopy using a LECO C-S 125 from 100 mg of powdered sample. Sediments for carbon and nitrogen isotopic compositions, particulate organic nitrogen (PON) and C/N ratios were weighed into silver cups and decarbonated using 1.2N HCl, and then analysed using an

elemental analyzer (ThermoFIsher® Scientific Flash 2000) coupled to an isotope ratio mass spectrometer (IRMS; Isoprime, GV Instruments®). IRMS daily drift was monitored using home-made standards (caseine, glycine) and, if necessary, data were corrected consequently. Elemental composition was calibrated against acetanilide and isotopic composition against home-made standards and reference material (IAEA-N2). All isotopic data were expressed in the conventional δ notation (‰):

$$\delta^{13}C_{sample} \text{ or } \delta^{15}N_{sample} = (R_{sample}/R_{reference} - 1) \times 1000$$

with R = $^{13}C/^{12}C$ or $^{15}N/^{14}N$, and the reference is PDB for $\delta^{13}C$ and atmospheric N_2 for $\delta^{15}N$.

Analytical associated uncertainties were ≤ 0.05% for TC, TS, PON and POC, ≤ 0.2‰ for $\delta^{13}C$ and $\delta 1^{5}N$, and ≤ 0.05 for C/N ratios.

2.3 Analytical methods for mercury

2.3.1 Mercury compounds analysis

The determination of Hg compounds was performed according to the procedure described by Monperrus et al., 2008. About 250 mg of crushed dried samples were digested with 5 mL nitric acid 6N under a microwave field (Discover system, CEM, 75 W, 4 min), and centrifuged to remove solid particles. The supernatant, stored at 4°C, was then submitted to derivatization using sodium tetraethylborate (1%). The samples were analyzed by compounds specific isotope dilution Gas Chromatography (Trace GC, Thermo Element) coupled to Inductively Coupled Plasma Mass Spectrometry (ICPMS X7, Thermo Element). The Gas Chromatograph was equipped with a capillary column MXT-1 (100% dimethylpolysiloxane 30m, i.d. 0.53 mm and 1 mm coating). The absolute detection limit based on three standard deviation of the digestion blank, was 0.02, 0.05 ng g^{-1} (as Hg, weight dry) for MeHg and Hg(II) respectively. The accuracy and precision of mercury analytical results were verified by analysing international certified materials (IAEA 405 estuarine sediment and BCR 580 estuarine sediment). Mean MeHg and Hg(II) recoveries were within the 95% confidence interval, indicating high accuracy (except for BCR580 MeHg where mean recovery was 110%). The coefficient of variation for five analyses for each certified materials was <3%, indicating high precision.

2.3.2 Set up of methylation and demethylation experiments

Hg compounds transformation potentials in sediments were determined through sediment slurry incubations spiked with isotopically enriched Hg compounds ($^{199}HgCl_2$ and $CH_3{}^{201}HgCl$) according to the incubation protocol, analyzes, and calculations of methylation

and demethylation potentials described elsewhere [189,190]. This methodology allows the simultaneous and quantitative determination of newly formed and remaining Hg compounds derived from each isotope, and the determination of specific formation/degradation yields. The formation of MeHg from the Hg(II) spike is taken as the methylation potential and the loss of spiked MeHg is taken as the demethylation potential.

Briefly, for each station, a slurry was prepared by mixing fresh sediment with overlying water (50:50, w:w). Incubation experiments were performed in 10 mL glass tubes sealed with PTFE stoppers filled with around 10 g of sediment slurry. For all assays under abiotic and biotic conditions, 0.02 mL of $^{199}HgCl_2$ (10 mg/L) and 0.02 mL of $Me^{201}HgCl$ (1 mg/L) were added. Control assays (initial time) were stopped immediately by storing samples at -80°C whereas incubated anaerobic assays were placed in the dark at 14°C (in situ temperature) and stopped at different elapsed times (1, 2, 4, 7, 11, 15 days). Slurries under abiotic condition (control condition), were twice sterilized for 20 min at 120 °C prior to spike with enriched Hg compounds. All assays, including initial time and other incubation times, were performed in triplicate.

2.3.3 Methylation / demethylation yields and rates

Quantification of isotopically labelled mercury compounds was performed according to the double-double spike isotopic dilution [189]. The sediment extract was spiked with enriched Hg compounds ($^{198}Hg(II)$ and $Me^{202}Hg$) compounds and then derivatized by ethylation and analyzed by GC–ICP MS. The amount of formed and recovered Hg compounds deriving from each enriched isotopes 199 and 201 ($Me^{199}Hg$, $Me^{201}Hg$, $^{199}Hg(II)$, $^{201}Hg(II)$) after the incubation period were calculated by isotopic pattern deconvolution methodology [190].

Hg transformation yields for methylation and demethylation (in %) can then be calculated by dividing the total amount of $Me^{199}Hg$ formed from the amount of $^{199}Hg(II)$ spiked and the total amount of $^{201}Hg(II)$ formed from the amount of $Me^{201}Hg$ added, respectively. Gross specific rates of methylation and demethylation (as represented by the rate constants k_M and k_D in % d^{-1}) were calculated from transformation yields in non-sterile condition (which include both abiotic and biotic processes), and incubation times and on the assumption those two reactions were independent and following a pseudo-first kinetic reaction order.

3 Results

3.1 Sediment characterization

Higher fine sediment fraction (i.e. the sum of silt and clay fraction) was found in canyon stations relatively to continental stations (78 ± 16 and 35 ± 13 %, respectively) where this fine fraction increased with the distance to the coast (Table S1, Supporting information). A strong correlation (Pearson correlation, r^2= 0.99, p-value < 0.0001, n=24) between silt and sand proportion (Fig. 2a) demonstrated that canyon stations accumulated more fine sediment fractions than continental shelf stations. TC and POC contents were higher in canyon stations than continental shelf stations with mean values of 3.3 ± 0.5 %, 1.8 ± 0.4 % and 1.8 ± 0.3 %, 0.6 ± 0.2 %, respectively. Canyon station sediments exhibited higher PON contents than continental shelf stations sediments with mean values of 0.18 ± 0.04 % and 0.06 ± 0.02 %, respectively. Significant correlations between fine fraction and TC, POC and PON proportions were observed (Fig. 2b, c and d, Pearson correlation, p-value < 0.001, n=24) indicating an enrichment of TC, POC and PON in fine particles and thus in canyon sediments. The same trend was observed for average TS contents with 0.32 ± 0.10 % in canyon sediments and 0.17 ± 0.11 % in continental shelf sediments (Table S2, Supporting information).

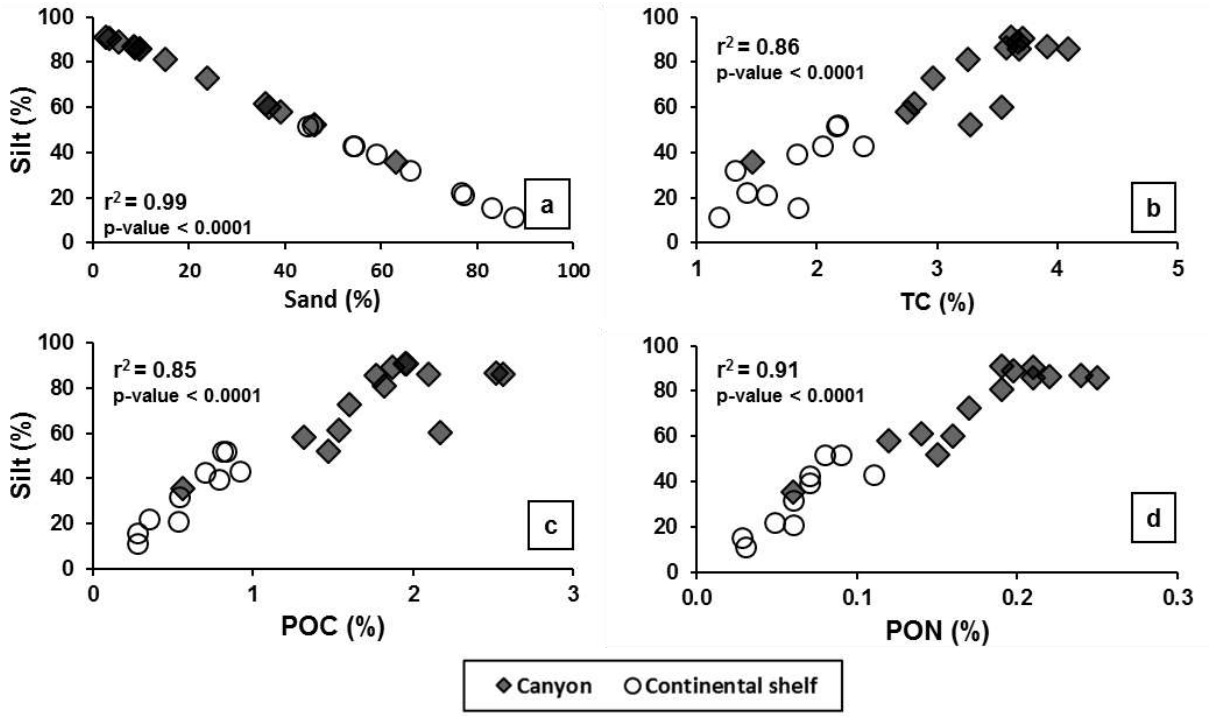

Figure 2 - Relationship between silt proportion and sand proportion (a), total carbon (TC) (b), particulate organic carbon (POC) (c) and particulate organic nitrogen (PON) (d) in surface sediments of Capbreton canyon. r2, Pearson correlation including all stations (n= 24). Canyon stations (grey diamonds) and continental shelf stations (white circle) are represented

Similar $\delta^{15}N$ values in continental shelf stations and canyon stations were measured in a narrow range of 5.2 ± 1.2 ‰ and 5.0 ± 0.5 ‰, respectively (Fig. 3a). The same pattern was observed for $\delta^{13}C$ mean values with -25.0 ± 0.6 ‰ for continental shelf stations and -25.4 ± 1.2 ‰ for canyon stations. The $\delta^{13}C$ and $\delta^{15}N$ values in the sediments appeared to vary according to station distance from the coast rather than by whether they were in the canyon or on the shelf. The $\delta^{13}C$ signatures of stations within the first 10 km to the coast are closed to those measured in suspended particle matter (SPM) of Adour and Gironde Estuaries, the most important tributaries of the eastern part of the Bay of Biscay [191,192]. The higher $\delta^{13}C$ values found in deepest stations (from G18 to G24) were close to marine phytoplankton signatures. Similar C:N ratios were observed between continental shelf stations and canyon stations which ranged between 10.2 and 15.6 in surface sediments (Fig. 26 b). Sediment C:N ratios were higher than those measured in continental SPM, especially from the Gironde Estuary (8.5 ± 0.8 mol mol^{-1}) and in marine phytoplankton (6-9 mol mol^{-1}) [191,192] may due to a depletion of organic nitrogen in sediments by early diagenesis [193].

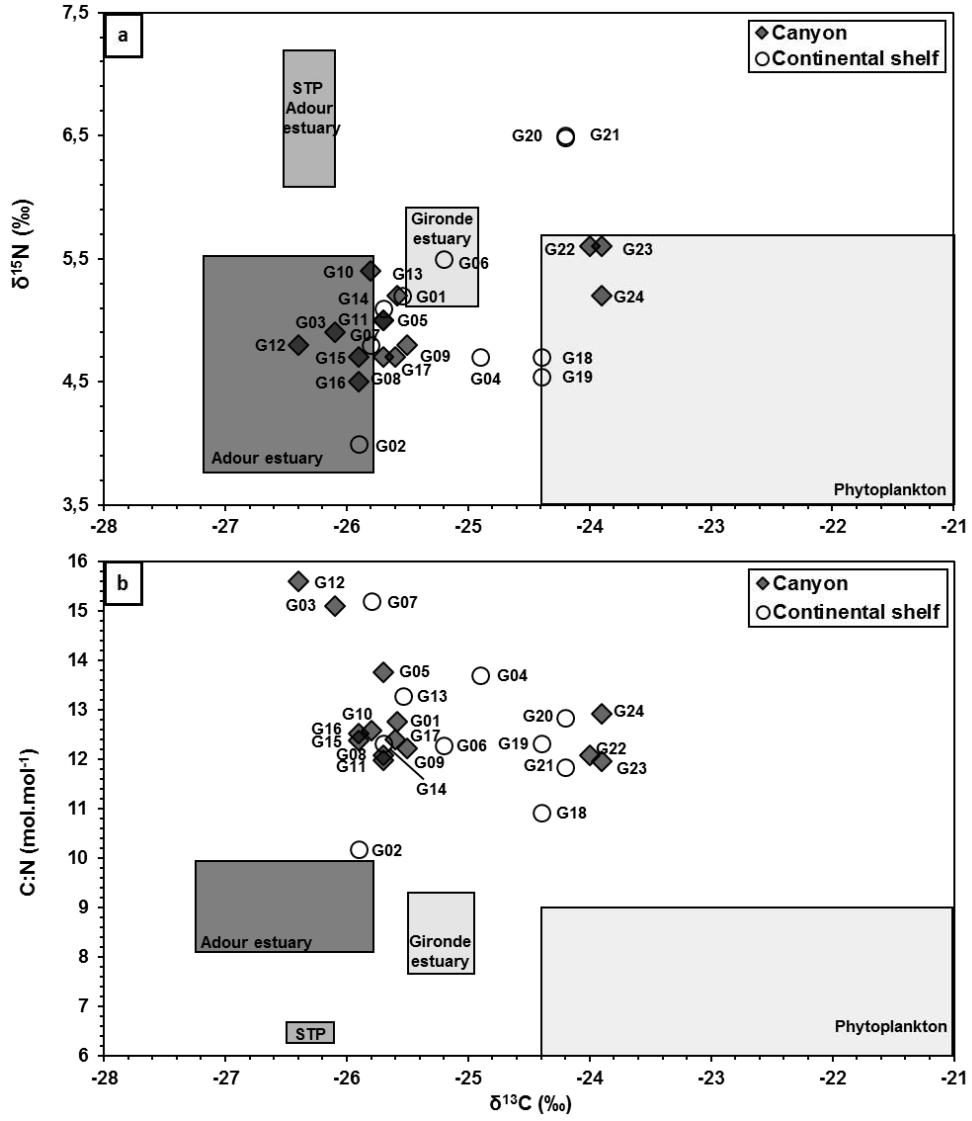

Figure 3 - Biplots showing δ13C, δ15N (a) and C:N molar ratios (b) of Capbreton canyon stations (grey diamonds) and adjacent continental shelf sediments (white circles). Reference sources of terrestrial particulate organic matter from the Adour estuary and from the Gironde estuary, particulate organic matter of Sewage Treatment Plants (STP) from the Adour estuary, and phytoplankton are represented by shaded areas (Liénart et al, 2016; Savoye et al, 2012).

3.2 Mercury compounds distribution and concentrations

Average Hg(II) concentrations in the studied sediments were higher in the canyon than the continental shelf (344.3 ± 246.0 ng g^{-1} and 101.6 ± 50.5 ng g^{-1}, respectively; Table S2, Supporting information). Hg(II) concentrations increased with the distance from the coast and the depth (Fig. 4). The average MeHg concentrations were also higher in the canyon than on the continental shelf (0.98 ± 0.48 ng g^{-1} and 0.31 ± 0.13 ng g^{-1}, respectively). No differences were observed in the proportion of total mercury (THg) as MeHg (% MeHg) between continental shelf and canyon stations. Higher % MeHg values were found for coastal stations with a maximum value at 0.9 % for the station G01 (Fig. 4).

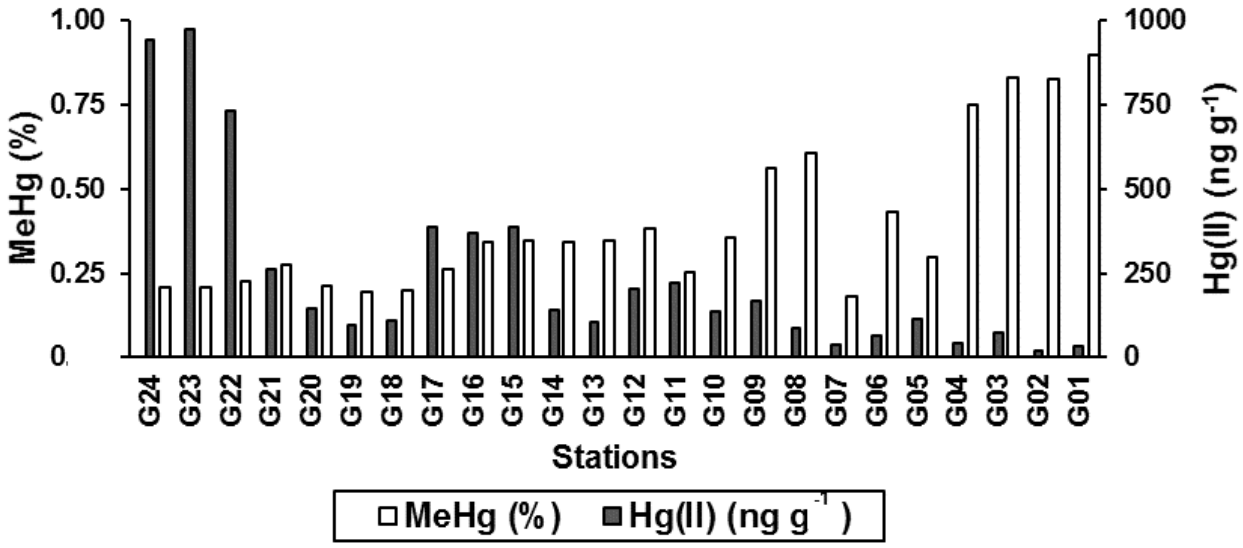

Figure 4 MeHg proportions and Hg(II) concentrations in the sediments along a canyon gradient from the coast (G01) to the off shore (G24).

3.3 Methylation / demethylation yields and rates

Higher methylation rates under biotic conditions was found in the nearshore station and decreasing along the canyon from 8.4% to 2.0 % in G10 and G24, respectively (Table 1). Very low methylation rates were observed for abiotic controls (0.2 %). For demethylation, abiotic control yields were significant and ranged between 13.9 and 17.0 %. High demethylation rates were found under biological conditions ranging between 32.2 and 44.1 % with higher yields for canyon stations (G10, G24) as compared to continental shelf station (G14).

Table 1 Methylation and demethylation rates (kM and kD), rate ratios and net production of MeHg in surface sediments under non sterile condition

Stations	k_M (% d^{-1})	k_D (% d^{-1})	k_M/k_D	Net prod. MeHg (ng g^{-1} d^{-1})
G10	0.63	1.64	0.65	0.85
G14	0.42	1.30	0.44	0.57
G24	0.14	1.83	0.14	1.24

Higher k_M was observed in coastal station, G10, with a progressive decrease in G14 until G24 with 0.63, 0.42 and 0.14 % day^{-1}, respectively (Table 1). That, clearly was demonstrated that ^{199}MeHg formed from the ^{199}Hg(II) was more rapidly formed in experiment with G10 sediment. No significant trend was observed for k_D in G10, G14 and G24 where k_D were 1.64, 1.30 and 1.83 % day^{-1}, respectively, demonstrating that Hg^{201} (II) formed from the $Me^{201}Hg$ was formed in same magnitude in all incubation experiments.

4 Discussion

4.1 Sediment inputs and transport in the canyon

Fine sediments (< 63 µm) were observed in the terraces and flanks of this canyon, although adjacent continental shelf sediment were sandy (Fig. 2a). This confirms the high activity of the canyon in the transport and trapping of fine sediments. Indeed, the Capbreton Canyon head was naturally disconnected from the Adour River in 1310 A.D., and in 1578 the river mouth was artificially relocated 15 km south of the canyon head, preventing reconnection. Despite the disconnection from the Adour River, the canyon remains active, meaning this canyon is currently being filled with suspended particulate matter from continent and column water as a result of strong particle remobilization processes [103,180]. Moreover, a strong affinity of OM for fine fraction in canyon sediments (Fig. 2a, b and c) was observed, demonstrated by strong correlations with TC, POC and PON contents. Several studies have shown the grain size and geochemical characteristics of sediments such as surface to volume ratio and OM were considered to influence chemical distribution of metals [194,195] such as mercury [196,197]. This suggests that fine fraction may have played a role and facilitated the Hg transport to the Capbreton Canyon sediments. $\delta^{13}C$ and $\delta^{15}N$ results (Fig. 23a) indicated a marine signature for OM in collected surface sediments [198–200,192,201]. Nevertheless, carbon origin was relatively different in offshore stations compared to coastal sediments. In details, stable isotope signatures and C:N ratios (Fig.3b) in nearshore stations seemed also to reveal a continental origin for the sediments with a mixture of SPM signatures mainly from the Adour estuary, and secondary from the Gironde

estuary [191,192]. The offshore bottom sediments showed a different contribution for this organic particulate material with a $\delta^{13}C$ signature close to marine phytoplankton values suggesting a hemipelagic sedimentation as complementary source of OM [103,191,192]. However, the high measured C:N ratios compared to continental SPM or marine phytoplankton and the particulate sulphur enrichment suggested a local production of OM in a N-depleted environment or intense OM mineralization processes which could lead to a N organic-depletion in the substrate by diffusion [202–205].

4.2 Mercury compounds concentrations

The National Oceanic and Atmospheric Administration (NOAA; USA) has established sediment quality guidelines for Hg that establishes concentration value for predicted with biological effects at the lower 10 percentile, Effects Range-Low (ER-L), and above median, Effects Range Median (ER-M) [206]. ERL and ERM guidelines for THg as 150 ng. g^{-1} and 710 ng g^{-1} dry weight, respectively. Similar criteria were adopted in Canada to protect aquatic life. Threshold Effect Level (TEL) and a Probable Effect Level (PEL) were reported by Canadian Council of Ministers of the Environments (CCME), for marine sediments as 130 and 700 ng g^{-1}, respectively. Hg(II) concentrations in the sediments from continental shelf of the Capbreton Canyon were lower or comparable to the NOAA and CCME recommendations while Hg(II) concentrations in the sediment collected from the slopes or terraces of Capbreton Canyon were higher than these recommendations, particularly in the deepest offshore stations. This suggests that those observed Hg concentrations could be affect the food web and indirectly the human by fish consumption. Moreover, according to Rodriguez et al. [57], Hg contents in canyon sediments were higher than the Basque country background concentration which is at 130 ng g^{-1}, except stations within the first 2.5 km to the coast. The high concentrations of Hg in the canyon indicate this canyon may act as a trap of Hg.

The Hg concentrations in the Capbreton Canyon sediments were higher than those of other Altantic Ocean submarine canyons, 10 times higher than concentrations in the Var Canyon located in the Mediterranean Sea (Table S3, Supporting information) and 20 times higher than concentrations found on the continental slope of the South West Atlantic Ocean [197]. Lamborg et al., [207] suggested that deep North Atlantic waters and most intermediate waters are anomalously enriched in mercury relative to the deep waters of the others oceans suggesting the high Hg concentrations in Capbreton Canyon may have an anthropogenic origin. Indeed, as seen elsewhere [185], a recent enrichment of anthropogenic Hg in sediments of the Cascais, Lisboa and Setubal canyons (North-Eastern Atlantic Ocean) was demonstrated, revealing human's activities have increased the Hg concentrations in these sediments via estuaries and effluents nearby these ecosystems [55]. Contrary to the

Capbreton Canyon, for example in the Nazaré Canyon (North-Eastern Atlantic Ocean), the highest Hg concentrations were found close to the coast, likely due to a natural dilution with non-contaminated sediments due to the Hg background 2 times lower in this ecosystem compared to the Basque country [57,54,185]. In accordance with the THg concentrations measured in sediments from coastal zone of Adour Estuary, nearby Capbreton Canyon, higher Hg concentrations were measured in Capbreton Canyon adjacent shelf (this study) than continental shelf sediments in the North-Eastern Atlantic Ocean (Table S3, Supporting information). This difference of concentration could be explained by the strong past metallurgic activities in the Basque country from the end of the 19th century to the early 1980s, one of the anthropogenic Hg source in environment.

4.3 Mercury compounds enrichment in the Canyon

Higher Hg compounds concentrations were found to be associated with sediment % clay (Fig. 6a and b) with strongly significant correlations for both Hg(II) and MeHg (Pearson correlation, r^2=0.70 and r^2=0.76, p-value < 0.0001, n=24, respectively). As the highest values of fine fractions were found in canyon sediments (Fig. 2a), the highest Hg concentrations were measured in the Capbreton canyon sediments as well. Hg compounds, like other trace metals, have a strong affinity with particulate material, especially fine factions (<63µm) due to adsorption process on their surface [208,209] and influence the availability of Hg [196,197]. This suggested that these sediments acted as storage and transport vectors for the Hg, determining the role of sediment particle size in their mobilization, deposition and dispersion.

Hg(II) and MeHg concentrations showed a modestly significant positive correlation with POC (Pearson correlation, r^2=0,32 and 0.54 with p-value = 0.004 and < 0.0001, respectively; Fig. 6c and d). Similar correlation between OM content and THg in sediments has been reported in several marine research studies [210,211,196,212,213] confirming the OM has a strong ability to bind with Hg [214] resulting in high concentrations of Hg associated with high concentrations of OM in those sediments.

Modestly significant correlations have been observed with PON where highest values were associated with the highest Hg compounds concentrations (Pearson correlations for Hg(II) and MeHg, r^2=0,36 and 0.58 with p-value = 0.002 and < 0.0001, respectively, Fig. 6e and f). Like carbon, nitrogen is a key component of life and a fundamental nutrient (proteins or enzymes). These results were confident with the Capbreton canyon dynamic, characterized by high sediments inputs, OM content and inputs, and substrate instability caused by bottom currents, small-scale environmental disturbances and re-sedimentation processes [215,216,103,180] leading to a Hg compounds enrichment in these canyon sediments.

The high Hg concentrations measured in canyon sediments with a strong Hg adsorption on the finest sediments particles were correlated with organic contents, suggesting that re-mobilization processes and primary production may have played a key role in Hg compounds distribution and deposition along the canyon axis [217] ,indirectly may affects methylation processes [218]. Moreover, the OM composition is a crucial factor influencing biological and abiotic processes in the sediment compartment [163,219] which enhance the methylation and demethylation processes and, hence influence the Hg biogeochemical cycle.

N:C ratios, PON, and POC contents in sediments of offshore stations were slightly lower than in coastal sediments (Fig. 3b; Table S2, Supporting information) indicating that OM was more refractory in offshore stations compare to coastal stations as previously observed by Mouret et al. [220]. Transport processes, such as bioturbation, bioirrigation, and sediment accumulation control the supply of substrates and terminal electron donors and therefore, exert an additional indirect influence on the degradation process influencing the biogeochemistry of Hg. OM deposition to the benthic zone, following increased loading of nutrients to the pelagic zone may increased the bacteria activity, such as methylating bacteria, and the MeHg formation rate increased with nutrient loading with a high Hg(II) availability for methylation, as seen elsewhere [219]. Nevertheless, Hg availability may depend of the state of degradation of OM. Indeed, the continuous alteration of OM during transport leads to a consumption of the most labile OM components and, thus, to increasingly refractory chemical structures of the sinking material [221,86,222]. Consequently, the availability of labile organic carbon in nearshore sediment might stimulate microbial activities involved in methylation process.

Althought nearshore sandy sediments were characterized by low values of the geochemical parameters and Hg(II) (Table S2, Supporting information), % MeHg of the THg were higher than offshore stations (Fig. 4). This suggests Hg(II) in coastal sediment was more available for the methylation mediated by micro-organisms, and/or Hg-methylating bacteria more active and/or the demethylation process might be less efficient than at offshore stations.

4.4 Sources of mercury compounds

Previous $\delta^{13}C$ and $\delta^{15}N$ results suggested G22, G23, and G24 sediments, where concentrations of MeHg and Hg(II) reached 2 ng g^{-1} and 973 ng g^{-1}, respectively and are associated with high clay and POC contents (Fig. 6a, b, c and d), may be controlled by hemipelagic sedimentation (Fig. 3a), local OM production and OM mineralization processes. Indeed, plankton blooms and a subsequent microbial decomposition of OM are the most

important factor influencing Hg concentrations and control the MeHg formation rate in marine sediments [219,84,223] could be responsible for the high observed Hg concentrations. Then, $\delta^{13}C$ and $\delta^{15}N$ results indicated sediments in south part of this canyon, (G03, G10, G12, G15 and G16, Fig. 1) arise mainly from Adour estuary suspended particulate matter (Fig. 3a), itself coming from turbid plumes according to Petus et al. [144], indicating Hg concentrations found in these stations may arise from terrigenous inputs. The relatively high Hg concentrations observed in the G03 location sediment, located in active gully [100] and likely indirectly connected to Adour Estuary reinforced this hypothesis. Moreover, previously reported, the MeHg and THg fluxes into the estuary, from the Adour River and various urban effluents were between 3.3 ± 5.2 g d^{-1} and 44.2 ± 28.1 g d^{-1}, respectively [224] supported by the similar fluxes in the Adour plume [82] could be a source of the Hg compounds observed in these south Capbreton Canyon locations.

These results could explain a part of high Hg concentrations found in Capbreton Canyon sediments which arose from Adour Estuary and phytoplankton. In addition, others sources such as atmospheric deposition regional-scale variability in air sea exchange of Hg, particulate settling, and lateral and vertical seawater flow are all important for determining the Hg concentrations in the open ocean [225]. Then, modern anthropogenic Hg emissions [226] are likely causing an anomalously Hg enrichment in the North Atlantic deep water [207] suggesting another source for these relatively high Hg concentrations in Capbreton Canyon sediments (Table S3, Supporting information). Additionally, a huge presence of marine snow has been recorded by HROV camera during the sampling cruise (HAPOGE, 2017) might constitute a source of MeHg because net Hg methylation can occur in it [227].

4.5 Methylation and demethylation processes and methylmercury production

The sediments collected in the canyon (G10 and G24) were characterized by higher values of POC, PON and clay fraction than the sediment collected in the continental shelf (G14). Hg compounds concentrations in G10 and G14 sediments were similar with same MeHg proportion while G24 sediment Hg compounds concentrations were higher but with a lower MeHg proportion (Fig. 4 and Table S2, Supporting information). These slurry incubation experiments demonstrate the highest methylation yield in the station nearest to the coast (G10) compared to the off shore stations (G14 and G24; Fig. 5). These results were consistent with higher MeHg proportion for coastal stations (Fig. 4). Moreover, the methylation process was mainly mediated by a bacterial activity likely influenced by the POC content (1.6, 0.92 and 1.95 % for G10, G14 and G24, respectively). Nevertheless, demethylation potential was due to both abiotic and biological processes, with a stronger biological component (Fig. 5). These experimental methylation and demethylation yields

observed highlighted the crucial role of microbial communities in the Hg cycle in such submarine canyon sediment. These results are consistent with the methylation and demethylation yields measured in sediment of the Adour Estuary [228] that is one of the most important tributary of the bay of Biscay. Additionally, the presence of anaerobic bacteria such as SRB, Hg-methylators, associated to particles of the Adour estuary plume [229,230], highlighted this hypothesis.

As previously demonstrated, the OM may be more refractory in deepest canyon sediments and hence this suggested methylation in offshore marine sediments was limited

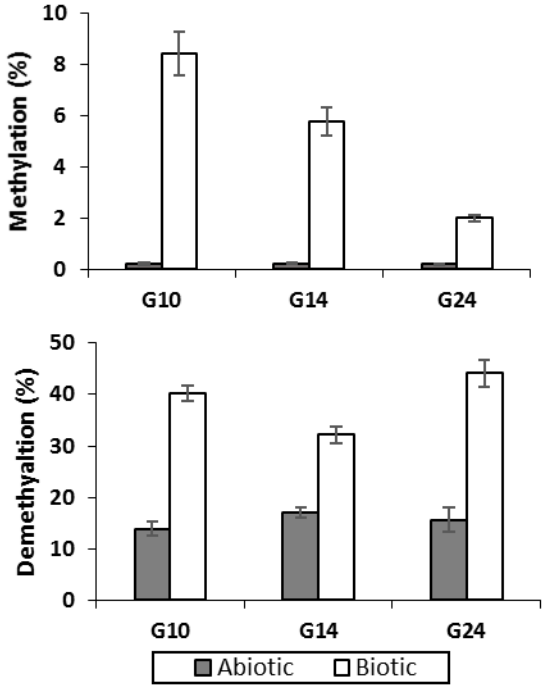

Figure 5 Methylation and demethylation yields after 2 weeks incubations of slurries from G10, G14 and G24 (70, 120 and 275 m depth of water, respectively) in biotic and abiotic conditions. Error bars represent the standard deviation of triplicate incubations.

by Hg(II) availability and the quality of OM. Consequently, Hg(II) in coastal sediment may be more available for the methylation. Moreover, the benthic mineralization of OM involves different organisms and oxidants. OM oxidation is coupled to the sequential utilization of terminal electron acceptors typically in the order of O_2, NO_{3-}, Mn(VI), Fe(III), and SO_4^{2-} followed by methanogenesis and/or fermentation [86]. Among various inorganic ligands, sulphur plays an important role in Hg complexation because TS contents are characteristic of black coloured anoxic surface sediments containing high amounts of sulphide compounds (e.g. pyrite, polysulphides). Sulphide is known to precipitate Hg(II) and consequently the high TS content could influence the availability of Hg(II) controlling the mercury speciation in

anaerobic environments [231]. Indeed, sulphate is used as electron acceptor by bacterial communities, such as SRB involving in Hg methylation and demethylation processes [83,87]. According to Benoit et al. [232], S-Hg complexation may inhibits the specific methylation rate and microbial uptake. Thus, while the higher carbon content was observed in offshore stations, possibly leading to bacterial activities, the high value of sulphur could limit the methylation process [163,231].

Results of this study suggested OM composition and S played major role in Hg biogeochemistry like MeHg formation and accumulation, as seen elsewhere [233]. The MeHg proportion (Fig. 4) ranged between 0.2 and 0.9% were consistent with the proportion generally found in marine sediments [234,51]. This quantity is determined as a steady-state condition representing the balance MeHg formation and removal processes. .The steady-state set point depends on such factors as its high sulphur content, organic carbon content, anaerobic conditions [235,236], dissolved OM [237] and calcium carbonate [162]. Moreover, the connection between the Capbreton Canyon and the Adour Estuary may be a supply of anthropogenic substances like antibiotic products which could impact the microbial composition in the sediment close to the shore [238] may be promoting the MeHg formation by selecting microbial group able to methylate the inorganic Hg.

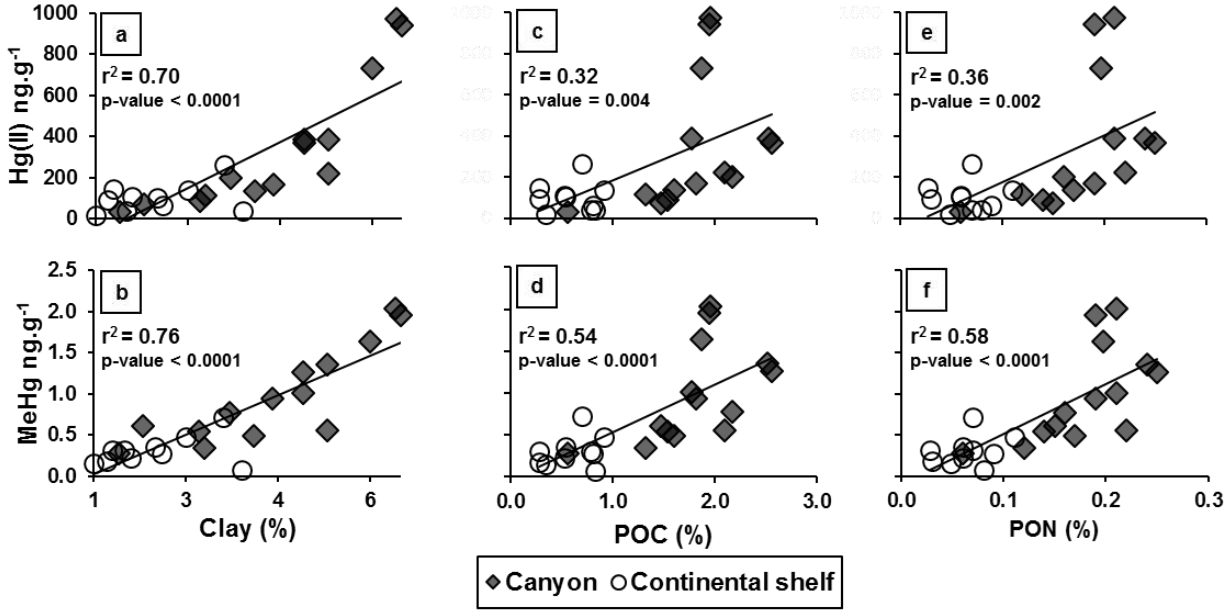

Figure 619 Relationship between Hg(II) and MeHg concentrations (ng g-1) against, clay (%) (a,b), Particulate Organic Carbon POC (%) (c,d) and Particulate Organic Nitrogen PON (%) (e,f) in surface sediment from Capbreton canyon. r2, Pearson correlation including all stations (n= 24). Continental shelf and canyon stations were represented with white circles and grey diamonds, respectively.

No data on methylation rates for submarine canyon sediments have been published, but regarding methylation rates for sediments located coastal and marine sediments, our

rates are relatively low (from 0.12 to 0.63 % day^{-1}, Table 1). Methylation rates previously found for deep sea sediments from Mediterrean Sea ranged between 0.14 and 0.71 % day^{-1} [239]; between 0.25 and 1.32 % day^{-1} in coastal sediments from the Thau Lagoon [179], between 1.6 and 8.2 % day^{-1} for near-shore marine sediments from Long Island Sound [236]. This suggested the production of MeHg in Capbreton Canyon sediments is relatively low compared to estuary and coastal ecosystems. Similar to methylation rates, our demethylation rates are relatively low (1.30 to 1.83 % day^{-1}) compared to tidal lagoon sediments from Arcachon Bay ranged between to 21 to 72 % day^{-1} [240]; 5.86 and 9.10 % day^{-1} in estuarine sediments from Adour estuary [228].

Furthermore, k_M/k_D ratio calculated from the potential rates can represent some index of the relative transformation rates for bioavailable Hg(II) and MeHg production considering these two competing processes. k_M/k_D ratios in these experimental incubations are inferior to 1 (Table 1) and consistent with those observed in the Adour Estuary [228], indicating that MeHg production may be limited by demethylation process. k_M/k_D ratio decrease along G10, G14 and G24 stations (Table 9) showing a relative low mercury reactivity in the most offshore station can explain the similar trend observed for % MeHg values (Fig. 4).

Methylation and demethylation rates at final kinetic time obtained via these current experimentations were allowed the calculation of net MeHg production with the following equation:

$$[MeHg]_{net\ production} = (k_M/100 * [Hg(II)]_{ambient}) - (k_D/100 * [MeHg]_{ambient})$$

With in situ ambient Hg(II) and MeHg concentrations, k_M and k_D kinetic constants expressed in % by day, net production of MeHg for G10, G14 and G24 are 0.85, 0.57 and 1.24 ng g^{-1} day^{-1}, respectively (Table 1). Assays of Hg methylation with added isotopes, however, overestimate the production of MeHg from the ambient Hg(II) because added Hg is more available for methylation [241]. Nevertheless, MeHg production results were positive, showing a potential MeHg source in this canyon. Although the results of experiments showed a stronger methylation potential in coastal stations, G10 and G14, compared to G24, the highest value of MeHg production was observed in G24 due to the highest concentration of Hg(II).

These results suggested that such deep marine canyon sediments accumulate Hg(II) by way of complex environmental factors (redox conditions, ambient Hg(II) concentration, availability of Hg(II), microbial activities, OM composition and origin) and may act as additionnal source of MeHg for these vulnerable ecosystems.

5 Conclusions

Concentrations of Hg compounds in Capbreton submarine canyon sediments were considerably higher than nearby continental shelf deposits and other submarine canyons. Grain size, OM composition, and sulphur content were controlled by the active transfer of particulate matter which occurs along this active canyon, and may have influenced the Hg distribution in these sediments. This study showed that submarine surface sediments are a favourable medium for methylation of Hg that mediated by biotic processes, are able to produce MeHg, and then can be a MeHg input pathway in the food web affecting the huge diversity found in those ecosystems. The presence of active submarine canyons across the world, around 120 according Harris et al. [98] feature significantly on the cycling of Hg and should be taken into account in global models. As many key processes in mercury biogeochemical cycles are still unknown or poorly characterized, a large array of investigations can be now accomplished using such experiments to unravel mercury cycling in submarine canyon systems.

Table S1 *Location, water depth and distance to the coast of sampled surface sediments in Capbreton canyon.*

Station	Latitude (N)	Longitude (W)	Depth (m)	Distance to coast (km)	Station	Latitude (N)	Longitude (W)	Depth (m)	Distance to coast (km)
Continental shelf					**Canyon**				
G02	3°39.795'	1°27.589'	61	1.4	G01	43°39.558'	1°27.592'	80	1.2
G04	3°39.841'	1°27.915'	70	1.8	G03	43°39.310'	1°27.821'	40	1.4
G06	3°40.036'	1°28.110'	80	2.3	G05	43°39.621'	1°28.176'	74	2.0
G07	3°39.528'	1°28.402'	40	2.3	G08	43°39.734'	1°28.427'	75	2.5
G13	3°40711'	1°32.750'	100	8.8	G09	43°39.775'	1°29.285'	153	3.7
G14	3°39.573'	1°33.104'	120	9.0	G10	43°39.516'	1°29.931'	70	4.4
G18	3°39.471'	1°34.858'	107	11.5	G11	43°39.910'	1°30.220'	119	5.1
G19	3°39.915'	1°36.238'	112	13.5	G12	43°39.783'	1°32.050'	100	7.6
G20	3°36.656'	1°41.368'	133	18.6	G15	43°39.732'	1°33.145'	193	9.1
G21	3°40.112'	1°40.105'	136	19.1	G16	43°39.767'	1°33.159'	193	9.2
					G17	43°42.278'	1°33.862'	138	10.6
					G22	43°38.168'	1°43.788'	399	23.3
					G23	43°38.201'	1°43.891'	248	23.5
					G24	43°63.805'	1°73.039'	275	23.5

Table S2 *Total Carbon TC (%), Particulate Organic Carbon POC (%), Particulate Organic Nitrogen PON (%), Total Sulfur TS (mg kg^{-1}), C:N ratio, carbon isotopic composition δ^{13}C (‰), nitrogen isotopic composition δ^{15}N (‰),sediment texture, HgII and MeHg concentrations (ng g^{-1}), and % of MeHg in surface sediments of Capbreton canyon and adjacent continental shelf.*

Station	TC (%)	POC (%)	PON (%)	TS (mg kg^{-1})	C:N	δ13C (‰)	δ15N (‰)	Sand (%)	Silt (%)	Clay (%)	[HgII] (ng g^{-1})	[MeHg] (ng g^{-1})	MeHg (%)
Continental shelf													
G02	1.41	0.35	0.05	0.12	10.2	-25.9	4.0	76.7	22.3	1	18.0	0.15	0.8
G04	1.83	0.79	0.07	0.20	13.7	-24.9	4.7	58.9	39.6	1.5	41.0	0.31	0.8
G06	2.17	0.81	0.09	0.25	12.3	-25.2	5.5	45.7	52.2	2.1	64.7	0.28	0.4
G07	2.16	0.83	0.08	0.59	15.2	-25.8	4.8	44.7	52.0	3.4	38.5	0.07	0.2
G13	1.32	0.54	0.06	0.09	13.3	-25.5	5.2	65.9	32.0	2	103.4	0.36	0.3
G14	2.04	0.92	0.11	0.15	12.3	-25.7	5.1	54.3	43.2	2.5	138.9	0.48	0.3
G18	1.58	0.53	0.06	0.08	10.9	-24.4	4.7	77.2	21.2	1.6	110.5	0.22	0.2
G19	1.18	0.28	0.03	0.05	12.3	-24.4	4.5	87.5	11.3	1.2	93.3	0.18	0.2
G20	1.84	0.28	0.03	0.07	12.8	-24.2	6.5	83	15.7	1.3	145.1	0.31	0.2
G21	2.38	0.7	0.07	0.11	11.8	-24.2	6.5	54.1	42.8	3.1	262.8	0.72	0.3
Canyon													
G01	1.46	0.56	0.06	0.14	12.8	-25.6	5.2	63	35.6	1.4	30.8	0.28	0.9
G03	3.28	1.47	0.15	0.27	15.1	-26.1	4.9	46.1	52.2	1.8	72.7	0.61	0.8
G05	2.75	1.32	0.12	0.51	13.8	-25.7	5.0	39.1	58.1	2.8	114.7	0.34	0.3
G08	2.81	1.54	0.14	0.26	12.1	-25.7	4.7	35.9	61.4	2.7	88.4	0.54	0.6
G09	3.26	1.82	0.19	0.42	12.2	-25.5	4.8	15.1	81.0	3.9	166.3	0.94	0.6
G10	2.97	1.6	0.17	0.42	12.6	-25.8	5.4	23.7	72.7	3.6	137.1	0.49	0.4
G11	3.58	2.1	0.22	0.53	12.0	-25.7	5.0	8.9	86.3	4.8	221.6	0.56	0.3
G12	3.54	2.17	0.16	0.39	15.6	-26.4	4.8	36.6	60.2	3.2	201.1	0.77	0.4
G15	3.92	2.52	0.24	0.36	12.4	-25.9	4.7	8.5	86.7	4.8	386.2	1.35	0.3
G16	4.09	2.56	0.25	0.29	12.5	-25.9	4.5	9.7	85.9	4.4	367.5	1.26	0.3
G17	3.68	1.77	0.21	0.24	12.4	-25.6	4.7	9.8	85.8	4.4	387.3	1.01	0.3
G22	3.67	1.87	0.20	0.21	12.1	-24.0	5.6	5.5	89	5.5	730.4	1.64	0.2
G23	3.71	1.96	0.21	0.20	12.0	-23.9	5.6	3.5	90.5	5.9	972.9	2.03	0.2
G24	3.62	1.95	0.19	0.24	12.9	-23.9	5.2	2.8	91	6.1	943.7	1.95	0.2

Table S3 *Comparison of mercury species concentrations in sediments from other marine sediments.*

Location	THg (ng g^{-1})	MeHg (ng g^{-1})	Authors
Capbreton canyon (Atl. Ocean)	31 - 973	0.28 - 2.03	This study
Continental shelf (Atl. Ocean)	18 - 263	0.07 - 0.72	This study
Cascais canyon (Atl. Ocean)	8 - 594		[55]
Cascais canyon (Atl. Ocean)	40 - 80		[185]
Nazaré canyon (Atl. Ocean)	2 - 363		[54]
Continental shelf (North-Eastern Alt. Ocean)	24 - 104		[54]
Adour estuary (Atl. Ocean)	20 - 461	0.10 - 0.24	[56]
Coastal zone of Adour estuary (Atl. Ocean)	25 - 477		[242]
Basque country background (Atl. Ocean)	30 - 270		[57]
Var canyon (Med. Sea)	18 - 61		[52]

Figure S1 *Relationship between Hg(II) (a) and MeHg concentrations (ng g^{-1}) (b) against, Total Sulfur (TS, mg kg^{-1}) in surface sediments from Capbreton canyon. Continental shelf and canyon stations were represented with whited and shaded plot symbols, respectively.*

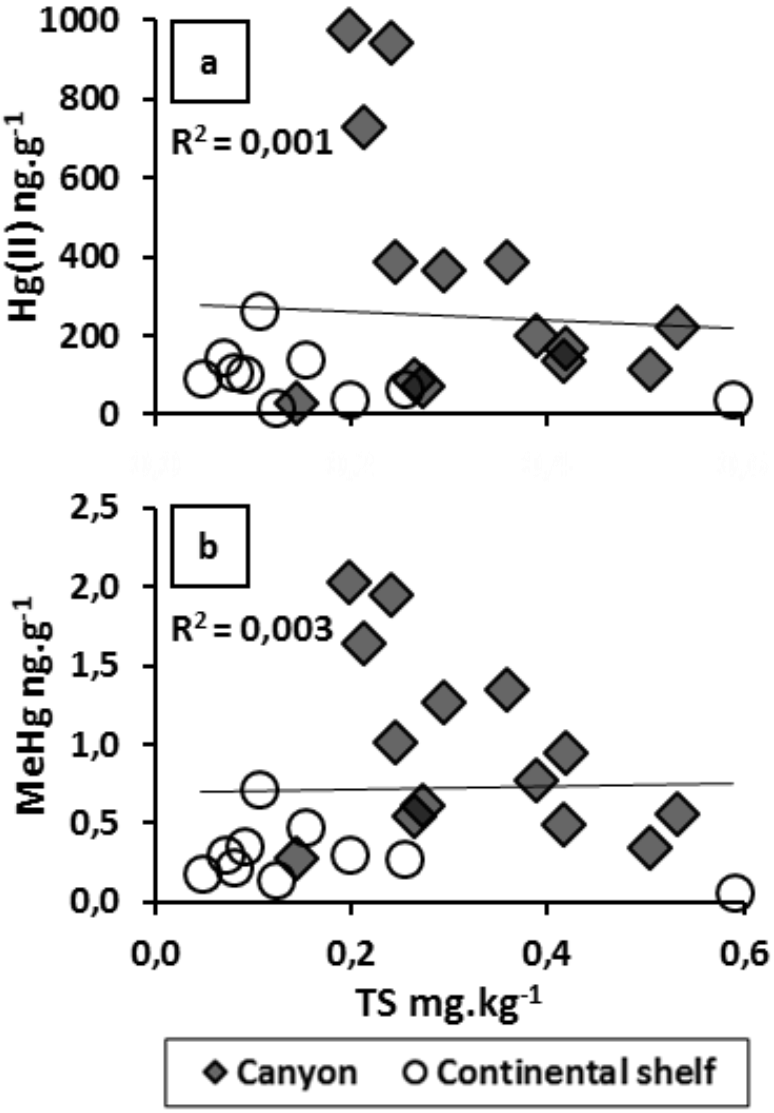

1.C - STABLE ISOTOPES OF CARBON AND MERCURY AS TRACERS OF PARTICULATE INPUTS IN SUBMARINE CANYON SEDIMENTS OF CAPBRETON (NORTH ATLANTIC OCEAN)

Alyssa Azaroff, Emmanuel Tessier, David Amouroux, Zoyne Pedredo Zayas, Rémy Guyoneaud, Mathilde Monperrus

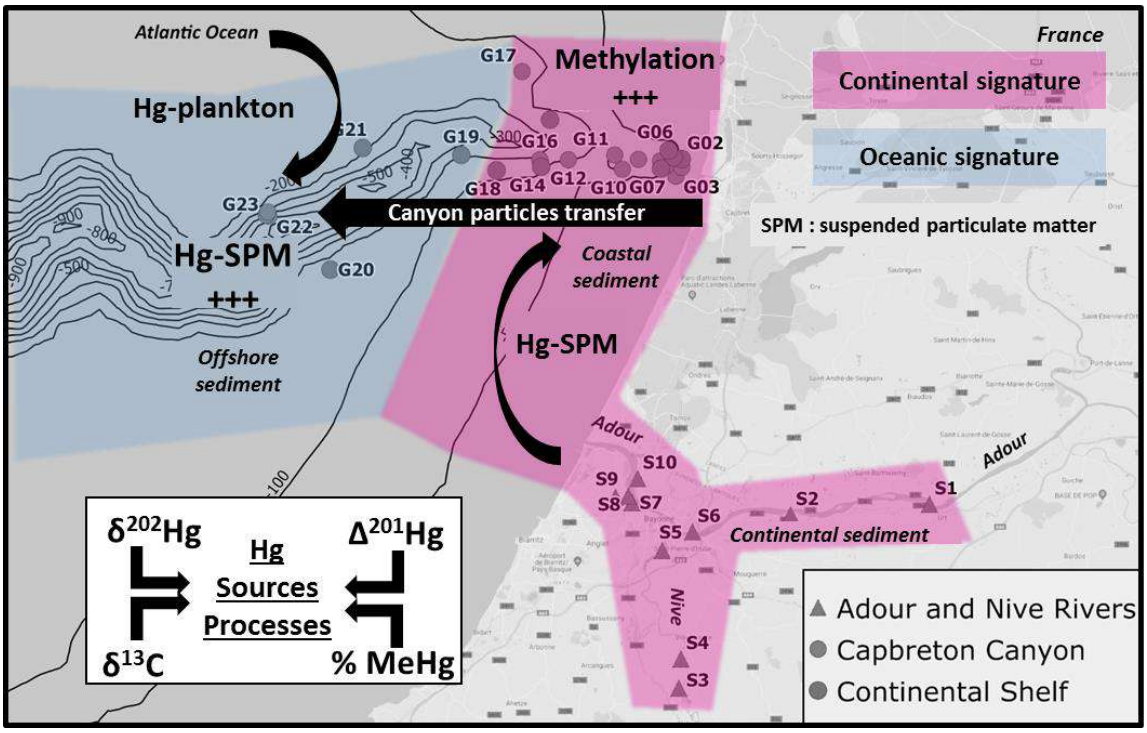

En préparation

Résumé

Le compartiment sédimentaire contitue une matrice intégrative pour le mercure (Hg) provenant à la fois de sources anthropiques et naturelles. Les variations spatiales des rapports isotopiques du Hg permet de renseigner sur les sources et sur les processus environnementaux. Dans cette étude, la composition isotopique du mercure a été étudiée dans les sédiments de surface d'un transect le long du canyon de Capbreton. La mise en relation de la composition isotopique du Hg en fonction des concentrations de mercure et de la composition isotopique du carbone (δ13C) a permis de mettre en évidence les sources potentielles de mercure. Aucune diférence significative de la composition isotopique n'a été observée entre les sédiments du canyon et du plateau continental. Cependant, les rapports isotopiques variaient en fonction des concentrations de mercure avec une augmentation de δ^{202}Hg de la côte vers le large. Les sédiments côtiers (10 premiers km) étaient caractérisés par des δ^{202}Hg plus faibles compris entre -0.94 ‰ to -0.48 ‰. En revanche, les stations les plus éloignées présentaient des valeurs de δ^{202}Hg comprises entre -0.62 ‰ to 0.-27 ‰. Ces résultats suggèrent des sources de mercure différentes entre les stations côtières et les stations au large (distance à la côte supérieure à 13km). Les ratios isotopiques retrouvés dans les sédiments côtiers étaient très similaires à ceux détectés dans l'estuaire de l'Adour, suggère que les apports de mercure d'origine continentale sont dominant dans les zones côtières. Les différentes origines de Hg observées dans ces sédiments sont renforcées par une corrélation positive entre le δ^{202}Hg et le δ^{13}C. Des MDF plus faibles pour les stations estuariennes et côtières suggèrent également une contribution plus importante de la méthylation du mercure microbienne. Des valeurs de MDF plus élevées observées dans les sédiments les plus éloignés peuvent indiquer que le pool de mercure est lié non seulement aux entrées de mercure provenant de l'estuaire de l'Adour, mais également à celles provenant de sources atmosphériques et hémipélagiques. De plus, des faibles valeurs de fractionnement indépendant de la masse (Δ^{199}Hg) ont été trouvées dans les sédiments, indiquant que le pool de mercure est peu influencé par les réactions photochimiques.

Mots clefs : Soruces de mercure, réactivité, composition isotopique du mercure, composition isotopique du carbone

Abstract

Sediments are an integrative compartment for mercury (Hg) originating from both anthropogenic and natural sources. The measurement of spatial variations of Hg isotope ratios in sediments may enable source identification and tracking of environmental processes. In this study, isotopic composition of Hg (was studied in surface sediments of a transect along the Capbreton Canyon. In order to track sources, Hg isotopic signature was related with the mercury concentrations and carbon isotope composition ($\delta^{13}C$). No distinct differences in Hg isotopic composition were observed between canyon and continental shelf sediments. However isotopic ratios varied according Hg concentrations levels with an increase of $\delta^{202}Hg$ from the coast to the deep ocean. The coastal sediments (first 10 km) showed lower $\delta^{202}Hg$ values ranging from -0.94 ‰ to -0.48 ‰. In contrast, the furthest stations exhibited $\delta^{202}Hg$ values from -0.62 ‰ to -0.27 ‰. These results suggest that coastal stations were impacted by different Hg sources or/and different Hg transport than deep sea stations. Isotope ratios found in the coastal sediments were very similar than those detected in the adjacent Adour estuary, suggested Hg terrestrial inputs as the dominating Hg source in near coastal regions. The different Hg origin in the canyon sediments is reinforced by a positive correlation between the $\delta^{202}Hg$ and the $\delta^{13}C$. Lower MDF for estuarine and coastal stations suggest also a higher contribution of microbial Hg methylation. Higher MDF values observed in the furthest sediments may indicate that Hg pool is not only related to the Hg inputs from the Adour estuary but also by atmospheric and hemipelagic sources. Moreover, low average of mass independent fractionation ($\Delta^{199}Hg$) at -0.04 ‰ ± 0.10 ‰ was found in sediments may indicate that the Hg pool is poorly influenced by photochemical reactions

Key words : Mercury sources, reactivity, mercury isotope composition, carbon isotope composition

1. Introduction

Mercury (Hg) is harmful toxicant which can be transported rapidly around the globe because of its high volatility and atmospheric transport [49]. Ocean play a very important role in global mercury (Hg) cycling [211]. Indeed, the global open oceans receive ~4.0×10^6 kg of Hg, mainly through atmospheric deposition [49]. High part of these inputs of Hg to the oceans come from anthropogenic Hg emissions, which have dramatically increased since the preindustrial era [207,243]. Hg can be easily converted into methylmercury (MeHg), a neurotoxin that can be biomagnified though higher trophic levels. Marine sediments are an integrative compartment for Hg originating from both anthropogenic and natural sources. While Hg inputs in marine ecosystem are mainly come from atmospheric deposits, sources of mercury (Hg) in these biologically productive systems remains unknown. Nevertheless, burial of Hg in ocean margin sediments represents a major sink in the global Hg biogeochemical cycle that has not been previously considered [244].

Capbreton submarine canyon is located at only 250 meters from the coast. Consequently that is a direct transfer zone between the continent (e.i. potential Hg anthropogenic inputs, rivers discharges) and the open ocean. An estimated 90% of river-derived Hg is buried in sediments at ocean margins [245], could be a potential Hg source in this canyon. First results about the mercury speciation (e.i. Hg(II) and MeHg) have demonstrated an enrichment of fine particles and mercury compounds in the Capbreton canyon sediments from the coast to the offshore [126] within the 30 first km. Hg(II) reached until almost 972 ng g^{-1}. This concentration was very high compare the local natural background (130 ng g^{-1}) [57] and others comparative areas [126]. Moreover, submarine canyons are home to important stocks of commercial fish species [107]. Hence, their consumption by human might represent a significant risk of exposure to monomethymercury (MeHg) accumulation [246].

Mercury has seven natural stable isotopes (^{196}Hg, ^{198}Hg, ^{199}Hg, ^{200}Hg, ^{201}Hg, ^{202}Hg, and ^{204}Hg). Research among these Hg stable isotopes biogeochemistry offer new insight for the mercury behavior. Studies of environmental samples demonstrated a large variation of Hg isotopic composition dependant about their sources [247]. Moreover, this approach can reveal biogeochemical processes though both mass-dependent fractionation (MDF, δ^{202}Hg) and mass-independent fractionation (MIF, Δ^{199}Hg) of the Hg isotopes [248]. Variation of MDF and MIF were observed during laboratory experiments demonstrated microbial-mediated reactions (e.i. reduction, methylation, demethylation), abiotic chemical reactions (e.i. photoreduction, chemical reduction) and physical processes (e.i. volatization, evaporation, adsorption and dissolution) [214]. Hence, the measurement of spatial variations of Hg

isotope ratios in sediments may enable source's tracking of environmental processes, through the study of mass dependant (MDF) and mass independent (MIF) fractionations of Hg isotopes.

The fate of mercury depends of several biogeochemical processes [249]. For instance the microbial methylation is responsible of the methylation of inorganic mercury (Hg(II)) into methylmercury (MeHg), a harmful toxicant for the environment and humans. More, micro-organisms in marine sediments are important in the organic matter decomposition for nutrient regeneration [250]. As Hg stable isotopes, carbon stable isotope ratios ($\delta^{13}C$) provide clues about the origins and transformations of organic matter [251]. Because, both mercury and carbon stable isotopes track sources and transformations of Hg and C, respectively, and mercury fate is influenced by the organic matter origin and states, it is interesting to study them together [252,253] as tools for understanding complex ecological processes involved in the Hg cycle.

The aim of this study is to investigated isotopic composition of surface sediments from a transect along the Capbreton Canyon to identify their sources and determine geochemical processes. Relationship with mercury concentrations and carbon isotope composition will also study in order to better understand mercury sources and fate in Capbreton Canyon sediments.

2. Material and methods

2.1 Study area and sampling strategy

The Capbreton Canyon (South-Eastern Bay of Biscay, NE Atlantic) begins 250 m from the coastline and reaches up to 3000 m water depth. Sediment were sampled in July 2017 during the HAPOGE oceanographic cruise. Twenty-four stations were sampled within the first 23.5 km of the Capbreton Canyon area with a Hybrid Remotely Operated Vehicle (HROV Ariane, Ifremer) and a Shipeck grab sampler. Fourteen stations were located in the Canyon and in adjacent slopes or terraces, between 40 and 399 m depth, extending from 1.2 km to 23.5 km from the coast (Fig. 1). Ten stations were located on the adjacent continental shelf between 40 and 136 m depth, extending from 1.4 km to 19.1 km from the shore (Fig. 1).

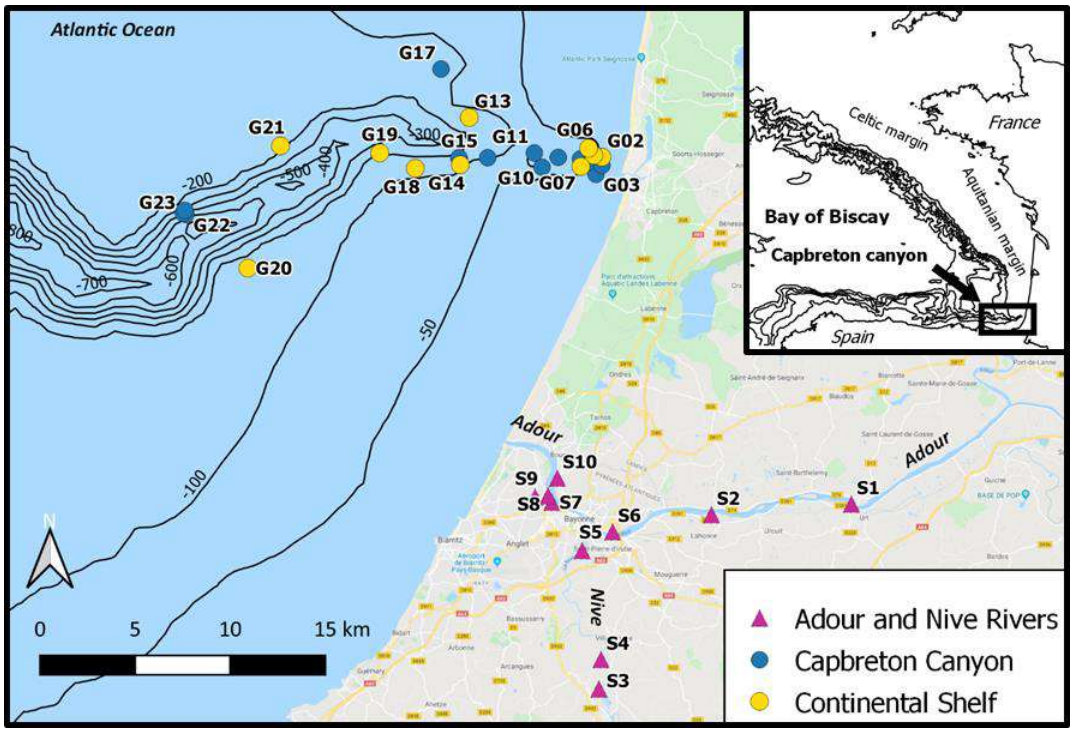

Fig. 1 – Sampling of surface sediments from Capbreton submarine Canyon and this adjacent continentan sheld and from the Adour estuary.

In order to identify Hg sources, data of mercury isotope composition from sediments of the Adour and Nive Rivers were also used to compare with Capbreton Canyon data. The focal point of the study corresponds to the middle and down estuary, between the mouth of the estuary (West) and upstream to the maximum salinity intrusion on the Adour (East) and Nive river (South-East). The Adour estuary has been drastically modified and canalized in the last century. The upstream part of the estuary flows through agricultural areas, while the downstream part is within the Bayonne urban district and is subjected to urban and industrial inputs. Briefly, 10 surface sediment samples (0-5 cm) were collected from the Adour estuary (Fig. 1) during three campaigns in the Adour estuary and Nive river: 09-11 May 2017 (ADOUR 1), 18-21 September 2017 (ADOUR 2) and from 31 January to 02 February 2018 (ADOUR 3). Sediments samples collected before by Stoichev et al. [17] in October 2000-June 2001, were also analyzed.

All samples were freeze-dried, homogenized and ground in an agate pestle and mortar before analytical procedures. Mercury isotope composition was analysed in all samples (described in 2.2 section). In parallel, for each samples of Capbreton Canyon area, carbon isotopes and THg concentration were already analysed [126].

2.2 Total mercury isotopes composition

The determination of total mercury (THg) isotopes composition was performed according to the procedure described by Perrot et al. [254]. Briefly, crushed dried samples

were pre-digested with 3 mL nitric acid (HNO_3 69-70 %, Instra) and 1 mL of chloric acid (HCl 33-36 % ,Ultrex) overnight before a total mineralization carried out with Digi-Prep Junior for 4 hours at 85°C (SCP Science, Quebec, Canada). Another cycle of mineralization (2 hours, 85°C) was carried after addition of 1 mL of peroxide (H_2O_2, Optima grade) in order to release carbonate. Then samples were centrifuged in order to remove solid particles (10 min). The supernatant, stored at 4°C, was then diluted with 2% HNO_3 to be at final concentration between 0.5 and 1 ppb.

Total Hg isotopic compositions of samples were measured for the six most abundant stable Hg-isotopes (^{198}Hg, ^{199}Hg, ^{200}Hg, ^{201}Hg, ^{202}Hg, and ^{204}Hg) relative to the bracketing standard NIST SRM-3133 reference material using cold-vapor-MC-ICP-MS (Nu Instruments, Wrexham, UK). A desolvating nebulizer system from Nu Instruments (Wrexham, UK) was used to introduce NIST SRM-997 thallium for the instrumental mass-bias correction using the exponential law. Reference materials UM-Almaden NIST 8610 (University of Michigan, USA) and certified materials, SRM 1944, IAEA405 and NIST-2702, were used as secondary standards. Results demonstrated a good accuracy and are in accordance with previous results (UM Almaden: $\delta^{202}Hg$= -0.55 ± 0.13, $\Delta^{199}Hg$= 0.04±0.12, n=43; IAEA 405: $\delta^{202}Hg$= -0.31 ± 0.12, $\Delta^{199}Hg$= -0.03 ± 0.09, n=3; SRM1944 : $\delta^{202}Hg$= 0.37 ± 0.14, $\Delta^{199}Hg$= 0.04 ± 0.08, n=6; NIST-2702 : $\delta^{202}Hg$= -0.71 ± 0.18, $\Delta^{199}Hg$= 0.00 ± 0.09, n=22) [255–257]. Reproducibility of the isotopic data was assessed by measuring replicate sample once every 10 samples.

Mass dependent fractionation (MDF) of samples are reported using delta notation according to the following equation, in permil (‰) (1) [247] :

(1) $\delta^{202}Hg_{\ sample} = (^{xxx/198}Hg_{\ sample} / {}^{xxx/198}Hg_{\ NIST\ 3133}) \times 1000$

Mass independent fractionation (MIF) signatures of odd isotopes ^{199}Hg and ^{201}Hg are expressed using capital delta notation, according to the following equations, in permil (‰) (2,3) [247]:

(2) $\Delta^{199}Hg = \delta^{199}Hg - 0.252 \times \delta^{202}Hg$

(3) $\Delta^{201}Hg = \delta^{201}Hg - 0.752 \times \delta^{202}Hg$

3 Results and discussion

3.1 Hg isotopic compositions in sediments from Capbreton Canyon area

The Hg isotope composition in sediments from the Capbreton canyon area (n=24, including samples from canyon and adjacent continental shelf) and the Adour and Nive rivers are presented in Table 1.A and B.

Average of $^{199}\Delta$Hg were at -0,04 ‰ ± 0,08 ‰ and -0,03 ‰ ± 0,14 ‰ for sediments from the Capbreton Canyon and the continental shelf, respectively (Table 1A). No significant difference was observed between the Canyon and the adjacent continent shelf. Overall, $^{199}\Delta$Hg, and $^{201}\Delta$Hg values extended from -0.14‰ to 0.02 ‰, and -0.18 ‰ to 0.04 ‰, respectively (Table 1A). Minor variation of MIF values ($^{199}\Delta$, $^{201}\Delta$) and values closed to 0 may indicate that Hg pool in sediments is a mixture of different reservoirs (atmospheric, organic matter, minerals)[226]. That is in accordance with high hydrodynamic in this submarine canyon leading to different inputs of Hg which can sink in the sediment compartment [103].

Photoreduction of Hg(II) and MeHg impart negative Hg-MIF ($\Delta 199Hg < 0$) in the produced Hg(0), and therefore cause positive Hg-MIF ($\Delta 199Hg > 0$) in residual Hg(II) [258]. The negative $^{199}\Delta$Hg results for all samples (or close to 0) from this area may indicate that Hg in sediments was poorly affected by photochemical processes [226]. It is likely due to the high affinity of Hg for the particles. Indeed, Hg binding on particles can inactive Hg reactivity and inhibit photochemical reduction [82]. That is reinforce with the strong correlation between fine fraction contents and mercury species concentrations observed in these sediments already demonstrated in a previous work [126].

Table 1 *– Isotopic composition of sediments sampled in Capbreton Canyon (CC) and this adjacent continental shelf (CS) (July 2017) (A) and in the Adour estuary (2017-2018 and 2000-2001 campaign) (B). Results in permil (‰).*

(A) Campaign	Site	202δ	201Δ	199Δ
Capbreton Canyon (July 2017)	G01	-0,75	-0,01	-0,04
	G02	-0,77	0,00	-0,13
	G03	-0,58	-0,11	-0,10
	G04	-0,55	0,04	0,08
	G05	-0,48	-0,13	-0,03
	G06	-0,67	-0,01	-0,03
	G07	-0,94	-0,18	-0,14
	G08	-0,73	-0,01	-0,10
	G09	-0,51	-0,08	0,01
	G10	-0,63	0,02	-0,03
	G11	-0,52	0,01	-0,03
	G12	-0,48	-0,09	-0,06
	G13	-0,51	-0,05	-0,04
	G14	-0,51	-0,08	-0,01
	G15	-0,62	0,00	-0,08
	G16	-0,55	-0,09	-0,09
	G17	-0,48	-0,06	0,00
	G18	-0,56	-0,12	-0,07
	G19	-0,44	-0,04	0,00
	G20	-0,29	-0,03	0,02
	G21	-0,27	-0,07	-0,02
	G22	-0,42	-0,04	0,00
	G23	-0,40	-0,04	-0,06
	G24	-0,32	-0,02	0,00
	Average CC	**-0,53**	**-0,05**	**-0,04**
	2 SD	0,24	0,09	0,08
	Average CS	**-0,56**	**-0,05**	**-0,03**
	2 SD	0,43	0,13	0,14
	Average	**-0,54**	**-0,05**	**-0,04**
	2 SD	0,31	0,11	0,10

(B) Campaign	Site	202δ	201Δ	199Δ
Adour1 (May 2017)	A1	-0,73	-0,06	-0,06
	A2	-1,02	-0,11	-0,12
	A3	-0,30	-0,13	-0,08
	A4	-0,74	-0,11	-0,08
	A5	-0,90	-0,12	-0,12
	A6	-0,72	-0,08	-0,12
	A7	-0,52	-0,04	-0,04

	A8	-0,84	-0,09	-0,03
	A9	-0,70	-0,04	-0,08
	A10	-1,02	-0,16	-0,11
	Average	**-0,75**	**-0,09**	**-0,08**
	2 SD	0,44	0,08	0,06
Adour2 (Sept. 2017)	A1	-1,00	-0,06	-0,03
	A2	-0,93	-0,07	-0,07
	A3	-0,76	-0,12	-0,10
	A4	-0,82	-0,13	-0,13
	A5	-0,97	-0,10	-0,13
	A6	-0,77	-0,03	-0,04
	A7	-0,67	-0,06	-0,07
	A8	-0,65	-0,03	-0,02
	A9	-0,82	-0,08	-0,04
	A10	-0,79	-0,08	-0,07
	Average	**-0,82**	**-0,08**	**-0,07**
	2 SD	0,23	0,07	0,08
Adour3 (Sept. 2018)	A1	-1,06	-0,10	-0,04
	A2	-0,97	-0,15	0,00
	A3	-0,09	0,01	0,00
	A4	-0,51	-0,12	-0,05
	A5	-0,90	-0,07	-0,03
	A6	-0,78	-0,08	-0,10
	A7	-0,54	-0,06	-0,01
	A8	-0,90	-0,06	-0,03
	A9	-0,88	-0,11	-0,07
	A10	-0,95	-0,09	-0,07
	Average	**-0,76**	**-0,08**	**-0,04**
	2 SD	0,59	0,09	0,06
Adour (2000-2001)	A1	-0,90	-0,06	-0,06
	A2	-0,88	-0,04	-0,05
	A3	-0,81	-0,07	-0,10
	A4	-0,85	-0,08	-0,10
	A6	-2,21	0,01	0,02
	A7	-1,32	-0,04	0,00
	A8	-1,10	-0,01	-0,10
	A9	-1,19	-0,17	-0,10
	A10	-1,00	-0,06	-0,07
	Average	**-1,14**	**-0,06**	**-0,06**
	2 SD	0,87	0,10	0,09

Average of $^{202}\delta$Hg were at -0.53 ‰ ± 0.23 ‰ and -0.56 ‰ ± 0.46 ‰ for sediments from Capbreton Canyon and the continental shelf, respectively (Table 1A). No significant difference of MDF was observed between sediments from the Capbreton Canyon and the

adjacent continental shelf. Nevertheless, high range of MDF was observed in all samples ranging from -0.94 ‰ to -0.29 ‰. According to Blum et al. [226], a high range of MDF suggests that several geological processes (sorption /desorption, OM burial, diagenesis) are involved in the Hg isotope fractionation. That confirms the Capbreton Canyon is a transfer zone of particles and the high affinity of mercury for these particle leading to mercury accumulation in the sediment compartment. Moreover this high extend can also suggest different potential sources described below.

The MDF and MIF from Capbreton Canyon sediments were similar to the MDF and MIF from sediments sampled of the continental slope near the Campos Basin (Brasil) (between 400 and 3000 meters depth) [197]. That may indicate that processes involved in Hg fate are similar in deep marine sediments. Moreover it was also comparable to marine surface sediment associated with point sources of Hg contamination [214,226]. That may indicate Hg in Capbreton Canyon sediments have anthropogenic sources.

3.2 Hg and C isotopes highlighting Hg sources in Capbreton Canyon sediments

The relationship between the $^{202}\delta$Hg (MDF) and THg concentrations demonstrated a strong difference for the Hg concentration between the Capbreton Canyon and this adjacent continental shelf while there is not significant difference for MDF (Fig. 2).

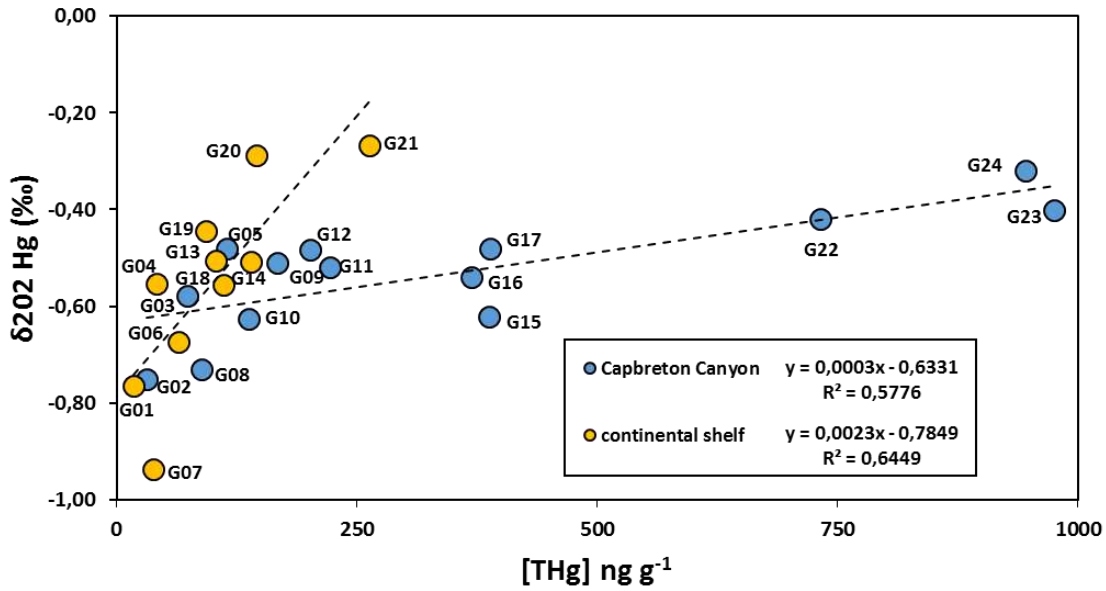

Fig. 2 – δ202Hg isotopic composition versus THg concentration in sediments from Capbreton Canyon and adjacent continental shelf. R² Determination coefficient, Pearson correlation, p-value < 0.05

Higher Hg concentrations and $^{202}\delta$Hg values were observed in offshore sediments. Indeed, more positive $^{202}\delta$Hg values were observed in offshore sediments compare to coastal sediments, with higher value at -0.21 ‰ in G21 (located at 19 km from the coast). This trend was comparable with others similar studies [55,259]. That may indicate a variation

of MDF with the distance to the coast. That reinforced with the relationship between $^{202}\delta$Hg values and the distance to the coast where $^{202}\delta$Hg values increased with the distance to the coast (Fig. 4A).

A strong adsorption of Hg with fine sediments and particulate organic carbon were also observed (p-value< 0.001, n=24)[126]. Indeed, Capbreton Canyon acts as sink for fine particles and POC with an enrichment of Hg species [126] suggesting that the Capbreton Canyon system is a trap for Hg. Relationship between THg concentration and δ^{202}Hg suggested that higher concentration of THg in sediments sampled in offshore with a MDF (Fig. 2, 3) according the distance to the coast (Fig 4.A). That could indicate different geological processes and/or a mixing of sources in offshore sediments compare sediments sampled close to the coast.

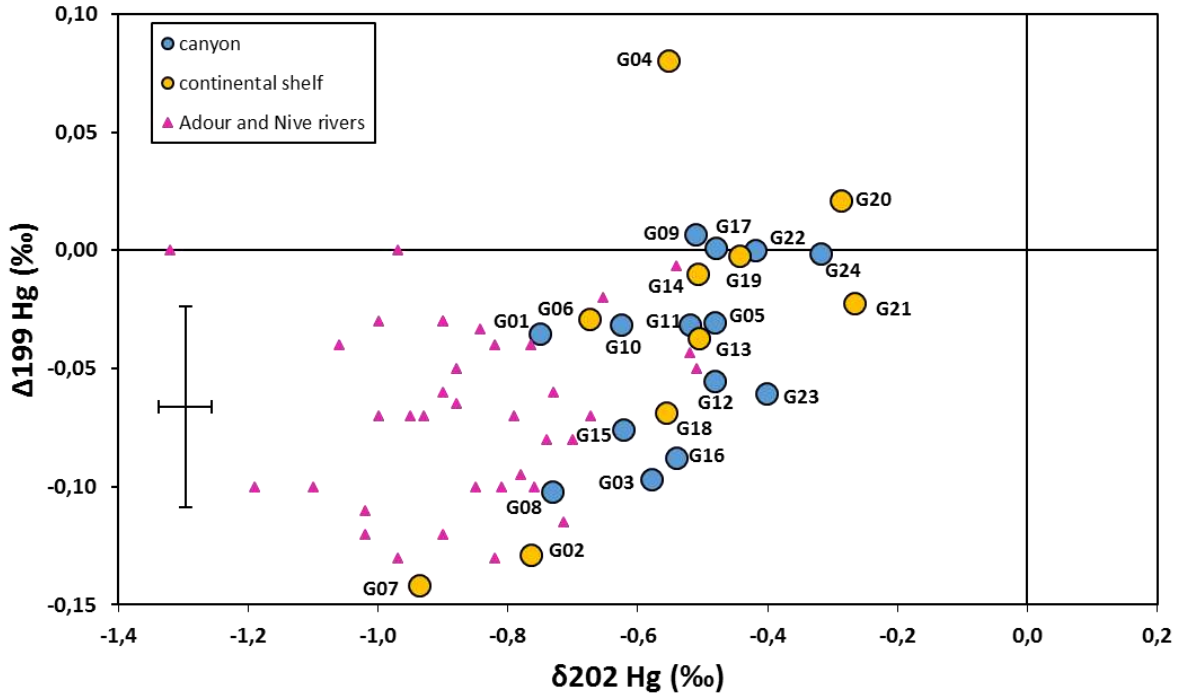

Fig. 3 - δ202Hg isotopic composition (MDF) versus 199ΔHg isotopic composition (MIF) in sediments from Capbreton canyon and continental sediments from Adour and Nive rivers and (unplublished data, Marchan Moreno, 2019). Average of uncertainties corresponded to 0.04 ‰ and 0.06 ‰ for Δ199 Hg and δ202 Hg, respectively

Comparison of $^{202}\delta$Hg values observed for the Adour watershed sediments and the Capbreton canyon sediments showed similar isotopic composition of Hg in sediments from the first 11.5 km of the Capbreton Canyon and those from the Adour and Nive rivers (Fig. 3, 4). Carbon isotopic composition confirmed that carbon originated from sediments sampled within the first 11.5 km of the Capbreton Canyon are related to the Adour particulate organic matter [191,192]. Contrary to these samples, sediments from offshore locations (superior to

13.5 km from the coast) showed a carbon composition related to a marine signature (e.i. plankton). .

Overall, isotopic compositions of Hg and C showed a terrigenous signature in sediments sampled in the first 11.5 km, where sediments can originate from gravitational sedimentation of continental suspended particulate matter. According the C isotope composition, offshore sediments exhibit a more oceanic signature. That suggests Hg sources along the canyon transect are mainly due to continental sources for the mouse of the then gradually replaced by oceanic sources (hemipelagic sedimentation, plankton). Moreover, Hg isotopes ratios in these sediments may indicate a point source of Hg contamination (i.e. metallurgic activities, industrialized runoff and/or atmospheric deposits)[226]. The river deliveries of Hg from industrial and urban sources and natural soils could be the main inputs of Hg in estuarine and coastal sediments [214]. In offshore sediments, we suggest plankton could pre-concentrate Hg in the column water [260] and then, may contribute to increase the Hg content in sediments through particles sedimentation.

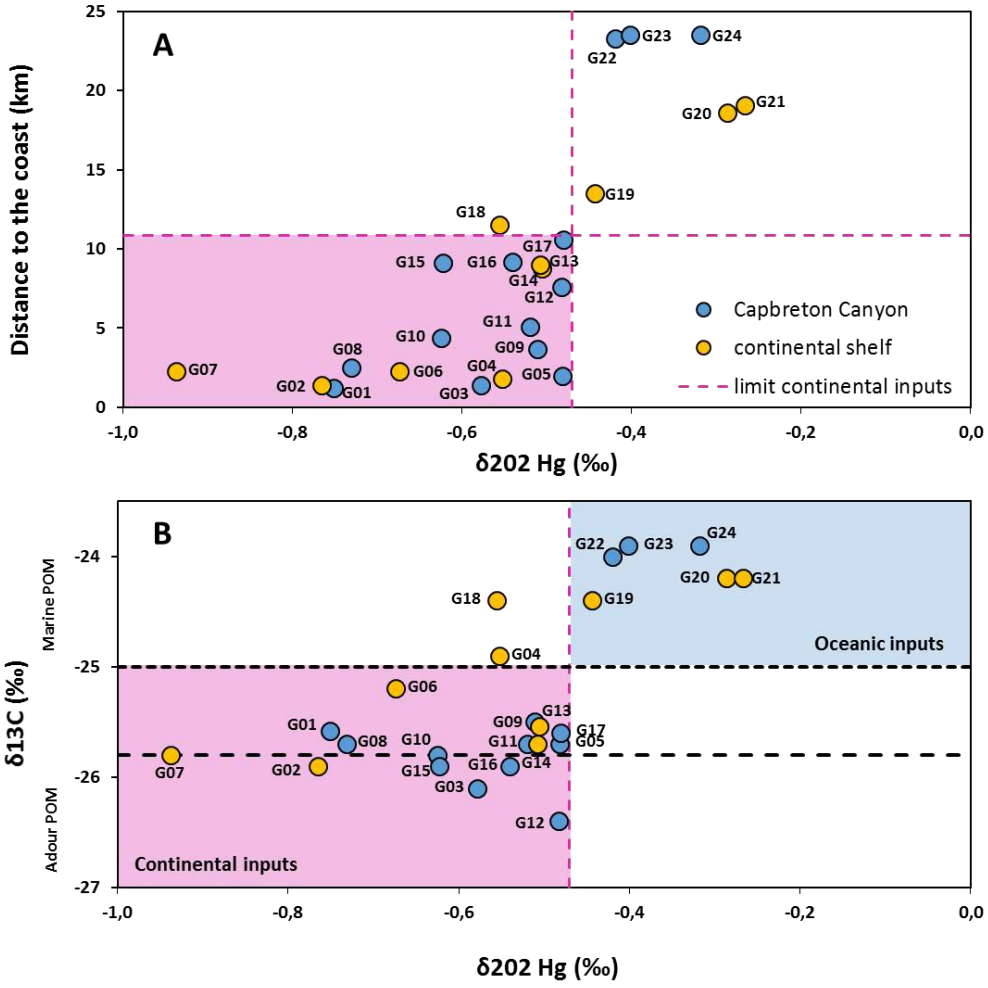

Fig. 4 – A : δ^{202}Hg isotopic composition (MDF) along the canyon transect (distance to the coast) and B : δ^{202}Hg isotopic composition (MDF) versus carbon isotopic composition (δ^{13}C). Marine and Adour

estuary POM from [191,192]. *Pink and blue squares show continental inputs and oceanic inputs, respectively. Analytical associated uncertainties were ≤ 0.2‰ for δ13C and ≤ 0.08‰ for δ202Hg.*

3.3 Hg isotope composition vs microbial methylation activities

It has been shown that microbial methylation of Hg(II) generates a lighter isotopic composition (MDF) for the reaction product (MeHg) than the reagent (Hg(II)) [261]. Thus, microbial methylation can generate a negative MDF. A previous study has demonstrated an high bio-methylation in coastal locations [126], may indicate that is one of the geochemical processes involved in the Hg fate in the Capbreton Canyon sediments [226] (Fig. 3). That suggests that the negative MDF observed in coastal sediments compare to the offshore sediments is coming from the higher microbial methylation in sediments close to the coast (Fig 3, Fig 4A) [226]. Nevertheless, Hg in environment depends also of the sources, biogeochemical cycling and reactions. That suggest others parameters conduct to these Hg isotopic compisition. Indeed, Yin et al. [214], demonstrated that the Hg is transported from large amount of suspended organic particle of riverine inputs could be less fractionated. Consequently, it is possible to identify potential sources of Hg because the signature is not altered. More, in deep ocean (here in offshore locations), source-related signatures of Hg isotopes may have been altered by natural (bio)geochemical processes (e.g., Hg2+ photoreduction and preferential adsorption processes, microbial methylation, thiol ligands), especially through the deposition by air to the surface of water [214].

Although Hg concentrations increased with the distance to the coast in this canyon, the % MeHg decreased with higher value in coastal location at 0.90 % in station G01. That suggested higher production of methylmercury in coastal sediments [126]. Stoichev et al. [56] had also showed high proportion of MeHg in the Adour estuary (ranged 0 - 1.8 %) due to microbial methylation in the sediment. Rodriguez et al had also demonstrated the involvement of sulfate reducing bacteria in the MeHg net methylation production especially in anoxic zones [85]. The Adour estuary is one of the most important tributary of SPM in the Capbreton Canyon [144].. However, higher biotic methylation potential was determined in coastal sediments compare to offshore sediments in this Canyon [126]. These results were consistent with the methylation potential measured in sediment of the Adour Estuary [228]. That highlight higher methylation in this area lead to increase the % of MeHg and to the decrease of the MDF.

Overall, the more negative values for the mass dependant fractionation observed in coastal sediments is in accordance with the proportion of MeHg and methylation potential results, confirming higher bio-methylation in sediments closed to the coast.

4. Conclusion

MDF and MIF in these sediments might indicate Hg pool in the sediments of the Capbreton canyon is under control of both microbial methylation and Hg sorption on particulate matter., Lower MDF in coastal sediments could be attributed to higher microbial methylation activities, as confirmed by higher methylation potential previously measured [126]. Isotope composition may indicate two main sources of Hg in these sediments with terrigenous inputs in coastal location (11.5 first km) and Hg related to particles (inorganic/phytoplankton) adsorption in offshore location. Nevertheless, the use of Hg isotopes as tracers in source attribution could be limited due to natural processes involved in the isotope fractionation such marine ecosystem.

CHAPITRE 2

DIVERSITE MICROBIENNE

ET

BIOTRANSFORMATION DES MICROPOLLUANTS

CHAPITRE 2 – DIVERSITE MICROBIENNE ET BIOTRANSFORMATION DES MICROPOLLUANTS

Le devenir des micropolluants est défini par un ensemble de paramètres dont leurs intéractions avec les paramètres géochimiques (e.i. pH, granulométrie, matière organique…) qui définiront par la même occasion leur biodispobilité vis-à-vis des communautés microbiennes.

Ces dernières sont reconnues pour être efficace et « éco-friendly » dans les stations de traitements de eaux usées par l'utilisaiton des boues dites activées. En conditions contrôlées (e.i. température, oxygénation, anaérobie), l'activité de consortiums microbiens est optimisée pour permettre la dégradation de la matière organique mais aussi de substances organiques de synthèse (e.i. prioritaires et émergentes)

Ce chapitre à pour objectif de répondre aux deux dernières problématiques qui sont :

- Mettre en relation la biodiversité bactérienne et la présence de ces micropolluants

- Evaluer la capacité résilience naturel d'un milieu marin profond à cet apport de micropolluants

Une première partie initulée « Microbial degradation of selected emerging contaminants in marine system : from sediments to pure strains » est consacrée à l'étude de la dégradation des micropolluants émergents (e.i HHCB, AHTN, ODPABA, OC et CBZ). La complémentarité des approches permet dans un premier temps d'estimer les temps de demi vie de trois de ces substances (e.i. HHCB, ODPABA et CBZ) par l'incubation de sédiments en conditions controlées. Ensuite, après des étapes d'enrchissement en présence de ces 5 micropolluants émergents des souches bactériennes ont été isolées et identifiées. Elles ont été comparé à la diversité des commnunuautés microbiennes *in situ*. Et finalement, des tests de dégradation ont été effectués pour estimer leur potentiel de bioremédiation.

Une seconde partie intitulée « Marine mercury-methylating microbial communities from coastal to Capbreton canyon sediments (North Atlantic Ocean) » est consacrée à l'étude des communautés microbiennes impliquées dans la méthylation du mercure. En effet, dans le chapitre précédent, il a été démontré une capacité de méthylation dans les sédiments du canyon de Capbreton avec un plus haut potentiel dans la zone cotière (chapitre 1.B). A partir de trois sédiments échantilllonnés le long du canyon, par une approche de cloning/sequencing, a été étudié le gène impliqué dans la méthylation du mercure afin d'identifier pour la première des bactéries et archeas porteuses de ce gène dans des sédiments marins profonds

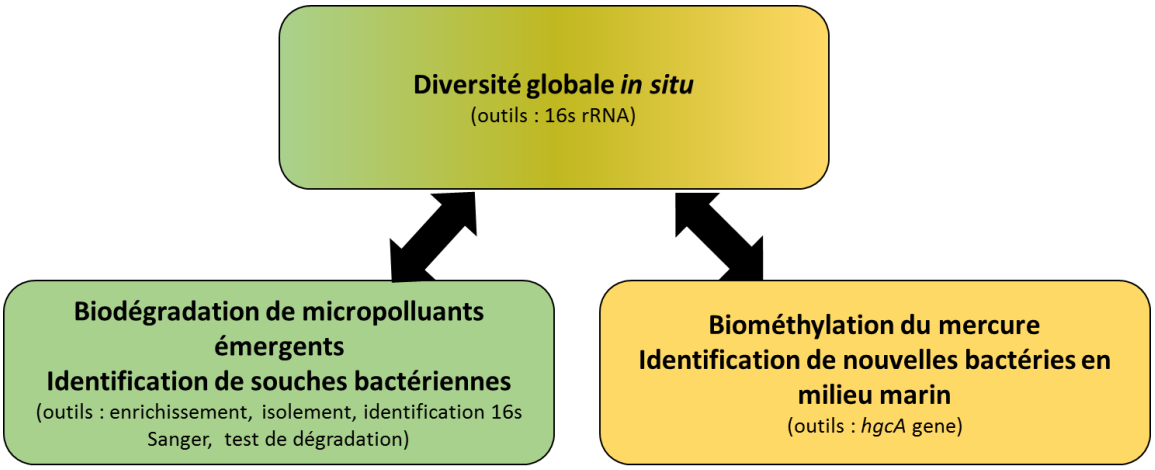

Valorisation de ce chapitre:

Publications:

Microbial degradation of selected emerging contaminants in marine system : from sediments to pure strains, Azaroff A, Monperrus M, Miossec C, Gassie C, Guyoneaud R. (***submitted in Hazardous Material***)

Marine mercury-methylating microbial communities from coastal to Capbreton canyon sediments (North Atlantic Ocean), (***published*** in Environmental Pollution Jounal) Azaroff A, Goni M, Gassie C, Monperrus M, Guyoneaud R

Présentations:

“Fate of emerging micropollutants and mercury in Capbreton Submarine Canyon sediment in controlled experimentations (Biscay Bay, SW France); Azaroff A., Monperrus. M, Gassie C., Tessier E., Guyoneaud R., USA, Sacramento , SETAC North America, November 2018. (***Poster***)

“Microbial activities versus mercury species reactivity in the deep sea sediment of the Capbreton Submarine Canyon (Biscay Bay, SW France)”; Azaroff A., Guyoneaud R., Tessier E., Gassie C., Deborde J., Monperrus M., USA, Sacramento , SETAC North America, November 2018. (***Oral***)

“Assessment of microbial communities and geochemical parameters determining the mercury methylation in Submarine Canyon sediments (Atlantic Ocean, SW France)”; Azaroff A., Guyoneaud R., Tessier E., Deborde J., Gassie C., Goni M., Monperrus. Krakow, Poland, The 14th International Conference on Mercury as a Global Pollutant (ICMGP), September 2019.(***Oral***)

2.A - MICROBIAL DEGRADATION OF SELECTED EMERGING CONTAMINANTS IN MARINE SYSTEM : FROM SEDIMENTS TO PURE STRAINS

Alyssa Azaroff, Mathilde Monperrus, Carole Miossec, Claire Gassie, Rémy Guyoneaud

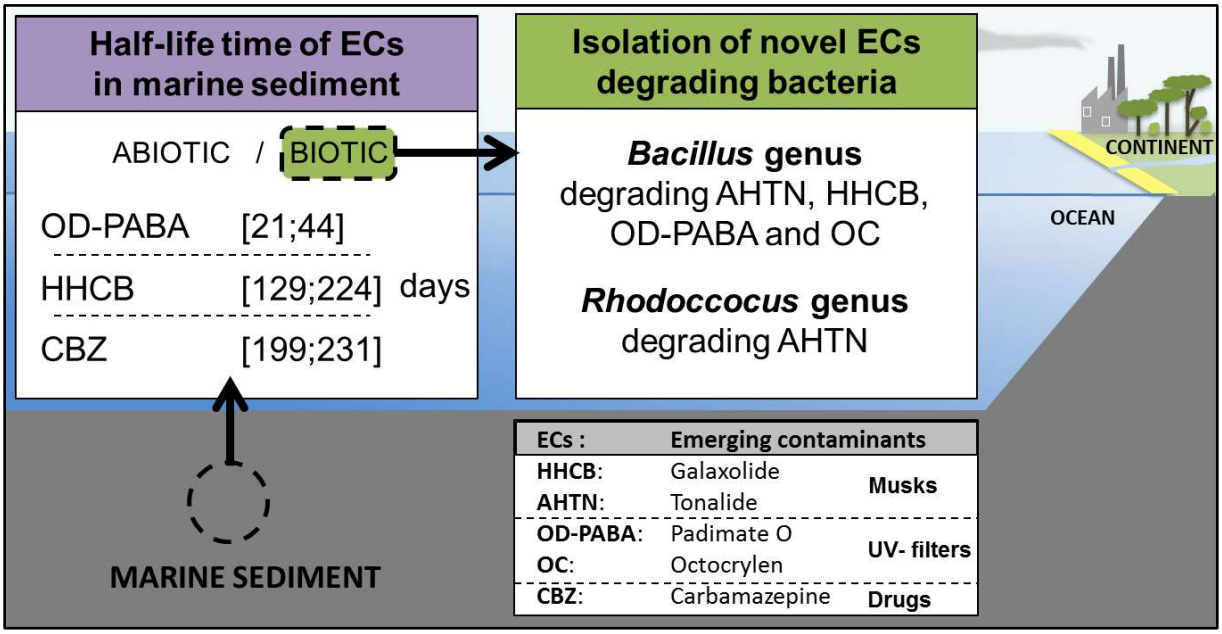

Submitted in Hazardous Material journal, 2020

Résumé

Bien que les polluants émergents soient de plus en plus étudiés dans les matrices environnementales, les données relatives aux environnements marins font encore défaut, en particulier en ce qui concerne leur devenir et leur potentiel de dégradation. Dans ce travail, pour la première fois, la dégradation de muscs synthétiques (galaxolide et tonalide), de filtres UV (O padimate et octoctrylène) et d'un composé pharmaceutique (carbamazépine) a été étudiée dans des échantillons de sédiment marin, en laboratoire. Après incubation, les temps de demi-vie en conditions biotiques ont été estimé à 21 jours, 129 jours et 199 jours pour O padimate, le galaxolide et la carbamazépine, respectivement. Ensuite, les enrichissements effectués dans des conditions à la fois anoxiques et oxiques ont démontré que, dans des conditions anaérobies, les dégradations après un mois d'incubation dans des conditions biotiques et abiotiques étaient limitées par rapport aux conditions aérobies. De nouvelles bactéries aérobies capables de dégrader les muscs synthétiques et les filtres UV ont été isolées. Ces nouvelles souches étaient principalement liées à *Bacillus megaterium*. Sur la base de ces résultats, les souches isolées capables de dégrader ces substances émergentes récalcitrantes pourraient avoir une forte implication dans la résilience naturelle en milieu marin et pourraient être également être utilisés dans les processus de dégradation artificiels.

Mots clefs : micropollutants émergents, muscs synthétiques, filtres UV, composés pharmaceutiques, dégradation, sédiments marins, souches bactériennes

Abstract

Despite emerging contaminants (ECs) are more and more monitored in environmental matrices, there is still a lack of data in marine ecosystems, especially on their fate and degradation potentials. In this work, for the first time, the degradation potential of synthetic musks (galaxolide and tonalide), UV filters (padimate O and octocrylene) and a pharmaceutical compound (carbamazepine) was studied in marine sediment samples, under laboratory conditions using sediment slurry incubations under biotic and abiotic conditions. Minimum half life times under biotic conditions were found at 21 days, 129 days and 199 days for padimate O, galaxolide and carbamazepine, respectively. Enrichments conducted under anoxic and oxic conditions demonstrated that degradations after one month of incubation either under both biotic and abiotic conditions were limited under anoxic conditions compared to oxic conditions for all the contaminants. Novel aerobic bacteria, able to degrade synthetic musks and UV filters have been isolated. These novel strains were mainly related to the Genus Bacillus. Based on these results, the isolated strains able to degrade such ECs, can have a strong implication in the natural resilience in marine environment, and could be used in remediation processes.

Key words : Emerging contaminants, musks, UV filters, pharmaceuticals, degradation, marine sediments, pure bacterial strains

1 Introduction

As a result of the last century, Man created and is still creating new synthetic substances. Contrary to the contaminants regulated in industrialized countries (European Commission, US, Japan), emerging contaminants (ECs) are not yet regulated. The scarce information available of their occurrence, reactivity and impact have led to a rising interest in identifying and screening these new compounds in the environment [58]. ECs in the environment are not necessarily new chemicals. They are substances whose occurence and significance were taken into account recently. (NORMAN project; http://www.norman-network.net). Among those ECs, pharmaceuticals and personal care products (PPCPs) are substances widely consumed and continuously released in the environment, mainly through wastewater, both treated and untreated[262,263].

Marine ecosystem is the final receptor for these organic ECs. They were found in marine sediments, mainly close to the high density population coast nearby the main estuaries [13,65,66]. ECs are characterized, for some of them, to be hazardous for the environment, endocrine disruptors, highly persistent due to their strong affinity for particles (log K_{ow} >4). Marine sediments act as integrative matrices reflecting the pollution state in a given area [116,117]. The affinities of contaminants with the suspended particulate matter (SPM) lead them to be readily scavenged from the water column and to be deposited in the sediments. Submarine canyons are known to act as transfer zones of suspended particulate matter and contaminants between the continent and the open ocean where organic pollutants can be accumulated [124,185,264] into these productive ecosystems containing important stocks of commercially important fishes. Capbreton Canyon is located nearby the coast, with important urban and agricultural activities. Additionally, wastewater treatment plants (WWTPs) are known to be an important pathway for introduction of ECs both through sewage water and particles released in aquatic environment [265,266]. In coastal areas, those WWTPs might be the main source of ECs in coastal and submarine sediments [264].

Microorganisms play a key role in ecological processes such as biogeochemical cycling and among them the carbon cycle and the organic compounds degradation. This bioremediation provides an important ecosystem service for the maintenance of the environment quality. The physicochemical properties of the sediment, such as organic carbon, grain size or pH, drive most of its interactions with the contaminants [118]. The bioavailability for the dwelling benthic organisms of these ECs depend of the adsorption, desorption and transformation processes which are themselves under control of the biogeochemical parameters. These compounds can be hazardous for the sediment-dwelling benthic organisms but also can be source of carbon for microorganisms that can degrade or

mineralise them. Consequently, the fates of ECs in submarine canyon sediments depend on physicochemical properties, and on the presence and activity of microorganisms that possess the ability to biodegrade them, i.e., use them as carbon and/or electron sources.

Several studies were performed to explore bioremediation by microorganisms of priority contaminants such as polycyclic aromatic hydrocarbons (PAHs) and polychlorinated biphenyl (PCBs) [11,267]. Few studies have shown the potential of bacteria and microbial consortia involvement in the ECs remediation [95]. Biotransformation potential of ECs in natural and oceanic environments is still unknown and it is urgent to better understand their fate in marine ecosystems [59].

The aim of this present work was to study the degradation potentials of ECs such as synthetic musks (galaxolide, HHCB; tonalide, AHTN), UV filters (padimate O, OD-PABA; octocrylene, OC) and an antiepileptic (carmabazepine, CBZ) in marine sediments in order to highlight, for the first time their natural resilience in a submarine canyon sediments. Moreover, a specific focus was put on the isolation of pure strains exposed to these hazardous substances in order to estimate their capacities in biotransformation of these contaminants in natural ecosystems and more particularly in marine sediments.

2 Material and methods

2.1 Study area and sampling strategy

The Capbreton Canyon (South-Eastern Bay of Biscay, NE Atlantic) begins 250 m from the coastline and reaches up to 3000 m water depth. In this study, we focused on two surface sediments (G10 and G14) sampled in the Capbreton Canyon area during the oceanographic cruise HAPOGE organized in July 2017. Surface sediments (0–10 cm) were sampled with Shipeck sampler grab. First sampling station was into the canyon (G10) and the second one was on the adjacent continental shelf (G14) at 4.4 and 9 km from the coast, and at 70 and 120 meters of depth, respectively (Fig. 1). After collection, the sediment samples were placed into sterile polyethylene bags sealed and stored in the dark at 4°C until slurry incubations in the laboratory (described further) within 48 h. In parallel, for each sample, contaminants analysis and geochemical parameters were analysed. Briefly, G10 sediments were more muddy than those in G14 and were characterized with particulate organic matter of 1.60 % and 0.92 %, respectively and fine grain size (<63 µm) of 76 % and 46%, respectively.

.

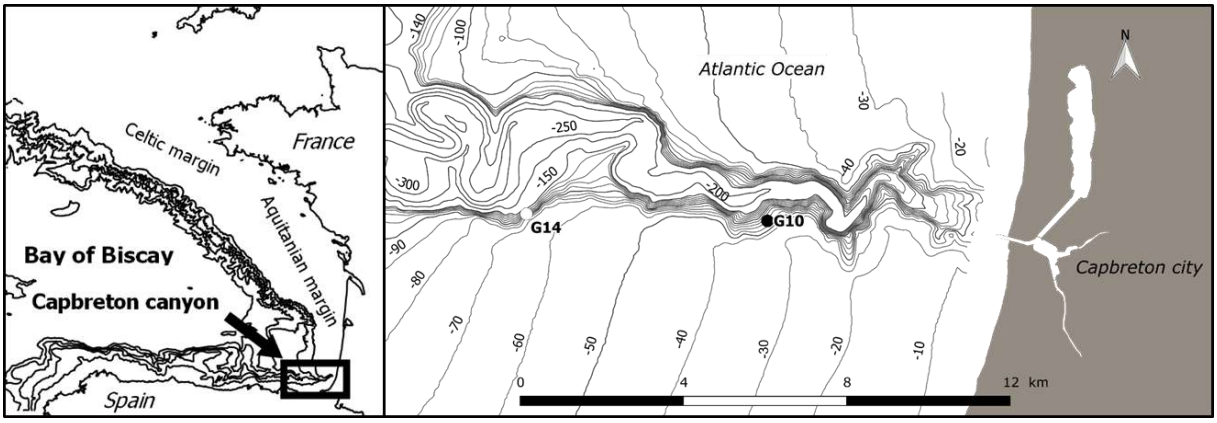

Fig. 1 Sediment sampling sites in the Capbreton Canyon (dark circle) and on the adjacent continental shelf (white circle). Isobath data from SEDIMAQ3 (Gillet 2012).

2.2 Chemicals

Ethyl acetate (EtOAc) and methanol were of analytical grade and supplied by Sigma Aldrich (Saint-Louis, USA). Acetone (laboratory reagent. 99.5%) used for cleaning the glassware was supplied by Fisher (Hampton, USA). Ultrapure water was obtained with a PURELAB Classic water purification system from Veolia (Paris, France). Reference standards of galaxolide (HHCB), octocrylene (OC), padimate O (OD-PABA) and carbamazepine (CBZ) were purchased from Sigma–Aldrich. Tonalide (AHTN) was purchased from LGC Standards (Molsheim, France). Internal standards musk xylene-d15 (MX-d15) (100 ng μL^{-1} in acetone) was purchased from LGC Standards and carbamazepine-d10 (CBZ-d10) (100 ng μL^{-1} in methanol) was purchased from Sigma Aldrich.

2.3 Determination of half life : sediment slurries incubations

In the laboratory slurry incubations spiked with HHCB, OD-PABA and CBZ were performed for 110 days in order to estimate the degradation potential (Fig. 2). Briefly, for each station (G10 and G14), a slurry was prepared by mixing fresh sediment with underlying water (50:50, w:w). Incubation experiments were performed in 10 mL glass tubes sealed with PTFE stoppers filled with 10 g of slurry. For all assays under abiotic and biotic conditions, HHCB, OD-PABA and CBZ were added independently, to have a final concentration at 100 $\mu g\ g^{-1}$. Initial time assays were stopped immediately by storing samples at -80°C whereas incubated assays were placed in the dark at 14°C (*in situ* temperature) and stopped at different elapsed times until 110 days. Slurries under abiotic condition (control), were twice sterilized for 20 min at 120 °C. All assays were performed in triplicate.

Based on the assumption that degradation reaction of these contaminants are of pseudo-first-order (1),biodegradation rate constants (k) were estimated with the following equation (2) :

(1) $Ln(C)= f(t)$

(2) $k= Ln(C_0/C_t)_t$

Where C_t is the concentration of the contaminant at the kinetic time t; C_0 is the initial contaminant concentration; k is the biodegradation rate constant and t is the time. Then, half time reactions were also determined by the following equation (3):

(3) $t_{1/2} = Ln(2)/k$

2.4 Enrichment experiments

In order to do a selective enrichment of microbial populations potentially involved in the ECs degradation, 0.5 grams of oxic (surface, 0.1 cm, clear yellow color) and 0.5 grams of anoxic (dark color) sediments (Fig. 2) were subsamples from the last days of sediment slurry incubations and were diluted with modified multipurpose medium [268] at 20 g L^{-1} of NaCl, called MM_{20} . The medium contained : 1 L of MilliQ water, 1 ml of SL_{12}, 1 mL SeTg, HEPES 10 mM, yeast extract 0.1 g L^{-1}, 20 g NaCl, 3 g $MgCl_26H_2O$, 0.15 g $CaCl_2 H_2O$, 0.25 g NH_4Cl, 0.5 g KCl. pH was ajusted at pH= 7.5 before sterilization and autoclave (20 min at 120°C). After autoclaving, 1 mL of solution V7 (vitamins) and KH_2PO_4 (final concentration of 0.2 g L^{-1}) were added with a syringe and a cellulose nitrate 0.2 µm filter (Fisher).

Emerging contaminants, HHCB, AHTN, OD-PABA, OC and CBZ were added independently at 100 µM final concentration (corresponding to 25, 25, 28, 36 and 24 ppm, respectively). These ECs have low solubility in water (Table 1), and they were added first into the tube with organic solvent (EtOAc, or methanol for CBZ) and evaporated at ambient temperature, under microbiological safety cabinet (MSC). This step was performed in order to release organic solvent, a potential carbon source [269]. Enrichment was performed in an agitator (120 rpm) [81] under oxic and anoxic conditions, at 27°C for one month. This enrichment was repeated three times, with each time a dilution at approximatively 1/11 of the previous assay. Briefly, under MSC, micropollutant was added in a falcon tube (50 mL) or penicillin tube (100 mL) (for oxic and anoxic conditions, respectively). Then 5.5 mL of the MM_{20} were added before the addition of 0.5 g of anoxic and oxic sediments from the slurry incubations (1st step, Fig 2). After one month in the agitator, new tubes were prepared with ECs by using the same protocol. Then 5 ml of MM_{20} were added and inoculated with 0.5 ml of the previous enrichment, corresponding to a 1/11 dilution (2nd and 3rd steps, Fig. 2).

Table 1 – Charateristics of the emerging contaminants used in this study. Log K_{ow} is octanol/water partition coefficient.

Compound	Family	Formula		Molar mass g mol^{-1}	Solubility in water mg L^{-1}	log K_{ow}	References
Galaxolide (HHCB)	Musk	$C_{18}H_{26}O$	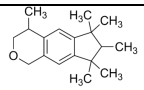	258,4	1,75	5,70	[270]
Tonalide (AHTN)	Musk	$C_{18}H_{26}O$	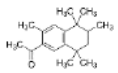	258,4	1,25	5,90	[270]
Padimate O (OD-PABA)	UV filter	$C_{17}H_{27}NO_2$		277,4	0,54	6,15	[147]
Octocrylen (OC)	UV filter	$C_{24}H_{27}NO_2$	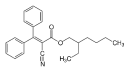	361,5	0,36	6,88	[155]
Carbamazepine (CBZ)	Pharmaceutical	$C_{15}H_{12}N_2O$	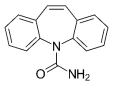	236,3	17,7	2,45	EPA's EPI Suite™

2.5 Strains isolation experiments

After the third enrichment step, in order to isolate the strains previously selected and enriched, solid medium of MM_{20} (with 20 g L^{-1} of agar bacteriologic, previously rinsed 3 times with ultrapure water) were prepared in Petri plates. Under MSC, micropollutants were added (274, 274, 306, 498 and 254 µl of HHCB, AHTN, OD-PABA, OC and CBZ at 1000 ppm, respectively) at the surface of the solid medium and organic solvent was evaporated. Then, inocula of the last enrichments were spread at the surface of the solid medium with sterile inoculator and sealed with parafilm before incubation for 1 month, at 27°C to favour the growth of colonies. After one month, colonies were selected and isolated by streak plates as described (A, B, C steps, Fig. 2). Then all strains isolated were stored at -80°C in sterile LB (20 g L) supplemented with NaCl (20 g L^{-1}), and glycerol 30% (v:v).

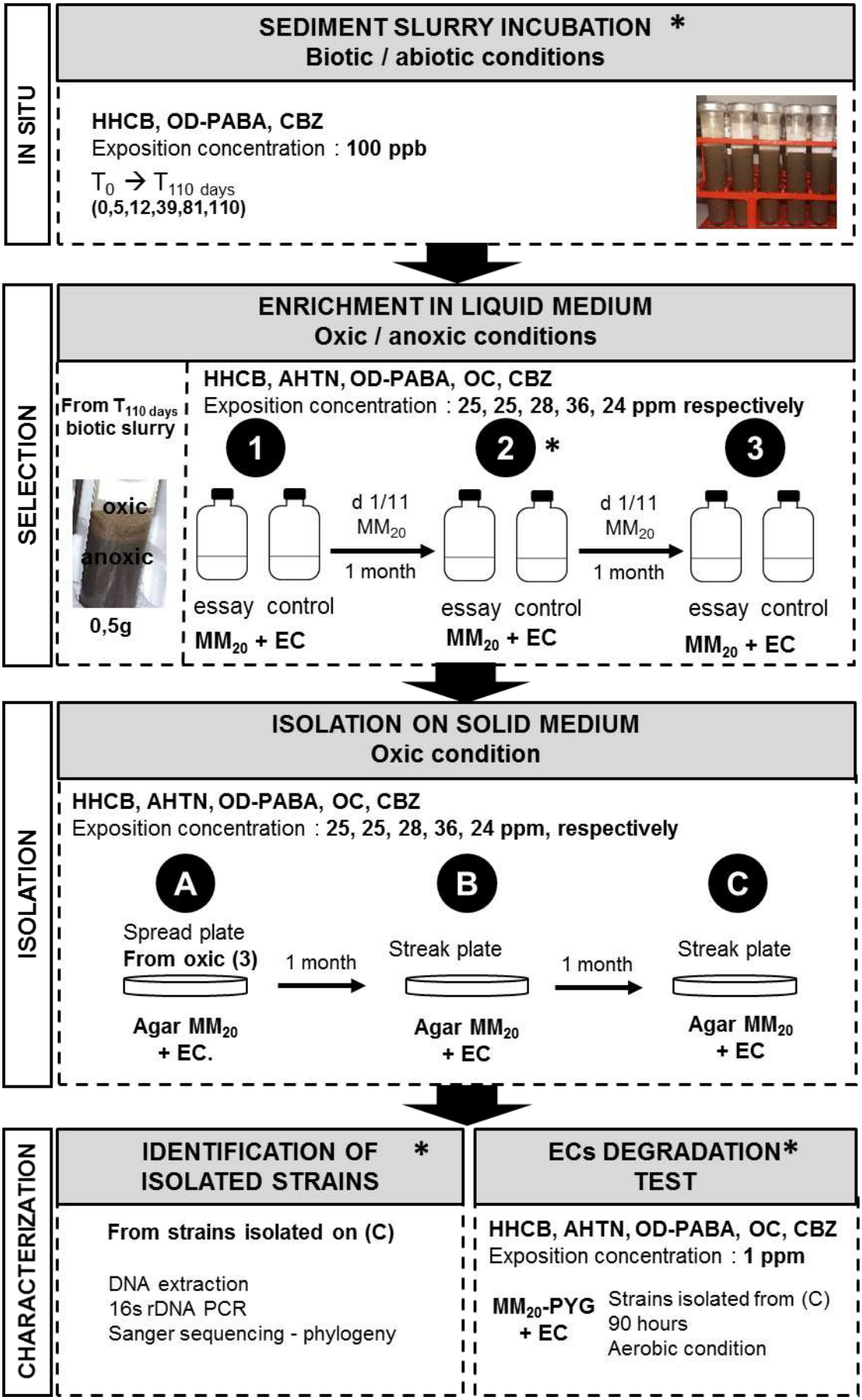
IN SITU
SEDIMENT SLURRY INCUBATION *
Biotic / abiotic conditions
HHCB, OD-PABA, CBZ
Exposition concentration : 100 ppb
T0 → T110 days
(0,5,12,39,81,110)
SELECTION
ENRICHMENT IN LIQUID MEDIUM
Oxic / anoxic conditions
From T110 days biotic slurry
oxic
anoxic
0,5g
HHCB, AHTN, OD-PABA, OC, CBZ
Exposition concentration : 25, 25, 28, 36, 24 ppm respectively
1
2 *
3
d 1/11 MM20
1 month
d 1/11 MM20
1 month
essay control
MM20 + EC
essay control
MM20 + EC
essay control
MM20 + EC
ISOLATION
ISOLATION ON SOLID MEDIUM
Oxic condition
HHCB, AHTN, OD-PABA, OC, CBZ
Exposition concentration : 25, 25, 28, 36, 24 ppm, respectively
A
B
C
Spread plate
From oxic (3)
1 month
Streak plate
1 month
Streak plate
Agar MM20 + EC.
Agar MM20 + EC
Agar MM20 + EC
CHARACTERIZATION
IDENTIFICATION OF ISOLATED STRAINS *
From strains isolated on (C)
DNA extraction
16s rDNA PCR
Sanger sequencing - phylogeny
ECs DEGRADATION* TEST
HHCB, AHTN, OD-PABA, OC, CBZ
Exposition concentration : 1 ppm
MM20-PYG + EC
Strains isolated from (C)
90 hours
Aerobic condition

*Fig. 2 – Design of experiments to determine natural resilience and microbial strains involved in the degradation of emerging contaminants (ECs): Galaxolide (HHCB), Padimate O (OD-PABA), Carbamazepine (CBZ), Tonalide (AHTN) and Octocrylen (OC). First step was the determination of in situ degradation constant rates from slurry sediments spiked with ECs under biotic and abiotic conditions at 100 ppb (AHTN and OC could not be measured). Second step was the selection of strains from the last slurry sediments incubation (days 110) through enrichments performed under oxic and anoxic conditions at 25, 25, 28, 36 and 24 ppm of HHCB, AHTN, OD-PABA, OC and CBZ, respectively (corresponding for each at 100 µM). These enrichments were repeated three times (1, 2, 3) with liquid multipurpose medium at 20 g L-1 of NaCl, called MM20. Third step was strains isolation from the last enrichment (3) where microbial consortia were separated (spread plates) on agar MM20 at same ECs exposition concentrations than the previous step (A). After one month of growth, colonies were twice isolated by streak plating (B, C). The last step was the characterisation of isolated strains through both their identification and the determination of their ECs degradation capacities. Isolated strains were identified by 16s rDNA amplification and Sanger sequencing. ECs degradation tests were performed at 1 ppm of ECs using liquid MM20 suppplemented with peptone (5 g L-1), yeast extract (2.5 g L-1) and glucose (5 g L-1), called MM20-PYG. * indicates that results are presented in following figures.*

2.6 Identification of isolated strains: DNA extraction, 16s rDNA amplification, sequencing and phylogenetic analysis

DNA was amplified from isolated strains after growth in LB Lennox medium. Amplification of the 16S rRNA was done with the universal primers 63F (5'-CAG GCC TAA CAC ATG CAA GTC-3') and 1387R (5'-GGG CGG WGT GTA CAA GGC-3')[271]. PCR amplification was performed using ampliTaq Gold® 360 master mix (Applied Biosystems, CA, USA), 0.2 µM of each primer and 1 µL of strain. PCR cycling was as following : after 10 min of initial denaturation at 95 °C (lysis of cells), 35 cycles of 40 s denaturation at 95 °C, 40 s annealing at 58 °C and 60 s elongation at 72 °C with 7 min final elongation at 72 °C. Amplicons were sequenced by SANGER sequencing at GATC (Köln, Germany). Sequences were trimmed with ChromasPro (Technelysium software) and were aligned with MUSCLE [272].A tree was generated using MEGA X software [273], with the Maximum Likelihood method and Tamura-Nei model [274] (with n replication boostraps = 500). Phylogenetic analysis were processed with NCBI (https://www.ncbi.nlm.nih.gov/) and corresponding reference type strains as defined by the bacteriological code of nomenclature for Prokaryotes (http://www.bacterio.net/-classifphyla.html). Sequences are archived in GenBank under accession numbers XXX.

In parallel, in order to compare with the isolated strains, DNA of *in situ* samples and from the final kinetic time of the slurry incubations were studied to determine the global diversity. DNA was extracted from frozen sediments with the QIAGEN DNeasy Powersoil kits (Qiagen Inc., Netherlands) according to the manufacturer's instructions. Diversity of the 16S rDNA were determined by sequencing the V4-V5 hypervariable regions of the 16S rDNA with universal primers V4-515F (5' GTGYCAGCMGCCGCGGTA 3') and V5-928R (5'-

ACTYAAAKGAATTGRCGGGG 3') [275–277]. PCR was performed using ampliTaq Gold® 360 master mix (Applied Biosystems, CA, USA), 0.5 µM of each primer and 3 ng of extracted DNA. PCR cycling was as following : after 10 min of initial denaturation at 95 °C, 30 cycles of 30 s denaturation at 95 °C, 30 s annealing at 60 °C and 40 s elongation at 72 °C with 7 min final elongation at 72 °C. Amplicons were sequenced using MiSeq 250-pair-end technology (Illumina, CA, USA) with V3 kit version, in Get-plage sequencing platform (INRA, Toulouse, France). Data were preprocessed using Galaxy FROGS pipeline [278]. Chimera and PhiX reads were removed, Operational Taxonomic Units (OTUs) clustering, after a de-noising step allows building fine clusters with minimal differences, with an aggregation distance equal or above 3. Data were normalized with the minimum number of reads. Taxonomic affiliation was performed using the Silva database v.128 [279]. Sequences data in situ and from the final kinetic time of the slurry incubations have been deposited in Genbank under the accession number PRJNA608532 and xxxxxx, respectively.

2.7 ECs degradation test

Isolated strains were re-cultivated in medium MM_{20}-PYG (MM_{20} medium supplemented with peptone, 5 g L^{-1}, yeast extracts, 2.5 g L^{-1} and glucose at 5 g L^{-1}) à 37 °C for 90 hours. Optical density (DO) at 600 nm was measured during the growth until the maximum growth using spectrophotometer (Spectronic 20). Degradation tests were performed in glass tubes with contaminants (HHCB, AHTN, OD-PABA, OC and CBZ) evaporated (Delgado-Moreno et al 2019) to be at 1 ppm final concentration, with 1 ml of the cultivated strains, 9 ml of MM_{20}-PYG at 27°C in agitator (120 rpm) [81]. 10 µL of micropollutant at 1000 ppm were added with sterile syringe and PTFE filter 0.2 µm (Fisher). Degradation was stopped when DO_{600} reached the maximum value. For initial and final times, chemical analysis were performed (in triplicates) to evaluate the ECs degradation (described below).

2.8 ECs analysis

HHCB, AHTN, OD-PABA, OC and CBZ were extracted by a liquid:liquid extraction, from initial and final degradation test for enrichment in liquid medium and for the degradation test (Fig.2). Briefly, 10 and 2 mL of EtOAc were added directly into the essay tube before to vortex for 1 min, respectively. Then, 20µL of the supernatant was diluted with EtoAC (960 µL) in GC-vial and spiked with 20 µL of an internal standard mixture at 10 µL ng^{-1} (CBZ-d10 and MX-d15) before analysis. Extracts were analysed by 7890A gas chromatograph coupled with 5975C mass spectrometer (GC/MS) with an Electron Ionization (EI) source using a Large Volume Injection (LVI) (Agilent Technologies). The GC/MS system was equipped with a single taper ultra-inert liner with glass wool and a HP-5MS UI capillary column (30 m length ×

0.25 mm diameter and 0.25 µm film thickness). Carrier gas was helium (He) with a purity greater than 99.999% (Linde). Separation was performed at a constant He flow of 1.5 mL min^{-1}, and the GC oven temperature was programmed to hold at 50 °C for 3 min, then increase at 25 °C min^{-1} until 195 °C (hold 1.5 min), then 8 °C min^{-1} until 265 °C (hold 1 min) and 20 °C min^{-1} until 310 °C (hold 5 min). Injection volume was 20 µL in splitless mode. Instrument control, data acquisition and data treatment were performed using Agilent Chemstation software. Quantification was carried out in Selected Ion Monitoring (SIM) mode, selecting two characteristics fragments ions for each compound. Calibrations with the target analytes (HHCB, AHTN, OD-PABA, OC and CBZ) were used to quantify target compounds. A six-point calibration curve was performed in EtOAc spiked with increasing pollutants concentration levels ranging from 0 to 500 µg L^{-1} as well as internal standards at 50 µg L^{-1} transferred into GC vials. Recoveries achieved for all target compounds with calibration point at 100 µg L^{-1} ranged from 81% ± 8% and 105% ± 1% (n=24).

3 Results and discussion

3.1 Degradation of HHCB, ODPABA and CBZ in slurry incubation

Based on kinetic degradation for 110 days under both abiotic and biotic conditions (Supplementary information, Fig. S1), degradation rate constants, k, were estimated from slurry incubations under biotic condition (Table 2). While CBZ in both sediment samples exhibited similar rates (0,0035 ± 0,0004 and 0,0029 ± 0,0001), HHCB and OD-PABA exhibited different rates of degradation according the location (e.g. G10 and G14) with a factor around 2 (Table 2). This suggested that ECs degradations were depending on the geochemical parameters of the sediments (e.i. grain size, organic matter content). For instance, a previous study demonstrated that ECs have a strong affinity for particles [147], as observed with sludge in wastewater treatment plants [280], suggesting those parameters and as well as environmental factors have to be taken in consideration to understand the fate of ECs in the ocean. Estimation of the half life time of reaction for these ECs indicated that the UV filter OD-PABA was between 21±1 and 44±4 days (Table 2). These results are similar with another UV filter degradation (i.e. EH-DPAB) estimated in marine sediments microcosm with a $t_{1/2}$ ranging from18 to 50 days [281]. Nevertheless, half life reaction for synthetic musk HHCB and anti-epileptic CBZ reached around 8 months and 7 months, respectively, indicated the high persistence of these contaminants in natural marine sediments compare to the UV filter OD-PABA (Table 2).

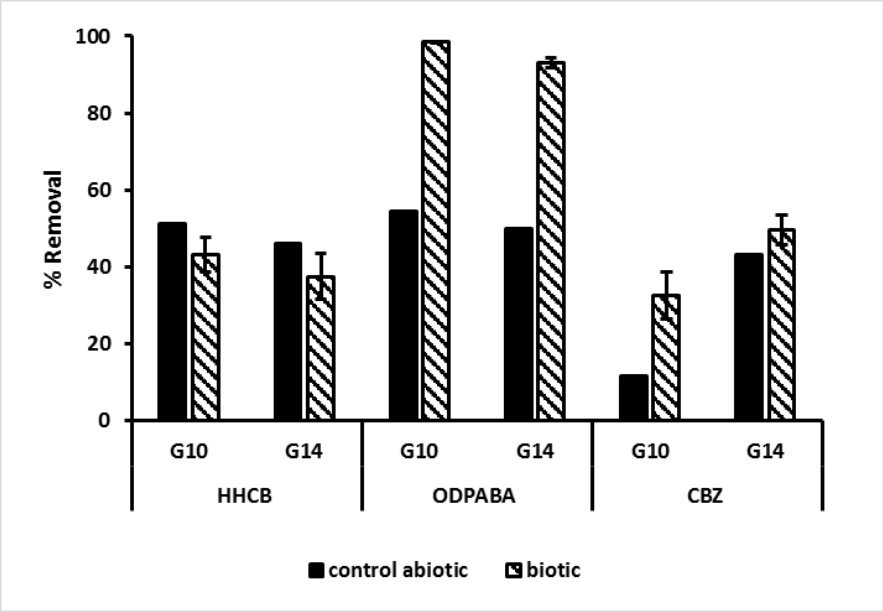

Fig. 3 - HHCB, OD-PABA and CBZ removal potential (%) at the final kinetic time of sediment incubation (after 110 days) and under abiotic control (slurry sterilized twice) from Capbreton Canyon sediments (G10, and G14). Initial exposure concentration was 100 ppb. Data are mean ± SD of three replicates

Lack of data on HHCB and CBZ degradation potentials in marine sediments does not allow comparison with these present data. Nevertheless, these preliminary results demonstrate the high persistence of these ECs in natural environment. In sediments, ECs may be associated to particulate matter, establishing equilibrium relations in the water-sediment interface, limiting their bioavailability. ECs remobilisation depends both of geochemical characteristics variations of the sediment, the overlying water column and pore water. Thus, ECs persistence in environment depend on coupling of abiotic and biotic factors [282,283], such as physicochemical properties of the ECs, environmental factors (e.i. temperature [284], pH [267], redox processes[285] photolysis process [286,287]) and the presence of microbial communities able to degrade these ECs [288]. It was also demonstrated that bioturbation or resuspension improved oxidation of anoxic sediments leading an increase of lability of ECs which can be more available for degradation processes [289].

Additionally, chemical characterization of the collected sediments revealed that the three-targeted ECs were not found at concentration detectable with the analytical method used [264]. The removal potential was observed under both abiotic and biotic conditions with percentage of removal for each compounds, HHCB, OD-PABA and CBZ, ranging from 37.5% to 51.4%, from 50.1% to 98.5% and from 11.6% to 49.6%, respectively (Fig. 3). Results of HHCB and CBZ slurry incubations suggested that the degradation was mainly driven by an abiotic process (except for G10 exposed with CBZ). Removal potential of OD-PABA under biotic condition was 2 times higher compared to the abiotic condition,

suggesting that micro-organisms in these sediments improved the degradation of this UV filter compound (Fig. 3).

T*able 2 – First-order rate constants k (in days-1) for degradation of HHCB, OD-PABA and CBZ in the slurry sediments incubations under biotic condition (in triplicate). Pearson determination coefficients ranged from 0.76 to 0.98 and p-values <0.05 for estimation of k. The corresponding half-lives (t1/2, in days) were calculated as ln(2)/k. G10 and G14 correspond to canyon surface sediment and continental shelf sediment, respectively*

Emerging contaminants	Slurry incub.	k ± SD ($days^{-1}$)	$t_{1/2}$ ± SD (days)
HHCB	G10	0,0032 ± 0,0005	224 ± 41
	G14	0,0065 ± 0,0029	129 ± 44
OD-PABA	G10	0,0324 ± 0,0014	21 ± 1
	G14	0,0158 ± 0,0014	44 ± 4
CBZ	G10	0,0035 ± 0,0004	199 ± 19
	G14	0,0029 ± 0,0001	231 ± 17

3.2 Enrichment in liquid medium

Results of the second enrichment in liquid medium (Fig. 4) demonstrated a higher removal in oxic conditions than under anoxic conditions for the five ECs studies (e.i. HHCB, AHTN, OD-PABA and CBZ). These ECs are well known to be observed in effluents of WWTP [290]. Although new advanced treatment processes, such as activated carbon adsorption, advanced oxidation processes, reverse osmosis or membrane bioreactors, are developed to increase the micropollutant removal of the WWTPs to struggle against the spread of micropollutants in aquatic environment, they are still observed in the WWTP effluents [291]. Those results suggested that oxic processes could improve the ECs removal and limit their spread from the WWTP sewage. Moreover, higher removals under abiotic anoxic conditions than biotic were observed. It is likely due to a higher ECs adsorption on cells present in biotic condition leading to trap ECs and reduce the quality of the liquid extraction [292,293]. Additionally, the high concentrations (ppm level) used for the selection of strains in these enrichments could inhibit microbial activity, thus could have mask their ECs removal capacities under anoxic condition [294].

Under oxic condition, similar removal potentials were observed for the abiotic and biotic condition, except for OC and CBZ (Fig. 4). That may indicate a potential involvement of microorganisms in the OC removal. Contrary to OC, CBZ removal was observed only in abiotic anoxic condition, likely due to the same explanations suggested previously for the removal potential under anoxic condition (e.i. adsorption on cells and/or high exposition concentrations). These results led to continue the study of ECs degradation with the isolated strains under oxic conditions.

Nevertheless, even though an efficient removal of ECs under oxic condition was observed, metabolites were not studied. Indeed, degradation of ECs to metabolites have been observed for CBZ [295], HHCB [81] and also for others UV filters [281]. These results highlighted the complexity of ECs removal under experimental conditions as well as in WWTPs, where their efficiency are dependant of both physical, chemical and biological processes but also to identify metabolites in further studies.

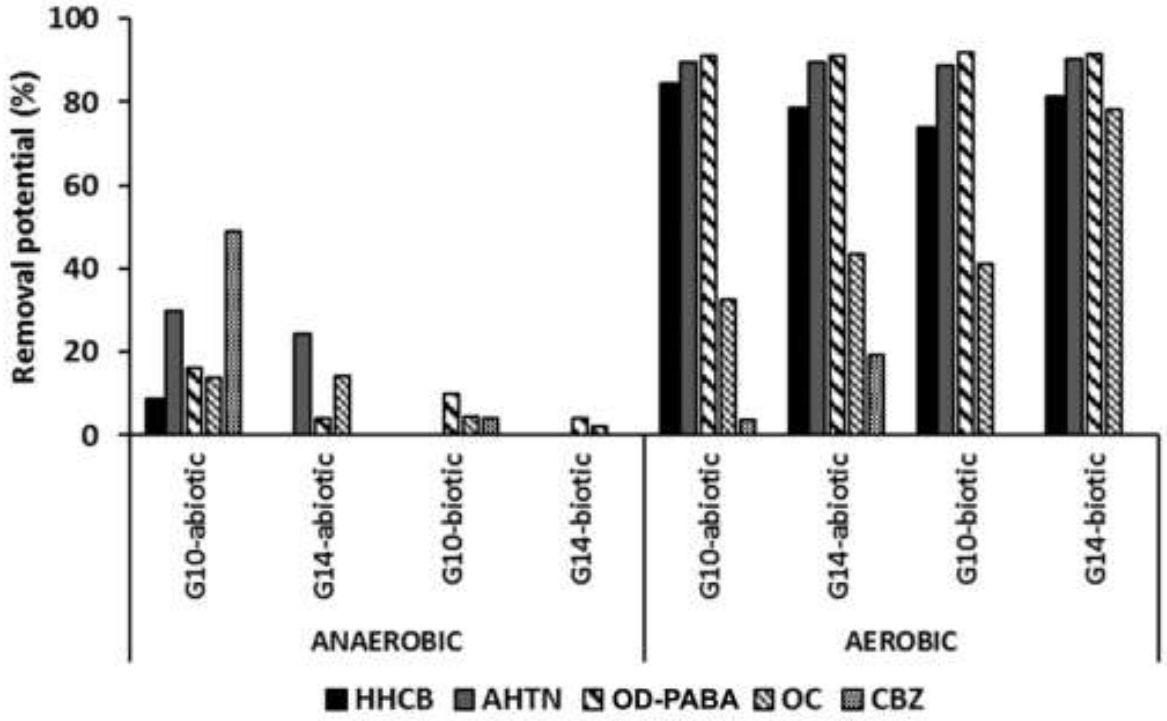

Fig. 4 – HHCB, AHTN, OD-PABA, OC and CBZ removal potential (%) at the final kinetic time (one month) of the second liquid enrichment under oxic or anoxic conditions with innoculum from G10 and G14 stations (biotic). Control was achieved without innoculum.

3.3 Isolated strains involved in ECs degradation

It is well known that degradation of complex organic substances increases under aerobic condition [296,297]. In accordance with this observation, isolation of strains and degradation test were consequently performed under aerobic condition. Twenty seven strains were isolated with the current method with 6, 8, 4, 4 and 5 strains constrained with HHCB, AHTN, OD-PABA, OC and CBZ, respectively (Supplementary information, Fig. S3). These strains were related to two families, dominated by the *Firmicutes,* followed by the *Actinobacteria* (Fig.5 A B).

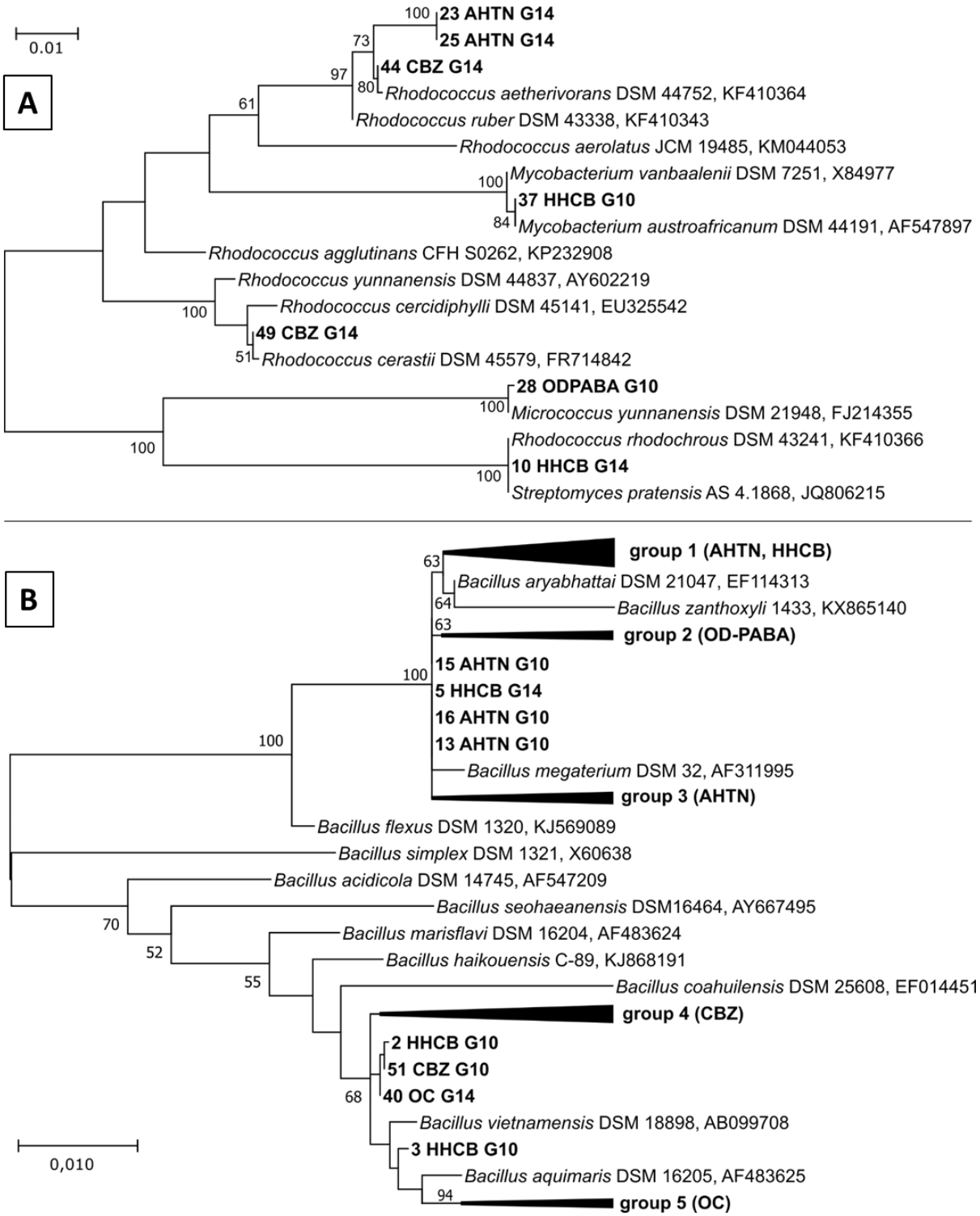

Fig. 5 – Phylogenic trees of strains obtained after the aerobic isolation in solid medium with different ECs (AHTN, HHCB, OC, OD-PABA and CBZ) from sediments collected in the submarine Canyon of Capbreton (stations G10 and G14). Fig.5A and Fig.5B correspond to Actinobacteria and Firmicutes, respectively. Isolated strains are in bold, reference strains are in italic. The evolutionary history was inferred by using the Maximum Likelihood method and Tamura-Nei model. The percentage in trees in which the associated taxa clustered together is shown next to the branches. The scale (0.01) indicates the dissimilarity between the strains. Groups 1, 2, 3, 4 and 5 included 10 (20, 21 AHTN-G10; 22, 27 AHTN-G14 4 and 6, 7, 8, 11, 12 HHCB- G14), 3 (33, 35, 36 ODPABA-G14), 4 (17, 18, 19 AHTN-G10 and

24 AHTN-G14), 6 (45, 46, 47, 48 CBZ-G14 and 50, 52 CBZ-G10) and 3 (41, 42, 43 OC-G10) isolated strains, respectively.

Within the *Actinobacteria*, *Rhodococcus* was the main bacteria genus isolated followed by *Streptomyces, Mycobacterium and Micrococcus*. Within the *Firmicutes*, only *Bacillus*-related strains were isolated (Fig. 5 A, B). Studies have shown that *Actinobacteria* were involved in degradation of some organic and inorganic compounds. For instance, *Rhodococcus* strains are involved in the removal of pharmaceutical compounds [298], tetrabromobisphenol A (TBBPA) [299] and dominant in naphthalene degrading enrichments [300]. It has also been demonstrated that the members of the genus *Streptomyces* produce laccase (i.e. ligninolytic enzymes) that can be involved in the removal of recalcitrant and ECs [301]. It has also been demonstrated that members of the genus *Streptomyces* were involved in the CBZ biodegradation [302,303]. Finally, experiments performed from marine sediments demonstrated that *Bacillus thuringiensis* was a novel group participating to the removal of PAHs and pesticides [304].

Within these isolated strains, only eight exhibited a capacity to degrade contaminants in the conditions used (1 ppm, 5 days, 37 degrees in rich organic medium) with 1, 2, 3 and 2 strains for HHCB, AHTN, OD-PABA and OC, respectively (Table 3). Seven were related to the genus *Bacillus* and one was related to the genus *Rhodoccocus* (23 AHTN G14). While studies have demonstrated high bioremediation capacities by *Actinobacteria*, this study demonstrated high capacity of marine *bacillus* to degrade ECs.

Table 3 – Removal capacity of isolated strain and their related affiliation based on phylogenetic tree (Fig. 5). % of removal is calculated relatively to the control removal and in triplicate, after 120 hours of experimentation at 1 ppm exposition concentration for each emerging contaminants. The strains for which degradation were not determined are not shown (Fig. 5

Isolated strains	***Phyla***	***Family***	**% of removal ± SD**
2 HHCB G10	*Firmicutes*	*Bacillus*	44 ± 31
17 AHTN G10	*Firmicutes*	*Bacillus*	68 ± 9
23 AHTN G14	*Actinobacteria*	*Rhodoccocus*	20 ± 7
33 ODPABA G14	*Firmicutes*	*Bacillus*	34 ± 19
35 ODPABA G14	*Firmicutes*	*Bacillus*	45 ± 9
36 ODPABA G14	*Firmicutes*	*Bacillus*	71 ± 19
40 OC G14	*Firmicutes*	*Bacillus*	17 ± 17
43 OC G10	*Firmicutes*	*Bacillus*	14 ± 13

These results suggested that the isolated *bacillus* were able to remove OD-PABA with a capacity ranging between 34% ± 19% and 71% ± 19% (Table 3). These strains could be involved in the biotic degradation observed in the slurry incubation experiment (Fig. 3).

Although CBZ slurry incubations experiments (G10) demonstrated a possible biotic degradation (Fig. 3), isolated strains did not exhibit a remediation for this pollutant under the conditions tested (Supplementary information, Fig. S3). Moreover, the $t_{1/2}$ of CBZ was estimated around 7 months, suggesting that the time should be expanded to observe a remediation capacity. Moreover, it is well known that in nature, the microbial consortia have to be considered to estimate biodegradation pollutant removal process [305].

Moreover, global microbial communities analysed *in situ*, in G10 and G14 demonstrated a relative abundance of the main phyla similar in both sediments (and similar to the final kinetic time of the slurry incubations, Supplementary information Fig. S2), with a dominance of *Proteobacteria* (relative abundance ranged between 47.9 and 49.4%), followed by *Bacteriodetes*, *Planctomycetes* and *Acidobacteria* (Fig. 6). Although the *Actinobacteria* and *Firmicutes* were minors *in situ* (Fig. 6), representing less than 1% of the total abundance, phylogenic trees based the sequences of the isolated strains (Fig. 5 A,B) demonstrated that these isolated strains were related to the *Actinobacteria* and *Firmicutes* families. This suggests a good selection process of these bacterial groups in the presence of these ECs exposition with the isolation method used.

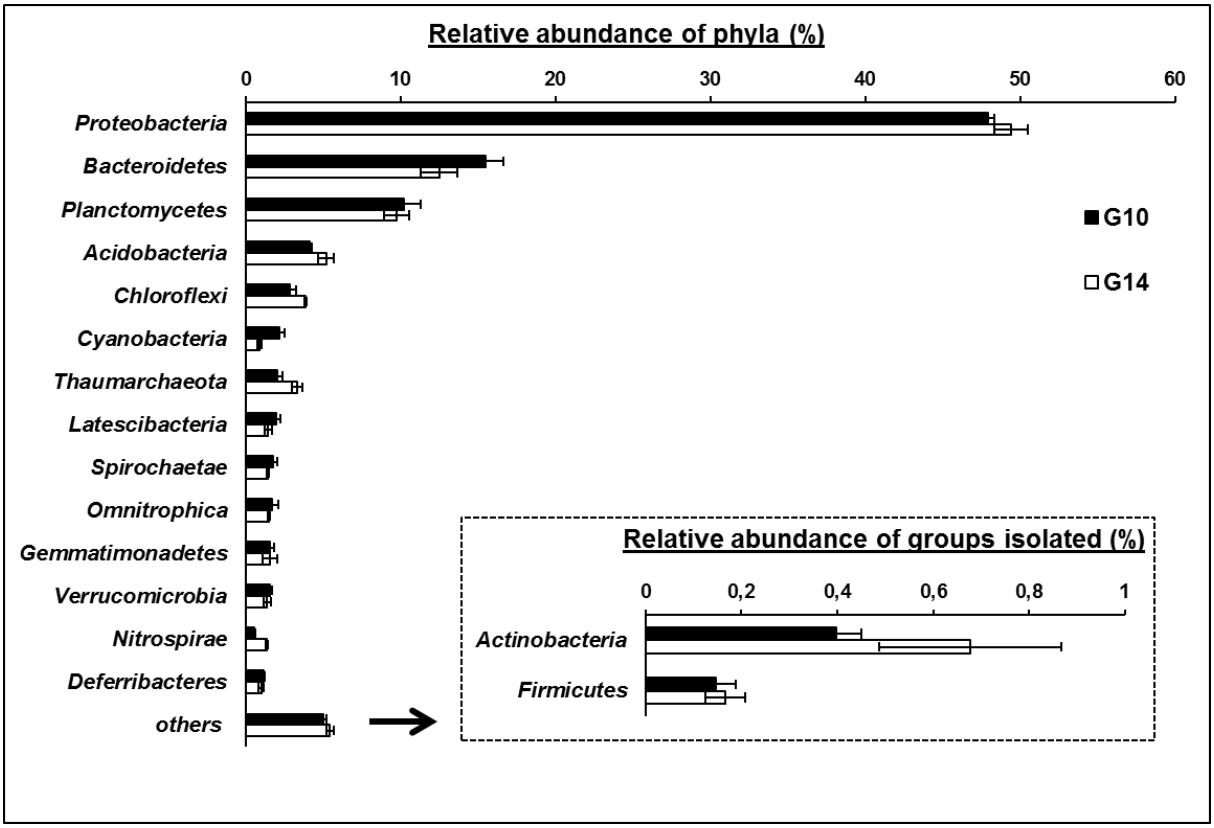

Fig. 6 –Relative abundance of prokaryotic 16S rDNA sequences (MiSEQ) from sediments of G10 and G14. Data are average percentages (± SE). Categories representing > 1% are shown. Relative abundances of phyla from which the isolated strains belonged are also shown.

In accordance with previous studies, the degradation test of isolated bacteria strains from the Capbreton Canyon sediments could be good candidate to degrade ECs. Nevertheless, in order to estimate the natural resilience of those ECs, it is crucial also to take account both the biological (e.i. biodegradation, biosorption/adsorption), physical and chemical processes, highlighting further studies are needed to decipher their fate in oceans.

4. Conclusion

This work characterized the degradation kinetics for ECs (HHCB, OD-PABA and CBZ) from marine sediments under in situ conditions (biotic, anaerobic and temperature) thought slurry sediment incubations. The half life times obtained demonstrated that half time live of OD-PABA was lower than HHCB and CBZ, with t1/2 ranging from few weeks to 8 months. This underlies that the ECs degradation in marine sediment is a long process and could be a high concern for the environment considering a chronical contamination from the coastal human activities (e.i. WWTPs sewage, agriculture…). Additionally, contrary to CBZ, different half lives were observed between muddy (G10) and sandy (G14) sediments for HHCB and OD-PABA. That indicates ECs degradation depends on the physicochemical properties of both chemicals and sediment.

Moreover, novel synthetic musks and UV filters degrading bacteria were isolated from marine sediment. Based on phylogenetic characteristics, microorganisms were mainly identified as Bacillus sp. dominated by Bacillus megaterium followed by Bacillus aquimaris and Bacillus vietnamensis. One other isolated strain which was able to degrade musk was related to Rhodococcus ruber. The isolated bacteria here, could have a strong potential to degrade a wide variety of organic pollutants (e.g. priority and emerging), such as synthetic musks and UV filters. Improving the knowledge about the microbial diversity in marine environment may lead to the development of technical tools with degradation abilities and high tolerance in the future but also highlight how microbial remediation contributes to the nature resilience in marine environment.

Fig. S1 *Concentration of emerging contaminants in G10 and G14 slurry incubations for each kinetic times (0, 5, 12, 39, 50, 81 and 110 days) under biotic condition. Data are ± SD of three replicates.*

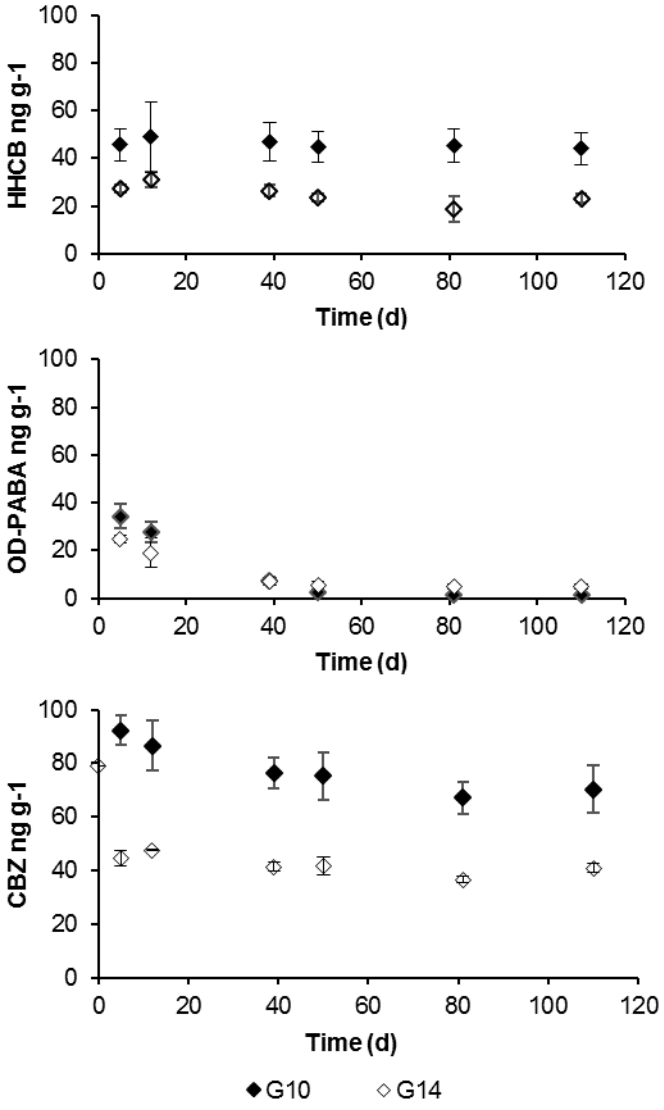

Fig. S2 *- Comparison of the relative abundance of prokaryotic 16S rDNA sequences (MiSEQ) affiliated with different phyla to the total number of sequences from the microcosm samples at initial time and final slurry incubation under biotic condition (110 days). Sequences not classified to any known phylum are included as Unclassified bacteria. The rare species with relative abundance less than 0.1 % are included as Others. Sediments were sampled in stations G10 and G14.*

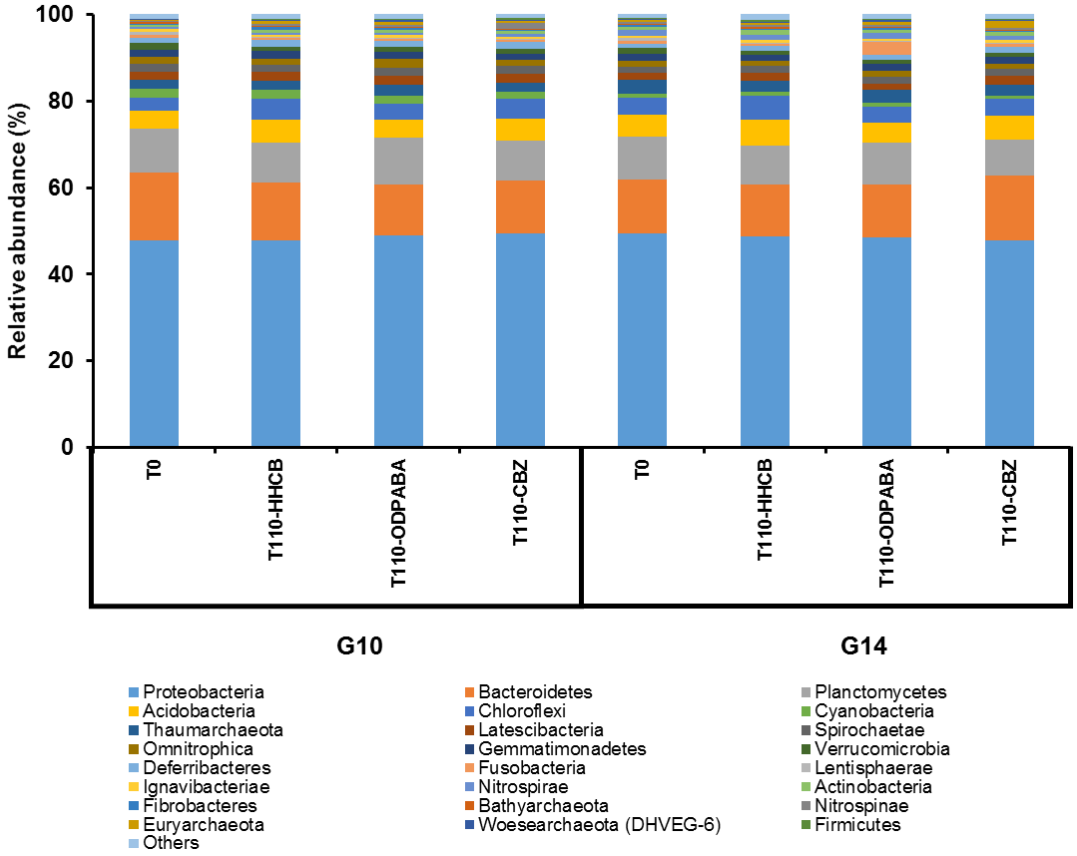

Fig. S3 *Growth (Log DO600) of isolated strains from isolation set up in aerobic condition in presence of 1 ppm of emerging contaminants, ECs, (HHCB, AHTN, OD-PABA, OC, CBZ) with 0.5 g L-1 of glucose. PCA20 + Glu medium without ECs supplementation was used as control. Abiotic control was constant and no growth was observed.*

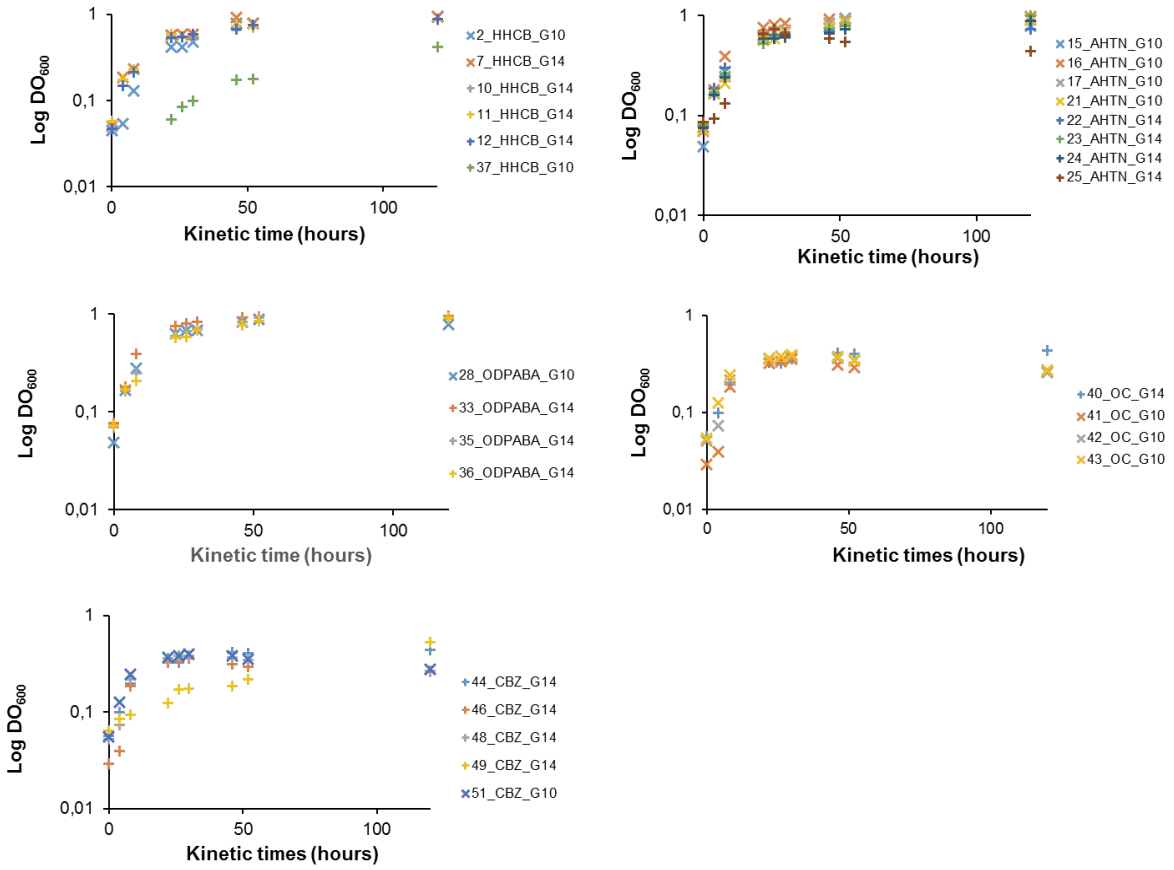

2.B - MARINE MERCURY-METHYLATING MICROBIAL COMMUNITIES FROM COASTAL TO CAPBRETON CANYON SEDIMENTS (NORTH ATLANTIC OCEAN)

Alyssa Azaroff, Marisol Goñi Urriza , Claire Gassie , Mathilde Monperrus, Rémy Guyoneaud

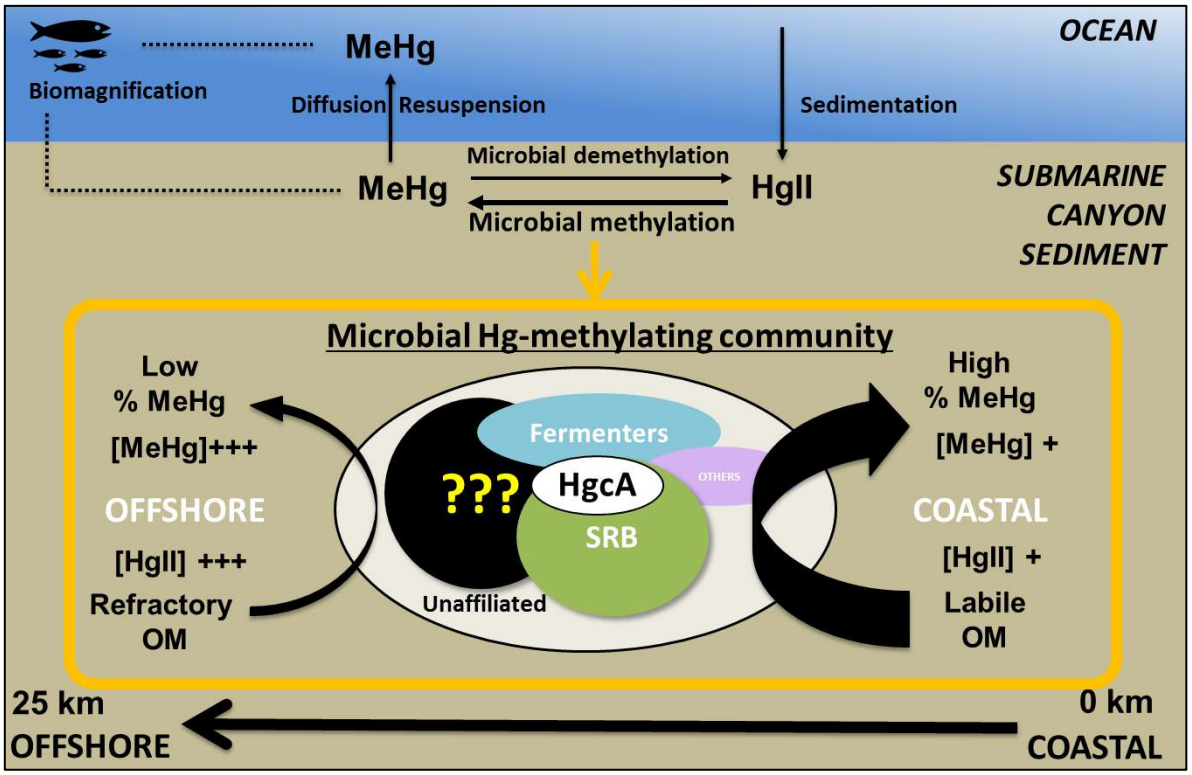

Published, Environmental Pollution Journal, 2020, https://doi.org/10.1016/j.envpol.2020.114333

Résumé

La méthylation microbienne du mercure (Hg) transforme le mercure inorganique (Hg(II)) en mercure organique (le méthylmercure (MeHg), un dangeureux neurotoxique) principalement dans les environnements anoxiques aquatiques. La difficulté d'échantillonnage dans les écosystèmes marins, en particulier dans les canyons sous-marins, conduit à un manque de connaissances sur le microbiome méthylant le mercure dans les sédiments marins. Une étude antérieure avait montré un enrichissement d'espèces mercurielles (Hg(II) et MeHg) dans les sédiments du canyon de Capbreton où les paramètres géochimiques et les activités microbiennes limitaient la production nette de MeHg. Afin de caractériser les communautés microbiennes méthylant le mercure des sédiments côtiers aux sédiments plus profonds, une analyse de la diversité des microorganismes (basée sur le séquençage de l'ADNr 16s) ainsi qu'une analyse des bactéries méthylante le mercure (basée sur le clonage et séquençage du gène *hgcA*) ont été réalisées. Les analyses de diversité (ADNr 16s et *hgcA*) ont démontré que les potentiels procaryotes présumés de méthylation du Hg se trouvaient parmi les *δ-protéobactéries*, dominée par des bactéries réductrices de composés soufrés (principalement sulfate). D'autres clades, tels que *Firmicutes*, *Chloroflexi* et *Euryarchaea* étaient mineurs. Néanmoins, 45 % des séquences de *hgcA* ne sont toujours pas affiliées, ce qui indique que des études supplémentaires en milieu marin sont nécessaires pour déchiffrer les implications de ces nouveaux microorganismes porteurs de *hgcA* dans la méthylation du Hg. Ces premiers résultats dans un écosystème marin productif suggèrent également l'implication du cycle du soufre dans la méthylation du mercure.

Mots clefs Sédiments de canyon sous-marin, mercure, méthylmercure, methylation du mercure, procaryotes méthylants le mercure, 16s rDNA MiSEQ, diversité HgcA

Abstract

Microbial mercury (Hg) methylation transforms inorganic mercury to neurotoxic methylmercury (MeHg) mainly in aquatic anoxic environments. Sampling challenges in marine ecosystems, particularly in submarine canyons, leads to a lack of knowledge about the Hg methylating microbia in marine sediments. A previous study showed an enrichment of mercury species in sediments from the Capbreton Canyon where both geochemical parameters and microbial activities constrained the net MeHg production. In order to characterize Hg-methylating microbial communities from coastal to deeper sediments, we analysed the diversity of microorganisms' (16S rDNA-based sequencing) and Hg methylators (*hgcA* based cloning and sequencing). Both, 16S rDNA and *hgcA* gene analysis demonstrated that the putative Hg-methylating prokaryotes were likely within the *Deltaproteobacteria,* dominated by sulfur-compounds based reducing bacteria (mainly sulfate reducers). Additionally, others clades were also identified as carrying HgcA gene, such as, *Chloroflexi, Spirochaetes, Elusimicrobia,* PVC superphylum (*Plantomycetes, Verrucomicrobia* and *Chlamydiae*) and *Euryarchaea*. Nevertheless, 61% of the *hgcA* sequences were not assigned to specific clade, indicating that further studies are needed to understand the implication of new microorganisms carrying *hgcA* in the Hg methylation in marine environments. These first results suggest that sulfur cycle drives the Hg-methylation in marine ecosystem.

Keywords: Mercury-methylation, Hg-methylating prokaryotes, 16S rDNA diversity, HgcA diversity, marine sediments

1 Introduction

Methylmercury (MeHg) is a neurotoxin that is biomagnified in aquatic food webs, with fish consumption as a primary route for human MeHg exposure [161,306]. In aquatic ecosystems, methylation of mercury (Hg) to MeHg is carried out by some anaerobic microorganisms. Studies have identified the sulfate-reducing bacteria (SRB) as the main contributors to Hg methylation [85]. MeHg production has also been associated with the activity of sulfur-reducing bacteria, iron-reducing bacteria (FeRB) and methanogenic archaea [165,307,308]. The recent identification of some genes required for Hg methylation, *hgcA and hgcB* [89], expanded our knowledge on the diversity of potential Hg methylators [87,90]. *hgcAB* genes are present in the genome of diverse sulfate, sulfur and iron reducing *Deltaproteobacteria*, in methanogens, but also in *Clostridia* (firmicutes), fermentative and acetogenic microorganisms [87,89,90,92,309]. Metagenomic data suggested the presence of *hgcAB* in members of others microbial phyla including the *Chloroflexi*, *Chrysiogenetes*, *Nitrospina*, the PVC superphylum (*Planctomycetes*, *Verrucomicrobia*, *Chlamydia*) and *Spirochaetes* [90,92,310,311]. Microbial Hg-methylating communities that have recently been described in wetlands, paddy soils, lakes, dam reservoir and sewage treatment plant effluent included methanogens, SRB, FeRB, syntrophs and also unaffiliated microorganisms [90,91,312–315]. Hg-methylating microbial communities in marine environment remain largely un-investigated with regards to their importance for methylation and the specific types of microorganisms involved.

The biogeochemical cycling of Hg remains understudied in the open ocean, particularly on continental margins and associated slopes [161]. Submarine canyons are large incisions into the continental margin which contribute to the enrichment of the sediments with organic matter (OM) and various trace metals [54,126,132]. Indeed, a previous study on the Capbreton Canyon (North Atlantic Ocean) has shown that the MeHg formation is driven by the OM and the sulfur content [126]. Comparatively to offshore canyon sediment, coastal sediment had the highest biological Hg methylation rates whereas ambient mercury compounds concentrations were lower [126]. Currently, no data exist about the microbial populations carrying *hgcA* in submarine canyons or even in marine sediments. Knowledge of the relationship between community composition and MeHg production may help to elucidate the origins of the large variability in MeHg/Hg ratios in oceanic ecosystem.

Building on these earlier discoveries and recognizing the implication of microbial communities on Hg methylation in Capbreton submarine canyon sediments, this study aimed to provide a mechanistic understanding of MeHg formation in sediments along the canyon transect. For this purpose, we linked sediment geochemistry and Hg speciation with parallel

analysis of the global prokaryotic diversity (16S rDNA) and microorganisms carrying *hgcA*. This is the first study in marine sediments, from coastal to canyon samples exploring the diversity of microorganisms involved in Hg methylation.

2 Material and method

2.1 Study area and sampling strategy

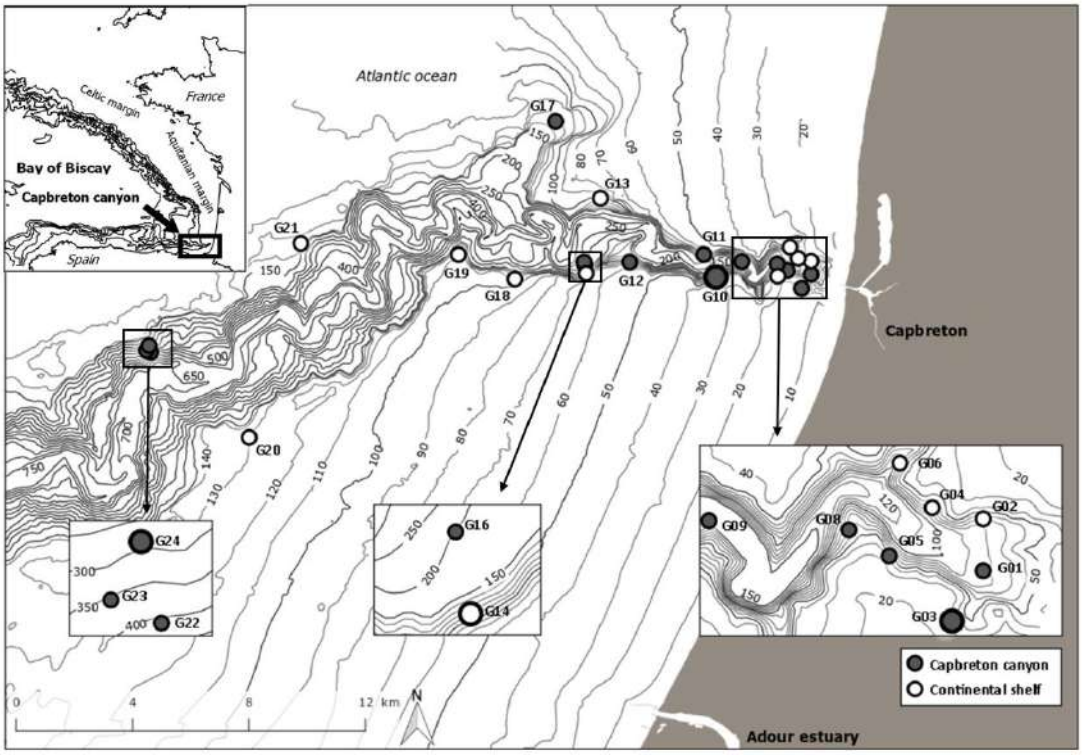

Figure 1 - Locations of sediment samples in the Capbreton Canyon (grey symbols) and the adjacent continental shelf (white symbols) included in this study. Enlarged symbols correspond to the four locations where hgcA diversity was studied. Bathymetric data are from SEDIMAQ3 cruise (Gillet H. (2012), RV Thalia, https://doi.org/10.17600/12070080).

The present study was undertaken in one of the longest canyons in the world, located in the North Atlantic Ocean: the Capbreton submarine canyon. It deeply incises the Aquitaine continental slope and shelf, and runs along the Spanish coast for 300 km and sinks into the abyssal plain at 3500 meters depth. Its head is at only 200 meters from the coast, where the population and human activities, are constantly increasing. Like many coastal ecosystems, it is a highly productive and ecologically rich zone due to large and continuous continental inputs of nutrients and organic matter coming from a rich network of effluents and the Adour estuary. Surface sediments were collected with a grab sampler and a core sampler along the canyon transect starting at 1.2 km from the coast to 23.5 km. Samples were located in slopes and terraces into the canyon (n=13) and in the adjacent continental shelf (n=9; Fig. 1). G03 is considered a canyon location because it is located in a gully connected to the mouth of this canyon [100]. For each sediment sample, Hg compounds analysis (Hg(II) and MeHg)

geochemical parameters as well as 16S rDNA diversity were analysed. *hgcA* diversity has been determined along the canyon transect at locations G03, G10, G14 and G24. On board, samples for DNA were collected in triplicate with sterile cryotubes then immediately frozen at -80 °C until analysis.

2.2 Chemical analysis

Sample processing, geochemical parameters (organic carbon (POC), total sulfur (TS)) and speciation of mercury (Hg(II) and MeHg) as well as the Hg transformation potential are detailed in a previous study [126].

2.3 DNA extraction and bacterial community composition: 16S rDNA gene

DNA was extracted from frozen sediments with the Power Soil DNA extraction kit (Mo-Bio Laboratories, Inc., Carlsbad, CA, USA) according to the manufacturer's instructions. Diversity of the 16S rDNA were determined by sequencing the V4-V5 hypervariable regions of the 16S rDNA with universal primers V4-515F (5' GTGYCAGCMGCCGCGGTA 3') and V5-928R (5′- ACTYAAAKGAATTGRCGGGG 3') [275,276,316]. PCR was performed using ampliTaq Gold® 360 master mix (Applied Biosystems, CA, USA), 0.5 µM of each primer and 3 ng of extracted DNA. PCR cycling was as following: after 10 min of initial denaturation at 95 °C, 30 cycles of 30 s denaturation at 95 °C, 30 s annealing at 60 °C and 40 s elongation at 72 °C with 7 min final elongation at 72 °C. Amplicons were sequenced by the Get-PlaGe sequencing service (INRA, Toulouse, France) using MiSeq 250 pb paired-end technology and reagent kit V3. Data were preprocessed using the Galaxy FROGS pipeline [278]. Chimeraic and PhiX reads were removed, Operational Taxonomic Units (OTUs) clustering, after a de-noising step allows building fine clusters with minimal differences, with an aggregation distance equal or above 3. Data were normalized to the minimum number of reads. Taxonomic assignments were performed using the Silva database v.128 [279]. Sequences data have been deposited in GenBank under the accession number PRJNA608532.

2.4 Hg methylation community composition: *hgcA* gene cloning and sequencing

hgcA gene diversity was studied in four surface sediments along the canyon gradient from the coast to the offshore (G03, G10, G14 and G24). Primers targeting *hgcAB* sequences were adopted from Christensen et al, 2016 [317] and *hgcAB* genes were amplified with the primer set ORNL-HgcAB-uni 268F (5′-AAYGTCTGGTGYGCNGVCGG-3′) and ORNL-HgcAB-uni 167R (5′-CABGCNCCRCAYTCCATRCA-3′). PCR was performed using ampliTaq Gold® 360 master mix (Applied Biosystems, CA, USA) and 1 µM of each

primer, with 2 min initial denaturation at 95 °C, 5 cycles of 30 s denaturation at 96 °C, 30 s annealing at 68 °C and 30 s elongation at 72 °C, then 30 cycles of 30 s denaturation at 96 °C, 30 s annealing at 63 °C and 1 min elongation at 72 °C with 7 min final elongation at 72 °C. PCR products were purified using GE Healthcare illustra™ GFX™ PCR DNA and Gel Band Purification Kit (GE Healthcare, Chicago, Illinois, US) according to the manufacturer's instructions. Purified products were ligated into a pCR™ 2.1-TOPO®, with TOPO™ TA Cloning™ Kit (Invitrogen, Carlsbad, CA, US), which was used to transform One Shot™ Mach1™ T1 Phage-Resistant Chemically Competent *E. coli*. Transformed *E. coli* were grown on lysogeny broth (LB) agar plates with 100 µg mL^{-1} ampicillin, 64 µg ml^{-1} X-gal and 160 mM IPTG. Successful transformants picked and screened by colony PCR with M13 primers (M13F; 5'GTAAAACGACGGCCAG-3' and M13R; 5'-CAGGAAACAGCTATGAC-3'). PCR was performed using ampliTaq Gold® 360 master mix (Applied Biosystems, CA, USA) and 0.2 µM of each primer, with 10 min initial denaturation at 95 °C, 30 cycles of 30 s denaturation at 95 °C, 30 s annealing at 54 °C and 40 s elongation at 72 °C with 10 min final elongation at 72 °C. Clones of the correct sized inserts were sequenced by SANGER sequencing at Eurofins Genomics (Ebersberg, Germany). Forward sequences were only used and converted to protein with ExPaSy tool (Swiss Institute of Bioinformatics, Lausanne, Switzerland) then, trimmed with Chromas Pro (Technelysium software). The obtained protein sequences were aligned with MUSCLE [272].The alignment was trimmed to the amplicon, and a tree was generated using MEGAX [273], with the Maximum Likelihood method based on the Poisson correction model [318] (with n replication bootstraps = 500). Phylogenetic analyses were processed using HgcA proteins homemade database including HgcA sequences from isolated strains' genomes and from metagenomes obtained from NCBI (https://www.ncbi.nlm.nih.gov/) and Integrated Microbial Genomes and Microbiomes platform (IMG/M, developed by the Joint Genome Institute, CA, USA, http://img.jgi.doe.gov/) [319] and previous studies (Supporting information, Table S3). HgcA sequences were also collected from Pfam database [320] using custom Pfam models (corrinoid-iron sulfur proteins (CFesP) classified under Pfam3599) according to Podar et al. [90]. From these references, we selected only sequences with the conservative cysteine in HgcA [321] within the CWA motif. All reference sequences are compiled in Supporting information, Table S3. Sequences are archived in GenBank under submission number .2316824

2.5 Statistical analysis

Pearson correlations were calculated between chemical parameters using the R software environment version (http://www.r-project.org/). To remove redundancy of the chemical parameters data in order to avoid collinearity, we used the variance inflation factor (VIF) with the mctest package [322] in R using the Farrar-Glauber test. Multivariate analysis

(Principal Component Analysis (PCA) were performed with FactomineR and Vegan package in R [130,323]. PCA for 16S rDNA diversity analysis was performed at the phylum level because of PCA constrains, with relative abundance above > 0.05%. We used the factoextra package [129] for extracting and visualizing the results. Hierarchical Clustering on Principal Components (HCPC) were performed using FactomineR package in R. Distances were calculated with the Canberra method and classification was applied to draw the trends of the dataset.

3 Results

3.1 Characterization of habitats and microbial community assemblies

In this study, we used previous chemical parameters in order to discriminate different habitats in the Capbreton canyon [126]. The variance in the relationship between depth, TS content, POC content, Hg(II) concentrations and MeHg proportion (selected among 10 parameters with the variance inflation factor, VIF, Supporting information, Table S1) was explained by two principal components contributing to 82.1% of the total variance contribution (Fig. 2). Surface sediments were separated into four distinct clusters corresponding to different areas in the Capbreton Canyon, with sediments from the mouth of the canyon, intermediate canyon, deep canyon and continental shelf (Fig. 2). Overall, the geochemical composition of sediments was dependent on the location (i.e. Canyon vs Continental Shelf), with an enrichment of TS, POC and Hg(II) levels in intermediate and offshore canyon locations (Fig. 2). Continental shelf sediments were characterized by a lower fine fraction content (<63µm), highlighting that Capbreton canyon enhances the transport and the accumulation of particles in the sediments [126]. In contrast, higher MeHg proportions of total Hg were found in coastal locations suggesting higher methylation activity close to the coast.

The composition of sediment microbial communities was investigated based on 16S rDNA gene sequences, normalized at 5024 reads per sample allowing assignment of 2600 OTUs for the whole set of data. Overall, the global diversity was quiet close across samples (Chao1 ranging from 1208 to 1685) and replicates (low standard deviation) and no particular trends in alpha diversity could be observed (Supporting information, Table S2).

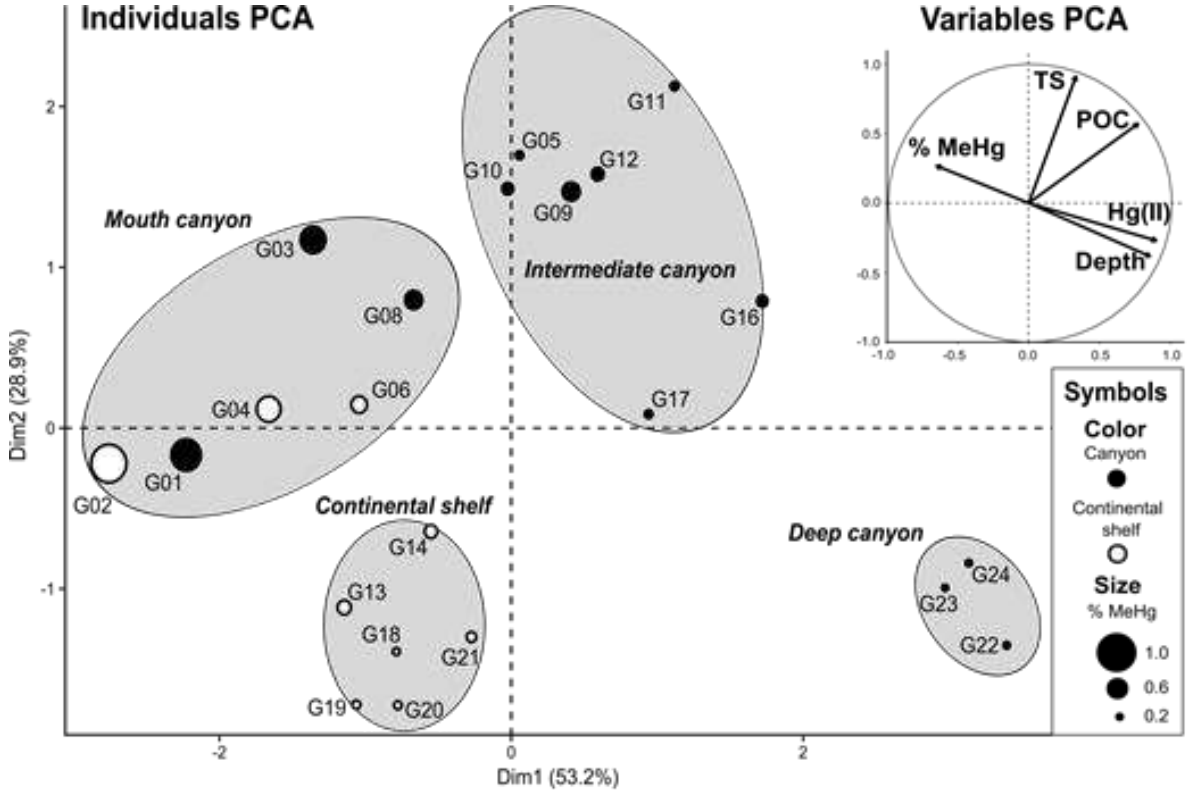

Figure 2 20- PCA of environmental parameters selected with the VIF method (depth, TS content, POC content, Hg(II) concentrations and MeHg proportion) for all locations sampled (n=22) in the Capbreton Canyon (grey symbols) and the adjacent continental shelf (white symbols). The size of symbols represents relative MeHg proportion of total Hg. Individual PCA illustrates position of samples on the two first dimensions (82.1 %) and variables PCA is the correlation circle of environmental parameters. Grey circles represent group of locations determined by using cluster analysis based on Euclidian distance (dendrogram in Supporting Information, Fig. S1).

Proteobacteria was the dominant phylum in terms of richness and relative abundance; they represented 921 OTUs and an average of 49.6 ± 3.6% of the total relative abundance, followed by *Bacteroidetes* and *Planctomycetes* representing 12.6 ± 5.7% and 8.6 ± 1.9%, respectively. A PCA analysis was performed on the relative abundance of phyla, in order to discriminate assemblies of microbial communities. The variance of the relationship between the relative abundance of phyla, was explained by the two first principal components contributing ~~with~~ 62.5% of the total variance (Fig. 3). Although the global pattern composition was uniform accross all locations, relative abundance variations led to three separate microbial community clusters along the canyon axis, distinguishing communities from mouth, intermediate and offshore locations (Fig. 3). Here, the distance to the coast seems to drive the microbial composition. Those multivariate analyses discriminated four different habitats colonized by three distinct microbial communities, themselves allocated along the canyon axis gradient.

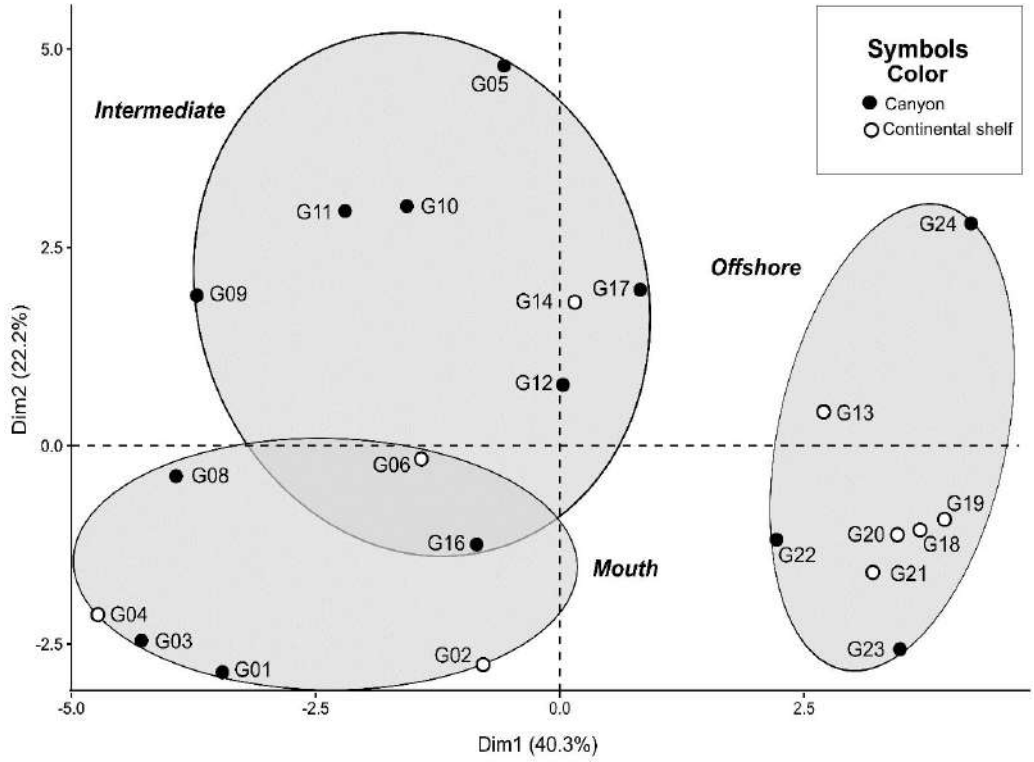

Figure 3 - PCA of prokaryotic phyla relative abundance (> 0.05%) from the 16S rDNA genes sequences for all locations sampled (n=22) in the Capbreton Canyon (grey symbols) and the adjacent continental shelf (white symbols). Individual PCA illustrates position of samples on the two first dimensions representing 62.5 % of inertia (correlation circle in Supporting Information, Fig. S2). Grey circles represent group of locations determined by using cluster analysis based of Euclidian distance (dendrogram in Supporting Information, Fig. S3).

3.2 Microorganisms involved in the Hg methylation: 16s rDNA versus *hgcA* gene

A previous study showed that the methylmercury proportion of total Hg decreased along the canyon axis, associated with a decrease of Hg methylation likely of biotic origin [126]. *hgcA* diversity was investigated in one sediment of each of previously defined habitat (three sediments into the canyon along the canyon axis (G03, G10 and G24) and one from the continental shelf (G14)) in order to observe the diversity of Hg-methylating microbial communities. In addition, known groups containing Hg-methylators were assessed using the 16S rDNA marker.

The alpha diversity in the different Capbreton canyon sediments was similar (Supporting information, table S2). *Deltaproteobacteria*, which includes most of the known Hg-methylating bacteria, were the most abundant and accounted for 50% of the *Proteobacteria* and 25% of the total reads (Fig. 4). Among phyla known to contain Hg-methylators members, *Planctomycetes* were observed at 8.6 ± 1.9% of total reads and *Chloroflexi* at 3.0 ± 1.9% of total reads.

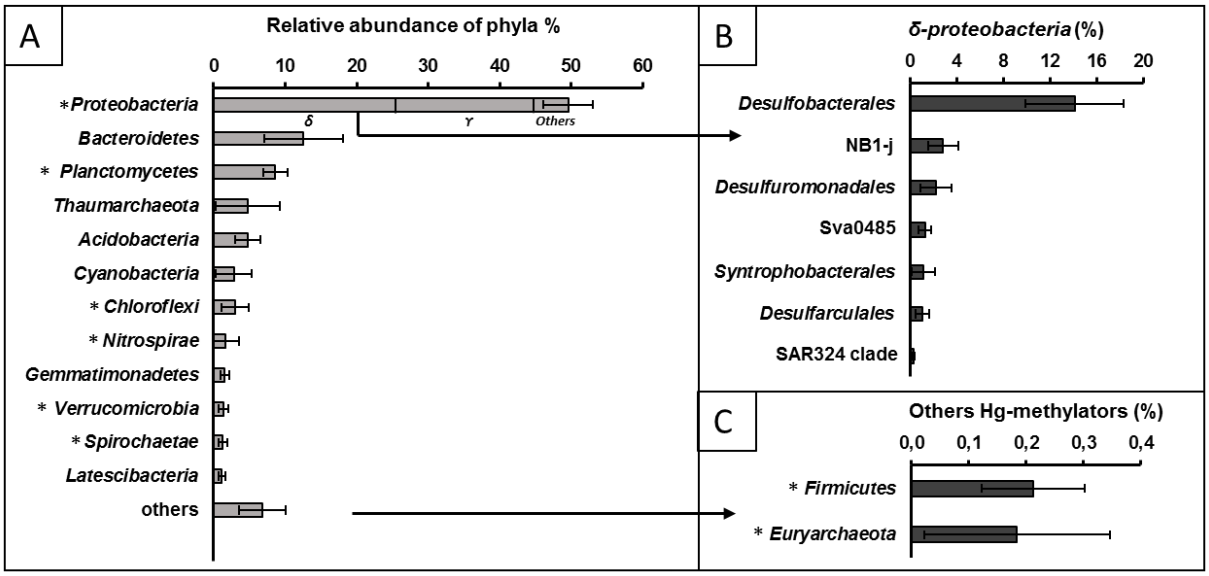

*Figure - 4 Relative abundance of prokaryotic 16S rDNA sequences from sediments of Capbreton canyon and adjacent continental shelf (n= 22) (A), within the Deltaproteobacteria (B) and the Firmicutes and the Euryarchaeota among others groups (C). Data are average percentages (± SE). Categories representing > 1% are shown. *represents known groups containing Hg-methylators.*

The relative abundance of the operational taxonomic units (OTUs) from 16S rDNA within the *Deltaproteobacteria* group, showed the dominance of *Desulfobacterales* over *Desulfuromonadales*, NB1-J, Sva0485, *Desulfarculales* and *Syntrophobacterales* (Fig. 5), with maximum total relative abundance of 20.8%, 5.4%, 4.9%, 1.8%, 2.2% and 3.3%, respectively. Genera within the *Deltaproteobacteria* known to methylate Hg (*Desulfobacteraceae*, *Desulfobulbaceae* and *Desulfuromonodaceae)* were dominated by *Desulfobulbus* and other uncultivated or unaffiliated genera. The relative abundance of *Desulfuromonadales* decreased along the canyon transect like the unknown genus of *Desulfobacterales*. SEEP, SRB1, *Desulfobulbus* follow the trend of the *Desulfobacterales* order trend and SVA0081 increased along this transect. Although *Geobacter sp.* were found as a crucial Hg-methylator in continental aquatic ecosystems [91,92,315], here, abundance of *Geobacteraceae* members peaked to only 0.17 ± 0.10% in the G03 location. Those results based on 16S rDNA may indicate that the bacterial sulfur-reduction, i.e sulfate and sulfur reduction, is the dominant metabolic guild in these marine sediments.

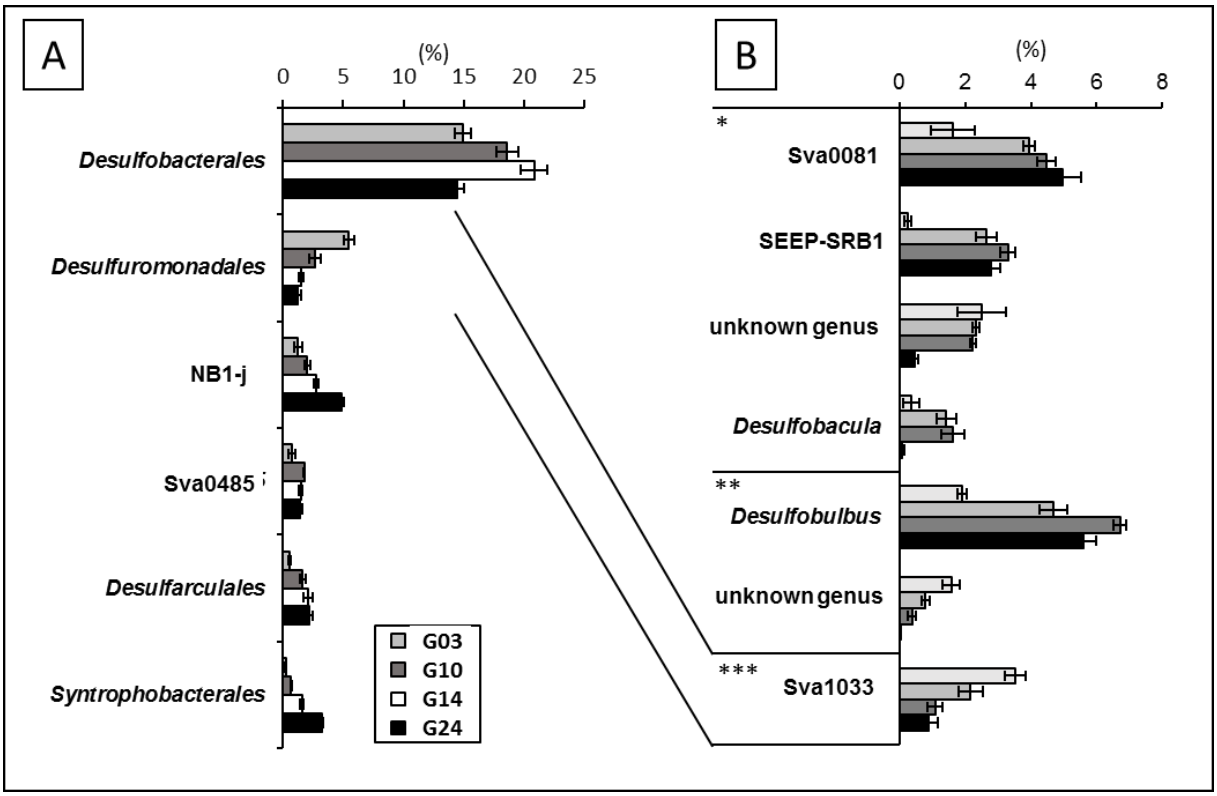

Figure 5 - Relative abundance of 16S rDNA sequences from Deltaproteobacteria in the sediments collected in the Capbreton canyon focused of the 4 selected locations (G03, G10, G14, G24) : order level (A) and genera or groups level (B) from (*) Desulfobacteraceae, (**) Desullfobulbaceae and (***) Desulfuromonodaceae families. Data are average percentages (± SE) from triplicate. Only categories representing > 1% are shown.

A total of 84 HgcA clones were obtained from locations G03, G10, G14 and G24 (n= 19, 22, 21, 22, respectively). They were mainly related to the *Deltaproteobacteria* (21% of the total HgcA clones), dominated by the SRB (10 HgcA clones) followed by ferrireducers (*Desulfuromodales*) and syntrophs (*Syntrophobacterales*) (Fig. 6 and Fig.7). HgcA clones were also related to recent new clades like *Chloroflexi*, *Atribacteria*, *Archae*, PVC superphylum, *Spirochaetes*, *Elusimicrobia* and *Bacteriodetes* (Fig. 6). Nevertheless, 61 % of the HgcA clones were unaffiliated (unaffiliated 1 to unafilliated 7 groups). While 18 clones of these unafilliated HgcA clones were unkown, 22 and 11 HgcA clones were likely related to *Deltaproteobacteria* (BSR like) and PVC superfphylum / *Aminicenantes,* respectively (Fig. 6 and Fig. 7) All together, almost half of HgcA clones (43 out of 84) obtained from the Capbreton submarine canyon sediments are likely related to *Deltaproteobacteria* with dominance of sulfate reducers. While HgcA clones cannot be representative of the Hg-methylators diversity due to the low number of clones per location and the selective approach used (cloning sequencing), those results follow the trend observed with the 16S rDNA approach, suggesting that microbial methylation is dominated by sulfate reduction.

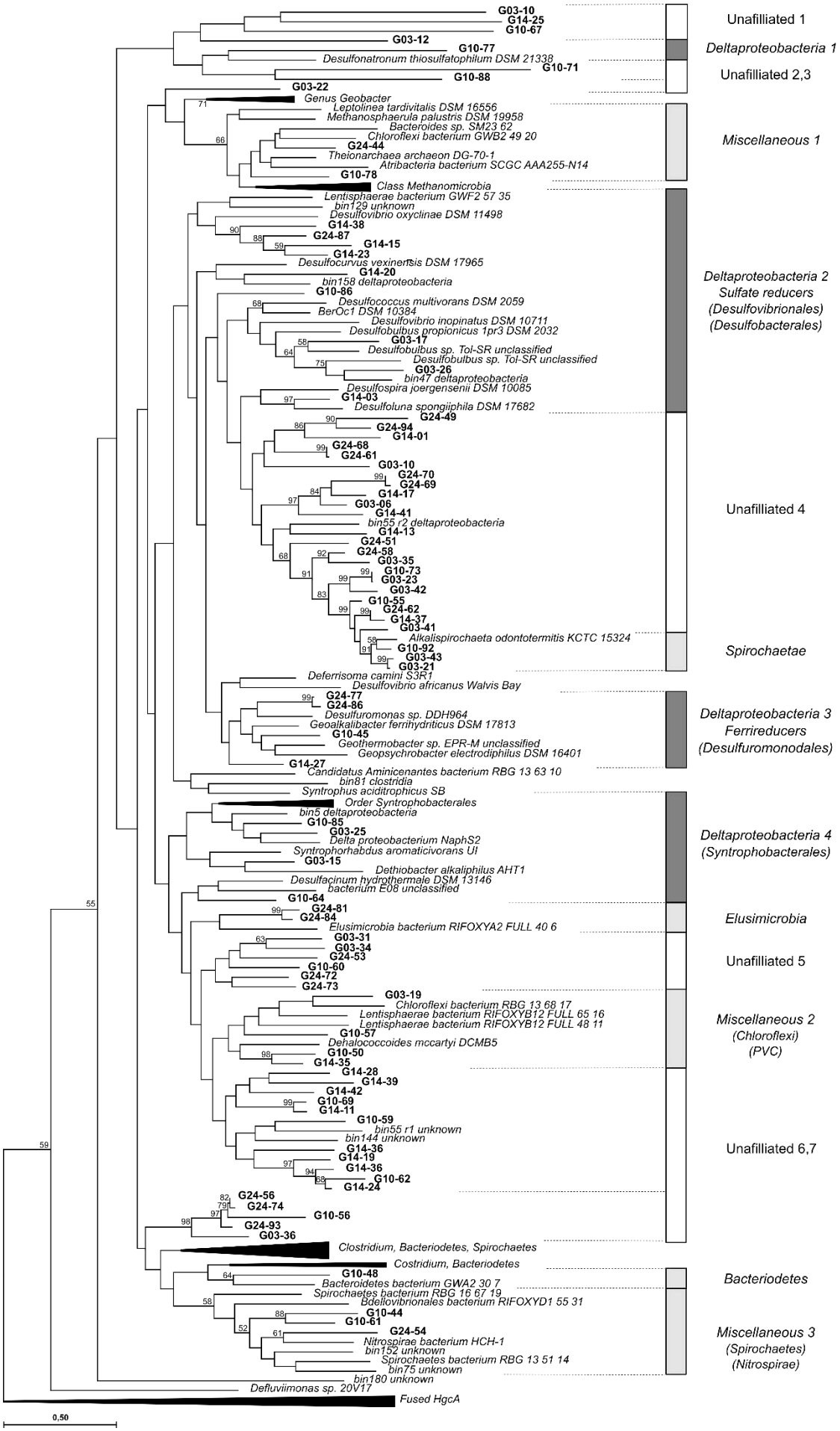
G03-10
G14-25
G10-67
G03-12
G10-77
Desulfonatronum thiosulfatophilum DSM 21338
G10-71
G10-88
G03-22
Genus Geobacter
Leptolinea tardivitalis DSM 16556
Methanosphaerula palustris DSM 19958
Bacteroides sp. SM23 62
Chloroflexi bacterium GWB2 49 20
G24-44
Theionarchaea archaeon DG-70-1
Atribacteria bacterium SCGC AAA255-N14
G10-78
Class Methanomicrobia
Lentisphaerae bacterium GWF2 57 35
bin129 unknown
Desulfovibrio oxyclinae DSM 11498
G14-38
G24-87
G14-15
G14-23
Desulfocurvus vexinensis DSM 17965
G14-20
bin158 deltaproteobacteria
G10-86
Desulfococcus multivorans DSM 2059
BerOc1 DSM 10384
Desulfovibrio inopinatus DSM 10711
Desulfobulbus propionicus 1pr3 DSM 2032
G03-17
Desulfobulbus sp. Tol-SR unclassified
Desulfobulbus sp. Tol-SR unclassified
G03-26
bin47 deltaproteobacteria
Desulfospira joergensenii DSM 10085
G14-03
Desulfoluna spongiiphila DSM 17682
G24-49
G24-94
G14-01
G24-68
G24-61
G03-10
G24-70
G24-69
G14-17
G03-06
G14-41
bin55 r2 deltaproteobacteria
G14-13
G24-51
G24-58
G03-35
G10-73
G03-23
G03-42
G10-55
G24-62
G14-37
G03-41
Alkalispirochaeta odontotermitis KCTC 15324
G10-92
G03-43
G03-21
Deferrisoma camini S3R1
Desulfovibrio africanus Walvis Bay
G24-77
G24-86
Desulfuromonas sp. DDH964
Geoalkalibacter ferrihydriticus DSM 17813
G10-45
Geothermobacter sp. EPR-M unclassified
Geopsychrobacter electrodiphilus DSM 16401
G14-27
Candidatus Aminicenantes bacterium RBG 13 63 10
bin81 clostridia
Syntrophus aciditrophicus SB
Order Syntrophobacterales
bin5 deltaproteobacteria
G10-85
G03-25
Delta proteobacterium NaphS2
Syntrophorhabdus aromaticivorans UI
G03-15
Dethiobacter alkaliphilus AHT1
Desulfacinum hydrothermale DSM 13146
bacterium E08 unclassified
G10-64
G24-81
G24-84
Elusimicrobia bacterium RIFOXYA2 FULL 40 6
G03-31
G03-34
G24-53
G10-60
G24-72
G24-73
G03-19
Chloroflexi bacterium RBG 13 68 17
Lentisphaerae bacterium RIFOXYB12 FULL 65 16
Lentisphaerae bacterium RIFOXYB12 FULL 48 11
G10-57
Dehalococcoides mccartyi DCMB5
G10-50
G14-35
G14-28
G14-39
G14-42
G10-69
G14-11
G10-59
bin55 r1 unknown
bin144 unknown
G14-36
G14-19
G14-36
G10-62
G14-24
G24-56
G24-74
G10-56
G24-93
G03-36
Clostridium, Bacteriodetes, Spirochaetes
Costridium, Bacteriodetes
G10-48
Bacteroidetes bacterium GWA2 30 7
Spirochaetes bacterium RBG 16 67 19
Bdellovibrionales bacterium RIFOXYD1 55 31
G10-44
G10-61
G24-54
Nitrospirae bacterium HCH-1
bin152 unknown
Spirochaetes bacterium RBG 13 51 14
bin75 unknown
bin180 unknown
Defluviimonas sp. 20V17
Fused HgcA
0,50
Unafilliated 1
Deltaproteobacteria 1
Unafilliated 2,3
Miscellaneous 1
Deltaproteobacteria 2
Sulfate reducers
(Desulfovibrionales)
(Desulfobacterales)
Unafilliated 4
Spirochaetae
Deltaproteobacteria 3
Ferrireducers
(Desulfuromonodales)
Deltaproteobacteria 4
(Syntrophobacterales)
Elusimicrobia
Unafilliated 5
Miscellaneous 2
(Chloroflexi)
(PVC)
Unafilliated 6,7
Bacteriodetes
Miscellaneous 3
(Spirochaetes)
(Nitrospirae)

Figure 6 - Maximum likelihood phylogenetic tree, based on aligned translated partial HgcA sequences (357 amino acid positions), conducted with Mega X [318,324]. HgcA sequences from the Capbreton canyon sediment are in bold, references sequences are in italic (composition of references groups are listed in Supplementary Information, Table S4). The sidebar denotes the different phylogenetic groups represented on the tree with the dark grey, light grey and white portions corresponding to Deltaproteobacteria, others phylogenetic groups and unaffiliated groups, respectively. Number at nodes indicates bootstrap values > 50.

4 Discussion

4.1 Geochemical conditions along Submarine canyons offer a diversity of ecological niches

We identified four distinct habitats along the canyon transect (Fig. 2) where Hg species, OM and TS contents were enriched. OM composition and TS play important roles in Hg biogeochemistry like MeHg formation and accumulation, as seen elsewhere [126,233,325,326]. Higher biotic methylation in coastal samples as compared to the offshore sediments as determined in ~~a~~ previous work, may be explained by a higher OM lability [327] and a differential sequestration of particulate matter along the canyon (i.e. gravitational sedimentation, hemipelagic sedimentation, remobilization). Otherwise, *Cyanobacteria* that might have come from the water released by the nearby Adour estuary [229], decrease along the canyon axis. As a primary producer, *Cyanobacteria* may contribute to the local OM, with higher production in coastal sediments than offshore sediments, and thus might control the MeHg production [328,329]. Moreover, Capbreton Canyon is still active, meaning it is still filled with particulate matter [103], where fine particulate matter is transported along the canyon transect (gravitational sedimentation), confirmed by the higher fine fraction measured in offshore sediment relative to the coastal sediments [126]. According to Mestre et al. [330] microbial community composition varied with particle size where, Bacteria were more diverse in larger size-fractions, whereas Archaea were more diverse in smaller particles determining diverse ecotypes with distinct size-fraction preferences. Considering colonization of the four habitats by three distinct bacterial communities (Fig. 2 and Fig. 3), different abundances of known groups containing Hg-methylators (Fig. 4) were correlated with the diverse metabolisms of Hg methylators identified along this canyon (Fig. 5), our results highlighted that geochemical conditions controlled both the global microbial communities and thus the Hg methylating microbial communities.

4.2 Hg-methylating communities in submarine canyon sediments: global and functional approaches

For the first time, in submarine canyon sediments, we identified Hg methylating communities using both 16S rDNA and *hgcA* gene. The organic carbon remineralization in marine sediments is dominated by bacterial sulfate reduction [331,332] performed by *Deltaproteobacteria* who are known to be the main group of Hg-methylating microorganisms [85,89–91,333]. Nevertheless, although 16S rDNA analysis showed the *Desulfobacterales* as dominant, *hgcA* analysis showed SRB were also related to *Desulfovibrionales.* That is in accordance with the results of SRB identified in the water column in this canyon [230]. *hgcA* clones within the “unafilliated 4”, likely affiliated with the *Deltaproteobacteria* [92], might be related to the uncultured or unknown bacteria from the 16S rDNA analysis (Fig.5 and Fig.6). We suggest putative Hg methylating bacteria of unknown genera within the *Desulfubacteracea*e, *Desulfobulbaceae* and Sva1033 within the *Desulfuromonadaceae*. The relative abundance of those genera followed the trend of Hg methylation potential along the canyon axis, suggesting their involvement in this process. Moreover, Sva1033 was related to *Desulfuromonas palmitatis* [334] and Kerin et al. 2006 [335] demonstrated that the latter, in pure culture under iron reducing conditions, was able to methylate Hg. Although sulfate reducing bacteria are widely studied and accepted as the major bacteria involved in mercury methylation in aquatic environments, these sulfate but also sulfur reducing bacteria remain largely unknown in marine environments.

Like in recent studies, *hgcA* analysis showed that the Hg methylators are also represented by fermentative organisms, or ferrireducers (Fig. 6) [90,92,333,336]. This highlighted the complexity between geochemical parameters and microorganisms involved in~~to~~ ~~the~~ MeHg formation. As recently discovered, HgcA clones were related to new phyla containing *hgcA* [92], such as *Aminicenantes*, *Bacteriodetes*, *Kiritimatiellaeota, Elusimicrobia* and Spirochaetes (Fig. 6).

Hg methylation is a strain-specific trait (Ranchou-Peyruse et al., 2009; Podar et al., 2013; Gilmour et al., 2013; Yu et al., 2013; Gilmour et al., 2018) that cannot be predicted purely by 16S rDNA taxonomic classification. Although another recent study demonstrated that 16s rRNA gene pyrosequencing did not have sufficient resolution to identify *hgcAB* harboring species in soil samples [333], this approach in marine sediments could provide indications about the *hgcA*-carrying *Prokaryotes*. The unknown *hgcA*-carrying populations are from uncultivated organisms, and consequently their identification, cultivation and specific contribution for MeHg remain to be explored.

MeHg proportion has previously been used as a proxy for methylation efficiency [337,338] and high MeHg proportion has also in a few cases been shown to correlate positively with the abundance of Hg(II) methylators [315]. Relative abundance of some phyla showed a strong correlation with MeHg proportion such as *Cyanobacteria* or *Gemmatimonadetes* (Table S5) suggesting that they could be involved, indirectly or directly, in MeHg formation. This may suggest that not only the Hg methylators themselves, i.e. *Deltaproteobacteria,* but also the supporting and interacting bacterial communities residing in the sediment may influence the MeHg formation across the studied submarine canyon sediments [315].

As previously demonstrated in these sediments, methylmercury production is under control of both methylation and demethylation processes [126]. Although the methylation seems to be controlled by microbial activities (for example *hgcA* gene is used as a proxy of microbial methylation), demethylation can be both abiotic (e.g. photoreduction) and biotic (e.g. reductive (performed by microorganisms carrying *operon mer*), oxidative (performed by methylotrophs)) processes [171,172,339]. Such biotic demethylation should be investigated in further studies to better understand microbial involvement in the Hg cycle in marine environment.

4.3 The S cycling and OM in marine sediments : drivers of Hg biomethylation ?

The mercury bioavailability for methylating microorganisms in marine sediments and indirectly the MeHg production, is controlled OM mineralization, thus depending on geochemical parameters [326,340] and the degree of OM lability. Only a small portion of the total inorganic mercury is likely available for cellular uptake [341]. Indeed, the relative partitioning of Hg(II) between various dissolved and particulate forms will govern the overall mobility of Hg in aquatic systems and the bioavailability of Hg to methylating microorganisms in anaerobic settings. OM could be more labile in coastal sediment [327], which may improve the microbial activities. This suggests that terrestrial inputs, from the high proximity of the canyon mouth to the coast, can influence Hg-methylating microbial composition and thus could explain the higher estimated methylation potential in coastal locations compared to the offshore sediments.

Putative Hg methylators were found among different anaerobic metabolic guilds, including sulfate and sulfur-reducing bacteria, dehalorespiring bacteria, syntrophs, and in some cases FeRB (Fig. 6) but also some newly identified micro-organims (*Chloroflexi, Spirochaetes, Elusimicrobia,* PVC superphylum). This suggests that Hg methylation potential is shared by organisms using a wide variety of carbon sources and electrons acceptors. This is in accordance with recent studies which demonstrated that the putative Hg methylators are

phylogenetically more diverse that previously, suggesting several independent horizontal gene transfer events [92,311].

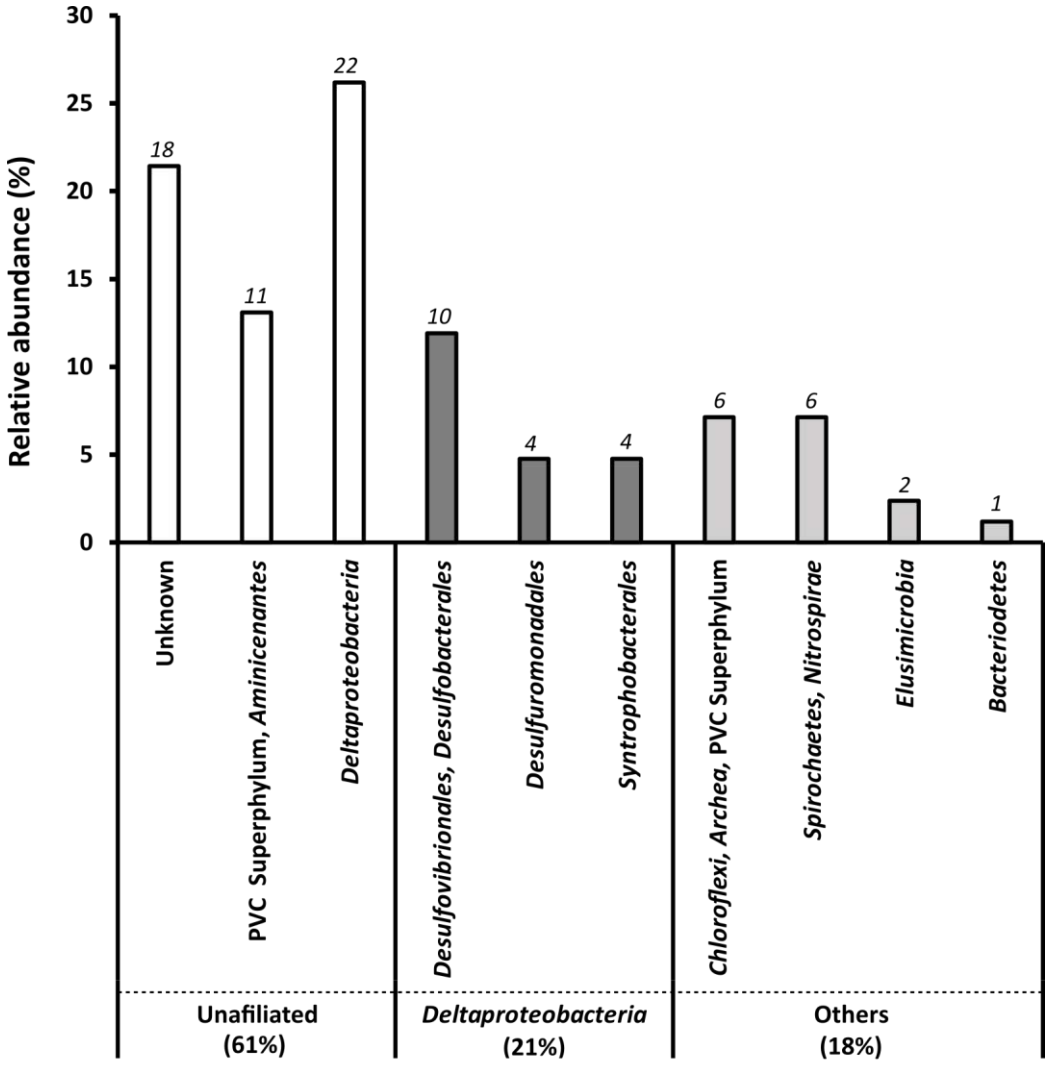

Figure 6 - Relative abundance (%) of Hg-methylating prokaryotes carrying hgcA in sediments from Capbreton Canyon. Italic numbers correspond to the number of HgcA sequences obtained for this study (total number=84).

Carbon cycling in marine sediments is dominated by sulfate-reduction that could mineralize 50% of the OM [331]. This is in accordance with the predominance of sulfur reducing bacteria (observed within 16S rDNA and HgcA) observed in these sediments. Fermenters were also observed in all studied sediments (Fig. 7). This suggests a fermentative degradation of OM from complex carbon molecules to small carbon products (i.e. proprionate, pyruvate, acetate) and dihydrogen production. They could be used as electron donors for the SRB and methanogens [309], improving the Hg biomethylation. Otherwise, OM degradation depends on the microbial composition and then both the methylating and non-methylating bacterial may control the MeHg formation [91,315]. Specific

populations of non-Hg(II) methylating bacteria actively decomposing OM seem also to create a niche that promotes Hg(II) methylation. Also, it has been demonstrated that bioturbating fauna disturbed mechanically the electrogenic sulfur oxidation through long filamentous bacteria (*Desulfobulbaceae*), which likely mediated the electron transport between the deep and surface marine sediments (at the centimetre scale; 50), could have profound implication for the sulfur cycle. This highlights the complexity of interspecific relationship at different scales for the S and the Hg cycling in marine sediments [343].

In oceans and seas, methylation of mercury occurs both in column water and sediment compartment [88,179,344]. At a global scale, Boyd et al. 2019 [345] showed that carbon sequestration in the open ocean is probably more influenced by solubility than biological activity. These insights into carbon sequestration can be taken into consideration to better understand the ~~Hg~~ biogeochemical cycle of mercury in ocean sediments. Although the OM is very reactive in the euphotic layer of the ocean, the carbon can directly sink to the bottom surface sediment [327] and could be an important carbon pump reacting into the Hg cycle, i.e. increase Hg methylation. Marine environment are the largest habitat on the earth accounting for more than 90% of total biosphere volume. The microorganisms colonizing marine habitats are responsible for more than 50% of the global primary production and nutrient cycling [112].

Carbon sedimentation at the bottom ocean of the ocean represents a significant fraction of global oceanic carbon sequestration [345] and could influence the bacterial composition, and consequently, can be a determinant for the formation of methylmercury [91,346–348]. The high anthropogenic Hg levels found in the North Atlantic ocean [162,207] associated with the high affinity of Hg for OM, could sink and trap Hg in those marine sediments. It is crucial to improve our knowledge of the Hg-methylating bacteria in marine sediments, in order to estimate their impact on MeHg production in ~~a~~ the global Hg cycle.

Conclusion

In this study, an assessment of marine Hg-methylating microbial communities was conducted in submarine canyon sediments by combining pluridisciplinary approaches including geochemical parameters, mercury speciation, global microbial diversity and *hgcA*-carrying bacteria diversity. Results highlighted that the distribution of microbial communities in submarine canyon sediments as well as methylation of mercury, were driven by the environmental parameters. Although Hg(II) and MeHg concentrations increased along the canyon axis from the coast to the offshore, the fraction of MeHg was higher in coastal locations due to the higher biomethylation potential estimated in coastal sediments [126]. These results may indicate that methylation of Hg in marine sediments is driven by OM

composition and the S cycle. Indeed, 16S rDNA and *hgcA* analysis suggested that *Deltaproteobacteria* dominated by sulfur-compounds-reducing bacteria are the main contributors for the methylation of Hg in marine sediments. Nevertheless, further studies are needed to identify and characterize/isolate the unaffiliated and unknown *hgcA* carrying microorganisms that could be novel Hg-methylators. Their methylation and demethylation capacities must be also determined in order to estimate their impacts on MeHg production in marine environments at the global scale. To fully understand and quantify the relationship between Hg, sulfur, OM and microorganisms, further studies are also needed to decipher the biogeochemical cycle of Hg in marine sediments.

File 1– Aligment of selected refences and HgcA sequences from HgcA with Muscle method (MEGA X) **(.fasta)**

Table S1 - Variance Inflector Factor (VIF) multicollinearity diagnostics of the geochemical parameters (MeHg proportion, inorganic Hg, depth, Total Sulfur and Particulate Organic Carbon) from Capbreton Canyon and the adjacent continental shelf sediments. Detection = 0 means collinearity is not detected by the test.

	VIF	**detection**
% MeHg	1.4	0
HgII	5.1	0
depth	4.3	0
TS	3.4	0
POC	4.8	0

Table S2 – Biodiversity indices based on 16s rDNA analysis of the sediments of Capbreton canyon. The data showed the mean and the standard deviation of three replicates.

Location	Chao1	Observed	Exp Shannon	1/Simpson
G01	1326 ± 30	903 ± 51	369 ± 49	154 ± 25
G02	1443 ± 16	1015 ± 13	461 ± 8	173 ± 1
G03	1311 ± 67	909 ± 16	386 ± 32	152 ± 25
G04	1363 ± 35	971 ± 12	431 ± 17	178 ± 9
G06	1621 ± 31	1113 ± 15	501 ± 14	192 ± 8
G05	1538 ± 35	1092 ± 20	528 ± 11	220 ± 5
G09	1472 ± 50	1001 ± 10	407 ± 9	156 ± 4
G08	1627 ± 62	1100 ± 3	498 ± 3	200 ± 3
G10	1622 ± 48	1110 ± 21	515 ± 12	203 ± 9
G11	1528 ± 134	1013 ± 17	421 ± 6	150 ± 6
G12	1685 ± 71	1189 ± 13	549 ± 12	192 ± 10
G13	1624 ± 36	1091 ± 40	466 ± 27	170 ± 3
G14	1702 ± 52	1153 ± 20	523 ± 18	195 ± 12
G16	1673 ± 115	1096 ± 18	394 ± 14	87 ± 7
G17	1644 ± 72	1110 ± 26	479 ± 18	169 ± 11
G18	1498 ± 13	1015 ± 8	391 ± 3	127 ± 9
G19	1483 ± 28	1037 ± 5	437 ± 8	154 ± 3
G21	1427 ± 241	1013 ± 137	410 ± 113	128 ± 65
G20	1418 ± 60	993 ± 53	425 ± 54	164 ± 28
G22	1449 ± 57	999 ± 25	383 ± 10	103 ± 5
G23	1208 ± 68	817 ± 34	243 ± 35	62 ± 7
G24	1380 ± 48	983 ± 17	417 ± 4	158 ± 2
All	1502 ± 62	1033 ± 26	438 ± 22	158 ± 12

Table S3 – Compilation of references carrying HgcA gene (n=189) from isolated strains' genomes, from metagenomes obtained from NCBI (https://www.ncbi.nlm.nih.gov/), ~~Imager~~ Integrated Microbial Genomes and Microbiomes platform (IMG/M, developed by the Joint Genome Institute, CA, USA, http://img.jgi.doe.gov/) and previous studies. HgcA sequences were also collected from Pfam database according to Podar et al, 2015 and Christensen et al 2019 using custom Pfam models (CFesP proteins classified under Pfam3599). From these references, we selected only sequences with the conservative cysteine in HgcA gene (Smith et al 2015) within the CWA motif. Others references were from metagenomic approach (Jones et al 2019) and others (references in the table).

Strains / Organisms	UnitProt / GenBank	Taxonomy ID	Reference
Acetivibrio cellulolyticus CD2 DSM 1870	WP_010243111		
Acetonema longum APO 1 DSM 6540	EGO62461.1		
Alkaliphilus peptidifermentans DSM 18978	A0A1G5LD09	1120976	
Alkalispirochaeta odontotermitis KCTC 15324	A0A0A0DNS7	1329640	*Sravanthi et al. (2016)*
Anaerocolumna jejuensis DSM 15929	A0A1M6W1F7	1121322	
Anaerocolumna xylanovorans DSM 12503	A0A1M7YNG5	1121345	
Anaerolineaceae bacterium 4572 32.2	A0A1W9UNX3	1971624	
Atribacteria bacterium SCGC AAA255-N14		192495	
bacterium E08 (2017) unclassified Bacteria	A0A202DIM8	1932693	
Bacteroidales bacterium 45-6 unclassified	A0A1Q3M6L0	1895719	
Bacteroides sp. SM23 62	A0A0S8K2G4	1703352	
Bacteroidetes bacterium GWA2 30 7	A0A1F3F194	1797313	
Bdellovibrionales bacterium RIFOXYD1 FULL 55 31	A0A1F3Y9R3	1797404	
BerOc1 DSM 10384	WP 071544503.1		*Ranchou-Peyruse et al. (2018)*
bin111 scaf8191 PROKKA 00002			*Jones et al. (2019)*
bin112 scaf12562 PROKKA 00011			*Jones et al. (2019)*
bin12 scaf63148 PROKKA 00003			*Jones et al. (2019)*
bin129 scaf31187 PROKKA 00005			*Jones et al. (2019)*
bin143 scaf1086 PROKKA 00017			*Jones et al. (2019)*
bin144 scaf3542 PROKKA 00009			*Jones et al. (2019)*
bin152 scaf19323 PROKKA 00003			*Jones et al. (2019)*
bin158 scaf9437 hgcAonly PROKKA 00009			*Jones et al. (2019)*
bin159 scaf27414 PROKKA 00003			*Jones et al. (2019)*
bin161 scaf119 PROKKA 00103			*Jones et al. (2019)*
bin180 scaf7379 PROKKA 00005			*Jones et al. (2019)*
bin26 scaf59132 PROKKA 00003			*Jones et al. (2019)*
bin43 scaf10320 PROKKA 00014			*Jones et al. (2019)*
bin47 scaf8582 PROKKA 00008			*Jones et al. (2019)*
bin5 scaf24242 PROKKA 00002			*Jones et al. (2019)*
bin55 scaf1218 PROKKA 00023			*Jones et al. (2019)*
bin55 scaf7203 PROKKA 00013			*Jones et al. (2019)*
bin61 scaf39489 PROKKA 00001			*Jones et al. (2019)*

bin67 scaf85604 PROKKA 00002			*Jones et al. (2019)*
bin75 scaf21842 PROKKA 00001			*Jones et al. (2019)*
bin77 scaf60597 PROKKA 00001			*Jones et al. (2019)*
bin81 scaf4680 PROKKA 00016			*Jones et al. (2019)*
bin85 scaf3615 PROKKA 00016			*Jones et al. (2019)*
bin93 scaf53 bin93 node53 PROKKA 00083			*Jones et al. (2019)*
bin95 scaf12911 PROKKA 00005			*Jones et al. (2019)*
bin97 scaf3218 PROKKA 00012			*Jones et al. (2019)*
Caloramator mitchellensis sp. VF08	A0A0R3JSA0	908809	*Ogg and Patel (2011)*
candidate division OP8 bacterium SCGC AAA252-F08			
candidate division OP9 bacterium SCGC AAA252-M02			
Candidatus Aminicenantes bacterium RBG 13 59 9	A0A1F5AV61	1797268	
Candidatus Aminicenantes bacterium RBG 13 63 1	A0A1F5B583	1797270	
Candidatus Aminicenantes bacterium RBG 13 63 10	A0A1F5BAE3	1797270	
Candidatus Bathyarchaeota archaeon RBG 13 38 9	A0A1F5DIG5	1797377	
Candidatus Heimdallarchaeota archaeon LC 2	A0A1Q9P5F1	1841597	
Candidatus Moduliflexus flocculans bacterium UASB14	A0A0S6VTP5	1499966	
Chloroflexi bacterium GWB2 49 20	A0A1F8KRX1	1797612	
Chloroflexi bacterium RBG 13 68 17	A0A1F8NXU3	1797638	
Clostridium cellobioparum DSM 1351	S0FI02	1121303	
Clostridium cellobioparum termitidis CT1112 DSM 5398	S0FI02	29371	
Clostridium cellulosi CS 4 4			
Clostridium sp. Bc-iso-3	A0A1E3C4D3	1848158	
Clostridium sp. Bc-iso-3	A0A1E3C4E8	1848158	
Clostridium straminisolvens JCM 21531	W4VBR0	1294263	
Clostridium tunisiense TJ	WP_017416929.1	219748	
Deferrisoma camini S3R1		1125863	
Defluviimonas sp. 20V17	A0A059ISM2	1417296	
Dehalobacter restrictus DSM 9455	WP_025205893.1	871738	
Dehalobacter sp 11DCA			
Dehalobacter sp UNSWDHB	EQB22247.1	1339256	
Dehalobacter sp. CF : CP003870	K4L0Y3	1131462	
Dehalococcoides mccartyi DCMB5	AGG05961.1	1193807	
delta proteobacterium MLMS-1	Q1NK61	262489	
delta proteobacterium NaphS2	D8FEF5	88274	
Desulfacinum hydrothermale DSM 13146	A0A1W1WXX7	1121390	
Desulfacinum infernum DSM 9756	A0A1M5E778	1121391	
Desulfamplus magnetovallimortis	A0A1W1HGL1	DSM 103535	*Descamps et al. (2017)*
Desulfitibacter sp. BRH c19	A0A101VAF2	1734395	
Desulfitobacterium dehalogenans JW/IU DC1 ATCC 51507	AFM01083.1	756499	
Desulfitobacterium dichloroeliminans LMG P 21439	L0F513	871963	
Desulfitobacterium metallireducens 853 15A DSM 15288	W0EDB0	871968	
Desulfobacterium vacuolatum DSM 3385	A0A1W2DTC2	1121400	
Desulfobulbus japonicus DSM 18378	WP_028582359.1	1121403	
Desulfobulbus mediterraneus DSM 13871	WP_028584587.1	1121404	
Desulfobulbus propionicus 1pr3 DSM 2032	E8RAX2	577650	
Desulfobulbus sp. Tol-SR unclassified	A0A0A2HT51	1536652	

Desulfocarbo indianensis DSM 28127	A0A0K9I5Q0	1348163	
Desulfococcus multivorans DSM 2059	S7U0P6	1121405	
Desulfocurvus vexinensis DSM 17965	WP_156939553.1	1121406	
Desulfofustis glycolicus DSM 9705	A0A1M5YF57	1121409	
Desulfoluna spongiiphila DSM 17682	A0A1G5HHN2	419481	*Ahn et al. (2009)*
Desulfomicrobium baculatum X DSM 4028	C7LVG1	525897	
Desulfomicrobium escambiense DSM 10707	WP_051307249.1	1121411	
Desulfomonile tiedjei DCB 1 DSM 6799	I4C2E8	706587	
Desulfonatronospira thiodismutans ASO3 1	D6SSN8	555779	
Desulfonatronovibrio hydrogenovorans DSM 9292	WP_051617342.1	1121413	
Desulfonatronum lacustre Z 7951 DSM 10312	WP_035262080.1	935942	
Desulfonatronum thiosulfatophilum DSM 21338	A0A1G6BW22	617002	
Desulfopila aestuarii DSM 18488	A0A1M7YCA7	1121416	
Desulfospira joergensenii DSM 10085	WP_153307583.1	1265505	
Desulfosporosinus acidiphilus SJ4 DSM 22704	I4D499	646529	
Desulfosporosinus lacus DSM 15449	A0A1M6A7D7	1121420	
Desulfosporosinus orientis Singapore I DSM 765	G7W8Z0	768706	
Desulfosporosinus sp. I2 unclassified	A0A0F2JK56	1617025	
Desulfosporosinus sp. OL unclassified	A0A1Q8QW16	1888891	
Desulfosporosinus sp. OT	G2G1C4	913865	
Desulfosporosinus sp. Tol-M unclassified	A0A0A2TIF6	1536651	
Desulfosporosinus youngiae JW/YJL B18 DSM 17734	H5XXI9	768710	
Desulfotalea sp. Unclassified	A0A2G2DVW0	2030813	
Desulfotignum balticum DSM 7044	WP_024336058.1	115781	
Desulfotignum phosphitoxidans FiPS 3 DSM 13687	S0G3G9	1286635	
desulfovibrio aespoeensis Aspo 2 DSM 10631	E6VW98	643562	
desulfovibrio africanus DSM 2603	WP_027367778.1	1121435	
desulfovibrio africanus PCS	EMG37847.1	1262666	
desulfovibrio africanus Walvis Bay	EGJ48477.2	690850	
Desulfovibrio alkalitolerans DSM 16529	S7UC14	1121439	*Abildgaard L et al. (2006) Spring S et al. (2019)*
Desulfovibrio bizertensis DSM 18034	A0A1T4VFM3	1121442	
Desulfovibrio desulfuricans ND132	F0JBF0	641491	
desulfovibrio inopinatus DSM 10711	WP_027186387.1	1121453	
desulfovibrio longus DSM 6739	WP_027189002.1	1121456	
desulfovibrio oxyclinae DSM 11498	WP_018125556.1	1121459	
Desulfovibrio putealis DSM 16056	WP_043644207.1	1121462	
Desulfovibrio sp. X2 unclassified	S7U091	941449	
Desulfuribacillus stibiiarsenatis DSM 28709	A0A1E5L9I2	1390249	*Abin and Hollibaugh (2017)*
Desulfuromonas soudanensis strain WTL	A0A0M4D2J5	1603606	*Badalamenti et al. (2016)*
Desulfuromonas sp. DDH964	A0A143BB07	1823759	
Dethiobacter alkaliphilus AHT1	C0GKZ8	555088	
Dethiosulfatarculus sandiegensis DSM 100305	A0A0D2JA33	1429043	
Elusimicrobia bacterium RIFOXYA2 FULL 40 6	A0A1F9X0Z7	1797958	
Ethanoligenens harbinense YUAN-3T DSM 18485	E6U3W1	663278	
Geoalkalibacter ferrihydriticus DSM 17813	A0A0C2HJE1	1121915	
Geobacter bemidjiensis Bem DSM 16622	B5EHJ2	404380	
Geobacter bremensis R1	WP_026842395.1	1304887	

Geobacter daltonii DSM 22248	B9M056	316067	
Geobacter metallireducens GS 15	Q39W98	269799	
Geobacter metallireducens RCH3	EHP88436.1	691164	
Geobacter pickeringii DSM 17153	A0A0B5BI21	345632	
Geobacter sp M18	E8WLC4	443143	
Geobacter sp M21	WP_015838335		
Geobacter sp. DSM 9736	A0A212PIJ7	1277350	
Geobacter sp. OR-1 unclassified	A0A0A8WU75	1266765	
Geobacter sulfurreducens DSM 12127	Q74D79	243231	
Geobacter uraniireducens (strain Rf4)	A5GCK4_GEO	351605	
Geobacter uraniireducens Rf4	A5GCK4	351605	
Geobacteraceae bacterium GWC2 53 11	A0A1G0N273	1798316	
Geopsychrobacter electrodiphilus DSM 16401	WP_156827088.1	1121918	
Geothermobacter sp. EPR-M unclassified	A0A1X0XMV0	1969733	
Gracilibacter sp. BRH c7a unclassified	A0A117S8Z7	1734398	
Kosmotoga pacifica SLHLJ1 : Ga0078918 11	A0A0G2ZE47	1330330	
Lentisphaerae bacterium GWF2 57 35	A0A1G0YCZ6	1798576	
Lentisphaerae bacterium RIFOXYA12 FULL 48 11	A0A1G1A528	1798578	
Lentisphaerae bacterium RIFOXYB12 FULL 65 16	A0A1G1C0D2	1798581	
Leptolinea tardivitalis DSM 16556	A0A0P6WXX6	229920	*Yamada et al. (2006)*
Lokiarchaeota archaeon (strain CR 4) unclassified	A0A1Q9MSN4	1849166	
Lokiarchaeum sp. (strain GC14 75) unclassified	A0A0F8XW16	1538547	*Spang et al. (2015)*
Methanocella arvoryzae MRE50	Q0W2F6	351160	
Methanocella paludicola SANAE	D1YWG8	304371	
Methanocorpusculum bavaricum DSM 4179	WP_042697303.1	1122230	
Methanofollis liminatans GKZPZ DSM 4140	J1L4E5	28892	
Methanolobus profundi DSM 21213	A0A1I4PLL0	487685	*Mochimaru et al. (2009)*
Methanolobus psychrophilus R15	K4M915	1094980	
Methanolobus sp. T82-4	A0A139CQ28	1794908	
Methanolobus tindarius DSM 2278	W9DU86	1090322	
Methanomassiliicoccales archaeon RumEn M1	A0A0Q4BFV7	1713724	
Methanomassiliicoccales archaeon RumEn M1	A0A0Q4BFV7	1713724	
Methanomassiliicoccus luminyensis B10	WP_019177913.1	1175296	
Methanomethylovorans hollandica DSM 15978	L0KTZ9	867904	
Methanoregula boonei DSM 21154	A7I5D0	456442	
Methanoregula formicica DSM 22288	L0HDZ2	593750	
Methanosarcina sp. Ant1	A0A1E7GGV6	1882735	
Methanosphaerula palustris DSM 19958	B8GGX7	521011	
Methanospirillum hungatei JF1 DSM 864	Q2FQB8	323259	
Natronincola peptidivorans DSM 18979	A0A1I0CAX9	426128	*Zhilina et al. (2009)*
Nitrospirae bacterium HCH-1	A0A109C0M4	1748249	
Paludibacter jiangxiensis JCM 17480	A0A170ZKK4	681398	*Qiu et al. (2016)*
Pelobacter seleniigenes DSM 18267	WP_029914612.1	1122946	
Peptoclostridium litorale DSM 5388	A0A069RKC8	1121324	
Pseudobacteroides cellulosolvens DSM 2933	A0A0L6JUS5	398512	
Pseudodesulfovibrio indicus DSM 101483	A0A126QSA6		*Cao et al. (2016)*
Pseudodesulfovibrio profundus DSM 11384	A0A2C8FBW6	57320	*Bale et al. (1997)* *Cao et al. (2016)*

Pyrococcus furiosus DSM 3638: AE009950	WP_011011854.1	186497	
Ruminiclostridium hungatei DSM 14427	A0A1V4SK86	48256	*Monserrate et al. (2001)*
scaf47750 bin89 PROKKA 00001			*Jones et al. (2019)*
Smithella sp. F21	A0A091B4M5	1538640	
Spirochaetes bacterium GWB1 36 13	A0A1G3L9D9	1802174	
Spirochaetes bacterium GWC1 61 12	A0A1G3MM08	1802180	
Spirochaetes bacterium GWF1 51 8	A0A1G3PL48	1802190	
Spirochaetes bacterium RBG 13 51 14	A0A1G3QH52	1802193	
Spirochaetes bacterium RBG 16 67 19	A0A1G3RAU2	1802196	
Syntrophaceae bacterium CG2 30 58 14	A0A1J5I533	1805378	
Syntrophobotulus glycolicus DSM 8271	F0SUS3	645991	
Syntrophorhabdus aromaticivorans UI			
Syntrophus aciditrophicus SB	Q2LXJ3	56780	
Syntrophus gentianae DSM 8423	A0A1H7ZYH0	43775	*Wallrabenstein et al. (1996)*
Theionarchaea archaeon DG-70-1	A0A151ENQ3	1803814	
WP 017952925.1 [Nitrospina]			*Gionfriddo et al. (2016)*

Table S4 – References sequences used within the different groups indicated in the phylogenetic tree in Fig. 6

Clusters	***References***
Genus Geobacter	*Geobacter sp M21* *Geobacter metallireducens RCH3* *Geobacter sp. DSM 9736* *Pelobacter seleniigenes DSM 18267*
Class Methanomicrobia	*Methanocella arvoryzae MRE50* *Methanomassiliicoccus luminyensis B10* *Methanoregula boonei DSM 21154* *Methanolobus profundi DSM 21213* *bin97 methanomicrobia* *Methanospirillum hungatei JF1 DSM 864*
Order Syntrophobacterales	*Smithella sp. F21* *bin26 deltaproteobacteria* *Syntrophaceae bacterium CG2 30 58 14* *bin85 deltaproteobacteria* *Desulfomonile tiedjei DCB 1 DSM 6799*
Clostridium, Bacteriodetes, Spirochaetes	*Pseudobacteroides cellulosolvens DSM 2933* *Acetivibrio cellulolyticus CD2 DSM 1870* *Dehalobacter restrictus DSM 9455* *Clostridium cellobioparum DSM 1351* *Desulfitobacterium metallireducens 853 15A DSM 15288* *Clostridium sp. Bc-iso-3* *Syntrophobotulus glycolicus DSM 8271* *bin161 clostridia* *Ethanoligenens harbinense YUAN-3T DSM 18485* *Desulfitibacter sp. BRH c19* *Acetonema longum APO 1 DSM 6540* *Spirochaetes bacterium GWF1 51 8*
Clostridium, Bacteriodetes	*Peptoclostridium litorale DSM 5388* *Clostridium tunisiense TJ* *Bacteroidales bacterium 45-6 unclassified*
Fused HgcA	*WP 017952925.1 MULTISPECIES: hypothetical protein [Nitrospina]* *Candidatus Bathyarchaeota archaeon RBG 13 38 9 unclassified* *Candidatus Heimdallarchaeota archaeon LC 2* *candidate division OP8 bacterium SCGC AAA252-F08* *Kosmotoga pacifica SLHLJ1 : Ga0078918 11* *candidate division OP9 bacterium SCGC AAA252-M02* *Pyrococcus furiosus DSM 3638: AE009950* *Anaerolineaceae bacterium 4572 32.2*

Table S5 - Determination coefficients between the % MeHg and the relative abundance of phyla based on 16s rDNA sequences. r^2 > to 0.3 are shown.

Phylum	**r^2**
Cyanobacteria	0,80
Gemmatimonadetes	0,68
Tenericutes	0,67
Verrucomicrobia	0,64
Acidobacteria	0,62
Bacteroidetes	0,52
Chloroflexi	0,47
Nitrospinae	0,38
Bathyarchaeota	0,35
Tectomicrobia	0,32
Thaumarchaeota	0,30

Fig. S1 – Dendrogram representing the clustering analysis (based of Euclidian distance) of PCA of environmental parameters selected with the VIF method (depth, TS content, POC content, Hg(II) concentrations and MeHg proportion) for all locations sampled (n=22) in the Capbreton Canyon and the adjacent continental shelf.

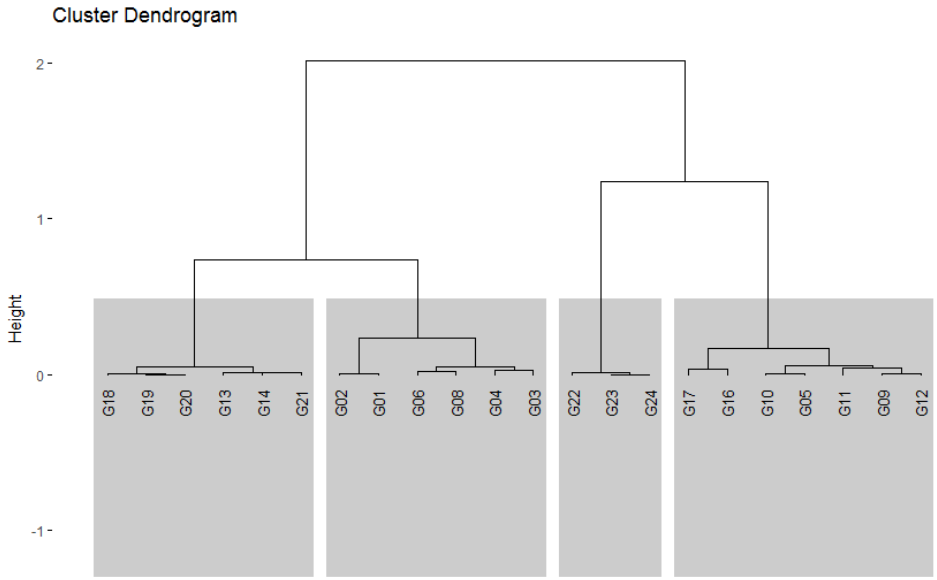

Fig. S2 : Variables PCA illustrates the correlations circle of prokaryotic phyla relative abundance (> 0.05%) from the 16S rDNA genes sequences for all locations sampled (n=22) in the Capbreton Canyon and the adjacent continental shelf, on the two first dimensions (62.5 %)

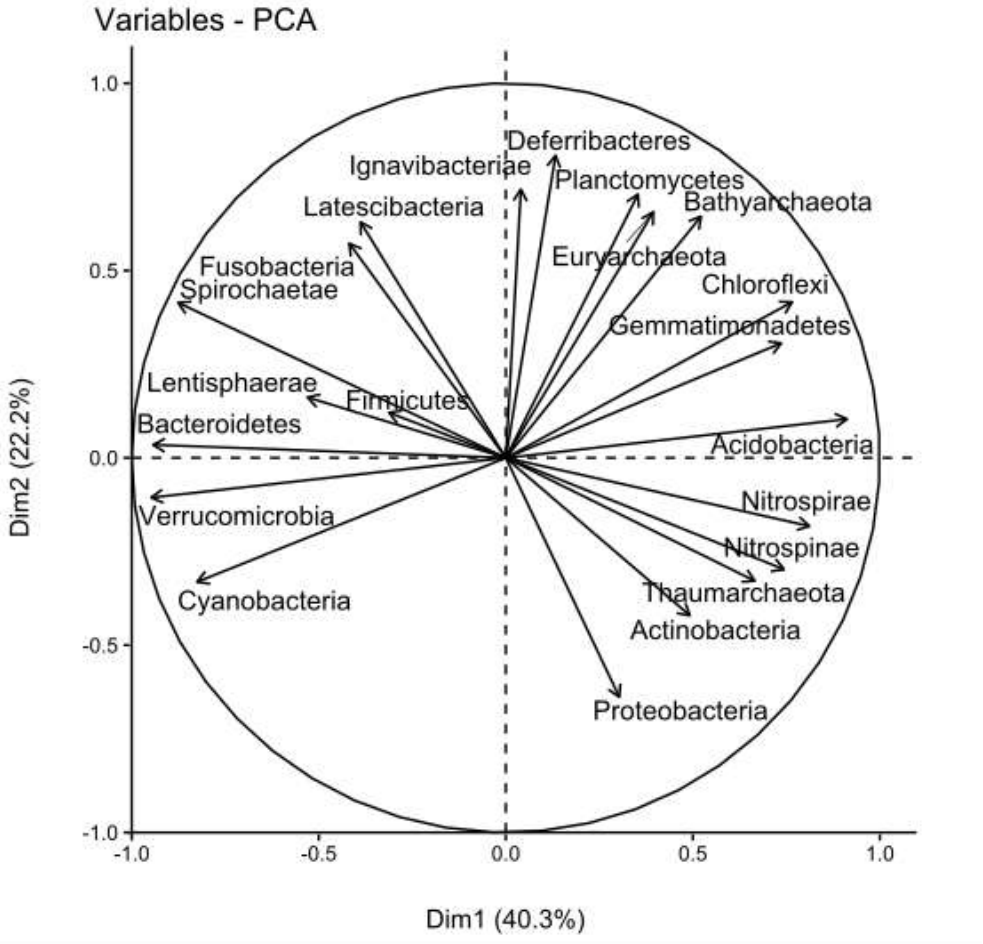

Fig. S3 : Dendrogram representing the clustering analysis (based of Euclidian distance) of PCA of prokaryotic phyla relative abundance (> 0.05%) from the 16S rDNA genes sequences for all locations sampled (n=22) in the Capbreton Canyon and the adjacent continental shelf.

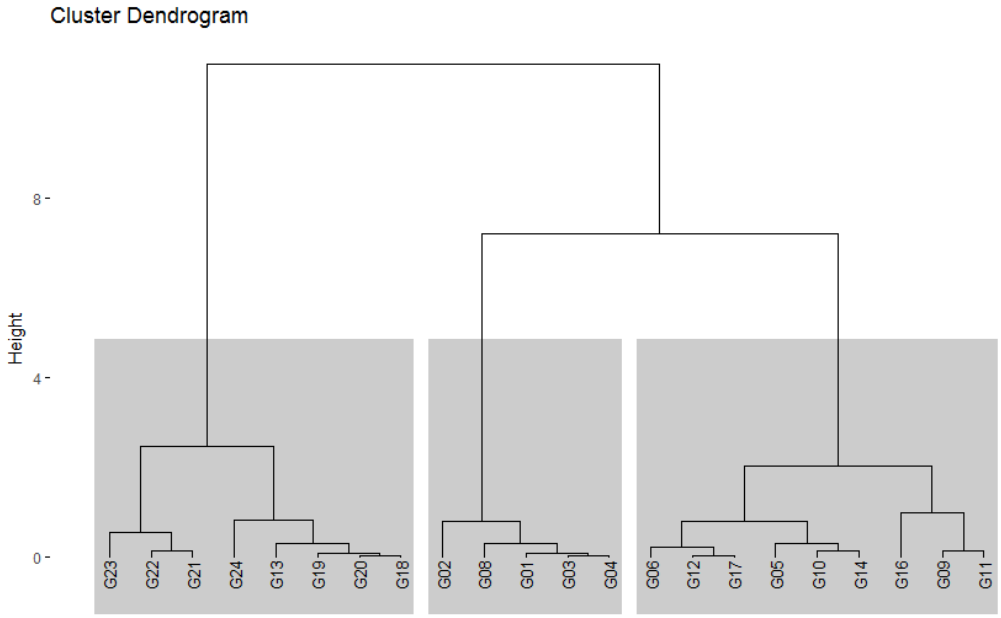

CONCLUSIONS ET PERSPECTIVES

Ce travail a permis l'étude de la réactivité et du devenir des micropolluants prioritaires et émergents dans un environnement marin particulier : le Canyon sous-marin de Capbreton. L'étude du compartiment sédimentaire, matrice intégratrice de l'état du milieu, a permis de répondre aux problématiques au travers des différentes études présentées précédemment. Ces travaux ont permis de renseigner sur l'impact des rejets de micropolluants dans les sédiments du Canyon de Capbreton, en mettant l'accent sur les interactions avec les microorganismes. Ici, seront discutés les résultats majeurs de ce travail en fonction des problématiques posées. Il sera ensuite proposé des recommandations et perspectives pour des études futures.

Le système du canyon de Capbreton : un milieu actif, intégratif et réactif

1. Un milieu actif : sources

Dans le cadre de ce travail, les signatures isotopiques du carbone (C), de l'azote (N) et du mercure (Hg) ont été étudiées afin de tracer les sources du matériel particulaire et du mercure. Les paramètres caractérisant le sédiment ont été aussi analysés pour renseigner la manière dont les sédiments se distribuent dans le canyon.

Nos résultats ont montré dans un premier temps une accumulation de particules fines sur le fond, les terrasses et les pentes du canyon. Au niveau du plateau continental les sédiments sont plutôt sableux. Cela confirme que le Canyon de Capbreton agit comme un piège à particules (minérales ou organiques) à la base de la forte activité primaire retrouvée dans ce type de milieu. Généralement, les sédiments prélevés dans le canyon (i.e., terrasses et pentes) sont aussi caractérisés par de fortes teneurs en carbone total, carbone organique et azote organique, pouvant être une source de nutriments pour les activités bactériennes.

Les signatures des isotopes stables du C, de N et du Hg, ne montrent pas de différences significatives entre les sédiments prélevés dans le canyon et sur le plateau continental adjacent. Cependant des différences ont été observées avec le gradient d'éloignement à la côte. Par exemple le $\delta^{13}C$, le $\delta^{15}N$ et le $\delta^{202}Hg$ montraient des sources plutôt « continentales » (similaires aux signatures de l'estuaire de l'Adour) sur les 10 premiers kilomètres du canyon alors que les stations au large (G17 à G24) montraient des signatures plutôt « océaniques » comparables à celles du phytoplancton.

Les canyons sous-marins sont une des caractéristiques géomorphologiques des plateaux continentaux qui permettent le transport de sédiment vers la plaine abyssale, sous l'effet de leur fort hydrodynamisme. Ils sont de véritables corridors sous-marins entre le continent et le milieu profond facilitant le transport de particules. Les rivières sont les sources majeures de ce matériel particulaire libéré sur les plateaux continentaux, démontrant le rôle

clef des panaches de rivières (chargés en particules en suspension) dans le contrôle de la distribution des sédiments dans la zone côtière. Le canyon de Capbreton débutant à 250 mètres de la côte est donc sous l'influence des apports continentaux dont le plus important est constitué par l'estuaire de l'Adour. Cet estuaire court le long de zones agricoles et urbaines avant de se jeter dans l'Océan Atlantique. Le canyon de Capbreton est un système actif de transport particulaire du continent vers la plaine abyssale. La forte affinité des micropolluants pour la phase particulaire constitue, dans le cas de cette étude, une des sources (potentielles) des micropolluants dans ce canyon. Nos résultats semblent le confirmer pour les sédiments des 10 premiers km de ce canyon.

Le cas du mercure est particulier ; puisque c'est un métal, il ne se dégrade pas. Cependant il subit des transformations qui le rendent ubiquiste et il se retrouve dans tous les compartiments (air, eau, sédiment et biote) sous différentes formes (gazeux, inorganique/organique, dissous/particulaire). Une de ces formes organiques, le méthylmercure, résultant de réactions de méthylation du mercure inorganique par l'intermédiaire de processus microbiens, est un neurotoxique capable de se bioaccumuler dans le réseau trophique. Les résultats de la composition isotopique du mercure semblent indiquer que le mercure est d'origine plutôt continentale dans les 10 premiers km. La signature océanique (i.e. phytoplanctonique) retrouvée dans les sédiments au large suggère que le mercure provient aussi en partie de la colonne d'eau, très probablement amené par la sédimentation de la matière organique (plancton ou/et fèces) qui résulte de la très forte productivité primaire de la zone euphotique. Il a été également estimé que le mercure dans l'océan provient essentiellement de l'atmosphère. Ceci suggère que ce mercure retrouvé au large dont la signature est marquée par des apports océaniques était initialement atmosphérique et qu'il a été transféré dans les fonds marins par sédimentation hémipélagique.

La distribution des micropolluants prioritaires et émergents a également été étudiée. Le seul fait de la présence de certains d'entre eux, est une preuve que le canyon agit comme une zone active qui facilite le transfert de micropolluants d'origines industrielles et domestiques, donc provenant du continent, vers le milieu profond. Les résultats ont montré la présence de micropolluants prioritaires (e.g., HAPs, de PCBs) et émergents (e.g., écrans anti UV et muscs de synthèse) dans les sédiments du canyon confirmant une fois encore le transfert de micropolluants d'origine continentale vers le milieu marin profond.

De plus, il a été démontré que les micropolluants retrouvés dans l'océan peuvent être aussi d'origine atmosphérique (e.g. le mercure, DDT, PCB, HAPs, composés de synthèse provenant de sources industrielles ou domestiques)[349]. Ainsi certains micropolluants

peuvent être transportés par les courants atmosphériques et se déposer dans l'océan (pluie/neige ou aérosols) en des endroits souvent éloignés de leur point d'émission à l'échelle régionale voire globale. Par exemple, l'étude de rapport de certain HAPs dans les sédiments du Canyon de Capbreton semble montrer une signature pyrogénique, c'est-à-dire liée à la combustion, et suggère une fois de plus une source additionnelle de micropolluants d'origine atmosphérique.

Perspectives de travail :

Afin d'identifier les sources des micropolluants organiques émergents, il pourrait être envisagé de suivre le fractionnement isotopique du carbone qui constituent ces molécules. Il serait pertinent de réaliser ces analyses dans tous les compartiments à savoir l'atmosphère, la colonne d'eau et le compartiment sédimentaire afin de déterminer les sources et identifier les voies de transport vers le milieu profond. En effet, la préoccupation est grandissante vis-à-vis du large panel de composés organiques de synthèses (généralement persistants, toxiques et à haut poids moléculaires) dont l'estimation des flux atmosphère/océan sont encore incertains [349] et seraient pourtant une voie d'entrée non négligeable pour les micropolluants émergents.

En ce qui concerne le mercure, de la même manière que pour les micropolluants émergents, il faudrait analyser la signature isotopique du mercure dans l'atmosphère (au-dessus de l'océan) et dans les MES de la colonne d'eau pour améliorer la compréhension de la dynamique de cet élément dans ce canyon.

2. Un milieu intégratif

Ce travail a permis de donner un premier aperçu de l'occurrence et des niveaux de concentrations des principales familles de micropolluants prioritaires (métaux traces, HAPs, PCBs, OCPs) et émergents (muscs de synthèse, écran anti UV, composés pharmaceutiques). Nos résultats ont montré des concentrations très élevées de micropolluants prioritaires et des micropolluants émergents dans les sédiments du canyon de Capbreton. Cela démontre que le piégeage et le transport des micropolluants le long du canyon de Capbreton pourraient conduire à une accumulation de ces micropolluants dans les sédiments.

L'évaluation des risques écologiques au travers des normes existantes pour les métaux traces, les micropolluants prioritaires et certains émergents, ont montré un risque potentiellement élevé pour les organismes benthiques (ex. HAPs, métaux traces, micropolluants émergents). En effet, certains HAPs peuvent causer de graves dommages sur les organismes, puisqu'ils sont mutagènes et cancérogènes. De plus, le risque potentiel

observé pour le mercure, le plomb, l'arsenic et certains micropolluants émergents peut jouer un effet synergique et par conséquent augmenter l'impact sur les organismes benthiques.

Bien que les HAPs et les métaux traces soient des substances prioritaires, donc réglementées, nos résultats semblent indiquer que les mesures restent inefficaces pour atteindre un bon état chimique et biologique (DCE, DCSMM). Néanmoins, les normes sur lesquelles sont basées l'évaluation du risque écotoxicologique sont établies selon différentes méthodes et nécessitent une harmonisation. Cela permettrait de comparer les résultats d'impacts entre eux. De plus, les normes ne sont pas établies pour toutes les substances notamment pour la plupart des micropolluants émergents, limitant ainsi une évaluation globale du risque. Bien que la DCE et la DCSMM aient formulé des recommandations pour atteindre l'objectif de concentration de contaminants ne causant pas d'effets de pollution en 2020, ces résultats montrent que cet objectif sera difficilement atteint dans le cas du Canyon de Capbreton.

Bien que l'effort analytique ait été considérable dans ce travail (près de 100 substances suivies) employant différentes méthodes analytiques (e.g. ICP-MS, GC-MS, LC-MS/MS, GC-ICP-MS) aucun composé issu de la dégradation des micropolluants organiques n'a été recherché. En effet, la dégradation de micropolluants organiques, souvent à haut poids moléculaire, peut conduire à la formation de métabolites de plus faible poids moléculaire, modifiant à la fois leurs propriétés physico-chimiques, leur biodisponibilité et leur toxicité. Par conséquent, la non identification d'un micropolluant émergent peut être du à i/ son absence dans le milieu, ii/ à une limite de quantification encore trop élevée pour la quantifier ou encore iii/ à sa dégradation totale ou partielle en métabolites de dégradation non identifiés.

Perspectives de travail

Ces premiers résultats soulignent qu'il faut continuer les investigations pour améliorer les connaissances sur les micropolluants dans le milieu marin. Afin d'atteindre l'objectif de la DCSMM, il faut également insister sur la détermination des sources des micropolluants que l'on retrouve dans le milieu marin pour soit, les supprimer, les réduire ou les remplacer par des substances moins nocives. Par exemple, des mesures pourraient être envisagées pour arrêter leur utilisation ou leur production, contrôler leur utilisation ou améliorer les procédés de traitements de rejets industriels et des eaux usées.

De plus, les micropolluants sélectionnés dans ce travail ont été ciblés selon leurs pertinences mais aussi en fonction de moyens analytiques déjà existants, dont les méthodes sont encore en cours de développement. Par conséquent, il n'est évalué qu'une fraction des

micropolluants rejetés dans le milieu, ce qui induit un biais dans l'évaluation de l'impact des activités humaines sur l'environnement. De plus, bien que de nombreuses méthodes analytiques aient été considérablement optimisées améliorant l'analyse d'un grand nombre de substances, dont les émergentes (réseau NORMAN), les niveaux de détection et de quantification peuvent être encore trop élevés pour observer la présence ou quantifier des substances à des niveaux du µg L^{-1} voire ng L^{-1} (ou kg^{-1}). L'optimisation de ces méthodes permettrait d'abaisser ces limites et d'améliorer la quantification des micropolluants.

La dégradation des micropolluants organiques génèrent des métabolites pouvant être plus toxiques. Des études sur la distribution de ces métabolites dans le canyon permettraient de documenter le devenir des micropolluants émergents libérés dans le milieu marin.

3. Un milieu réactif

Comme les zones côtières, les canyons sous-marins sont des aires de forte productivité primaire induisant une forte diversité et abondance d'espèces. En terme de réactivité, la proximité du canyon de Capbreton avec la côte (200 mètres) lui confère les caractéristiques d'une zone côtière particulière en associant une productivité primaire intense et une forte dynamique hydro-sédimentaire (ex. vagues, marées (au niveau de la tête du canyon), courants internes, courants turbiditiques lors d'événements de crues générant un transfert très énergétique de particules vers les zones profondes, les avalanches sous-marines le long des pentes, les courants d'advection, les upwellings … etc.). Ainsi, le canyon de Capbreton peut être considéré comme un réacteur dans lequel des substrats (dont les micropolluants) sont ajoutés. Tant en phase dissoute que solide, les processus de transport répartissent ces substrats dans le réacteur où des processus biogéochimiques modifient les particules et l'eau interstitielle associée. Cela entraîne des échanges à l'interface eau/sédiment qui sont un point clef dans les cycles du carbone, des nutriments et des micropolluants. L'étude de la réactivité des micropolluants est indispensable pour comprendre leur devenir dans les sédiments marins.

De plus, les activités microbiennes sont essentielles dans le cycle biogéochimique à l'échelle globale car elles servent à catalyser les transformations majeures de l'azote, du soufre et du carbone. Dans le milieu marin, les bactéries anaérobies sont présentes dans les milieux dépourvus d'oxygène tels que les particules qui sédimentent, dans la zone minimum d'oxygène (sous la zone de très forte productivité primaire de la zone euphotique jusqu'à 300 mètres sous la surface de l'eau) ou encore dans les sédiments. Par conséquent, ces bactéries utilisent d'autres accepteurs d'électrons que l'oxygène (e.g. le Fer(III), le nitrate, le

sulfate) où les donneurs d'électrons proviennent de la matière organique produite par le système, de composés organiques issues de la dégradation de la cette matière ou bien de l'apport de micropolluants organiques anthropiques. L'étude des micro-organismes apparaît donc indispensable pour compléter les connaissances et améliorer la compréhension du devenir des micropolluants dans les sédiments marins.

3.1 Potentiels de dégradation de micropolluants émergents et potentiels de méthylation/déméthylation du mercure

Cette étude a permis d'une part d'estimer les potentiels de dégradation de certains micropolluants émergents (i.e. HHCB, OD-PABA et CBZ) et d'autre part d'estimer les potentiels de méthylation/déméthylation du mercure en condition expérimentale au laboratoire à partir de sédiment prélevés dans le canyon de Capbreton.

3.1.1 Micropolluants organiques émergents

Les résultats ont démontré une forte persistance du galaxolide (HHCB) et de la carbamazépine (CBZ). Dans le cas du galaxolide, cela pourrait expliquer qu'il ait été retrouvé dans 40 % des sédiments prélevés dans le canyon à des concentrations allant jusqu'à 3.6 ng g^{-1}. Par contre, l'absence de CBZ dans les sédiments du canyon suggère que les quantités déversées dans le milieu marin seraient trop faibles pour être quantifiées. Il est également possible que les procédés de dégradation des stations de traitement des eaux soient efficaces et rejettent des eaux décontaminées vis-à-vis de cette molécule.

Cependant les temps de demi vie estimés de l'OD-PABA sont de 16 et 44 jours, indiquant une dégradation relativement rapide. Cela pourrait expliquer que l'OD PABA n'ait été quantifié que sur un seul des échantillons de sédiment prélevé dans le canyon. Cela suggère que l'OD-PABA est dégradé pendant son transport dans le canyon par un ensemble de processus biologiques et abiotiques (i.e. transformation microbienne, photodégradation, hydrolyse, …)

Perspectives de travail :

Contrairement aux métaux, les composés organiques bien que persistants subissent des processus de transformations amenant à leur dégradation totale ou partielle conduisant à la formation de produits de dégradation, appelés métabolites. C'est pour cette raison notamment qu'il est plus difficile de suivre le cycle biogéochimique des composés organiques de synthèse comparativement au métaux dont les cycles biogéochimiques dans l'océan sont relativement bien étudiés[349].

De la même manière qu'il faudrait analyser ces métabolites dans l'environnement, il pourrait être envisagé de les analyser pour améliorer les connaissances sur les processus de transformations impliqués dans leur dégradation au travers d'expérimentation en laboratoire.

3.1.2 Le mercure

Notre travail a montré de très fortes concentrations de mercure inorganique (Hg(II)) et de mercure organique (MeHg) dans les sédiments du Canyon de Capbreton avec un facteur d'enrichissement de la côte vers le large de 50 et 15, respectivement pour le Hg(II) et MeHg. Cela suggère que le canyon de Capbreton est un piège pour le mercure. Etonnamment le pourcentage de MeHg était quant à lui plus élevé sur les stations côtières. Or, il est admis que le MeHg résulte d'une réaction de méthylation microbienne. Cela suggère que les potentiels de méthylation du mercure sont plus important dans les sédiments côtiers qu'au large.

En laboratoire, des incubations de sédiments collectés à différentes distances à la côte ont montré que les potentiels de méthylation et de déméthylation du mercure étaient comparables à ceux retrouvés dans les sédiments profonds de la mer Méditerranée [239] mais relativement faibles comparés à des sédiments de zones côtières et estuariennes [350,351]. Cela suggère que le canyon de Capbreton est une zone côtière particulière associant profondeur et une forte dynamique hydrosédimentaire. De plus, ces expérimentations ont permis de confirmer que la méthylation nette du mercure était essentiellement un processus biotique et qu'elle était plus importante dans les sédiments à proximité de la côte. Ensuite, des estimations basées sur ces potentiels et sur les concentrations de méthylmercure et de mercure inorganique, montrent que le canyon de Capbreton serait un réacteur qui induit une production nette du méthylmercure.

Une partie du mercure apporté dans les zones côtières provient des rivières et puis se dilue dans l'océan. Ce mercure est rapidement adsorbé sur les particules (matière organique ou inorganique) de la colonne d'eau puis la sédimentation de ces particules favorise le stockeage du mercure dans le compartiment sédimentaire. Les sources continentales de carbone sur les stations proches de la côte suggèrent que la matière organique est encore fraîche, c'est-à-dire labile et disponible pour les microorganismes, notamment pour ceux impliqués dans la méthylation du mercure. Cela donnerait un des éléments de réponse au plus fort potentiel de biométhylation observé à proximité de la côte. De plus, en condition réelle, les zones côtières sont sous l'influence d'un très fort hydrodynamisme (vagues, marées) qui pourraient favoriser une plus forte remise en

suspension du sédiment de surface conduisant à un renouvellement rapide de matière organique labile.

Bien que ce travail ait montré une voie d'entrée de méthylmercure dans le milieu marin par la production de méthylmercure dans le compartiment sédimentaire, il faut garder à l'esprit que les potentiels ont été estimés par l'ajout de traceurs qui peuvent surestimer les réactions en conditions *in situ*. De plus, dans les sédiments le mercure peut être stocké/immobilisé par précipitation avec du sulfure sous forme de cinabre. Sous cette forme, le mercure ne serait plus biodisponible et donc ne pourrait plus être transformé en méthylmercure. Cela réduirait considérablement le risque de transfert de méthylmercure du sédiment vers la colonne d'eau et son transfert dans la chaîne alimentaire qui aurait lieu lors de phénomènes de remise en suspension/diffusion pour les organismes benthiques.

Perspective de travail :

Ce travail a notamment montré que la granulométrie, la composition de la matière organique et la teneur en soufre étaient contrôlées par le transfert actif de matière particulaire le long du canyon et pourraient influencer la distribution des espèces de mercure et les activités des bactéries méthylant, faisant de ces sédiments marins un producteur net de méthylmercure. Or, d'après Harris et Whiteway [98], environ 150 canyons sous marins actifs comme celui de Capbreton existent à l'échelle globale. Ils pourraient donc avoir une place importante dans le cycle du mercure et ils devraient être pris en comptent dans les cycles globaux. Étant donné que de nombreux processus clés dans les cycles biogéochimiques du mercure sont encore inconnus ou mal caractérisés, un large éventail d'études peut maintenant être réalisé en utilisant de telles expériences pour la compréhension du cycle du mercure dans les systèmes de canyon sous-marins. Ce travail a été initié au cours de ma mobilité internationale à l'Université de Californie, Santa Cruz où une étude comparative a été réalisée entre le Canyon de Capbreton et le Canyon de Monterey. Cela a permis pour la première fois de comparer deux canyons, l'un dans l'Océan Atlantique et l'autre dans l'Océan Pacifique. La distribution des espèces de mercure (Hg(II) et MeHg) et l'étude des potentiels de méthylation et de déméthylation en condition biotique et abiotique ont été étudiés. Les résultats ont montré que les concentrations en Hg(II) et MeHg étaient plus faibles dans le Canyon de Monterey par rapport à celui de Capbreton. Cependant, cette étude semble confirmer que la méthylation du mercure est principalement biotique et plus importante dans les stations proches de la côte comparées aux stations éloignées (Annexe 1). Cela suggère qu'il faut continuer à prospecter pour confirmer cette hypothèse mais aussi qu'il serait judicieux d'identifier les bactéries responsables de cette méthylation dans les sédiments océaniques.

3.2 Implication des micro-organismes dans le devenir des micropolluants

Cette étude a permis d'une part d'isoler et d'identifier des bactéries pouvant être impliquées dans les processus de dégradation de certains micropolluants émergents (i.e. HHCB, AHTN, OD-PABA, OC et CBZ) avant d'estimer leur potentiel de dégradation. D'autre part, ce travail a permis l'identification de bactéries potentiellement impliquées dans la méthylation du mercure.

3.2.1 Les bactéries comme acteurs clefs dans la dégradation des micropolluants émergents

Dans le cadre de cette étude, des bactéries capables de dégrader des micropolluants émergent tels que des muscs de synthèse (HHCB, AHTN), des écran anti-UV (OD-PABA, OC) et un antiépileptique (CBZ) ont été enrichies et isolées à partir de sédiments collectés dans le Canyon de Capbreton. Une première étape d'enrichissement effectuée dans des conditions anoxiques et oxiques a montré que les dégradations après un mois d'incubation, que ce soit dans des conditions biotiques ou abiotiques, étaient limitées en condition anoxique par rapport à la condition oxique, et ce pour tous les contaminants. L'anoxie dans les sédiments marins est rapidement atteinte après l'interface eau/sédiment. Cela suggère qu'en condition anoxique, les micropolluants émergents sont dégradés très lentement, comme le démontre les temps de demi-vie du HHCB et de la CBZ estimés à partir des incubations de sédiments. Par ailleurs, les micropolluants émergents (e.g. HHCB, AHTN, musc kétone (MK), OC et 2-ethyl-hexyl-4-trimethoxycinnamate (EHMC)) ont été retrouvées essentiellement dans la station la plus profonde du canyon (à 399 mètres) et la plus éloignée de la côte (à 23 km) ayant les plus fortes concentrations par rapport aux autres échantillons de sédiments. Cela démontre que les micropolluants émergents provenant des activités domestiques sont transportés jusque dans les sédiments marins profonds. Néanmoins l'absence d'autres micropolluants émergents ou leurs plus faibles concentrations de ceux listés précédemment suggèrent que les micropolluants émergents se dégradent probablement pendant leur transfert dans la colonne d'eau, donc en conditions oxiques. Cependant, les fortes concentrations retrouvées dans cette station suggèrent que les micropolluants n'ont pas subit de dégradation lors du leur transfert suggérant soit une accumulation rapide dans les sédiments ou un transport dans des particules suffisamment grosses pour être en anaérobiose ralentissant leur dégradation (e.g. neige marine).

Ce travail a également permis l'isolement de souches bactériennes aérobies capables de dégrader le HHCB, AHTN, OC et OD-PABA. Elles sont probablement

impliquées dans les processus de dégradation de micropolluants organiques et favorisent la résilience naturelle du milieu.

Perspectives de travail :

Des travaux plus poussés sur les souches bactériennes aérobies capables de dégrader les micropolluants émergents pourraient être envisagés afin d'identifier les conditions optimales de dégradation. Les micropolluants émergents proviennent majoritairement d'activités humaines domestiques, par conséquent ils sont principalement libérés dans l'environnement via les eaux traitées rejetées par les stations de traitement des eaux usées (STEUs). Ces STEUs sont équipées de nombreuses technologies qui permettent entre autres de dégrader la matière organique dont les micropolluants organiques émergents. Parmi ces technologies les boues activées sont à l'image du compartiment sédimentaire naturel. Ce sont des technologies « ecofriendly » et efficace pour la remédiation des micropolluants. En effet, elles permettent à la fois immobilisation des micropolluants par des processus d'adsorption et des processus de biorémédiation microbiennes. Dans ce cadre, les bactéries isolées des sédiments du Canyon de Capbreton, capables de dégrader des micropolluants émergents, pourraient faire l'objet d'un nouvel outil biotechnologique pour améliorer leur biorémédiation au niveau des stations de traitement des eaux usées (au niveau des boues activées par exemple). Ces boues des STEUs peuvent être revalorisées pour l'épandage de parcelles agricoles. Alors qu'elles permettaient de réduire le rejet de micropolluants dans les eaux rejetées par les STEUs, les micropolluants peuvent être remobilisés dans les sols, puis amenés dans les cours d'eaux par ruissellement jusqu'à aboutir dans l'océan. L'analyse de micropolluants émergents et les métabolites de dégradation permettrait d'évaluer le risque qu'ils posent pour les milieux aquatiques.

La présence de neige marine dans l'océan peut également jouer un rôle majeur dans les processus de dégradation des micropolluants émergents. La neige marine résulte de l'agrégation particules qui sédimentent dans la colonne d'eau (e.i. diatomés, phytoplancton, fèces, matière organique). Ces particules de neige marine favorisent les activités bactériennes. De petites tailles, l'oxygène pourra diffuser et favoriser la décomposition de la matière organique et la dégradation des micropolluants émergents. De plus grandes tailles, ces particules peuvent être de micro-environnements anaérobies pouvant limiter la dégradation des micropolluants émergents. Basé sur ces hypothèses, des études futures sur la dégradation des micropolluants émergents dans des particules de neige marine en fonction de leur taille pourrait renseigner sur le rôle de la neige marine dans la résilience du milieu marin.

3.2.2 Les bactéries comme acteurs clefs dans la méthylation du mercure

La forme toxique et bioaccumulable du mercure est le MeHg qui se peut se former dans les sédiments en condition anaérobie par des bactéries sulfato-réductrices (BSR) qui incorpore le HgS^0 et méthyle le mercure. Ce processus apparaît surtout dans les milieux où la sulftato-réduction est importante. Dans ces conditions, les sédiments sont une source importante de méthylmercure dans le milieu marin (colonne d'eau, biote).

La découverte récente du gène *hgcA* [90], impliqué dans la méthylation du mercure, a permis d'identifier d'autres groupes microbiens potentiellement impliqués dans la méthylation du mercure tels que des ferri-réducteur (parmi les *δproteobacteria*), des fermentaires ou encore des Archées méthanogènes.

Les résultats de la réactivtié du mercure ont démontré une forte implication biologique dans le processus de méthylation dans les sédiments de ce canyon, très probablement à l'origine de la formation de méthylmercure dans le milieu marin. Par une approche de clonage et de séquençage, des bactéries potentiellement impliquées dans la méthylation du mercure (gène *hgcA*)ont été identifiées à partir de sédiments prélevés dans l'axe du canyon de Capbreton. Les résultats obtenus par cette méthode clonage/séquençage ont permis d'identifier pour la première fois des bactéries méthylant le mercure dans des sédiments marins. En accord avec les résultats de diversité globale des communautés microbiennes (16s rDNA), l'analyse de la diversité du gène *hgcA* a démontré que les procaryotes portant ce gène étaient essentiellement des *δ-proteobacteria* dominés par des bactéries réduisant les composés soufrés. D'autres groupes mineurs ont été identifiés tels que *Firmicutes*, les *Chloroflexi* et les *Euryarchaea.* Néanmoins, presque la moitié des séquences *hgcA* n'ont pas pu être affiliées. En effet, les séquences du gène *hgcA* ne sont pas systématiquement affiliées aux méthylateurs connus et cultivables au laboratoire. Cela n'est pas étonnant puisque les bactéries marines sont difficiles à cultiver [352].

Nos résultats sur la réactivité du Hg et l'identificaton de procaryotes potentiellement impliquées dans le méthylation du Hg, suggèrent que le cycle biogéochimique du Hg dans le milieu marin est très fortement lié à celui du soufre. En effet, la méthylation bactérienne du mercure dans des conditions de sulfato-réduction, telles dans les sédiments, est également contrôlée par la spéciation du mercure à la fois sous forme solide ou dissoute [166]. Par exemple, des premiers travaux sur la méthylation microbienne dans les environnements anoxiques ont montré l'implication des complexes Hg-S neutres dissous par diffusion passive. Plus récemment des études ont montré une voie de méthylation par transport actif de complexes thiol-Hg dissous de faible poids moléculaire (les thiols sont des composés organiques soufrés qui se lient fortement au mercure)[350,353,354]. D'après le programme

des Nations Unies pour l'Environnement [355], la spéciation chimique du mercure inorganique, qui contrôle la méthylation du mercure, reste encore à étudier dans le milieu marin pour déterminer l'impact du MeHg sur l'environnement et les êtres humains.

Perspectives de travail :

Ce travail a révélé le manque de données issues de la littérature scientifique concernant les bactéries méthylant le mercure dans le milieu marin. De nouvelles études seraient nécessaires pour préciser l'implication de ces nouveaux microorganismes porteurs du gène *hgcA* pour mieux comprendre la méthylation du mercure dans l'océan (i.e. quels métabolismes sont impliqués). Pour cela, les souches identifiées pourraient être caractérisées dans un premier temps et puis leur capacité à méthyler le mercure pourraient être également déterminée dans les conditions *in situ.*

De plus, des études ont montré de fortes teneurs en MeHg dans le minimum d'oxygène sous-thermocline dans la colonne d'eau [356–358] suggérant que la méthylation du mercure dans les systèmes marins pourrait être provoquées par des processus microbiens liés à la reminéralisation de la matière organique en sédimentation. Il est donc indispensable de poursuivre les efforts pour identifier et cultiver les bactéries possédant le gène *hgcA* à la fois dans les sédiments et la colonne d'eau pour mieux comprendre la méthylation du mercure dans les milieux marins.

De plus, la forte implication des bactéries sulfato-réductrices dans la décomposition de la matière organique [359] et dans la méthylation du mercure indique que le soufre est déterminant dans les processus de méthylation microbiennes. Ainsi en plus d'étudier l'isotopie du Hg, du C, l'isotopie du soufre permettrait de décrypte encore plus finement les processus de transformation qui ont lieu dans les sédiments marins.

4. Ouverture : modélisation du devenir des micropolluants dans les canyons sous-marins

L'ensemble de nos résultats ont démontré que le canyon de Capbreton à proximité de la côte est un milieu actif, intégratif et réactif favorisant le transport de micropolluants vers les fonds marins profonds où ils subissent des transformations à la fois abiotique et biotique (notamment par les activités microbiennes). Les résultats de ce travail renforcent l'idée selon laquelle les canyons sous-marins sont des canaux où transitent des micropolluants et par conséquent une voie d'entrée en milieu profond de substances d'origine anthropiques, souvent persistantes, avec des effets néfastes pour l'environnement. A ce jour, 153 canyons sous-marins ont été identifiés [98] comme étant connectés aux effluents continentaux, ce qui suppose qu'ils pourraient aussi jouer un rôle clef dans le transfert de micropolluants dans les

fonds marins à l'échelle globale. D'autant plus que ce nombre de canyons dit aussi « actif » est sûrement sous-estimé. Une étude récente a montré la présence de microplastiques dans la colonne du canyon de Monterey [360] suggérant que ces canyons favorisent aussi le transfert de plastique dans les fonds marins. Or il a été aussi démontré que les micropolluants ont une très forte affinité pour le plastique, ce qui suggère que le transfert de ces microplastiques peut favoriser le transfert et l'accumulation de micropolluants dans les fonds marins. Afin d'intégrer l'ensemble de ces résultats aux données géomorphologiques et hydrysédimentaires déjà existantes, il pourra être envisagé d'utiliser le canyon de Capbreton comme modèle de transfert de micropolluants vers les fonds marins basé sur un modèle dynamique de transfert particulaire intégrant les flux entre les compartiments sédimentaire et aquatique et les constantes de réactions biotique et abiotique des micropolluants

.

REFERENCES

REFERENCES

[1] R. Carson, E.O. Wilson, L. Lear, Silent Spring, 40th Anniversary ed., Mariner Books, Boston, 2002.

[2] F. Ramade, Ecotoxicologie, Ecotoxicologie. 9 (1979). http://bases.bireme.br/cgi-bin/wxislind.exe/iah/online/?IsisScript=iah/iah.xis&src=google&base=REPIDISCA&lang=p&nextAction=lnk&exprSearch=150049&indexSearch=ID (accessed October 3, 2019).

[3] Directive 2013/39/EU of the European Parliament and of the Council of 12 August 2013 amending Directives 2000/60/EC and 2008/105/EC as regards priority substances in the field of water policy Text with EEA relevance, 2013. http://data.europa.eu/eli/dir/2013/39/oj/eng.

[4] J.C.G. Sousa, A.R. Ribeiro, M.O. Barbosa, C. Ribeiro, M.E. Tiritan, M.F.R. Pereira, A.M.T. Silva, Monitoring of the 17 EU Watch List contaminants of emerging concern in the Ave and the Sousa Rivers, Sci. Total Environ. 649 (2019) 1083–1095. https://doi.org/10.1016/j.scitotenv.2018.08.309.

[5] C. Briand, A. Bressy, C. Ghassan, J.-F. Deroubaix, S. Deshayes, J.-C. Deutsch, J. Gasperi, M.-C. Gromaire, J.L. Roux, R. Moilleron, B. Tassin, G. Varrault, S. Barraud, J.-L. Bertrand-Krajewski, V. Ruban, C. Boussac, C. Dianoux, G. Lemkine, C. Leval, P. Neveu, J. Paupardin, R. Quillien, A. Rabier, V. Rocher, Z. Zeglil, Que sait-on des micropolluants dans les eaux urbaines ?, 2018. https://hal-enpc.archives-ouvertes.fr/hal-01803319 (accessed October 3, 2019).

[6] V. Tornero, G. Hanke, Potential chemical contaminants in the marine environment: An overview of main contaminant lists, EUR 28925. (2017).

[7] J. Knoery, J. Tronczynki, Directive Cadre Stratégie pour le Milieu Marin (DCSMM) Définition du Bon Etat Ecologique (BEE) - Rapport final pour le descripteur 8 «le niveau de concentration des contaminants ne provoque pas d'effets dus à la pollution», Ifremer, 2012.

[8] R.P. Schwarzenbach, B.I. Escher, K. Fenner, T.B. Hofstetter, C.A. Johnson, U. von Gunten, B. Wehrli, The Challenge of Micropollutants in Aquatic Systems, Science. 313 (2006) 1072–1077. https://doi.org/10.1126/science.1127291.

[9] A.J. Jamieson, T. Malkocs, S.B. Piertney, T. Fujii, Z. Zhang, Bioaccumulation of persistent organic pollutants in the deepest ocean fauna, Nat. Ecol. Evol. 1 (2017) 0051. https://doi.org/10.1038/s41559-016-0051.

[10] R.A. Hites, R.E. Laflamme, J.W. Farrington, Sedimentary Polycyclic Aromatic Hydrocarbons: The Historical Record, Science. 198 (1977) 829–831. https://doi.org/10.1126/science.198.4319.829.

[11] R. Duran, C. Cravo-Laureau, Role of environmental factors and microorganisms in determining the fate of polycyclic aromatic hydrocarbons in the marine environment, FEMS Microbiol. Rev. 40 (2016) 814–830. https://doi.org/10.1093/femsre/fuw031.

[12] A. Alebic-Juretic, Polycyclic aromatic hydrocarbons in marine sediments from the Rijeka Bay area, Northern Adriatic, Croatia, 1998–2006, Mar. Pollut. Bull. 62 (2011) 863–869. https://doi.org/10.1016/j.marpolbul.2011.01.035.

[13] M.G. Pintado-Herrera, C. Wang, J. Lu, Y.-P. Chang, W. Chen, X. Li, P.A. Lara-Martín, Distribution, mass inventories, and ecological risk assessment of legacy and emerging contaminants in sediments from the Pearl River Estuary in China, J. Hazard. Mater. 323 (2017) 128–138. https://doi.org/10.1016/j.jhazmat.2016.02.046.

[14] P. Baumard, H. Budzinski, Q. Michon, P. Garrigues, T. Burgeot, J. Bellocq, Origin and Bioavailability of PAHs in the Mediterranean Sea from Mussel and Sediment Records, Estuar. Coast. Shelf Sci. 47 (1998) 77–90. https://doi.org/10.1006/ecss.1998.0337.

[15] J. Viguri, J. Verde, A. Irabien, Environmental assessment of polycyclic aromatic hydrocarbons (PAHs) in surface sediments of the Santander Bay, Northern Spain, Chemosphere. 48 (2002) 157–165. https://doi.org/10.1016/S0045-6535(02)00105-4.

[16] H. Budzinski, I. Jones, J. Bellocq, C. Piérard, P. Garrigues, Evaluation of sediment contamination by polycyclic aromatic hydrocarbons in the Gironde estuary, Mar. Chem. 58 (1997) 85–97. https://doi.org/10.1016/S0304-4203(97)00028-5.

[17] K.T. Benlahcen, A. Chaoui, H. Budzinski, J. Bellocq, Ph. Garrigues, Distribution and sources of polycyclic aromatic hydrocarbons in some Mediterranean coastal sediments, Mar. Pollut. Bull. 34 (1997) 298–305. https://doi.org/10.1016/S0025-326X(96)00098-7.

[18] F. Botsou, I. Hatzianestis, Polycyclic aromatic hydrocarbons (PAHs) in marine sediments of the Hellenic coastal zone, eastern Mediterranean: levels, sources and toxicological significance, J. Soils Sediments. 12 (2012) 265–277. https://doi.org/10.1007/s11368-011-0453-1.

[19] T. Combi, M.G. Pintado-Herrera, P.A. Lara-Martin, S. Miserocchi, L. Langone, R. Guerra, Distribution and fate of legacy and emerging contaminants along the Adriatic Sea: A comparative study, Environ. Pollut. 218 (2016) 1055–1064. https://doi.org/10.1016/j.envpol.2016.08.057.

[20] M. Sprovieri, M.L. Feo, L. Prevedello, D.S. Manta, S. Sammartino, S. Tamburrino, E. Marsella, Heavy metals, polycyclic aromatic hydrocarbons and polychlorinated biphenyls in surface sediments of the Naples harbour (southern Italy), Chemosphere. 67 (2007) 998–1009. https://doi.org/10.1016/j.chemosphere.2006.10.055.

[21] N. Valette-Silver, M. Jawed Hameedi, D.W. Efurd, A. Robertson, Status of the Contamination in Sediments and Biota from the Western Beaufort Sea (Alaska), Mar. Pollut. Bull. 38 (1999) 702–722. https://doi.org/10.1016/S0025-326X(99)00034-X.

[22] T.F. da Silva, D. de A. Azevedo, F.R. de Aquino Neto, Distribution of polycyclic aromatic hydrocarbons in surface sediments and waters from Guanabara Bay, Rio de Janeiro, Brazil, J. Braz. Chem. Soc. 18 (2007) 628–637. https://doi.org/10.1590/S0103-50532007000300021.

[23] W. Huang, Z. Wang, W. Yan, Distribution and sources of polycyclic aromatic hydrocarbons (PAHs) in sediments from Zhanjiang Bay and Leizhou Bay, South China, Mar. Pollut. Bull. 64 (2012) 1962–1969. https://doi.org/10.1016/j.marpolbul.2012.05.023.

[24] M.G. Pintado-Herrera, C. Wang, J. Lu, Y.-P. Chang, W. Chen, X. Li, P.A. Lara-Martín, Distribution, mass inventories, and ecological risk assessment of legacy and emerging contaminants in sediments from the Pearl River Estuary in China, J. Hazard. Mater. 323 (2017) 128–138. https://doi.org/10.1016/j.jhazmat.2016.02.046.

[25] D.R. Dudhagara, R.K. Rajpara, J.K. Bhatt, H.B. Gosai, B.K. Sachaniya, B.P. Dave, Distribution, sources and ecological risk assessment of PAHs in historically contaminated surface sediments at Bhavnagar coast, Gujarat, India, Environ. Pollut. 213 (2016) 338–346. https://doi.org/10.1016/j.envpol.2016.02.030.

[26] A.O. Barakat, A. Mostafa, T.L. Wade, S.T. Sweet, N.B. El Sayed, Distribution and characteristics of PAHs in sediments from the Mediterranean coastal environment of Egypt, Mar. Pollut. Bull. 62 (2011) 1969–1978. https://doi.org/10.1016/j.marpolbul.2011.06.024.

[27] H.M. Hassan, A.B. Castillo, O. Yigiterhan, E.A. Elobaid, A. Al-Obaidly, E. Al-Ansari, J.P. Obbard, Baseline concentrations and distributions of Polycyclic Aromatic Hydrocarbons in surface sediments from the Qatar marine environment, Mar. Pollut. Bull. 126 (2018) 58–62. https://doi.org/10.1016/j.marpolbul.2017.10.093.

[28] W.E. Pereira, F.D. Hostettler, S.N. Luoma, A. van Geen, C.C. Fuller, R.J. Anima, Sedimentary record of anthropogenic and biogenic polycyclic aromatic hydrocarbons in San Francisco Bay, California, Mar. Chem. 64 (1999) 99–113. https://doi.org/10.1016/S0304-4203(98)00087-5.

[29] J. Weber, C.J. Halsall, D. Muir, C. Teixeira, J. Small, K. Solomon, M. Hermanson, H. Hung, T. Bidleman, Endosulfan, a global pesticide: A review of its fate in the environment and occurrence in the Arctic, Sci. Total Environ. 408 (2010) 2966–2984. https://doi.org/10.1016/j.scitotenv.2009.10.077.

[30] M. Margni, D. Rossier, P. Crettaz, O. Jolliet, Life cycle impact assessment of pesticides on human health and ecosystems, Agric. Ecosyst. Environ. 93 (2002) 379–392. https://doi.org/10.1016/S0167-8809(01)00336-X.

[31] R. Faasen, Agricultural pesticide use a threat to the European environment?, Eur. Water Pollut. Control. 2 (1995) 34–40.

[32] J.P. Butault, N. Delame, F. Jacquet, G. Zardet, L'utilisation des pesticides en France : état des lieux et perspectives de réduction, Ministère Agric. Aliment. Pêche Rural. Aménage. Territ. (2011) 7–26.

[33] S. Gómez, D. Gorri, Á. Irabien, Organochlorine pesticide residues in sediments from coastal environment of Cantabria (northern Spain) and evaluation of the Atlantic Ocean, Environ. Monit. Assess. 176 (2011) 385–401. https://doi.org/10.1007/s10661-010-1591-4.

[34] A.D. Syakti, L. Asia, F. Kanzari, H. Umasangadji, L. Malleret, Y. Ternois, G. Mille, P. Doumenq, Distribution of organochlorine pesticides (OCs) and polychlorinated biphenyls (PCBs) in marine sediments directly exposed to wastewater from Cortiou, Marseille, Environ. Sci. Pollut. Res. Int. 19 (2012) 1524–1535. https://doi.org/10.1007/s11356-011-0640-z.

[35] F. Kanzari, L. Asia, A.D. Syakti, A. Piram, L. Malleret, G. Mille, P. Doumenq, Distribution and risk assessment of hydrocarbons (aliphatic and PAHs), polychlorinated biphenyls (PCBs), and pesticides in surface sediments from an agricultural river (Durance) and an industrialized urban lagoon (Berre lagoon), France, Environ. Monit. Assess. 187 (2015) 591. https://doi.org/10.1007/s10661-015-4823-9.

[36] C.A. Gillis, N.L. Bonnevie, S.H. Su, J.G. Ducey, S.L. Huntley, R.J. Wenning, DDT, DDD, and DDE contamination of sediment in the Newark Bay estuary, New Jersey, Arch. Environ. Contam. Toxicol. 28 (1995) 85–92. https://doi.org/10.1007/BF00213973.

[37] L. Yang, X. Li, P. Zhang, M.E. Melcer, Y. Wu, U. Jans, Concentrations of DDTs and dieldrin in Long Island Sound sediment, J. Environ. Monit. 14 (2012) 878–885. https://doi.org/10.1039/C2EM10642F.

[38] O. Wurl, J.P. Obbard, Organochlorine pesticides, polychlorinated biphenyls and polybrominated diphenyl ethers in Singapore's coastal marine sediments, Chemosphere. 58 (2005) 925–933. https://doi.org/10.1016/j.chemosphere.2004.09.054.

[39] B.J. Richardson, G.J. Zheng, Chlorinated hydrocarbon contaminants in Hong Kong surficial sediments, Chemosphere. 39 (1999) 913–923. https://doi.org/10.1016/S0045-6535(99)00041-7.

[40] R. Yang, A. Lv, J. Shi, G. Jiang, The levels and distribution of organochlorine pesticides (OCPs) in sediments from the Haihe River, China, Chemosphere. 61 (2005) 347–354. https://doi.org/10.1016/j.chemosphere.2005.02.091.

[41] A. Sarkar, R. Nagarajan, S. Chaphadkar, S. Pal, S.Y.S. Singbal, Contamination of organochlorine pesticides in sediments from the Arabian Sea along the west coast of India, Water Res. 31 (1997) 195–200. https://doi.org/10.1016/S0043-1354(96)00210-2.

[42] R.-A. Doong, C.-K. Peng, Y.-C. Sun, P.-L. Liao, Composition and distribution of organochlorine pesticide residues in surface sediments from the Wu-Shi River estuary, Taiwan, Mar. Pollut. Bull. 45 (2002) 246–253. https://doi.org/10.1016/S0025-326X(02)00102-9.

[43] S.W. Fowler, Critical review of selected heavy metal and chlorinated hydrocarbon concentrations in the marine environment, Mar. Environ. Res. 29 (1990) 1–64. https://doi.org/10.1016/0141-1136(90)90027-L.

[44] M.G. Pintado-Herrera, T. Combi, C. Corada-Fernández, E. González-Mazo, P.A. Lara-Martín, Occurrence and spatial distribution of legacy and emerging organic pollutants in marine sediments from the Atlantic coast (Andalusia, SW Spain), Sci. Total Environ. 605–606 (2017) 980–994. https://doi.org/10.1016/j.scitotenv.2017.06.055.

[45] F. Kanzari, A.D. Syakti, L. Asia, L. Malleret, A. Piram, G. Mille, P. Doumenq, Distributions and sources of persistent organic pollutants (aliphatic hydrocarbons, PAHs, PCBs and pesticides) in surface sediments of an industrialized urban river (Huveaune), France, Sci. Total Environ. 478 (2014) 141–151. https://doi.org/10.1016/j.scitotenv.2014.01.065.

[46] F. Léauté, Biogéochimie des contaminants organiques HAP, PCB et pesticides organochlorés dans les sédiments de l'étang de Thau, (2008). https://tel.archives-ouvertes.fr/tel-00449516 (accessed October 7, 2019).

[47] M. Frignani, L.G. Bellucci, C. Carraro, S. Raccanelli, Polychlorinated biphenyls in sediments of the Venice Lagoon, Chemosphere. 43 (2001) 567–575. https://doi.org/10.1016/S0045-6535(00)00408-2.

[48] L. Guzzella, C. Roscioli, L. Viganò, M. Saha, S.K. Sarkar, A. Bhattacharya, Evaluation of the concentration of HCH, DDT, HCB, PCB and PAH in the sediments along the lower stretch of Hugli estuary, West Bengal, northeast India, Environ. Int. 31 (2005) 523–534. https://doi.org/10.1016/j.envint.2004.10.014.

[49] C.T. Driscoll, R.P. Mason, H.M. Chan, D.J. Jacob, N. Pirrone, Mercury as a global pollutant: sources, pathways, and effects, Environ. Sci. Technol. 47 (2013) 4967–4983. https://doi.org/10.1021/es305071v.

[50] M. Harada, Minamata Disease : Methylmercure poisoning in Japan caused by envronmental pollution, Crit. Rev. Toxicol. (1995). https://doi.org/10.3109/10408449509089885.

[51] B. Gworek, O. Bemowska-Kałabun, M. Kijeńska, J. Wrzosek-Jakubowska, Mercury in Marine and Oceanic Waters—a Review, Water. Air. Soil Pollut. 227 (2016) 371. https://doi.org/10.1007/s11270-016-3060-3.

[52] L.-E. Heimbürger, D. Cossa, B. Thibodeau, A. Khripounoff, V. Mas, J.-F. Chiffoleau, S. Schmidt, C. Migon, Natural and anthropogenic trace metals in sediments of the Ligurian Sea (Northwestern Mediterranean), Chem. Geol. 291 (2012) 141–151. https://doi.org/10.1016/j.chemgeo.2011.10.011.

[53] A.M. Costa, M. Mil-Homens, S.M. Lebreiro, T.O. Richter, H. de Stigter, W. Boer, M.A. Trancoso, Z. Melo, F. Mouro, M. Mateus, J. Canário, V. Branco, M. Caetano, Origin and transport of trace metals deposited in the canyons off Lisboa and adjacent slopes (Portuguese Margin) in the last century, Mar. Geol. 282 (2011) 169–177. https://doi.org/10.1016/j.margeo.2011.02.007.

[54] A. Oliveira, C. Palma, M. Valença, Heavy metal distribution in surface sediments from the continental shelf adjacent to Nazaré canyon, Deep Sea Res. Part II Top. Stud. Oceanogr. 58 (2011) 2420–2432. https://doi.org/10.1016/j.dsr2.2011.04.006.

[55] M. Mil-Homens, J. Blum, J. Canário, M. Caetano, A.M. Costa, S.M. Lebreiro, M. Trancoso, T. Richter, H. de Stigter, M. Johnson, V. Branco, R. Cesário, F. Mouro, M. Mateus, W. Boer, Z. Melo, Tracing anthropogenic Hg and Pb input using stable Hg and Pb isotope ratios in sediments of the central Portuguese Margin, Chem. Geol. 336 (2013) 62–71. https://doi.org/10.1016/j.chemgeo.2012.02.018.

[56] T. Stoichev, D. Amouroux, J.C. Wasserman, D. Point, A. De Diego, G. Bareille, O.F.X. Donard, Dynamics of mercury species in surface sediments of a macrotidal estuarine–coastal system (Adour River, Bay of Biscay), Estuar. Coast. Shelf Sci. 59 (2004) 511–521. https://doi.org/10.1016/j.ecss.2003.10.007.

[57] J.G. Rodríguez, I. Tueros, A. Borja, M.J. Belzunce, J. Franco, O. Solaun, V. Valencia, A. Zuazo, Maximum likelihood mixture estimation to determine metal background values in estuarine and coastal sediments within the European Water Framework Directive, Sci. Total Environ. 370 (2006) 278–293. https://doi.org/10.1016/j.scitotenv.2006.08.035.

[58] J.A. Field, C.A. Johnson, J.B. Rose, What is “emerging”?, Environ. Sci. Technol. 40 (2006) 7105–7105. https://doi.org/10.1021/es062982z.

[59] M. Gavrilescu, K. Demnerová, J. Aamand, S. Agathos, F. Fava, Emerging pollutants in the environment: present and future challenges in biomonitoring, ecological risks and bioremediation, New Biotechnol. 32 (2015) 147–156. https://doi.org/10.1016/j.nbt.2014.01.001.

[60] L. Arpin-Pont, M.J.M. Bueno, E. Gomez, H. Fenet, Occurrence of PPCPs in the marine environment: a review, Environ. Sci. Pollut. Res. 23 (2016) 4978–4991. https://doi.org/10.1007/s11356-014-3617-x.

[61] C.G. Daughton, T.A. Ternes, Pharmaceuticals and personal care products in the environment: agents of subtle change?, Environ. Health Perspect. 107 Suppl 6 (1999) 907–938. https://doi.org/10.1289/ehp.99107s6907.

[62] K. Bester, Analysis of musk fragrances in environmental samples, J. Chromatogr. A. 1216 (2009) 470–480. https://doi.org/10.1016/j.chroma.2008.08.093.

[63] K. Bester, Retention characteristics and balance assessment for two polycyclic musk fragrances (HHCB and AHTN) in a typical German sewage treatment plant, Chemosphere. 57 (2004) 863–870. https://doi.org/10.1016/j.chemosphere.2004.08.032.

[64] V. Homem, J.A. Silva, N. Ratola, L. Santos, A. Alves, Prioritisation approach to score and rank synthetic musk compounds for environmental risk assessment, J. Chem. Technol. Biotechnol. 90 (2015) 1619–1630. https://doi.org/10.1002/jctb.4628.

[65] M. Beretta, V. Britto, T.M. Tavares, S.M.T. da Silva, A.L. Pletsch, Occurrence of pharmaceutical and personal care products (PPCPs) in marine sediments in the Todos os Santos Bay and the north coast of Salvador, Bahia, Brazil, J. Soils Sediments. 14 (2014) 1278–1286. https://doi.org/10.1007/s11368-014-0884-6.

[66] W. Huang, Z. Xie, W. Yan, W. Mi, W. Xu, Occurrence and distribution of synthetic musks and organic UV filters from riverine and coastal sediments in the Pearl River estuary of China, Mar. Pollut. Bull. 111 (2016) 153–159. https://doi.org/10.1016/j.marpolbul.2016.07.018.

[67] J.M. Brausch, G.M. Rand, A review of personal care products in the aquatic environment: Environmental concentrations and toxicity, Chemosphere. 82 (2011) 1518–1532. https://doi.org/10.1016/j.chemosphere.2010.11.018.

[68] F. Henkler, T. Tralau, J. Tentschert, C. Kneuer, A. Haase, T. Platzek, A. Luch, M.E. Götz, Risk assessment of nanomaterials in cosmetics: a European union perspective, Arch. Toxicol. 86 (2012) 1641–1646. https://doi.org/10.1007/s00204-012-0944-x.

[69] L. Preud'homme, A. Depues, S. Noiset, Cosmetic regulatory writing, Med. Writ. 23 (2014) 186–189. https://doi.org/10.1179/2047480614Z.000000000238.

[70] K.H. Langford, K.V. Thomas, Inputs of chemicals from recreational activities into the Norwegian coastal zone, J. Environ. Monit. 10 (2008) 894–898. https://doi.org/10.1039/B806198J.

[71] M.M.P. Tsui, H.W. Leung, B.K.Y. Kwan, K.-Y. Ng, N. Yamashita, S. Taniyasu, P.K.S. Lam, M.B. Murphy, Occurrence, distribution and ecological risk assessment of multiple classes of UV filters in marine sediments in Hong Kong and Japan, J. Hazard. Mater. 292 (2015) 180–187. https://doi.org/10.1016/j.jhazmat.2015.03.025.

[72] E. Barón, P. Gago-Ferrero, M. Gorga, I. Rudolph, G. Mendoza, A.M. Zapata, S. Díaz-Cruz, R. Barra, W. Ocampo-Duque, M. Páez, R.M. Darbra, E. Eljarrat, D. Barceló, Occurrence of hydrophobic organic pollutants (BFRs and UV-filters) in sediments from South America, Chemosphere. 92 (2013) 309–316. https://doi.org/10.1016/j.chemosphere.2013.03.032.

[73] G. Moulin, S. Roux, Suivi des ventes de médicaments vétérinaires contenant des antibiotiques en France en 2001., Anses, 2002.

[74] Z. Li, M.P. Maier, M. Radke, Screening for pharmaceutical transformation products formed in river sediment by combining ultrahigh performance liquid chromatography/high resolution mass spectrometry with a rapid data-processing method, Anal. Chim. Acta. 810 (2014) 61–70. https://doi.org/10.1016/j.aca.2013.12.012.

[75] L.A. Maranho, M.C. Garrido-Pérez, R.M. Baena-Nogueras, P.A. Lara-Martín, R. Antón-Martín, T.A. DelValls, M.L. Martín-Díaz, Are WWTPs effluents responsible for acute toxicity? Seasonal variations of sediment quality at the Bay of Cádiz (SW, Spain), Ecotoxicol. Lond. Engl. 24 (2015) 368–380. https://doi.org/10.1007/s10646-014-1385-5.

[76] K.A. Maruya, D.E. Vidal-Dorsch, S.M. Bay, J.W. Kwon, K. Xia, K.L. Armbrust, Organic contaminants of emerging concern in sediments and flatfish collected near outfalls discharging treated wastewater effluent to the Southern California Bight, Environ. Toxicol. Chem. 31 (2012) 2683–2688. https://doi.org/10.1002/etc.2003.

[77] E.R. Long, M. Dutch, S. Weakland, B. Chandramouli, J.P. Benskin, Quantification of pharmaceuticals, personal care products, and perfluoroalkyl substances in the marine sediments of Puget Sound, Washington, USA, Environ. Toxicol. Chem. 32 (2013) 1701–1710. https://doi.org/10.1002/etc.2281.

[78] M. Stewart, G. Olsen, C.W. Hickey, B. Ferreira, A. Jelić, M. Petrović, D. Barcelo, A survey of emerging contaminants in the estuarine receiving environment around Auckland, New Zealand, Sci. Total Environ. 468–469 (2014) 202–210. https://doi.org/10.1016/j.scitotenv.2013.08.039.

[79] K. Chen, J.L. Zhou, Occurrence and behavior of antibiotics in water and sediments from the Huangpu River, Shanghai, China, Chemosphere. 95 (2014) 604–612. https://doi.org/10.1016/j.chemosphere.2013.09.119.

[80] S. Gaw, K.V. Thomas, T.H. Hutchinson, Sources, impacts and trends of pharmaceuticals in the marine and coastal environment, Philos. Trans. R. Soc. B Biol. Sci. 369 (2014) 20130572. https://doi.org/10.1098/rstb.2013.0572.

[81] L. Vallecillos, Y. Sadef, F. Borrull, E. Pocurull, K. Bester, Degradation of synthetic fragrances by laccase-mediated system, J. Hazard. Mater. 334 (2017) 233–243. https://doi.org/10.1016/j.jhazmat.2017.04.003.

[82] A. Sharif, M. Monperrus, E. Tessier, S. Bouchet, H. Pinaly, P. Rodriguez-Gonzalez, P. Maron, D. Amouroux, Fate of mercury species in the coastal plume of the Adour River estuary (Bay of Biscay, SW France), Sci. Total Environ. 496 (2014) 701–713. https://doi.org/10.1016/j.scitotenv.2014.06.116.

[83] R. Bridou, M. Monperrus, P.R. Gonzalez, R. Guyoneaud, D. Amouroux, Simultaneous determination of mercury methylation and demethylation capacities of various sulfate-reducing bacteria using species-specific isotopic tracers, Environ. Toxicol. Chem. 30 (2011) 337–344. https://doi.org/10.1002/etc.395.

[84] S. Zhu, Z. Zhang, D. Žagar, Mercury transport and fate models in aquatic systems: A review and synthesis, Sci. Total Environ. 639 (2018) 538–549. https://doi.org/10.1016/j.scitotenv.2018.04.397.

[85] G.C. Compeau, R. Bartha, Sulfate-Reducing Bacteria: Principal Methylators of Mercury in Anoxic Estuarine Sediment, Appl. Environ. Microbiol. 50 (1985) 498–502.

[86] S. Arndt, B.B. Jørgensen, D.E. LaRowe, J.J. Middelburg, R.D. Pancost, P. Regnier, Quantifying the degradation of organic matter in marine sediments: A review and synthesis, Earth-Sci. Rev. 123 (2013) 53–86. https://doi.org/10.1016/j.earscirev.2013.02.008.

[87] C.C. Gilmour, M. Podar, A.L. Bullock, A.M. Graham, S.D. Brown, A.C. Somenahally, A. Johs, R.A. Hurt, K.L. Bailey, D.A. Elias, Mercury Methylation by Novel Microorganisms from New Environments, Environ. Sci. Technol. 47 (2013) 11810–11820. https://doi.org/10.1021/es403075t.

[88] G. Rosati, L.E. Heimbürger, D.M. Canu, C. Lagane, L. Laffont, M.J.A. Rijkenberg, L.J.A. Gerringa, C. Solidoro, C.N. Gencarelli, I.M. Hedgecock, H.J.W.D. Baar, J.E. Sonke, Mercury in the Black Sea: New Insights From Measurements and Numerical Modeling, Glob. Biogeochem. Cycles. 32 (2018) 529–550. https://doi.org/10.1002/2017GB005700.

[89] J.M. Parks, A. Johs, M. Podar, R. Bridou, R.A. Hurt, S.D. Smith, S.J. Tomanicek, Y. Qian, S.D. Brown, C.C. Brandt, A.V. Palumbo, J.C. Smith, J.D. Wall, D.A. Elias, L. Liang, The genetic basis for bacterial mercury methylation, Science. 339 (2013) 1332–1335. https://doi.org/10.1126/science.1230667.

[90] M. Podar, C.C. Gilmour, C.C. Brandt, A. Soren, S.D. Brown, B.R. Crable, A.V. Palumbo, A.C. Somenahally, D.A. Elias, Global prevalence and distribution of genes and microorganisms involved in mercury methylation, Sci. Adv. 1 (2015) e1500675. https://doi.org/10.1126/sciadv.1500675.

[91] A.G. Bravo, J. Zopfi, M. Buck, J. Xu, S. Bertilsson, J.K. Schaefer, J. Poté, C. Cosio, Geobacteraceae are important members of mercury-methylating microbial communities of sediments impacted by waste water releases, ISME J. 12 (2018) 802. https://doi.org/10.1038/s41396-017-0007-7.

[92] D.S. Jones, G.M. Walker, N.W. Johnson, C.P.J. Mitchell, J.K.C. Wasik, J.V. Bailey, Molecular evidence for novel mercury methylating microorganisms in sulfate-impacted lakes, ISME J. (2019) 1. https://doi.org/10.1038/s41396-019-0376-1.

[93] C. Munschy, N. Olivier, B. Veyrand, P. Marchand, Occurrence of legacy and emerging halogenated organic contaminants in marine shellfish along French coasts, Chemosphere. 118 (2015) 329–335. https://doi.org/10.1016/j.chemosphere.2014.09.106.

[94] A. Singh, O.P. Ward, Biotechnology and Bioremediation — An Overview, in: A. Singh, O.P. Ward (Eds.), Biodegrad. Bioremediation, Springer Berlin Heidelberg, Berlin, Heidelberg, 2004: pp. 1–17. https://doi.org/10.1007/978-3-662-06066-7_1.

[95] M.C. Ncibi, B. Mahjoub, O. Mahjoub, M. Sillanpää, Remediation of Emerging Pollutants in Contaminated Wastewater and Aquatic Environments: Biomass-Based Technologies, CLEAN – Soil Air Water. 45 (2017) 1700101. https://doi.org/10.1002/clen.201700101.

[96] D. Springael, E.M. Top, Horizontal gene transfer and microbial adaptation to xenobiotics: new types of mobile genetic elements and lessons from ecological studies, Trends Microbiol. 12 (2004) 53–58. https://doi.org/10.1016/j.tim.2003.12.010.

[97] F.P. Shepard, Submarine geology, Harper & Row, 1963.

[98] P.T. Harris, T. Whiteway, Global distribution of large submarine canyons: Geomorphic differences between active and passive continental margins, Mar. Geol. 285 (2011) 69–86. https://doi.org/10.1016/j.margeo.2011.05.008.

[99] F. Sanchez, M. Santurtun, SYNThèse et Analyse des données eXistantes sur un écosystème profond transfrontalier : le gouf de Capbreton – « SYNTAX », (2013). https://archimer.ifremer.fr/doc/00137/24787/ (accessed October 3, 2019).

[100] A. Mazières, H. Gillet, B. Castelle, T. Mulder, C. Guyot, T. Garlan, C. Mallet, High-resolution morphobathymetric analysis and evolution of Capbreton submarine canyon head (Southeast Bay of Biscay—French Atlantic Coast) over the last decade using descriptive and numerical modeling, Mar. Geol. 351 (2014) 1–12. https://doi.org/10.1016/j.margeo.2014.03.001.

[101] Cirac Pierre, Gillet Hervé, Mazières Alaïs, S. Laure, Carte des formations superficielles du plateau aquitain (2016), (2016). https://doi.org/10.12770/602a30c5-c338-4e75-a591-baccb8ba1f79.

[102] M. Cremer, S. Brocheray, H. Gillet, V. Hanquiez, Capbreton canyon: evidence of its formation by differential sedimentation, in: XII Int. Symp. Oceanogr. Bay Biscay Santander Spain, 2012.

[103] M. Gaudin, T. Mulder, P. Cirac, S. Berné, P. Imbert, Past and present sedimentary activity in the Capbreton Canyon, southern Bay of Biscay, Geo-Mar. Lett. 26 (2006) 331. https://doi.org/10.1007/s00367-006-0043-1.

[104] H. Gillet, A. Mazières, L. Biscara, M. Cremer, Morphobathymetric evolution and sedimentary processes in the upper part of the Capbreton submarine canyon, International canyons workshop, Ifremer Brest, 2012.

[105] T. Salles, T. Mulder, M. Gaudin, M.C. Cacas, S. Lopez, P. Cirac, Simulating the 1999 Capbreton canyon turbidity current with a Cellular Automata model, Geomorphology. 97 (2008) 516–537. https://doi.org/10.1016/j.geomorph.2007.09.005.

[106] T. Mulder, S. Zaragosi, T. Garlan, J. Mavel, M. Cremer, A. Sottolichio, N. Sénéchal, S. Schmidt, Present deep-submarine canyons activity in the Bay of Biscay (NE Atlantic), Mar. Geol. 295–298 (2012) 113–127. https://doi.org/10.1016/j.margeo.2011.12.005.

[107] De Leo Fabio C., Smith Craig R., Rowden Ashley A., Bowden David A., Clark Malcolm R., Submarine canyons: hotspots of benthic biomass and productivity in the deep sea, Proc. R. Soc. B Biol. Sci. 277 (2010) 2783–2792. https://doi.org/10.1098/rspb.2010.0462.

[108] E.W. Vetter, C.R. Smith, F.C.D. Leo, Hawaiian hotspots: enhanced megafaunal abundance and diversity in submarine canyons on the oceanic islands of Hawaii, Mar. Ecol. 31 (2010) 183–199. https://doi.org/10.1111/j.1439-0485.2009.00351.x.

[109] J.A. Santora, R. Zeno, J.G. Dorman, W.J. Sydeman, Submarine canyons represent an essential habitat network for krill hotspots in a Large Marine Ecosystem, Sci. Rep. 8 (2018) 1–9. https://doi.org/10.1038/s41598-018-25742-9.

[110] M.-C. Fabri, L. Pedel, L. Beuck, F. Galgani, D. Hebbeln, A. Freiwald, Megafauna of vulnerable marine ecosystems in French mediterranean submarine canyons: Spatial distribution and

anthropogenic impacts, Deep Sea Res. Part II Top. Stud. Oceanogr. 104 (2014) 184–207. https://doi.org/10.1016/j.dsr2.2013.06.016.

[111] D.E. Alexander, R.W. Fairbridge, eds., Encyclopedia of Environmental Science, Springer Netherlands, 1999. https://www.springer.com/gp/book/9781402044946 (accessed October 3, 2019).

[112] F.M. Lauro, D. McDougald, T. Thomas, T.J. Williams, S. Egan, S. Rice, M.Z. DeMaere, L. Ting, H. Ertan, J. Johnson, S. Ferriera, A. Lapidus, I. Anderson, N. Kyrpides, A.C. Munk, C. Detter, C.S. Han, M.V. Brown, F.T. Robb, S. Kjelleberg, R. Cavicchioli, The genomic basis of trophic strategy in marine bacteria, Proc. Natl. Acad. Sci. 106 (2009) 15527. https://doi.org/10.1073/pnas.0903507106.

[113] Directive 2008/105/EC of the European Parliament and of the Council of 16 December 2008 on environmental quality standards in the field of water policy, amending and subsequently repealing Council Directives 82/176/EEC, 83/513/EEC, 84/156/EEC, 84/491/EEC, 86/280/EEC and amending Directive 2000/60/EC of the European Parliament and of the Council, 2008. http://data.europa.eu/eli/dir/2008/105/oj/eng.

[114] DIRECTIVE, Marine Strategy Framework. Directive 2008/56/EC of the European Parliament and of the Council of 17 June 2008 establishing a framework for community action in the field of marine environmental policy., Off. J. Eur. Union L. (2008) vol. 164, 19-40.

[115] Y. Yang, Y.S. Ok, K.-H. Kim, E.E. Kwon, Y.F. Tsang, Occurrences and removal of pharmaceuticals and personal care products (PPCPs) in drinking water and water/sewage treatment plants: A review, Sci. Total Environ. 596–597 (2017) 303–320. https://doi.org/10.1016/j.scitotenv.2017.04.102.

[116] J. Bellas, Ó. Nieto, R. Beiras, Integrative assessment of coastal pollution: Development and evaluation of sediment quality criteria from chemical contamination and ecotoxicological data, Cont. Shelf Res. 31 (2011) 448–456. https://doi.org/10.1016/j.csr.2010.04.012.

[117] D.A. Roberts, Causes and ecological effects of resuspended contaminated sediments (RCS) in marine environments, Environ. Int. 40 (2012) 230–243. https://doi.org/10.1016/j.envint.2011.11.013.

[118] L.H. Nowell, P.W. Moran, R.J. Gilliom, D.L. Calhoun, C.G. Ingersoll, N.E. Kemble, K.M. Kuivila, P.J. Phillips, Contaminants in Stream Sediments From Seven United States Metropolitan Areas: Part I: Distribution in Relation to Urbanization, Arch. Environ. Contam. Toxicol. 64 (2013) 32–51. https://doi.org/10.1007/s00244-012-9813-0.

[119] D. Fichet, G. Boucher, G. Radenac, P. Miramand, Concentration and mobilisation of Cd, Cu, Pb and Zn by meiofauna populations living in harbour sediment: their role in the heavy metal flux from sediment to food web, Sci. Total Environ. 243–244 (1999) 263–272. https://doi.org/10.1016/S0048-9697(99)00401-5.

[120] D. Rial, R. Beiras, Prospective ecological risk assessment of sediment resuspension in an estuary, J. Environ. Monit. 14 (2012) 2137–2144. https://doi.org/10.1039/C2EM30225J.

[121] E.R. Long, D.D. Macdonald, S.L. Smith, F.D. Calder, Incidence of adverse biological effects within ranges of chemical concentrations in marine and estuarine sediments, Environ. Manage. 19 (1995) 81–97. https://doi.org/10.1007/BF02472006.

[122] S. Brocheray, M. Cremer, S. Zaragosi, S. Schmidt, F. Eynaud, L. Rossignol, H. Gillet, 2000 years of frequent turbidite activity in the Capbreton Canyon (Bay of Biscay), Mar. Geol. 347 (2014) 136–152. https://doi.org/10.1016/j.margeo.2013.11.009.

[123] P. Puig, A. Palanques, J. Martín, Contemporary Sediment-Transport Processes in Submarine Canyons, Annu. Rev. Mar. Sci. 6 (2014) 53–77. https://doi.org/10.1146/annurev-marine-010213-135037.

[124] C.K. Paull, H.G. Greene, W. Ussler, P.J. Mitts, Pesticides as tracers of sediment transport through Monterey Canyon, Geo-Mar. Lett. 22 (2002) 121–126. https://doi.org/10.1007/s00367-002-0110-1.

[125] C.R. McClain, J.P. Barry, Habitat heterogeneity, disturbance, and productivity work in concert to regulate biodiversity in deep submarine canyons, Ecology. 91 (2010) 964–976. https://doi.org/10.1890/09-0087.1.

[126] A. Azaroff, E. Tessier, J. Deborde, R. Guyoneaud, M. Monperrus, Mercury and methylmercury concentrations, sources and distribution in submarine canyon sediments (Capbreton, SW France): Implications for the net methylmercury production, Sci. Total Environ. 673 (2019) 511–521. https://doi.org/10.1016/j.scitotenv.2019.04.111.

[127] C. Miossec, L. Lanceleur, M. Monperrus, Adaptation and validation of QuEChERS method for the simultaneous analysis of priority and emerging pollutants in sediments by gas chromatography—mass spectrometry, Int. J. Environ. Anal. Chem. 98 (2018) 695–708. https://doi.org/10.1080/03067319.2018.1496245.

[128] G. Siedlewicz, M. Borecka, A. Białk-Bielińska, K. Sikora, P. Stepnowski, K. Pazdro, Determination of antibiotic residues in southern Baltic Sea sediments using tandem solid-phase extraction and liquid chromatography coupled with tandem mass spectrometry, Oceanologia. 58 (2016) 221–234. https://doi.org/10.1016/j.oceano.2016.04.005.

[129] A. Kassambara, F. Mundt, Package 'factoextra'. Extract and visualize the results of multivariate data analyses, 76 (2017).

[130] S. Lê, J. Josse, F. Husson, FactoMineR: An R Package for Multivariate Analysis, J. Stat. Softw. 25 (2008) 1–18. https://doi.org/10.18637/jss.v025.i01.

[131] EC, Guidance Document No. 27. Technical Guidance For Deriving Environmental Quality Standards, (2011). https://doi.org/10.2779/43816.

[132] A. Palanques, P. Masqué, P. Puig, J.A. Sanchez-Cabeza, M. Frignani, F. Alvisi, Anthropogenic trace metals in the sedimentary record of the Llobregat continental shelf and adjacent Foix Submarine Canyon (northwestern Mediterranean), Mar. Geol. 248 (2008) 213–227. https://doi.org/10.1016/j.margeo.2007.11.001.

[133] A. Larrose, A. Coynel, J. Schäfer, G. Blanc, L. Massé, E. Maneux, Assessing the current state of the Gironde Estuary by mapping priority contaminant distribution and risk potential in surface sediment, Appl. Geochem. 25 (2010) 1912–1923. https://doi.org/10.1016/j.apgeochem.2010.10.007.

[134] J.-J. Jiang, C.-L. Lee, M.-D. Fang, J.T. Liu, Polycyclic aromatic hydrocarbons in coastal sediments of southwest Taiwan: An appraisal of diagnostic ratios in source recognition, Mar. Pollut. Bull. 58 (2009) 752–760. https://doi.org/10.1016/j.marpolbul.2008.12.017.

[135] M.B. Yunker, R.W. Macdonald, R. Vingarzan, R.H. Mitchell, D. Goyette, S. Sylvestre, PAHs in the Fraser River basin: a critical appraisal of PAH ratios as indicators of PAH source and composition, Org. Geochem. 33 (2002) 489–515. https://doi.org/10.1016/S0146-6380(02)00002-5.

[136] L. Gouriou, G. Trut, I. Auby, L. Rigouin, C. Meteigner, H. Oger-Jeanneret, Valorisation des données de la surveillance chimique DCE dans les masses d'eau du bassin Adour- Garonne (2008- 2015), (2018). https://archimer.ifremer.fr/doc/00422/53364/ (accessed May 14, 2019).

[137] J.A. Salvadó, J.O. Grimalt, J.F. López, A. Palanques, S. Heussner, C. Pasqual, A. Sanchez-Vidal, M. Canals, Transfer of lipid molecules and polycyclic aromatic hydrocarbons to open marine waters by dense water cascading events, Prog. Oceanogr. 159 (2017) 178–194. https://doi.org/10.1016/j.pocean.2017.10.002.

[138] B. Matturro, C. Ubaldi, P. Grenni, A.B. Caracciolo, S. Rossetti, Polychlorinated biphenyl (PCB) anaerobic degradation in marine sediments: microcosm study and role of autochthonous microbial communities, Environ. Sci. Pollut. Res. 23 (2016) 12613–12623. https://doi.org/10.1007/s11356-015-4960-2.

[139] S. Gómez-Lavín, D. Gorri, Á. Irabien, Assessment of PCDD/Fs and PCBs in Sediments from the Spanish Northern Atlantic Coast, Water. Air. Soil Pollut. 221 (2011) 287–299. https://doi.org/10.1007/s11270-011-0790-0.

[140] C. Ribeiro, A.R. Ribeiro, M.E. Tiritan, Occurrence of persistent organic pollutants in sediments and biota from Portugal versus European incidence: A critical overview, J. Environ. Sci. Health Part B. 51 (2016) 143–153. https://doi.org/10.1080/03601234.2015.1108793.

[141] A. Beyer, M. Biziuk, Environmental Fate and Global Distribution of Polychlorinated Biphenyls, in: D.M. Whitacre (Ed.), Rev. Environ. Contam. Toxicol. Vol 201, Springer US, Boston, MA, 2009: pp. 137–158. https://doi.org/10.1007/978-1-4419-0032-6_5.

[142] HERA, Environmental Risk Assessment on Ingredients of Household Cleaning Products− Polycyclic Musks AHTN (CAS 1506-02-1) and HHCB (CAS 1222-05-05)Environmental Section Version, 2 (2004) 1–81.

[143] J. Cavalheiro, O. Zuloaga, A. Prieto, H. Preudhomme, D. Amouroux, M. Monperrus, Occurrence and Fate of Organic and Organometallic Pollutants in Municipal Wastewater Treatment Plants and Their Impact on Receiving Waters (Adour Estuary, France), Arch. Environ. Contam. Toxicol. 73 (2017) 619–630. https://doi.org/10.1007/s00244-017-0422-9.

[144] C. Petus, G. Chust, F. Gohin, D. Doxaran, J.-M. Froidefond, Y. Sagarminaga, Estimating turbidity and total suspended matter in the Adour River plume (South Bay of Biscay) using MODIS 250-m imagery, Cont. Shelf Res. 30 (2010) 379–392. https://doi.org/10.1016/j.csr.2009.12.007.

[145] N.R. Sumner, C. Guitart, G. Fuentes, J.W. Readman, Inputs and distributions of synthetic musk fragrances in an estuarine and coastal environment; a case study, Environ. Pollut. 158 (2010) 215–222. https://doi.org/10.1016/j.envpol.2009.07.018.

[146] R. Rodil, M. Moeder, R. Altenburger, M. Schmitt-Jansen, Photostability and phytotoxicity of selected sunscreen agents and their degradation mixtures in water, Anal. Bioanal. Chem. 395 (2009) 1513–1524. https://doi.org/10.1007/s00216-009-3113-1.

[147] S. Li, G. Lu, Z. Xie, J. Ding, J. Liu, Y. Li, Sorption and degradation of selected organic UV filters (BM-DBM, 4-MBC, and OD-PABA) in laboratory water-sediment systems, Environ. Sci. Pollut. Res. 23 (2016) 9679–9689. https://doi.org/10.1007/s11356-016-6126-2.

[148] E. Barón, P. Gago-Ferrero, M. Gorga, I. Rudolph, G. Mendoza, A.M. Zapata, S. Díaz-Cruz, R. Barra, W. Ocampo-Duque, M. Páez, R.M. Darbra, E. Eljarrat, D. Barceló, Occurrence of hydrophobic organic pollutants (BFRs and UV-filters) in sediments from South America, Chemosphere. 92 (2013) 309–316. https://doi.org/10.1016/j.chemosphere.2013.03.032.

[149] Y. Kameda, K. Kimura, M. Miyazaki, Occurrence and profiles of organic sun-blocking agents in surface waters and sediments in Japanese rivers and lakes, Environ. Pollut. 159 (2011) 1570–1576. https://doi.org/10.1016/j.envpol.2011.02.055.

[150] H.W. Leung, T.B. Minh, M.B. Murphy, J.C.W. Lam, M.K. So, M. Martin, P.K.S. Lam, B.J. Richardson, Distribution, fate and risk assessment of antibiotics in sewage treatment plants in Hong Kong, South China, Environ. Int. 42 (2012) 1–9. https://doi.org/10.1016/j.envint.2011.03.004.

[151] J. Dong, X. Xia, Y. Zhai, Investigating particle concentration effects of polycyclic aromatic hydrocarbon (PAH) sorption on sediment considering the freely dissolved concentrations of PAHs, J. Soils Sediments. 13 (2013) 1469–1477. https://doi.org/10.1007/s11368-013-0736-9.

[152] J.A. Salvadó, J.O. Grimalt, J.F. López, A. Palanques, M. Canals, Influence of deep water formation by open-sea convection on the transport of low hydrophobicity organic pollutants in the NW Mediterranean Sea, Sci. Total Environ. 647 (2019) 597–605. https://doi.org/10.1016/j.scitotenv.2018.07.458.

[153] K. Amstaetter, E. Eek, G. Cornelissen, Sorption of PAHs and PCBs to activated carbon: Coal versus biomass-based quality, Chemosphere. 87 (2012) 573–578. https://doi.org/10.1016/j.chemosphere.2012.01.007.

[154] A. Nuzzo, A. Negroni, G. Zanaroli, F. Fava, Identification of two organohalide-respiring Dehalococcoidia associated to different dechlorination activities in PCB-impacted marine sediments, Microb. Cell Factories. 16 (2017) 127. https://doi.org/10.1186/s12934-017-0743-4.

[155] P. Gago-Ferrero, M.S. Díaz-Cruz, D. Barceló, An overview of UV-absorbing compounds (organic UV filters) in aquatic biota, Anal. Bioanal. Chem. 404 (2012) 2597–2610. https://doi.org/10.1007/s00216-012-6067-7.

[156] S. Romero-Romero, L. Herrero, M. Fernández, B. Gómara, J.L. Acuña, Biomagnification of persistent organic pollutants in a deep-sea, temperate food web, Sci. Total Environ. 605–606 (2017) 589–597. https://doi.org/10.1016/j.scitotenv.2017.06.148.

[157] S. Koenig, P. Fernández, J.B. Company, D. Huertas, M. Solé, Are deep-sea organisms dwelling within a submarine canyon more at risk from anthropogenic contamination than those from the adjacent open slope? A case study of Blanes canyon (NW Mediterranean), Prog. Oceanogr. 118 (2013) 249–259. https://doi.org/10.1016/j.pocean.2013.07.016.

[158] P.T. Harris, M. Macmillan-Lawler, J. Rupp, E.K. Baker, Geomorphology of the oceans, Mar. Geol. 352 (2014) 4–24. https://doi.org/10.1016/j.margeo.2014.01.011.

[159] D. Kaiser, A. Sieratowicz, H. Zielke, M. Oetken, H. Hollert, J. Oehlmann, Ecotoxicological effect characterisation of widely used organic UV filters, Environ. Pollut. Barking Essex 1987. 163 (2012) 84–90. https://doi.org/10.1016/j.envpol.2011.12.014.

[160] N.E. Selin, D.J. Jacob, R.J. Park, R.M. Yantosca, S. Strode, L. Jaeglé, D. Jaffe, Chemical cycling and deposition of atmospheric mercury: Global constraints from observations, J. Geophys. Res. Atmospheres. 112 (2007) D02308. https://doi.org/10.1029/2006JD007450.

[161] R.P. Mason, A.L. Choi, W.F. Fitzgerald, C.R. Hammerschmidt, C.H. Lamborg, A.L. Soerensen, E.M. Sunderland, Mercury biogeochemical cycling in the ocean and policy implications, Environ. Res. 119 (2012) 101–117. https://doi.org/10.1016/j.envres.2012.03.013.

[162] C.H. Lamborg, C.R. Hammerschmidt, K.L. Bowman, An examination of the role of particles in oceanic mercury cycling, Philos. Transact. A Math. Phys. Eng. Sci. 374 (2016). https://doi.org/10.1098/rsta.2015.0297.

[163] S.M. Ullrich, T.W. Tanton, S.A. Abdrashitova, Mercury in the Aquatic Environment: A Review of Factors Affecting Methylation, Crit. Rev. Environ. Sci. Technol. 31 (2001) 241–293. https://doi.org/10.1080/20016491089226.

[164] T. Barkay, I. Wagner-Döbler, Microbial Transformations of Mercury: Potentials, Challenges, and Achievements in Controlling Mercury Toxicity in the Environment, in: Adv. Appl. Microbiol., Academic Press, 2005: pp. 1–52. https://doi.org/10.1016/S0065-2164(05)57001-1.

[165] E.J. Fleming, E.E. Mack, P.G. Green, D.C. Nelson, Mercury Methylation from Unexpected Sources: Molybdate-Inhibited Freshwater Sediments and an Iron-Reducing Bacterium, Appl. Environ. Microbiol. 72 (2006) 457–464. https://doi.org/10.1128/AEM.72.1.457-464.2006.

[166] S. Jonsson, U. Skyllberg, M.B. Nilsson, E. Lundberg, A. Andersson, E. Björn, Differentiated availability of geochemical mercury pools controls methylmercury levels in estuarine sediment and biota, Nat. Commun. 5 (2014) 4624. https://doi.org/10.1038/ncomms5624.

[167] J.M. Benoit, R.P. Mason, C.C. Gilmour, G.R. Aiken, Constants for mercury binding by dissolved organic matter isolates from the Florida Everglades, Geochim. Cosmochim. Acta. 65 (2001) 4445–4451. https://doi.org/10.1016/S0016-7037(01)00742-6.

[168] J. Schäfer, S. Castelle, G. Blanc, A. Dabrin, M. Masson, L. Lanceleur, C. Bossy, Mercury methylation in the sediments of a macrotidal estuary (Gironde Estuary, south-west France), Estuar. Coast. Shelf Sci. 90 (2010) 80–92. https://doi.org/10.1016/j.ecss.2010.07.007.

[169] W. Zheng, L. Liang, B. Gu, Mercury Reduction and Oxidation by Reduced Natural Organic Matter in Anoxic Environments, Environ. Sci. Technol. 46 (2012) 292–299. https://doi.org/10.1021/es203402p.

[170] T. Jiang, U. Skyllberg, S. Wei, D. Wang, S. Lu, Z. Jiang, D.C. Flanagan, Modeling of the structure-specific kinetics of abiotic, dark reduction of Hg(II) complexed by O/N and S functional groups in humic acids while accounting for time-dependent structural rearrangement, Geochim. Cosmochim. Acta. 154 (2015) 151–167. https://doi.org/10.1016/j.gca.2015.01.011.

[171] R.S. Oremland, C.W. Culbertson, M.R. Winfrey, Methylmercury Decomposition in Sediments and Bacterial Cultures: Involvement of Methanogens and Sulfate Reducers in Oxidative Demethylation, Appl. Environ. Microbiol. 57 (1991) 130–137.

[172] * Mark Marvin-DiPasquale, † Jennifer Agee, † Chad McGowan, † Ronald S. Oremland, ‡ Martha Thomas, § and David Krabbenhoft, C.C. Gilmour#, Methyl-Mercury Degradation

Pathways: A Comparison among Three Mercury-Impacted Ecosystems, (2000). https://doi.org/10.1021/es0013125.

[173] T. Barkay, S.M. Miller, A.O. Summers, Bacterial mercury resistance from atoms to ecosystems, FEMS Microbiol. Rev. 27 (2003) 355–384. https://doi.org/10.1016/S0168-6445(03)00046-9.

[174] J.K. Schaefer, J. Yagi, J.R. Reinfelder, T. Cardona, K.M. Ellickson, S. Tel-Or, T. Barkay, Role of the Bacterial Organomercury Lyase (MerB) in Controlling Methylmercury Accumulation in Mercury-Contaminated Natural Waters, Environ. Sci. Technol. 38 (2004) 4304–4311. https://doi.org/10.1021/es049895w.

[175] R.S. Oremland, L.G. Miller, P. Dowdle, T. Connell, T. Barkay, Methylmercury oxidative degradation potentials in contaminated and pristine sediments of the carson river, nevada., Appl Env. Microbiol. 61 (1995) 2745–2753.

[176] M.C. Marvin-DiPasquale, R.S. Oremland, Bacterial Methylmercury Degradation in Florida Everglades Peat Sediment, Environ. Sci. Technol. 32 (1998) 2556–2563. https://doi.org/10.1021/es971099l.

[177] L. Lambertsson, M. Nilsson, Organic Material: The Primary Control on Mercury Methylation and Ambient Methyl Mercury Concentrations in Estuarine Sediments, Environ. Sci. Technol. 40 (2006) 1822–1829. https://doi.org/10.1021/es051785h.

[178] N.M. Mazrui, S. Jonsson, S. Thota, J. Zhao, R.P. Mason, Enhanced availability of mercury bound to dissolved organic matter for methylation in marine sediments, Geochim. Cosmochim. Acta. 194 (2016) 153–162. https://doi.org/10.1016/j.gca.2016.08.019.

[179] M. Monperrus, E. Tessier, D. Point, K. Vidimova, D. Amouroux, R. Guyoneaud, A. Leynaert, J. Grall, L. Chauvaud, G. Thouzeau, O.F.X. Donard, The biogeochemistry of mercury at the sediment–water interface in the Thau Lagoon. 2. Evaluation of mercury methylation potential in both surface sediment and the water column, Estuar. Coast. Shelf Sci. 72 (2007) 485–496. https://doi.org/10.1016/j.ecss.2006.11.014.

[180] S. Schmidt, H. Howa, A. Diallo, J. Martín, M. Cremer, P. Duros, C. Fontanier, B. Deflandre, E. Metzger, T. Mulder, Recent sediment transport and deposition in the Cap-Ferret Canyon, South-East margin of Bay of Biscay, Deep Sea Res. Part II Top. Stud. Oceanogr. 104 (2014) 134–144. https://doi.org/10.1016/j.dsr2.2013.06.004.

[181] J.P. Walsh, C.A. Nittrouer, Understanding fine-grained river-sediment dispersal on continental margins, Mar. Geol. 263 (2009) 34–45. https://doi.org/10.1016/j.margeo.2009.03.016.

[182] P. Puig, M. Canals, J.B. Company, J. Martín, D. Amblas, G. Lastras, A. Palanques, A.M. Calafat, Ploughing the deep sea floor, Nature. 489 (2012) 286–289. https://doi.org/10.1038/nature11410.

[183] L. Buhl-Mortensen, P.B. Mortensen, Distribution and diversity of species associated with deep-sea gorgonian corals off Atlantic Canada, in: Cold-Water Corals Ecosyst., Springer, Berlin, Heidelberg, 2005: pp. 849–879. https://doi.org/10.1007/3-540-27673-4_44.

[184] A.L. Post, P.E. O'Brien, R.J. Beaman, M.J. Riddle, L.D. Santis, Physical controls on deep water coral communities on the George V Land slope, East Antarctica, Antarct. Sci. 22 (2010) 371–378. https://doi.org/10.1017/S0954102010000180.

[185] A.M. Costa, M. Mil-Homens, S.M. Lebreiro, T.O. Richter, H. de Stigter, W. Boer, M.A. Trancoso, Z. Melo, F. Mouro, M. Mateus, J. Canário, V. Branco, M. Caetano, Origin and transport of trace metals deposited in the canyons off Lisboa and adjacent slopes (Portuguese Margin) in the last century, Mar. Geol. 282 (2011) 169–177. https://doi.org/10.1016/j.margeo.2011.02.007.

[186] M. Papale, A. Conte, M. Del Core, E. Zito, M. Sprovieri, F. De Leo, C. Rizzo, C. Urzì, E. De Domenico, G.M. Luna, L. Michaud, A. Lo Giudice, Heavy-metal resistant microorganisms in sediments from submarine canyons and the adjacent continental slope in the northeastern Ligurian margin (Western Mediterranean Sea), Prog. Oceanogr. 168 (2018) 155–168. https://doi.org/10.1016/j.pocean.2018.09.015.

[187] W.D. Nesteroff, S. Duplaix, J. Sauvage, Y. Lancelot, F. Melieres, E. Vincent, Les depots recents du canyon de Cap-Breton, Bull. Société Géologique Fr. S7-X (1968) 218–252. https://doi.org/10.2113/gssgfbull.S7-X.2.218.

[188] F.P. Shepard, R. Dill, Marine Geology. (Book Reviews: Submarine Canyons and Other Sea Valleys), Science. 154 (1966) 1433–1434. https://doi.org/10.1126/science.154.3755.1433.

[189] M. Monperrus, P.R. Gonzalez, D. Amouroux, J.I.G. Alonso, O.F.X. Donard, Evaluating the potential and limitations of double-spiking species-specific isotope dilution analysis for the accurate quantification of mercury species in different environmental matrices, Anal. Bioanal. Chem. 390 (2008) 655–666. https://doi.org/10.1007/s00216-007-1598-z.

[190] P. Rodriguez-Gonzalez, S. Bouchet, M. Monperrus, E. Tessier, D. Amouroux, In situ experiments for element species-specific environmental reactivity of tin and mercury compounds using isotopic tracers and multiple linear regression, Environ. Sci. Pollut. Res. 20 (2013) 1269–1280. https://doi.org/10.1007/s11356-012-1019-5.

[191] N. Savoye, V. David, F. Morisseau, H. Etcheber, G. Abril, I. Billy, K. Charlier, G. Oggian, H. Derriennic, B. Sautour, Origin and composition of particulate organic matter in a macrotidal turbid estuary: The Gironde Estuary, France, Estuar. Coast. Shelf Sci. 108 (2012) 16–28. https://doi.org/10.1016/j.ecss.2011.12.005.

[192] C. Liénart, N. Susperregui, V. Rouaud, J. Cavalheiro, V. David, Y. Del Amo, R. Duran, B. Lauga, M. Monperrus, T. Pigot, S. Bichon, K. Charlier, N. Savoye, Dynamics of particulate organic matter in a coastal system characterized by the occurrence of marine mucilage – A stable isotope study, J. Sea Res. 116 (2016) 12–22. https://doi.org/10.1016/j.seares.2016.08.001.

[193] M.F. Lehmann, S.M. Bernasconi, A. Barbieri, J.A. McKenzie, Preservation of organic matter and alteration of its carbon and nitrogen isotope composition during simulated and in situ early sedimentary diagenesis, Geochim. Cosmochim. Acta. 66 (2002) 3573–3584. https://doi.org/10.1016/S0016-7037(02)00968-7.

[194] S. Maslennikova, N. Larina, S. Larin, The effect of sediment grain size on heavy metal content, Lakes Reserv. Ponds. 6 (2012) 43–54.

[195] C. Zhang, Z. Yu, G. Zeng, M. Jiang, Z. Yang, F. Cui, M. Zhu, L. Shen, L. Hu, Effects of sediment geochemical properties on heavy metal bioavailability, Environ. Int. 73 (2014) 270–281. https://doi.org/10.1016/j.envint.2014.08.010.

[196] P. Chakraborty, A. Sarkar, K. Vudamala, R. Naik, B.N. Nath, Organic matter — A key factor in controlling mercury distribution in estuarine sediment, Mar. Chem. 173 (2015) 302–309. https://doi.org/10.1016/j.marchem.2014.10.005.

[197] B.F. Araujo, H. Hintelmann, B. Dimock, M.G. Almeida, C.E. Rezende, Concentrations and isotope ratios of mercury in sediments from shelf and continental slope at Campos Basin near Rio de Janeiro, Brazil, Chemosphere. 178 (2017) 42–50. https://doi.org/10.1016/j.chemosphere.2017.03.056.

[198] P.A. Meyers, Preservation of elemental and isotopic source identification of sedimentary organic matter, Chem. Geol. 114 (1994) 289–302. https://doi.org/10.1016/0009-2541(94)90059-0.

[199] J.J. Middelburg, P.M.J. Herman, Organic matter processing in tidal estuaries, Mar. Chem. 106 (2007) 127–147. https://doi.org/10.1016/j.marchem.2006.02.007.

[200] N. Ohkouchi, N.O. Ogawa, Y. Chikaraishi, H. Tanaka, E. Wada, Biochemical and physiological bases for the use of carbon and nitrogen isotopes in environmental and ecological studies, Prog. Earth Planet. Sci. 2 (2015) 1. https://doi.org/10.1186/s40645-015-0032-y.

[201] Y. Li, H. Zhang, C. Tu, C. Fu, Y. Xue, Y. Luo, Sources and fate of organic carbon and nitrogen from land to ocean: Identified by coupling stable isotopes with C/N ratio, Estuar. Coast. Shelf Sci. 181 (2016) 114–122. https://doi.org/10.1016/j.ecss.2016.08.024.

[202] S. Dubois, N. Savoye, A. Grémare, M. Plus, K. Charlier, A. Beltoise, H. Blanchet, Origin and composition of sediment organic matter in a coastal semi-enclosed ecosystem: An elemental and isotopic study at the ecosystem space scale, J. Mar. Syst. 94 (2012) 64–73. https://doi.org/10.1016/j.jmarsys.2011.10.009.

[203] J. Brahney, A.P. Ballantyne, B.L. Turner, S.A. Spaulding, M. Otu, J.C. Neff, Separating the influences of diagenesis, productivity and anthropogenic nitrogen deposition on sedimentary

δ15N variations, Org. Geochem. 75 (2014) 140–150. https://doi.org/10.1016/j.orggeochem.2014.07.003.

[204] A. Barber, K. Lalonde, A. Mucci, Y. Gélinas, The role of iron in the diagenesis of organic carbon and nitrogen in sediments: A long-term incubation experiment, Mar. Chem. 162 (2014) 1–9. https://doi.org/10.1016/j.marchem.2014.02.007.

[205] Y. Hong, J. Wu, F. Guan, W. Yue, A. Long, Nitrogen removal in the sediments of the Pearl River Estuary, China: Evidence from the distribution and forms of nitrogen in the sediment cores, Mar. Pollut. Bull. 138 (2019) 115–124. https://doi.org/10.1016/j.marpolbul.2018.11.040.

[206] E.R. Long, D.D. Macdonald, S.L. Smith, F.D. Calder, Incidence of adverse biological effects within ranges of chemical concentrations in marine and estuarine sediments, Environ. Manage. 19 (1995) 81–97. https://doi.org/10.1007/BF02472006.

[207] C.H. Lamborg, C.R. Hammerschmidt, K.L. Bowman, G.J. Swarr, K.M. Munson, D.C. Ohnemus, P.J. Lam, L.-E. Heimbürger, M.J.A. Rijkenberg, M.A. Saito, A global ocean inventory of anthropogenic mercury based on water column measurements, Nature. 512 (2014) 65–68. https://doi.org/10.1038/nature13563.

[208] J.M. Everaarts, C.V. Fischer, The distribution of heavy metals (Cu, Zn, Cd, Pb) in the fine fraction of surface sediments of the North Sea, Neth. J. Sea Res. 29 (1992) 323–331. https://doi.org/10.1016/0077-7579(92)90072-M.

[209] J. Unda-Calvo, E. Ruiz-Romera, S. Fdez-Ortiz de Vallejuelo, M. Martínez-Santos, A. Gredilla, Evaluating the role of particle size on urban environmental geochemistry of metals in surface sediments, Sci. Total Environ. 646 (2019) 121–133. https://doi.org/10.1016/j.scitotenv.2018.07.172.

[210] C.R. Hammerschmidt, W.F. Fitzgerald, Methylmercury cycling in sediments on the continental shelf of southern New England, Geochim. Cosmochim. Acta. 70 (2006) 918–930. https://doi.org/10.1016/j.gca.2005.10.020.

[211] C.T. Driscoll, C.Y. Chen, C.R. Hammerschmidt, R.P. Mason, C.C. Gilmour, E.M. Sunderland, B.K. Greenfield, K.L. Buckman, C.H. Lamborg, Nutrient supply and mercury dynamics in marine ecosystems: A conceptual model, Environ. Res. 119 (2012) 118–131. https://doi.org/10.1016/j.envres.2012.05.002.

[212] P. Chakraborty, R.P. Mason, S. Jayachandran, K. Vudamala, K. Armoury, A. Sarkar, S. Chakraborty, P. Bardhan, R. Naik, Effects of bottom water oxygen concentrations on mercury distribution and speciation in sediments below the oxygen minimum zone of the Arabian Sea, Mar. Chem. 186 (2016) 24–32. https://doi.org/10.1016/j.marchem.2016.07.005.

[213] C.A. Kelly, J.W.M. Rudd, Transport of mercury on the finest particles results in high sediment concentrations in the absence of significant ongoing sources, Sci. Total Environ. 637–638 (2018) 1471–1479. https://doi.org/10.1016/j.scitotenv.2018.04.234.

[214] R. Yin, X. Feng, B. Chen, J. Zhang, W. Wang, X. Li, Identifying the Sources and Processes of Mercury in Subtropical Estuarine and Ocean Sediments Using Hg Isotopic Composition, Environ. Sci. Technol. 49 (2015) 1347–1355. https://doi.org/10.1021/es504070y.

[215] T. Mulder, S. Migeon, B. Savoye, J.-C. Faugères, Inversely graded turbidite sequences in the deep Mediterranean: a record of deposits from flood-generated turbidity currents?, Geo-Mar. Lett. 21 (2001) 86–93. https://doi.org/10.1007/s003670100071.

[216] P. Anschutz, F.J. Jorissen, G. Chaillou, R. Abu-Zied, C. Fontanier, Recent turbidite deposition in the eastern Atlantic: Early diagenesis and biotic recovery, J. Mar. Res. 60 (2002) 835–854. https://doi.org/10.1357/002224002321505156.

[217] T.S. Figueiredo, A.L.S. Albuquerque, C.J. Sanders, L.G.M.S. Cordeiro, E.V. Silva-Filho, Mercury deposition during the previous century in an upwelling region; Cabo Frio, Brazil, Mar. Pollut. Bull. 76 (2013) 389–393. https://doi.org/10.1016/j.marpolbul.2013.07.049.

[218] C.A. da Silva, E. Tessier, V.T. Kütter, J.C. Wasserman, O.F.X. Donard, E.V. Silva-Filho, Mercury speciation in fish of the Cabo Frio upwelling region, SE-Brazil, Braz. J. Oceanogr. 59 (2011) 259–266. https://doi.org/10.1590/S1679-87592011000300006.

[219] V. Liem-Nguyen, S. Jonsson, U. Skyllberg, M.B. Nilsson, A. Andersson, E. Lundberg, E. Björn, Effects of Nutrient Loading and Mercury Chemical Speciation on the Formation and Degradation of Methylmercury in Estuarine Sediment, Environ. Sci. Technol. 50 (2016) 6983–6990. https://doi.org/10.1021/acs.est.6b01567.

[220] A. Mouret, P. Anschutz, B. Deflandre, G. Chaillou, C. Hyacinthe, J. Deborde, H. Etcheber, J.-M. Jouanneau, A. Grémare, P. Lecroart, Oxygen and organic carbon fluxes in sediments of the Bay of Biscay, Deep Sea Res. Part Oceanogr. Res. Pap. 57 (2010) 528–540. https://doi.org/10.1016/j.dsr.2009.12.009.

[221] B. Dauwe, J.J. Middelburg, P.M.J. Herman, C.H.R. Heip, Linking diagenetic alteration of amino acids and bulk organic matter reactivity, Limnol. Oceanogr. 44 (1999) 1809–1814. https://doi.org/10.4319/lo.1999.44.7.1809.

[222] K. Wang, J. Chen, H. Jin, H. Li, W. Zhang, Organic matter degradation in surface sediments of the Changjiang estuary: Evidence from amino acids, Sci. Total Environ. 637–638 (2018) 1004–1013. https://doi.org/10.1016/j.scitotenv.2018.04.242.

[223] J. Bełdowski, M. Szubska, M. Bełdowska, K. Jankowska, E. Kotlarska, B. Graca, Seasonal changes of mercury speciation in the coastal sediments, J. Soils Sediments. (2018). https://doi.org/10.1007/s11368-018-1993-4.

[224] D. Point, Spéciation et biogéochimie des éléments traces métalliques dans l'estuaire de l'Adour., thesis, Pau, 2004. http://www.theses.fr/2004PAUU3029 (accessed December 19, 2018).

[225] E.M. Sunderland, R.P. Mason, Human impacts on open ocean mercury concentrations, Glob. Biogeochem. Cycles. 21 (2007). https://doi.org/10.1029/2006GB002876.

[226] J.D. Blum, L.S. Sherman, M.W. Johnson, Mercury Isotopes in Earth and Environmental Sciences, Annu. Rev. Earth Planet. Sci. 42 (2014) 249–269. https://doi.org/10.1146/annurev-earth-050212-124107.

[227] V.L. Ortiz, R.P. Mason, J. Evan Ward, An examination of the factors influencing mercury and methylmercury particulate distributions, methylation and demethylation rates in laboratory-generated marine snow, Mar. Chem. 177 (2015) 753–762. https://doi.org/10.1016/j.marchem.2015.07.006.

[228] R.C. Rodríguez Martín-Doimeadios, E. Tessier, D. Amouroux, R. Guyoneaud, R. Duran, P. Caumette, O.F.X. Donard, Mercury methylation/demethylation and volatilization pathways in estuarine sediment slurries using species-specific enriched stable isotopes, Mar. Chem. 90 (2004) 107–123. https://doi.org/10.1016/j.marchem.2004.02.022.

[229] M.S. Goñi-Urriza, D. Point, D. Amouroux, R. Guyoneaud, O.F.X. Donard, P. Caumette, R. Duran, Bacterial community structure along the Adour estuary (French Atlantic coast): influence of salinity gradient versus metal contamination, Aquat. Microb. Ecol. 49 (2007) 47–56. https://doi.org/10.3354/ame01128.

[230] Y. Colin, M. Goñi-Urriza, C. Gassie, E. Carlier, M. Monperrus, R. Guyoneaud, Distribution of Sulfate-Reducing Communities from Estuarine to Marine Bay Waters, Microb. Ecol. 73 (2017) 39–49. https://doi.org/10.1007/s00248-016-0842-5.

[231] J.M. Benoit, C.C. Gilmour, R.P. Mason, A. Heyes, Sulfide Controls on Mercury Speciation and Bioavailability to Methylating Bacteria in Sediment Pore Waters, Environ. Sci. Technol. 33 (1999) 951–957. https://doi.org/10.1021/es9808200.

[232] J.M. Benoit, C.C. Gilmour, R.P. Mason, The Influence of Sulfide on Solid-Phase Mercury Bioavailability for Methylation by Pure Cultures of Desulfobulbus propionicus (1pr3), Environ. Sci. Technol. 35 (2001) 127–132. https://doi.org/10.1021/es001415n.

[233] D. Cossa, R. Buscail, P. Puig, J.-F. Chiffoleau, O. Radakovitch, G. Jeanty, S. Heussner, Origin and accumulation of trace elements in sediments of the northwestern Mediterranean margin, Chem. Geol. 380 (2014) 61–73. https://doi.org/10.1016/j.chemgeo.2014.04.015.

[234] K. Kannan, J. Falandysz, Speciation and Concentrations of Mercury in Certain Coastal Marine Sediments, Water. Air. Soil Pollut. 103 (1998) 129–136. https://doi.org/10.1023/A:1004967112178.

[235] J.H. Weber, R. Evans, S.H. Jones, M.E. Hines, Conversion of mercury(II) into mercury(0), monomethylmercury cation, and dimethylmercury in saltmarsh sediment slurries, Chemosphere. 36 (1998) 1669–1687. https://doi.org/10.1016/S0045-6535(97)10042-X.

[236] C.R. Hammerschmidt, W.F. Fitzgerald, Geochemical Controls on the Production and Distribution of Methylmercury in Near-Shore Marine Sediments, Environ. Sci. Technol. 38 (2004) 1487–1495. https://doi.org/10.1021/es034528q.

[237] A.T. Schartup, U. Ndu, P.H. Balcom, R.P. Mason, E.M. Sunderland, Contrasting Effects of Marine and Terrestrially Derived Dissolved Organic Matter on Mercury Speciation and Bioavailability in Seawater, Environ. Sci. Technol. 49 (2015) 5965–5972. https://doi.org/10.1021/es506274x.

[238] P. Liang, S. Wu, C. Zhang, J. Xu, P. Christie, J. Zhang, Y. Cao, The role of antibiotics in mercury methylation in marine sediments, J. Hazard. Mater. 360 (2018) 1–5. https://doi.org/10.1016/j.jhazmat.2018.07.096.

[239] N. Ogrinc, M. Monperrus, J. Kotnik, V. Fajon, K. Vidimova, D. Amouroux, D. Kocman, E. Tessier, S. Žižek, M. Horvat, Distribution of mercury and methylmercury in deep-sea surficial sediments of the Mediterranean Sea, Mar. Chem. 107 (2007) 31–48. https://doi.org/10.1016/j.marchem.2007.01.019.

[240] S. Bouchet, P. Rodriguez-Gonzalez, R. Bridou, M. Monperrus, E. Tessier, P. Anschutz, R. Guyoneaud, D. Amouroux, Investigations into the differential reactivity of endogenous and exogenous mercury species in coastal sediments, Environ. Sci. Pollut. Res. 20 (2013) 1292–1301. https://doi.org/10.1007/s11356-012-1068-9.

[241] J.M. Benoit, C.C. Gilmour, A. Heyes, R.P. Mason, C.L. Miller, Geochemical and Biological Controls over Methylmercury Production and Degradation in Aquatic Ecosystems, in: Biogeochem. Environ. Important Trace Elem., American Chemical Society, 2002: pp. 262–297. https://doi.org/10.1021/bk-2003-0835.ch019.

[242] M. Monperrus, D. Point, J. Grall, L. Chauvaud, D. Amouroux, G. Bareille, O. Donard, Determination of metal and organometal trophic bioaccumulation in the benthic macrofauna of the Adour estuary coastal zone (SW France, Bay of Biscay), J. Environ. Monit. 7 (2005) 693–700. https://doi.org/10.1039/B500288E.

[243] W.F. Fitzgerald, C.H. Lamborg, C.R. Hammerschmidt, Marine biogeochemical cycling of mercury, Chem. Rev. 107 (2007) 641–662. https://doi.org/10.1021/cr050353m.

[244] H.M. Amos, D.J. Jacob, D. Kocman, H.M. Horowitz, Y. Zhang, S. Dutkiewicz, M. Horvat, E.S. Corbitt, D.P. Krabbenhoft, E.M. Sunderland, Global biogeochemical implications of mercury discharges from rivers and sediment burial, Environ. Sci. Technol. 48 (2014) 9514–9522. https://doi.org/10.1021/es502134t.

[245] R. Chester, The transport of material to the oceans: relative flux magnitudes, in: R. Chester (Ed.), Mar. Geochem., 2nd ed., Blackwell science : Oxford, Dordrecht, 2003: pp. 98–134. https://doi.org/10.1007/978-94-010-9488-7_6.

[246] C. Chen, A. Amirbahman, N. Fisher, G. Harding, C. Lamborg, D. Nacci, D. Taylor, Methylmercury in marine ecosystems: spatial patterns and processes of production, bioaccumulation, and biomagnification, EcoHealth. 5 (2008) 399–408.

[247] J.D. Blum, B.A. Bergquist, Reporting of variations in the natural isotopic composition of mercury, Anal. Bioanal. Chem. 388 (2007) 353–359. https://doi.org/10.1007/s00216-007-1236-9.

[248] R. Yin, X. Feng, X. Li, B. Yu, B. Du, Trends and advances in mercury stable isotopes as a geochemical tracer, Trends Environ. Anal. Chem. 2 (2014) 1–10. https://doi.org/10.1016/j.teac.2014.03.001.

[249] D.W. Boening, Ecological effects, transport, and fate of mercury: a general review, Chemosphere. 40 (2000) 1335–1351. https://doi.org/10.1016/S0045-6535(99)00283-0.

[250] R.N. Glud, F. Wenzhöfer, M. Middelboe, K. Oguri, R. Turnewitsch, D.E. Canfield, H. Kitazato, High rates of microbial carbon turnover in sediments in the deepest oceanic trench on Earth, Nat. Geosci. 6 (2013) 284–288. https://doi.org/10.1038/ngeo1773.

[251] B. Fry, E.B. Sherr, δ13C Measurements as Indicators of Carbon Flow in Marine and Freshwater Ecosystems, in: P.W. Rundel, J.R. Ehleringer, K.A. Nagy (Eds.), Stable Isot. Ecol. Res., Springer New York, 1989: pp. 196–229.

[252] D.B. Senn, E.J. Chesney, J.D. Blum, M.S. Bank, A. Maage, J.P. Shine, Stable Isotope (N, C, Hg) Study of Methylmercury Sources and Trophic Transfer in the Northern Gulf of Mexico, Environ. Sci. Technol. 44 (2010) 1630–1637. https://doi.org/10.1021/es902361j.

[253] X. Xu, Q. Zhang, W.-X. Wang, Linking mercury, carbon, and nitrogen stable isotopes in Tibetan biota: Implications for using mercury stable isotopes as source tracers, Sci. Rep. 6 (2016) 25394. https://doi.org/10.1038/srep25394.

[254] V. Perrot, M.V. Pastukhov, V.N. Epov, S. Husted, O.F.X. Donard, D. Amouroux, Higher mass-independent isotope fractionation of methylmercury in the pelagic food web of Lake Baikal (Russia), Environ. Sci. Technol. 46 (2012) 5902–5911. https://doi.org/10.1021/es204572g.

[255] C. Feng, Z. Pedrero, P. Li, B. Du, X. Feng, M. Monperrus, E. Tessier, S. Berail, D. Amouroux, Investigation of Hg uptake and transport between paddy soil and rice seeds combining Hg isotopic composition and speciation, Elem Sci Anth. 4 (2016) 000087. https://doi.org/10.12952/journal.elementa.000087.

[256] M. Jiménez-Moreno, J.P.G. Barre, V. Perrot, S. Bérail, R.C. Rodríguez Martín-Doimeadios, D. Amouroux, Sources and fate of mercury pollution in Almadén mining district (Spain): Evidences from mercury isotopic compositions in sediments and lichens, Chemosphere. 147 (2016) 430–438. https://doi.org/10.1016/j.chemosphere.2015.12.094.

[257] L.S. Sherman, J.D. Blum, Mercury stable isotopes in sediments and largemouth bass from Florida lakes, USA, Sci. Total Environ. 448 (2013) 163–175. https://doi.org/10.1016/j.scitotenv.2012.09.038.

[258] R. Yin, X. Feng, J.P. Hurley, D.P. Krabbenhoft, R.F. Lepak, R. Hu, Q. Zhang, Z. Li, X. Bi, Mercury Isotopes as Proxies to Identify Sources and Environmental Impacts of Mercury in Sphalerites, Sci. Rep. 6 (2016) 18686. https://doi.org/10.1038/srep18686.

[259] P. Donovan, J. Blum, D. Yee, G. Gehrke, M. Singer, An isotopic record of mercury in San Francisco Bay sediment, Chem. Geol. s 349–350 (2013) 87–98. https://doi.org/10.1016/j.chemgeo.2013.04.017.

[260] S. Le Faucheur, P.G.C. Campbell, C. Fortin, V.I. Slaveykova, Interactions between mercury and phytoplankton: Speciation, bioavailability, and internal handling, Environ. Toxicol. Chem. 33 (2014) 1211–1224. https://doi.org/10.1002/etc.2424.

[261] P. Rodríguez-González, V.N. Epov, R. Bridou, E. Tessier, R. Guyoneaud, M. Monperrus, D. Amouroux, Species-specific stable isotope fractionation of mercury during Hg(II) methylation by an anaerobic bacteria (Desulfobulbus propionicus) under dark conditions, Environ. Sci. Technol. 43 (2009) 9183–9188. https://doi.org/10.1021/es902206j.

[262] W.C. Li, Occurrence, sources, and fate of pharmaceuticals in aquatic environment and soil, Environ. Pollut. 187 (2014) 193–201. https://doi.org/10.1016/j.envpol.2014.01.015.

[263] S. Rainieri, A. Barranco, M. Primec, T. Langerholc, Occurrence and toxicity of musks and UV filters in the marine environment, Food Chem. Toxicol. 104 (2017) 57–68. https://doi.org/10.1016/j.fct.2016.11.012.

[264] A. Azaroff, C. Miossec, L. Lanceleur, R. Guyoneaud, M. Monperrus, Priority and emerging micropollutants distribution from coastal to continental slope sediments: A case study of Capbreton Submarine Canyon (North Atlantic Ocean), Sci. Total Environ. 703 (2020) 135057. https://doi.org/10.1016/j.scitotenv.2019.135057.

[265] C. Miège, J.M. Choubert, L. Ribeiro, M. Eusèbe, M. Coquery, Fate of pharmaceuticals and personal care products in wastewater treatment plants – Conception of a database and first results, Environ. Pollut. 157 (2009) 1721–1726. https://doi.org/10.1016/j.envpol.2008.11.045.

[266] P. Verlicchi, M. Al Aukidy, E. Zambello, Occurrence of pharmaceutical compounds in urban wastewater: Removal, mass load and environmental risk after a secondary treatment—A review, Sci. Total Environ. 429 (2012) 123–155. https://doi.org/10.1016/j.scitotenv.2012.04.028.

[267] L.W. Perelo, Review: In situ and bioremediation of organic pollutants in aquatic sediments, J. Hazard. Mater. 177 (2010) 81–89. https://doi.org/10.1016/j.jhazmat.2009.12.090.

[268] F. Widdel, F. Bak, Gram-Negative Mesophilic Sulfate-Reducing Bacteria, in: A. Balows, H.G. Trüper, M. Dworkin, W. Harder, K.-H. Schleifer (Eds.), Prokaryotes Handb. Biol. Bact. Ecophysiol. Isol. Identif. Appl., Springer New York, New York, NY, 1992: pp. 3352–3378. https://doi.org/10.1007/978-1-4757-2191-1_21.

[269] L. Delgado-Moreno, S. Bazhari, R. Nogales, E. Romero, Innovative application of biobed bioremediation systems to remove emerging contaminants: Adsorption, degradation and bioaccesibility, Sci. Total Environ. 651 (2019) 990–997. https://doi.org/10.1016/j.scitotenv.2018.09.268.

[270] F. Balk, R.A. Ford, Environmental risk assessment for the polycyclic musks AHTN and HHCB in the EU. I. Fate and exposure assessment, Toxicol. Lett. 111 (1999) 57–79. https://doi.org/10.1016/s0378-4274(99)00169-1.

[271] J.R. Marchesi, T. Sato, A.J. Weightman, T.A. Martin, J.C. Fry, S.J. Hiom, W.G. Wade, Design and Evaluation of Useful Bacterium-Specific PCR Primers That Amplify Genes Coding for Bacterial 16S rRNA, Appl Env. Microbiol. 64 (1998) 795–799.

[272] R.C. Edgar, MUSCLE: multiple sequence alignment with high accuracy and high throughput, Nucleic Acids Res. 32 (2004) 1792–1797. https://doi.org/10.1093/nar/gkh340.

[273] S. Kumar, G. Stecher, M. Li, C. Knyaz, K. Tamura, MEGA X: Molecular Evolutionary Genetics Analysis across Computing Platforms, Mol. Biol. Evol. 35 (2018) 1547–1549. https://doi.org/10.1093/molbev/msy096.

[274] K. Tamura, M. Nei, Estimation of the number of nucleotide substitutions in the control region of mitochondrial DNA in humans and chimpanzees, Mol. Biol. Evol. 10 (1993) 512–526. https://doi.org/10.1093/oxfordjournals.molbev.a040023.

[275] A.E. Parada, D.M. Needham, J.A. Fuhrman, Every base matters: assessing small subunit rRNA primers for marine microbiomes with mock communities, time series and global field samples, Environ. Microbiol. 18 (2016) 1403–1414. https://doi.org/10.1111/1462-2920.13023.

[276] W. Walters, E.R. Hyde, D. Berg-Lyons, G. Ackermann, G. Humphrey, A. Parada, J.A. Gilbert, J.K. Jansson, J.G. Caporaso, J.A. Fuhrman, A. Apprill, R. Knight, Improved Bacterial 16S rRNA Gene (V4 and V4-5) and Fungal Internal Transcribed Spacer Marker Gene Primers for Microbial Community Surveys, MSystems. 1 (2015). https://doi.org/10.1128/mSystems.00009-15.

[277] Y. Wang, P.-Y. Qian, Conservative Fragments in Bacterial 16S rRNA Genes and Primer Design for 16S Ribosomal DNA Amplicons in Metagenomic Studies, PLOS ONE. 4 (2009) e7401. https://doi.org/10.1371/journal.pone.0007401.

[278] F. Escudié, L. Auer, M. Bernard, M. Mariadassou, L. Cauquil, K. Vidal, S. Maman, G. Hernandez-Raquet, S. Combes, G. Pascal, FROGS: Find, Rapidly, OTUs with Galaxy Solution, Bioinforma. Oxf. Engl. 34 (2018) 1287–1294. https://doi.org/10.1093/bioinformatics/btx791.

[279] E. Pruesse, C. Quast, K. Knittel, B.M. Fuchs, W. Ludwig, J. Peplies, F.O. Glöckner, SILVA: a comprehensive online resource for quality checked and aligned ribosomal RNA sequence data compatible with ARB, Nucleic Acids Res. 35 (2007) 7188–7196. https://doi.org/10.1093/nar/gkm864.

[280] Y.-S. Liu, G.-G. Ying, A. Shareef, R.S. Kookana, Occurrence and removal of benzotriazoles and ultraviolet filters in a municipal wastewater treatment plant, Environ. Pollut. Barking Essex 1987. 165 (2012) 225–232. https://doi.org/10.1016/j.envpol.2011.10.009.

[281] A. Volpe, M. Pagano, G. Mascolo, P. Grenni, S. Rossetti, Biodegradation of UV-filters in marine sediments, Sci. Total Environ. 575 (2017) 448–457. https://doi.org/10.1016/j.scitotenv.2016.10.001.

[282] N. Lee Wolfe, D.L. Macalady, New perspectives in aquatic redox chemistry: Abiotic transformations of pollutants in groundwater and sediments, J. Contam. Hydrol. 9 (1992) 17–34. https://doi.org/10.1016/0169-7722(92)90048-J.

[283] J.-R. Jeon, K. Murugesan, P. Baldrian, S. Schmidt, Y.-S. Chang, Aerobic bacterial catabolism of persistent organic pollutants — potential impact of biotic and abiotic interaction, Curr. Opin. Biotechnol. 38 (2016) 71–78. https://doi.org/10.1016/j.copbio.2015.12.016.

[284] C. Lange, B. Kuch, J.W. Metzger, Occurrence and fate of synthetic musk fragrances in a small German river, J. Hazard. Mater. 282 (2015) 34–40. https://doi.org/10.1016/j.jhazmat.2014.06.027.

[285] J.-R. Jeon, K. Murugesan, I.-H. Nam, Y.-S. Chang, Coupling microbial catabolic actions with abiotic redox processes: A new recipe for persistent organic pollutant (POP) removal, Biotechnol. Adv. 31 (2013) 246–256. https://doi.org/10.1016/j.biotechadv.2012.11.002.

[286] S. Chiron, C. Minero, D. Vione, Photodegradation Processes of the Antiepileptic Drug Carbamazepine, Relevant To Estuarine Waters, Environ. Sci. Technol. 40 (2006) 5977–5983. https://doi.org/10.1021/es060502y.

[287] D. Vogna, R. Marotta, R. Andreozzi, A. Napolitano, M. d'Ischia, Kinetic and chemical assessment of the UV/H2O2 treatment of antiepileptic drug carbamazepine, Chemosphere. 54 (2004) 497–505. https://doi.org/10.1016/S0045-6535(03)00757-4.

[288] K.M. Onesios, J.T. Yu, E.J. Bouwer, Biodegradation and removal of pharmaceuticals and personal care products in treatment systems: a review, Biodegradation. 20 (2009) 441–466. https://doi.org/10.1007/s10532-008-9237-8.

[289] K. Booij, E.P. Achterberg, B. Sundby, Release rates of chlorinated hydrocarbons from contaminated sediments, Neth. J. Sea Res. 29 (1992) 297–310. https://doi.org/10.1016/0077-7579(92)90070-U.

[290] P. Krzeminski, C. Schwermer, A. Wennberg, K. Langford, C. Vogelsang, Occurrence of UV filters, fragrances and organophosphate flame retardants in municipal WWTP effluents and their removal during membrane post-treatment, J. Hazard. Mater. 323 (2017) 166–176. https://doi.org/10.1016/j.jhazmat.2016.08.001.

[291] Y. Luo, W. Guo, H.H. Ngo, L.D. Nghiem, F.I. Hai, J. Zhang, S. Liang, X.C. Wang, A review on the occurrence of micropollutants in the aquatic environment and their fate and removal during wastewater treatment, Sci. Total Environ. 473–474 (2014) 619–641. https://doi.org/10.1016/j.scitotenv.2013.12.065.

[292] J.P. Bell, M. Tsezos, Removal of Hazardous Organic Pollutants by Biomass Adsorption, J. Water Pollut. Control Fed. 59 (1987) 191–198.

[293] M. Tsezos, J.P. Bell, Comparison of the biosorption and desorption of hazardous organic pollutants by live and dead biomass, Water Res. 23 (1989) 561–568. https://doi.org/10.1016/0043-1354(89)90022-5.

[294] A. Barra Caracciolo, E. Topp, P. Grenni, Pharmaceuticals in the environment: Biodegradation and effects on natural microbial communities. A review, J. Pharm. Biomed. Anal. 106 (2015) 25–36. https://doi.org/10.1016/j.jpba.2014.11.040.

[295] A. König, C. Weidauer, B. Seiwert, T. Reemtsma, T. Unger, M. Jekel, Reductive transformation of carbamazepine by abiotic and biotic processes, Water Res. 101 (2016) 272–280. https://doi.org/10.1016/j.watres.2016.05.084.

[296] M. Biel-Maeso, C. González-González, P.A. Lara-Martín, C. Corada-Fernández, Sorption and degradation of contaminants of emerging concern in soils under aerobic and anaerobic conditions, Sci. Total Environ. 666 (2019) 662–671. https://doi.org/10.1016/j.scitotenv.2019.02.279.

[297] G.-G. Ying, X.-Y. Yu, R.S. Kookana, Biological degradation of triclocarban and triclosan in a soil under aerobic and anaerobic conditions and comparison with environmental fate modelling, Environ. Pollut. 150 (2007) 300–305. https://doi.org/10.1016/j.envpol.2007.02.013.

[298] I. Ivshina, E. Tyumina, E. Vikhareva, Biodegradation of emerging pollutants: focus on pharmaceuticals, Microbiol. Aust. 39 (2018) 117–122. https://doi.org/10.1071/MA18037.

[299] S. Xu, Y.-F. Wang, L.-Y. Yang, R. Ji, A.-J. Miao, Transformation of tetrabromobisphenol A by Rhodococcus jostii RHA1: Effects of heavy metals, Chemosphere. 196 (2018) 206–213. https://doi.org/10.1016/j.chemosphere.2017.12.173.

[300] S.-K. Rhee, X. Liu, L. Wu, S.C. Chong, X. Wan, J. Zhou, Detection of Genes Involved in Biodegradation and Biotransformation in Microbial Communities by Using 50-Mer Oligonucleotide Microarrays, Appl. Environ. Microbiol. 70 (2004) 4303–4317. https://doi.org/10.1128/AEM.70.7.4303-4317.2004.

[301] J.-A. Majeau, S.K. Brar, R.D. Tyagi, Laccases for removal of recalcitrant and emerging pollutants, Bioresour. Technol. 101 (2010) 2331–2350. https://doi.org/10.1016/j.biortech.2009.10.087.

[302] C. Popa, L. Favier, R. Dinica, S. Semrany, H. Djelal, A. Amrane, G. Bahrim, Potential of newly isolated wild Streptomyces strains as agents for the biodegradation of a recalcitrant pharmaceutical, carbamazepine, Environ. Technol. 35 (2014) 3082–3091. https://doi.org/10.1080/09593330.2014.931468.

[303] C. Popa Ungureanu, L. Favier, G. Bahrim, A. Amrane, Response surface optimization of experimental conditions for carbamazepine biodegradation by Streptomyces MIUG 4.89, New Biotechnol. 32 (2015) 347–357. https://doi.org/10.1016/j.nbt.2014.12.005.

[304] L. Ferreira, E. Rosales, A.S. Danko, M.A. Sanromán, M.M. Pazos, Bacillus thuringiensis a promising bacterium for degrading emerging pollutants, Process Saf. Environ. Prot. 101 (2016) 19–26. https://doi.org/10.1016/j.psep.2015.05.003.

[305] Y. Wu, J. He, L. Yang, Evaluating Adsorption and Biodegradation Mechanisms during the Removal of Microcystin-RR by Periphyton, Environ. Sci. Technol. 44 (2010) 6319–6324. https://doi.org/10.1021/es903761y.

[306] E.M. Sunderland, Mercury Exposure from Domestic and Imported Estuarine and Marine Fish in the U.S. Seafood Market, Environ. Health Perspect. 115 (2007) 235–242. https://doi.org/10.1289/ehp.9377.

[307] M. Ranchou-Peyruse, M. Monperrus, R. Bridou, R. Duran, D. Amouroux, J.C. Salvado, R. Guyoneaud, Overview of Mercury Methylation Capacities among Anaerobic Bacteria Including Representatives of the Sulphate-Reducers: Implications for Environmental Studies, Geomicrobiol. J. 26 (2009) 1–8. https://doi.org/10.1080/01490450802599227.

[308] S. Hamelin, M. Amyot, T. Barkay, Y. Wang, D. Planas, Methanogens: principal methylators of mercury in lake periphyton, Environ. Sci. Technol. 45 (2011) 7693–7700. https://doi.org/10.1021/es2010072.

[309] C.C. Gilmour, A.L. Bullock, A. McBurney, M. Podar, D.A. Elias, Robust Mercury Methylation across Diverse Methanogenic Archaea, MBio. 9 (2018). https://doi.org/10.1128/mBio.02403-17.

[310] C.M. Gionfriddo, M.T. Tate, R.R. Wick, M.B. Schultz, A. Zemla, M.P. Thelen, R. Schofield, D.P. Krabbenhoft, K.E. Holt, J.W. Moreau, Microbial mercury methylation in Antarctic sea ice, Nat. Microbiol. 1 (2016) 16127. https://doi.org/10.1038/nmicrobiol.2016.127.

[311] E.A. McDaniel, B. Peterson, S.L.R. Stevens, P.Q. Tran, K. Anantharaman, K.D. McMahon, Expanded Phylogenetic Diversity and Metabolic Flexibility of Microbial Mercury Methylation, BioRxiv. (2020) 2020.01.16.909358. https://doi.org/10.1101/2020.01.16.909358.

[312] Y.-R. Liu, R.-Q. Yu, Y.-M. Zheng, J.-Z. He, Analysis of the Microbial Community Structure by Monitoring an Hg Methylation Gene (hgcA) in Paddy Soils along an Hg Gradient, Appl Env. Microbiol. 80 (2014) 2874–2879. https://doi.org/10.1128/AEM.04225-13.

[313] J.K. Schaefer, R.-M. Kronberg, F.M.M. Morel, U. Skyllberg, Detection of a key Hg methylation gene, hgcA, in wetland soils, Environ. Microbiol. Rep. 6 (2014) 441–447. https://doi.org/10.1111/1758-2229.12136.

[314] H. Du, M. Ma, T. Sun, X. Dai, C. Yang, F. Luo, D. Wang, Y. Igarashi, Mercury-methylating genes dsrB and hgcA in soils/sediments of the Three Gorges Reservoir, Environ. Sci. Pollut. Res. 24 (2017) 5001–5011. https://doi.org/10.1007/s11356-016-8213-9.

[315] J. Xu, M. Buck, K. Eklöf, O.O. Ahmed, J.K. Schaefer, K. Bishop, U. Skyllberg, E. Björn, S. Bertilsson, A.G. Bravo, Mercury methylating microbial communities of boreal forest soils, Sci. Rep. 9 (2019) 518. https://doi.org/10.1038/s41598-018-37383-z.

[316] Y. Wang, P.-Y. Qian, Conservative Fragments in Bacterial 16S rRNA Genes and Primer Design for 16S Ribosomal DNA Amplicons in Metagenomic Studies, PLoS ONE. 4 (2009). https://doi.org/10.1371/journal.pone.0007401.

[317] G.A. Christensen, A.M. Wymore, A.J. King, M. Podar, R.A. Hurt, E.U. Santillan, A. Soren, C.C. Brandt, S.D. Brown, A.V. Palumbo, J.D. Wall, C.C. Gilmour, D.A. Elias, Development and Validation of Broad-Range Qualitative and Clade-Specific Quantitative Molecular Probes for Assessing Mercury Methylation in the Environment., Appl Env. Microbiol. (2016) AEM.01271-16. https://doi.org/10.1128/AEM.01271-16.

[318] E. Zuckerkandl, L. Pauling, Evolutionary divergence and convergence in proteins. In : Evolving genes and proteins., Acad. Press. (1965) 97–166.

[319] V.M. Markowitz, I.-M.A. Chen, K. Palaniappan, K. Chu, E. Szeto, Y. Grechkin, A. Ratner, B. Jacob, J. Huang, P. Williams, M. Huntemann, I. Anderson, K. Mavromatis, N.N. Ivanova, N.C. Kyrpides, IMG: the integrated microbial genomes database and comparative analysis system, Nucleic Acids Res. 40 (2012) D115–D122. https://doi.org/10.1093/nar/gkr1044.

[320] R.D. Finn, P. Coggill, R.Y. Eberhardt, S.R. Eddy, J. Mistry, A.L. Mitchell, S.C. Potter, M. Punta, M. Qureshi, A. Sangrador-Vegas, G.A. Salazar, J. Tate, A. Bateman, The Pfam protein families database: towards a more sustainable future, Nucleic Acids Res. 44 (2016) D279–D285. https://doi.org/10.1093/nar/gkv1344.

[321] S.D. Smith, R. Bridou, A. Johs, J.M. Parks, D.A. Elias, R.A. Hurt, S.D. Brown, M. Podar, J.D. Wall, Site-Directed Mutagenesis of HgcA and HgcB Reveals Amino Acid Residues Important for Mercury Methylation, Appl. Environ. Microbiol. 81 (2015) 3205–3217. https://doi.org/10.1128/AEM.00217-15.

[322] M. Imdadullah, M. Aslam, S. Altaf, Mctest: An R package for detection of collinearity among regressors, R J. 8 (n.d.) 499–509.

[323] J. Oksanen, Multivariate Analysis of Ecological Communities in R: Vegan Tutorial, UR Httpcc Oulu Fi~ Jarioksaopetusmetodivegantutor Pdf. 1 (2007).

[324] K. Tamura, G. Stecher, D. Peterson, A. Filipski, S. Kumar, MEGA6: Molecular Evolutionary Genetics Analysis Version 6.0, Mol. Biol. Evol. 30 (2013) 2725–2729. https://doi.org/10.1093/molbev/mst197.

[325] S.-C. Choi, R. Bartha, Environmental factors affecting mercury methylation in estuarine sediments, Bull. Environ. Contam. Toxicol. 53 (1994) 805–812. https://doi.org/10.1007/BF00196208.

[326] A.G. Bravo, S. Bouchet, J. Tolu, E. Björn, A. Mateos-Rivera, S. Bertilsson, Molecular composition of organic matter controls methylmercury formation in boreal lakes, Nat. Commun. 8 (2017) 14255. https://doi.org/10.1038/ncomms14255.

[327] S.G. Wakeham, C. Lee, Limits of our knowledge, part 2: Selected frontiers in marine organic biogeochemistry, Mar. Chem. (2019). https://doi.org/10.1016/j.marchem.2019.02.005.

[328] W.L. Lázaro, S. Díez, A.G. Bravo, C.J. da Silva, Á.R.A. Ignácio, J.R.D. Guimaraes, Cyanobacteria as regulators of methylmercury production in periphyton, Sci. Total Environ. 668 (2019) 723–729. https://doi.org/10.1016/j.scitotenv.2019.02.233.

[329] A.L. Müller, C. Pelikan, J.R. de Rezende, K. Wasmund, M. Putz, C. Glombitza, K.U. Kjeldsen, B.B. Jørgensen, A. Loy, Bacterial interactions during sequential degradation of cyanobacterial necromass in a sulfidic arctic marine sediment, Environ. Microbiol. 20 (2018) 2927–2940. https://doi.org/10.1111/1462-2920.14297.

[330] M. Mestre, I. Ferrera, E. Borrull, E. Ortega-Retuerta, S. Mbedi, H.-P. Grossart, J.M. Gasol, M.M. Sala, Spatial variability of marine bacterial and archaeal communities along the particulate matter continuum, Mol. Ecol. 26 (2017) 6827–6840. https://doi.org/10.1111/mec.14421.

[331] B.B. Jørgensen, The sulfur cycle of a coastal marine sediment (Limfjorden, Denmark)1, Limnol. Oceanogr. 22 (1977) 814–832. https://doi.org/10.4319/lo.1977.22.5.0814.

[332] B.B. Jørgensen, A Thiosulfate Shunt in the Sulfur Cycle of Marine Sediments, Science. 249 (1990) 152–154. https://doi.org/10.1126/science.249.4965.152.

[333] G.A. Christensen, C.M. Gionfriddo, A.J. King, J.G. Moberly, C.L. Miller, A.C. Somenahally, S.J. Callister, H. Brewer, M. Podar, S.D. Brown, A.V. Palumbo, C.C. Brandt, A.M. Wymore, S.C. Brooks, C. Hwang, M.W. Fields, J.D. Wall, C.C. Gilmour, D.A. Elias, Determining the Reliability of Measuring Mercury Cycling Gene Abundance with Correlations with Mercury and Methylmercury Concentrations, Environ. Sci. Technol. 53 (2019) 8649–8663. https://doi.org/10.1021/acs.est.8b06389.

[334] K. Ravenschlag, K. Sahm, J. Pernthaler, R. Amann, High Bacterial Diversity in Permanently Cold Marine Sediments, Appl Env. Microbiol. 65 (1999) 3982–3989.

[335] E.J. Kerin, C.C. Gilmour, E. Roden, M.T. Suzuki, J.D. Coates, R.P. Mason, Mercury Methylation by Dissimilatory Iron-Reducing Bacteria, Appl Env. Microbiol. 72 (2006) 7919–7921. https://doi.org/10.1128/AEM.01602-06.

[336] H.-S. Bae, F.E. Dierberg, A. Ogram, Syntrophs Dominate Sequences Associated with the Mercury Methylation-Related Gene hgcA in the Water Conservation Areas of the Florida Everglades, Appl. Environ. Microbiol. 80 (2014) 6517–6526. https://doi.org/10.1128/AEM.01666-14.

[337] U. Skyllberg, A. Drott, L. Lambertsson, E. Björn, T. Karlsson, T. Johnson, S.-A. Heinemo, H. Holmström, Net methylmercury production as a basis for improved risk assessment of mercury-contaminated sediments, Ambio. 36 (2007) 437–442.

[338] A. Drott, L. Lambertsson, E. Björn, U. Skyllberg, Do Potential Methylation Rates Reflect Accumulated Methyl Mercury in Contaminated Sediments?, Environ. Sci. Technol. 42 (2008) 153–158. https://doi.org/10.1021/es0715851.

[339] X. Lu, W. Gu, L. Zhao, M.F.U. Haque, A.A. DiSpirito, J.D. Semrau, B. Gu, Methylmercury uptake and degradation by methanotrophs, Sci. Adv. 3 (2017) e1700041. https://doi.org/10.1126/sciadv.1700041.

[340] M. Goñi-Urriza, Y. Corsellis, L. Lanceleur, E. Tessier, J. Gury, M. Monperrus, R. Guyoneaud, Relationships between bacterial energetic metabolism, mercury methylation potential, and hgcA/hgcB gene expression in Desulfovibrio dechloroacetivorans BerOc1, Environ. Sci. Pollut. Res. Int. 22 (2015) 13764–13771. https://doi.org/10.1007/s11356-015-4273-5.

[341] H. Hsu-Kim, K.H. Kucharzyk, T. Zhang, M.A. Deshusses, Mechanisms Regulating Mercury Bioavailability for Methylating Microorganisms in the Aquatic Environment: A Critical Review, Environ. Sci. Technol. 47 (2013) 2441–2456. https://doi.org/10.1021/es304370g.

[342] S.Y. Malkin, A.M. Rao, D. Seitaj, D. Vasquez-Cardenas, E.-M. Zetsche, S. Hidalgo-Martinez, H.T. Boschker, F.J. Meysman, Natural occurrence of microbial sulphur oxidation by long-range electron transport in the seafloor, ISME J. 8 (2014) 1843–1854. https://doi.org/10.1038/ismej.2014.41.

[343] J. Liu, T. Jiang, F. Wang, J. Zhang, D. Wang, R. Huang, D. Yin, Z. Liu, J. Wang, Inorganic sulfur and mercury speciation in the water level fluctuation zone of the Three Gorges Reservoir, China: The role of inorganic reduced sulfur on mercury methylation, Environ. Pollut. 237 (2018) 1112–1123. https://doi.org/10.1016/j.envpol.2017.11.045.

[344] K.L. Smith, H.A. Ruhl, C.L. Huffard, M. Messié, M. Kahru, Episodic organic carbon fluxes from surface ocean to abyssal depths during long-term monitoring in NE Pacific, Proc. Natl. Acad. Sci. 115 (2018) 12235–12240. https://doi.org/10.1073/pnas.1814559115.

[345] P.W. Boyd, H. Claustre, M. Levy, D.A. Siegel, T. Weber, Multi-faceted particle pumps drive carbon sequestration in the ocean, Nature. 568 (2019) 327. https://doi.org/10.1038/s41586-019-1098-2.

[346] J.K. King, F.M. Saunders, R.F. Lee, R.A. Jahnke, Coupling mercury methylation rates to sulfate reduction rates in marine sediments, Environ. Toxicol. Chem. 18 (1999) 1362–1369. https://doi.org/10.1002/etc.5620180704.

[347] J.K. King, J.E. Kostka, M.E. Frischer, F.M. Saunders, Sulfate-Reducing Bacteria Methylate Mercury at Variable Rates in Pure Culture and in Marine Sediments, Appl Env. Microbiol. 66 (2000) 2430–2437. https://doi.org/10.1128/AEM.66.6.2430-2437.2000.

[348] J.K. King, J.E. Kostka, M.E. Frischer, F.M. Saunders, R.A. Jahnke, A Quantitative Relationship that Demonstrates Mercury Methylation Rates in Marine Sediments Are Based on the Community Composition and Activity of Sulfate-Reducing Bacteria, Environ. Sci. Technol. 35 (2001) 2491–2496. https://doi.org/10.1021/es001813q.

[349] R.A. Duce, Atmospheric Input of Pollutants, in: J.K. Cochran, H.J. Bokuniewicz, P.L. Yager (Eds.), Encycl. Ocean Sci. Third Ed., Academic Press, Oxford, 2001: pp. 243–251. https://doi.org/10.1016/B978-0-12-813081-0.00045-8.

[350] C.R. Hammerschmidt, W.F. Fitzgerald, C.H. Lamborg, P.H. Balcom, P.T. Visscher, Biogeochemistry of methylmercury in sediments of Long Island Sound, Mar. Chem. 90 (2004) 31–52. https://doi.org/10.1016/j.marchem.2004.02.024.

[351] M. Monperrus, E. Tessier, D. Amouroux, A. Leynaert, P. Huonnic, O.F.X. Donard, Mercury methylation, demethylation and reduction rates in coastal and marine surface waters of the Mediterranean Sea, Mar. Chem. 107 (2007) 49–63. https://doi.org/10.1016/j.marchem.2007.01.018.

[352] J.S. Bowman, H.W. Ducklow, Bacterioplankton☆, in: J.K. Cochran, H.J. Bokuniewicz, P.L. Yager (Eds.), Encycl. Ocean Sci. Third Ed., Academic Press, Oxford, 2019: pp. 500–507. https://doi.org/10.1016/B978-0-12-409548-9.11404-6.

[353] D. Cossa, M. Coquery, C. Gobeil, J.-M. Martin, Mercury Fluxes at the Ocean Margins, in: W. Baeyens, R. Ebinghaus, O. Vasiliev (Eds.), Glob. Reg. Mercury Cycles Sources Fluxes Mass Balanc., Springer Netherlands, Dordrecht, 1996: pp. 229–247. https://doi.org/10.1007/978-94-009-1780-4_11.

[354] C.H. Lamborg, W.F. Fitzgerald, A. Skoog, P.T. Visscher, The abundance and source of mercury-binding organic ligands in Long Island Sound, Mar. Chem. 90 (2004) 151–163. https://doi.org/10.1016/j.marchem.2004.03.014.

[355] AMAP/UNEP (2018) Technical background report for the global mercury assessment, (n.d.). http://www.mercuryconvention.org/Resources/Information/Publications/tabid/3429/language/ en-US/Default.aspx.

[356] D. Obrist, J.L. Kirk, L. Zhang, E.M. Sunderland, M. Jiskra, N.E. Selin, A review of global environmental mercury processes in response to human and natural perturbations: Changes of emissions, climate, and land use, Ambio. 47 (2018) 116–140. https://doi.org/10.1007/s13280-017-1004-9.

[357] K.L. Bowman, C.R. Hammerschmidt, C.H. Lamborg, G. Swarr, Mercury in the North Atlantic Ocean: The U.S. GEOTRACES zonal and meridional sections, Deep Sea Res. Part II Top. Stud. Oceanogr. 116 (2015) 251–261. https://doi.org/10.1016/j.dsr2.2014.07.004.

[358] H. Hsu-Kim, C.S. Eckley, D. Achá, X. Feng, C.C. Gilmour, S. Jonsson, C.P.J. Mitchell, Challenges and opportunities for managing aquatic mercury pollution in altered landscapes, Ambio. 47 (2018) 141–169. https://doi.org/10.1007/s13280-017-1006-7.

[359] B.B. Jørgensen, The sulfur cycle of a coastal marine sediment (Limfjorden, Denmark)1, Limnol. Oceanogr. 22 (1977) 814–832. https://doi.org/10.4319/lo.1977.22.5.0814.

[360] C.A. Choy, B.H. Robison, T.O. Gagne, B. Erwin, E. Firl, R.U. Halden, J.A. Hamilton, K. Katija, S.E. Lisin, C. Rolsky, K.S.V. Houtan, The vertical distribution and biological transport of marine microplastics across the epipelagic and mesopelagic water column, Sci. Rep. 9 (2019) 7843. https://doi.org/10.1038/s41598-019-44117-2.

ANNEXES

Annexe1

COMPARISON OF THE MERCURY REACTIVITY IN TWO SUBMARINE CANYONS (ATL. OCEAN AND PAC. OCEAN)

Alyssa Azaroff[1], Emmanuel Tessier[2], Carl Lamborg[3], Laurent Lanceleur[1], Rémy Guyoneaud[2], Mathilde Monperrus[1]

[1]CNRS/ UNIV PAU & PAYS ADOUR/ E2S UPPA, Institut des Sciences Analytiques et de Physicochimie pour l'Environnement et les Materiaux – MIRA, UMR 5254, 64600, Anglet, FRANCE
[2] CNRS/ UNIV PAU & PAYS ADOUR/ E2S UPPA, Institut des Sciences Analytiques et de Physicochimie pour l'Environnement et les Materiaux – MIRA, UMR 5254, 64000, Pau, FRANCE
[3] University of California, Santa Cruz, Department of Ocean Sciences, Santa Cruz, CA 95064, USA

Context

Submarine canyons are home to important stocks of commercially important fisheries, the consumption of which is the main monomethymercury (MeHg) human exposure. Currently, biogeochemistry of mercury in these biologically productive systems is unknown. Here, inorganic mercury (Hg(II)) and organic mercury (MeHg) distributions as well as the Hg reactivity were measured in surface sediments of two submarine canyons: Monterey Canyon in NE Pacific Ocean and the Capbreton Canyon in the NE Atlantic Ocean

Capbreton Canyon
Atlantic Ocean

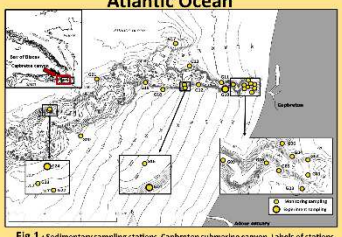

Fig.1 : Sedimentary sampling stations, Capbreton submarine canyon. Labels of stations are attributed according to distance to the coast (HaPoGé cruise, July 2017)

Monterey Canyon
Pacific Ocean

Fig.2 : Sedimentary sampling stations, Monterey submarine canyon. Labels of stations are attributed according to distance to the coast (Moss Landing Marine Lab., Oct. 2018)

Research questions

1- What is the Hg species distribution in two submarine canyon from two different ocean ?
2- Are submarine canyons sediments involved in MeHg production ?

Material and methods

To investigate the difference of Hg species, e.i. inorganic mercury (Hg(II)) and organic mercury (MeHg), and Hg transformations between two different canyon systems, sediments were sampled in Capbreton submarine canyon (Atlantic Ocean) and Monterey submarine canyon (Pacific Ocean) (Fig. 1 and Fig. 2) in 2017 and 2018.

Sampling sediments

Hg distribution

Isotopic Dilution method, GC – ICPMS

Hg transformation

Enriched isotopic tracers
$Me^{201}Hg$ and $^{199}HgII$

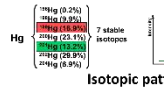

Isotopic pattern deconvolution

$$M = \frac{{}^{MeHg}x_{spike} \cdot {}^{MeHg}N_m}{N_{spike}} \qquad D = \frac{{}^{m_2}x_{spike} \cdot {}^{m_2}N_m}{N_{spike}}$$

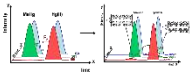

Kinetic times (days) : 0,1, 2, 4, 7, 11,
In biotic and abiotic conditions

Double spiked Isotopic Dilution method, GC – ICPMS

1- Hg distribution

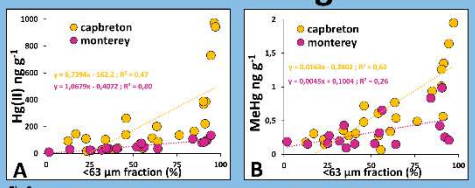

Fig.3 : Relationship between fine fraction and Hg species concentrations, Hg(II) (A) and MeHg (B), in surface sediments of Capbreton submarine canyon area and Monterey submarine canyon (p-value <0,05).

- Strong correlations between fine sediments (<63µm fraction) and total carbon content in both of two canyons (R^2= 0,86 and 0,63; with p-value < 0,0001 for Capbreton and Monterey, respectively)
- Hg(II) and MeHg concentrations are strongly related to fine fraction in both canyons, with an increase along canyon transect (Fig. 3A, B)
- Mercury levels are up to 7 times higher in the Capbreton Canyon than the Monterey Canyon

Fig.4 : HgII concentrations and proportion of MeHg in surface sediments of Capbreton submarine canyon area.

High % MeHg levels are observed close to the coast and decrease along with the distance to the coast (Fig. 4)

$$\%\,MeHg = \frac{MeHg}{\underbrace{(Hg(II)+MeHg)}_{THg}} \times 100$$

2- Hg transformations

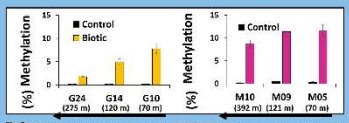

Fig.5 : Methylation yields (%) after 11 days incubations of slurries from Capbreton (yellow) and Monterey (pink) in biotic and control (abiotic) conditions. Error bars represent the standard deviation of triplicate incubations. Between brackets, depth of sampling in meter (m).

- Methylation is a biotic process, higher in Monterey than Capbreton canyon, where yields (Fig.5) and kM (Table 1) are high in coastal sediments.

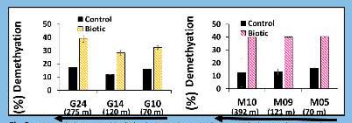

Fig.6 : Demethylation yields (%) after 11 days incubations of slurries from Capbreton (yellow) and Monterey (pink) in biotic and control (abiotic) conditions. Error bars represent the standard deviation of triplicate incubations. Between brackets, depth of sampling in meter (m).

- Demethylation is mediated by biotic and abiotic processes, similar in both canyons (Fig. 5, Table 1).

Stations	[HgII] ng g^{-1}	[MeHg] ng g^{-1}	MeHg %	kM %.d^{-1}	kD %.d^{-1}	MeHg net prod. ng g^{-1} day^{-1}
G10	137	0,49	0,36	0,72	1,42	0,98
G14	139	0,48	0,34	0,42	1,21	0,58
G24	944	1,95	0,21	0,15	2,05	1,35
M05	30	0,18	0,61	1,06	2,65	0,31
M09	48	0,16	0,33	1,01	2,10	0,47
M10	137	0,29	0,21	0,77	1,85	1,04

Table 1 : Parameters of Hg transformations in three surface sediments along the canyon transect in Capbreton and Monterey canyons. kM and kD are methylation and demethylation rates, respectively.

Positive net production of MeHg are estimated (Table 1) in both canyons, associated to inorganic Hg ambiant concentrations.

$$[MeHg]_{net\ production} = (k_M/100 \times [Hg(II)]_{ambient}) - (k_D/100 \times [MeHg]_{ambient})$$

1- Hg distribution

- Positive correlations between TC, fine fraction, and Hg species concentrations were shown, suggest canyon sediments accumulate fine particulate matter and concentrate mercury.
- Higher mercury levels in Capbreton canyon sediments may indicate more important local (rivers discharges) and regional sources (geological background, high anthropgenic Hg in Atlantic ocean[1]).
- Capbreton canyon is more stable than Monterey canyon (high frequency of "flushing events"[2]), with high particulate accumulation potential[3], could improve Hg enrichment in sediment compartment.

2- Hg transformations

- Studies on sediments have identified the sulfate-reducing bacteria (SRB) as the main contributors to Hg methylation[4]. High % MeHg observed in coastal locations in both canyons might indicate higher biotic activities nearby the coast.
- Results confirm that the net MeHg production is controlled by competing simultaneous methylation and demethylation processes, mainly mediated by biotic process.

Conclusion

This comparative study presents, for the first time, Hg species distribution in two submarine canyons, where higher Hg levels were observed in Atlantic ocean than Pacific ocean. Slurry incubation experiments demonstrated a biotic process might enhance the production of MeHg, a harmful global pollutant for the environment and human health. Overall, this study demonstrated submarine canyons might contribute to the global ocean MeHg cycle.

References :

1. Lamborg, C. H. et al. A global ocean inventory of anthropogenic mercury based on water column measurements. Nature (2014).
2. Okey, T. A. Sediment flushing observations, earthquake slumping, and benthic community changes in Monterey Canyon head. Cont. Shelf Res. (1997).
3. Mulder, T. et al. Present deep-submarine canyons activity in the Bay of Biscay (NE Atlantic). Mar. Geol. (2012).
4. Compeau GC, Bartha R. Sulfate-Reducing Bacteria: Principal Methylators of Mercury in Anoxic Estuarine Sediment. Appl Environ Microbiol. (1985).

The **Micropolit** research **program** "State and evolution of the quality of the South Atlantic coastal environment" is co-financed by the European Union and the Adour Garonne Water Agency. Europe commits to New Aquitaine with the European Regional Development Fund.

Résumé : Ce travail a permis d'acquérir de nouvelles connaissances sur la pollution marine issue des activités anthropiques dans le Canyon sous-marin de Capbreton, une zone de transfert de matériel particulaire du continent vers l'océan profond. Un état des lieux a été réalisé sur la présence de micropolluants prioritaires et émergents dans les sédiments des 25 premiers kilomètres de ce canyon. Les sédiments prélevés dans le canyon présentaient des concentrations de micropolluants plus importantes que dans les sédiments prélevés sur le plateau continental suggérant que le canyon est à la fois un piège à particules et à micropolluants. La détermination des sources par des outils isotopiques a démontré une forte contribution d'apports provenant des effluents côtiers pour les zones proches de la côte et une contribution d'apports pélagiques pour les zones plus éloignées. La réactivité de certains micropolluants émergents et du mercure a été examinée par des expériences en conditions contrôlées afin d'identifier les processus de transformation et les bactéries impliquées. La dégradation des micropolluants émergents est lente en condition anoxique et bien plus rapide en condition oxique. La capacité de dégradation observée pour des bactéries isolées de ces sédiments suggère leur potentielle implication dans les processus de biorémédiation des micropolluants organiques dans le milieu marin. Les potentiels de méthylation et de déméthylation du mercure ont montré une forte biométhylation dans les sédiments côtiers anoxiques, associée à des bactéries du cycle du soufre notamment. Ces travaux confirment que le canyon de Capbreton, comme certainement d'autres canyons sous-marins, sont des zones importantes en terme de processus de transfert et de transformations des micropolluants.

Mots clefs : micropolluants prioritaires, micropolluants émergents, sources, réactivité, activités et diversité bactériennes, sédiments de canyon sous marin

Abstract : This work improved our knowledge about the marine pollution from anthropogenic activities in the submarine Canyon of Capbreton, a transfer zone of particulate matter from the continent to the deep sea. An inventory of the priority and emerging micropollutants has been performed from sediments of the first 25 kilometres of this canyon. Higher concentrations of micropollutants were observed in the canyon compare to the continental shelf suggesting that this canyon is both a trap for particles and micropollutants. Tracking of sources with isotopic tools demonstrated high contribution of runoff inputs for coastal sediments and a contribution of the hemipelagic inputs for the offshore sediments. Reactivity of emerging micropollutants and mercury was assessed by experiments under controlled conditions in order to identify transformations processes and Prokaryotes involved. Emerging micropollutants degradation is slow under anoxic condition and much higher under oxic condition. The capacity of degradation observed for bacteria isolated from those sediments suggests their implication for the organic micropollutants bioremediation in the marine environment. Mercury methylation and demethylation potentials demonstrated a high biomethylation in coastal anoxic sediments, linked to bacteria related to the sulphur cycle. This work confirm that Capbreton Canyon, likely as others submarine canyons, are important ecosystems for the transfer and micropollutants transformations processes.

Key words : priority micropollutants, emerging micropollutants, sources, reactivity, reactivity and diversity of bacteria, submarine canyon sediments